1-1-2016

# Studies Towards Broadening The Substrate Profile And Regulation Of Histone Deacetylase 1

Dhanusha Ashanthi Nalawansha
*Wayne State University,*

# STUDIES TOWARDS BROADENING THE SUBSTRATE PROFILE AND REGULATION OF HISTONE DEACETYLASE 1

by

**DHANUSHA ASHANTHI NALAWANSHA**

**DISSERTATION**

Submitted to the Graduate School

of Wayne State University,

Detroit, Michigan

in partial fulfillment of the requirements

for the degree of

**DOCTOR OF PHILOSOPHY**

2016

MAJOR: CHEMISTRY (Biochemistry)

Approved By:

_____

Advisor Date

_____

_____

_____

_____

## DEDICATION

The dissertation is dedicated to my father (T.R. Nalawansha), my mother (W. Jayalath), my husband (Kusal Samarasinghe), my son (Thiveyn Samarasinghe), and my dissertation advisor, Prof. Mary Kay Pflum

## ACKNOWLEDGEMENTS

I am truly indebted to my advisor, Prof. Mary Kay Pflum for her guidance, valuable advice, encouragement and constant support throughout the last five years. She always believed in me and that led me to become a skilled and independent scientist. She helped me to get through hard times and always came up with valuable suggestions to overcome the hurdles. Thank you very much Dr. Pflum for your unending support and I am so blessed to have you as a mentor in my career. I wish you all the best for your future and professional career.

I would like to express my sincere gratitude to my dissertation committee, Prof. Tamara L. Hendrickson, Prof. G. Andres Cisneros, and Prof. Lori A. Pile. I greatly appreciate the comments and invaluable suggestions given over the years. I wish you all the best in your future endeavors.

I would also like to acknowledge Dr. Joseph Caruso at the Proteomic core facility, Wayne State University for analyzing the mass spectrometric data and Dr. Yin long in the Department of Pathology for help with the real time PCR instrument. I would like to thank Rashmi Chandra (Dr. Joy Alcedo lab) and Divya Subramonium (Dr. Xiang Dong Zhang lab) for helping me with the fluorescence microscope in the Department of Biological Sciences.

I would like to thank my past lab mates, Todd Faner, Dr. Magdalene K Wambua, Dr. Satish Garre, Dr. Geetha Padige, Dr. Chamara Senenviratne, and present lab mates Dr. Thilani Anthony, Maheeka Embogama, Pavithra Dedigama, Dr. Ahmed Fouda, Ahmed Negmeldin, Inosha Gomes, Aparni Gamage, Vindya Harshani, and Nuwan Acharige.

I am also very grateful to Department of Chemistry, Wayne State University for providing the facilities and instrumentation to pursue my Ph.D. studies.

I am truly grateful to my dear parents for believing in me and supporting me from the beginning to become the person who I am today. Your unconditional love, support, and advice always inspired me to achieve my goals and I am forever indebted to you.

My greatest gratitude goes to my beloved and supportive husband who is always by my side and has helped me a lot to achieve my goals. Thanks for all the suggestions and unending support to make this journey a reality. It would not be possible without you. I am also grateful to my dearest son for all the happiness given to me during the last two years.

## TABLE OF CONTENTS

## LIST OF TABLES

## LIST OF FIGURES

## LIST OF SCHEMES

## LIST OF ABBREVIATIONS

DNA – Deoxyribonucleic Acid

cDNA – complementary DNA

RNA – Ribonucleic Acid

SWI/SNF – SWItch/Sucrose Non Fermentable

ISWI – Imitation SWItch

hBRG1 – Human Brahma Related Gene 1

hBRM – Human Brahma

DNMT – DNA Methyltransferase

PTMs – Post Translational Modifications

ADP – Adenosine Dinucleotide Phosphate

ATP – Adenosine Trinucleotide Phosphate

HAT – Histone Acetyltransferase

HDAC – Histone Deacetylase

SAHA – Suberoyl Anilide Hydroxamic Acid

SHI-1:2 – HDAC1/2 Selective Inhibitor

MTA-1 – Metastasis-associated protein

NuRD – Nucleosome Remodelling and Deacetylation

NCOR1 – Nuclear receptor corepressor 1

CoREST – Corepressor for element 1-silencing transcription factor

NCOR/SMRT – Nuclear receptor co-repressor/silencing mediator of retinoid and thyroid receptor

SNP – Single Nucleotide Polymorphism

KIF11 – Kinesin like Protein 11

HyDn-SNP-S – Hypothesis driven SNP-search

LC-MS/MS – Liquid Chromatography-tandem mass spectrometry

SDS-PAGE – Sodium Dodecyl Sulfate PolyAcrylamide Gel Electrophoresis

HEK293 – Human Embryonic Kidney 293

DAPI – (4',6-diamidino)-2-phenylindole

BSA – Bovine Serum Albumin

PBS – Phosphate Buffered Saline

TBS – Tris Buffered Saline

JLB – Jurkat Lysis Buffer

FBS – Fetal Bovine Serum

DMSO – Dimethyl Sulfoxide

EDTA – Ethylenediaminetetraacetic acid

TEMED – TEtraMEthylthyleneDiamine

APS – Ammonium PerSulfate

IPTG – IsoPropyl-1-Thio-β-D-Galactopyranoside

DTT – Dithiothreitol

BME – β-Mercaptoethanol

TCEP – (tris(2-carboxyethyl)phosphine

FDR – False Discovery Rate

LSD1 – Lysine Specific histone Demethylase 1

AcLys – Acetyl lysine

PCR – Polymerase Chain Reaction

RT-PCR – Real Time PCR

CIP – Calf Intestinal Phosphatase

# CHAPTER 1. INTRODUCTION

## 1.1 Nucleosome

DNA is the genetic material that stores information in the cell and transfers it from one generation to another (1). In eukaryotes, DNA is packaged into nucleosomes, which is further condensed into higher order chromatin (Figure 1.1). The nucleosome, which is the basic subunit of chromatin, consists of an octamer of histone proteins, two each of H2A, H2B, H3 and H4, with 146 bp of DNA wrapped around each unit. Positively charged amino acids, such as lysines and arginines, in the histone proteins form tight interactions with the negatively charged DNA. Hence, the interaction between DNA and histone proteins has a direct impact on the conformation of chromatin. DNA in the context of chromatin is involved in multiple processes, such as transcription, replication, DNA repair and recombination. Therefore, cells deploy versatile mechanisms to modulate chromatin structure to mediate gene expression.

## 1.2 Epigenetics

The heritable changes in gene expression that occur without changes in DNA sequence are referred to as epigenetics (2). Epigenetic regulation of gene expression involves chromatin remodeling factors, DNA methylation, and histone modifications (Figure 1.1). Multiple enzymes are involved in epigenetic gene regulation. As a consequence, mutations or aberrant activity of epigenetic modifiers have been implicated in several diseases including cancer (3). Given the involvement of epigenetic enzymes in cancer, they are emerging as attractive anti-cancer targets.

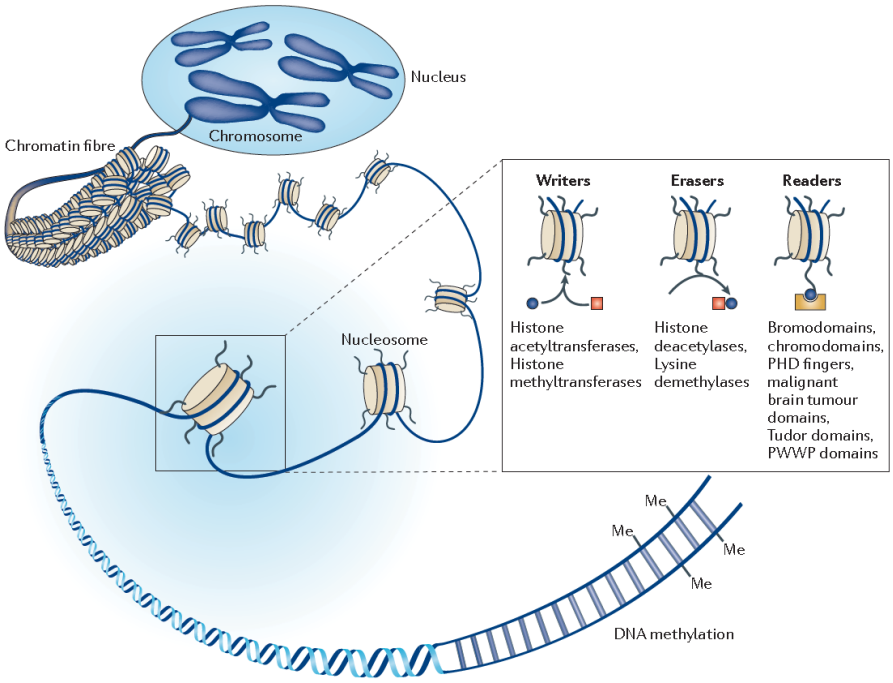


**Figure 1.1 – Chromatin and the nucleosome**. DNA is packaged inzato higher order chromatin structure, which consists of an array of nucleosomes. DNA and four different types of histone proteins form the nucleosome. Writers, readers, and erasers are involved in epigenetic gene regulation through modification of the N-terminal tails of the histone proteins. Copyright permission was obtained from *Nat rev Drug disc.* 2012,11 (2).

### 1.2.1 Chromatin Remodeling

Several chromatin remodeling complexes are involved in dynamically regulating chromatin structure (4). These proteins utilize the energy of ATP hydrolysis to alter the interaction between DNA and histone proteins. Three major chromatin remodeling complexes are known to date: SWI2/SNF2, ISWI and CHD. SWI2/SNF2 was the first remodeling complex isolated from yeast. Humans also have homologous complexes related to yeast SWI2/SNF2 complex, such as the hBRG1 and hBRM complexes. The structural changes mediated by chromatin remodeling complexes include sliding of the

histone octamer along the DNA, changing the DNA conformation, and replacement of histone proteins.

### 1.2.2 DNA methylation

DNA methylation plays a crucial role in gene repression. DNA methyltransferases (DNMTs) catalyzes the transfer of methyl groups from S-adenosyl-L-methionine to cytosine bases in DNA (5). Methylation of cytosines in the promoter regions is often linked to gene repression. DNMT enzymes are also found in chromatin remodeling complexes and other corepressor complexes. Methyl CpG binding proteins in the corepressor complexes recruit histone modifying enzymes to further repress transcription through histone deacetylation. Aberrant patterns of DNA methylation are also linked to disease formation (6). Therefore, DNMT enzymes have emerged as anti-cancer therapeutics.

### 1.2.3 Histone modifications

The N–terminal tails of histone proteins undergo a myriad of post translational modifications (PTMs), such as acetylation, methylation, phosphorylation, ubiquitination, sumoylation, and ADP ribosylation (Figure 1.2) ; (Scheme 1.1) (7). These PTMs modulate chromatin structure and gene expression. Multiple epigenetic enzymes are involved in regulating histone modifications, which are categorized into readers, writers and erasers (Figure 1.1) (2). Readers assist in recognizing a particular histone mark. For example, bromodomains recognize acetylated lysines, whereas chromodomains identify methylated lysines. Reader proteins then recruit writers or erasers to carry out their function. Writers catalyze the addition of a particular histone mark, such as an acetyl or methyl group. Erasers catalyze the removal of a histone mark. Combined, action of all these enzymes are critical to regulate gene expression.

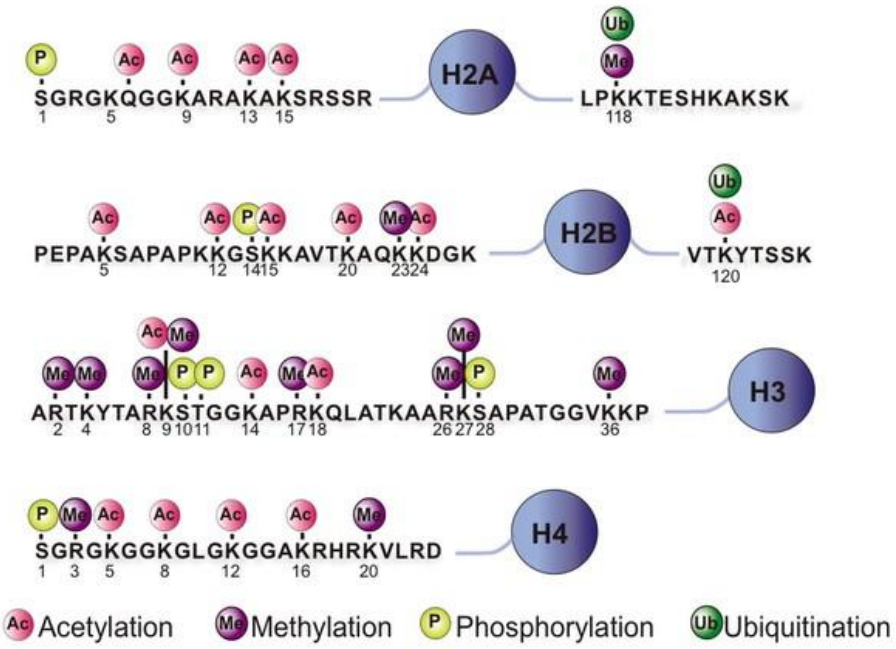


**Figure 1.2 – Covalent post-translational modifications of histone proteins.** N-terminal tails of histone proteins undergo multiple PTMs to regulate gene transcription. Acetylation (pink color) and ubiquitination (green color) occur on lysine residues whereas methylation (purple color) occurs on both arginines and lysines. Phosphorylation (yellow color) occurs on serine and threonine residues. Copyright permission was obtained from Kato. S. *et al. IBMS Bonekey.* 2010, 7 (8).

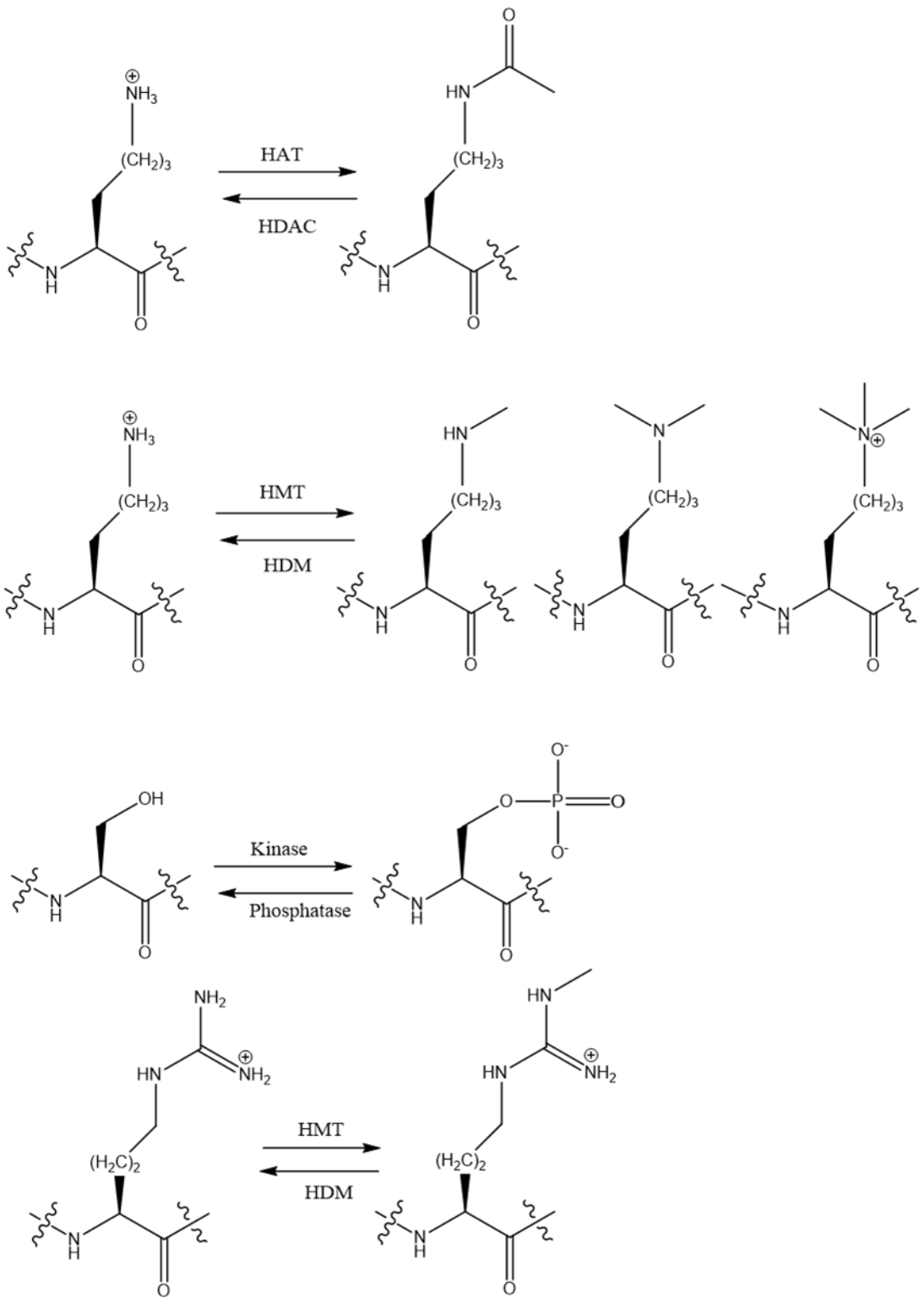


**Scheme 1.1 - Post-translational modification of histone proteins. A)** HATs catalyzes the transfer of acetyl group to the lysines of the N-terminal tails of histone proteins,

whereas HDACs remove acetyl groups from lysines to regulate gene expression. B) and D) Histone methylation is regulated by histone methyltransferases (HMT) and demethylases (HDM). C) Histone phosphorylation is catalyzed by kinases and phosphatases.

Expression of a particular gene is modulated by a single or a combination of several histone modifications (3). Acetylation and methylation of lysine residues of histone tails have a significant impact on transcriptional activity. Acetylation is mediated by the interplay between histone acetyl transferases and histone deacetylases, which will be discussed in greater detail in the next section (1.4). With an essential role in gene expression, epigenetic deregulation is often linked to cancer formation (3). For example, aberrant expression of histone demethylases are implicated in many diseases, including cancer. As a consequence, the aberrant activities of epigenetic enzymes have been targeted by anti-cancer therapeutics.

**1.3 Histone methylation and demethylation**

Histone methylation of lysines can be either activating or repressing of gene expression depending on the residue (9). For example, methylation at lysine 4 and lysine 36 of histone H3 are linked to transcriptional activation, whereas methylation at lysine 9 or lysine 27 mediates gene repression (10). Methylation can also occur on arginine residues in histones. Histone methyltransferase (HMT) and demethylase (HDM) proteins govern histone methylation (scheme 1.1B and D) to regulate transcription (11).

Histone demethylases have been classified in two families: the Monoamine oxidase family and the Jumonji (JmjC) family. Lysine specific demethylase1 (LSD1) was the first identified histone demethylase; it belongs to the monoamine oxidase superfamily,

which uses flavin adenine dinucleotide (FAD) as a cofactor during catalysis. LSD1 catalyzes the demethylation of mono and dimethylated H3K4 and H3K9 to regulate gene expression. LSD1 is involved in multiple cellular processes including embryonic development, cell proliferation and metastasis. LSD1 is also overexpressed in multiple cancers, such as breast, Acute Myeloid Leukemia, prostate, colon, lung and neuroblastoma. Genetic knockdown of LSD1 inhibits cell proliferation. Hence, LSD1 has emerged as a potential anti-cancer drug target (12,13). LSD1 will be discussed in greater detail in Chapter 3.

**1.4 Histone acetylation and deacetylation**

Acetylation is a well-studied post translational modification that directly affects chromatin structure (14). Acetylation is usually associated with euchromatin (relaxed and active chromatin) regions, whereas deacetylation is typically found with heterochromatin (condensed and silent chromatin). The balance between acetylation and deacetylation is governed by the interplay between histone acetyltransferases (HATs) and histone deacetylases (HDACs) (scheme 1.1A).

The acetylation of lysines on histone proteins reduces the interaction between negatively charged DNA and histones, leading to a less compact chromatin structure. Hence, acetylation is linked to transcriptional activation (Figure 1.3B). In contrast, histone deacetylases (HDACs) catalyze deacetylation to restore the positive charge on the lysines, which tightens the interaction between DNA and histones to form condensed or more compact chromatin (Figure 1.3A). Thus, deacetylation is usually associated with transcriptional repression (15).

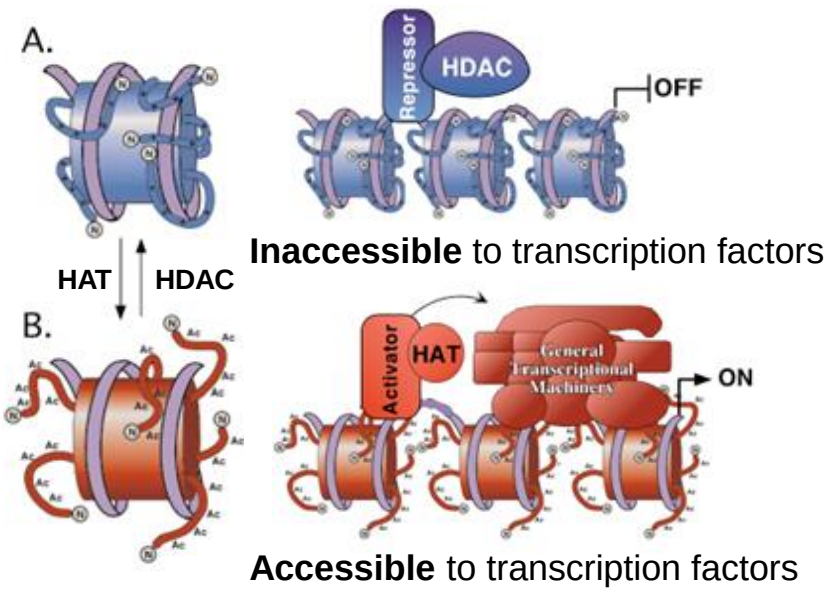


**Figure 1.3 – Acetylation maintains chromatin structure in ON and OFF states.** Acetylation of lysines on the histone tails produce more relaxed and open chromatin structure, which is accessible to the transcription machinery; hence transcription is turned ON. Deacetylation, mediated by HDACs, forms more compact and closed chromatin, which is inaccessible to transcription factors; hence transcription is turned OFF (picture credit – Dr. Mary Kay Hamm Pflum).

### 1.5 Histone deacetylases (HDACs)

#### 1.5.1 Classification of HDACs

To date, eighteen human HDAC proteins have been identified and grouped into four classes based on catalytic mechanism, size, sub-cellular localization, and similarity to yeast enzymes (Figure 1.4) (16). Class I, II and IV proteins require metal ions for enzymatic activity. Class I comprises HDAC1, HDAC2, HDAC3 and HDAC8, which are homologous to the yeast Rpd3 protein (17-21). Class I HDACs are smaller in size compared to class II and have molecular weight ranges from 49-55 kDa. Class I HDAC proteins are expressed in all tissues and localize predominantly in the nucleus. Members

of class II include HDAC4, HDAC5, HDAC6, HDAC7, HDAC9 and HDAC10 and are similar to yeast HDA1 (22-24). Class II HDACs are large in size in the range from 80-131 kDa. Among all the HDAC isoforms, HDAC6 and HDAC10 have two deacetylase domains, although only HDAC6 has two active domains. Class II members are tissue specific and shuttle between the nucleus and the cytoplasm (25). Class IV consists of only HDAC11, which is 39 kDa and shares some similarity with both class I and II (26). HDAC11 is expressed in a tissue specific manner and is mainly found in the nucleus.

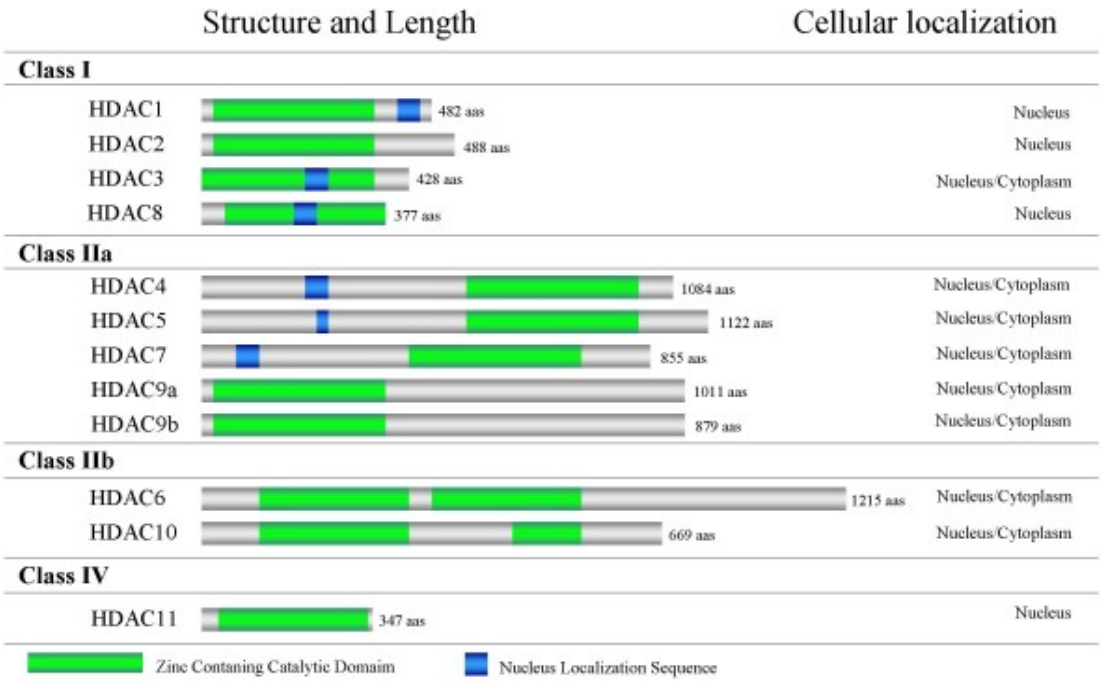


**Figure 1.4 – Classification of histone deacetylases (HDACs).** HDACs are divided into four different classes based on their size, subcellular localization, and similarity to yeast proteins. Class I, II and IV require metal for their enzymatic activity. Copyright permission was obtained from Lucio-Eterovic, A. K*. et al. BMC cancer*, 2008, 8. (27).

Class III HDACs are sirtuins that require NAD+ for their catalytic activity. They also share sequence similarity to yeast sirt2. There are seven class III members named Sirt

1-Sirt7. The focus of this dissertation work is on the Class I, II and IV proteins, which require metal ions for enzymatic activity. Therefore, sirtuins will not be discussed in detail.

### 1.5.2 Structure of HDACs

Crystal structures of HDAC1-4, 6, 7 and 8 have been reported (28-36). The structures revealed that HDAC proteins contain a narrow 11Å active site channel with an adjacent 14 Å cavity (Figure 1.5). The Zn metal lies at the bottom of the 11 Å channel. The hydrophobic linker of HDAC inhibitor; SAHA (Vorinostat, Suberoyl Anilide Hydroxamic Acid) or the acetylated substrate interacts with the 11 Å active site and form hydrophobic interactions with the enzyme. The carbonyl oxygen of the hydroxamic acid of SAHA coordinates to the Zn metal. Polar and charged residues in the 14 Å internal cavity stabilize the acetate byproduct and facilitate acetate escape (37). In prior work, residues in the 11 Å and 14 Å channels of HDAC1 were mutated to alanine to study structure and function (37,38). Almost all mutants displayed reduced enzymatic activity, confirming the importance of these structural features for deacetylation reaction.

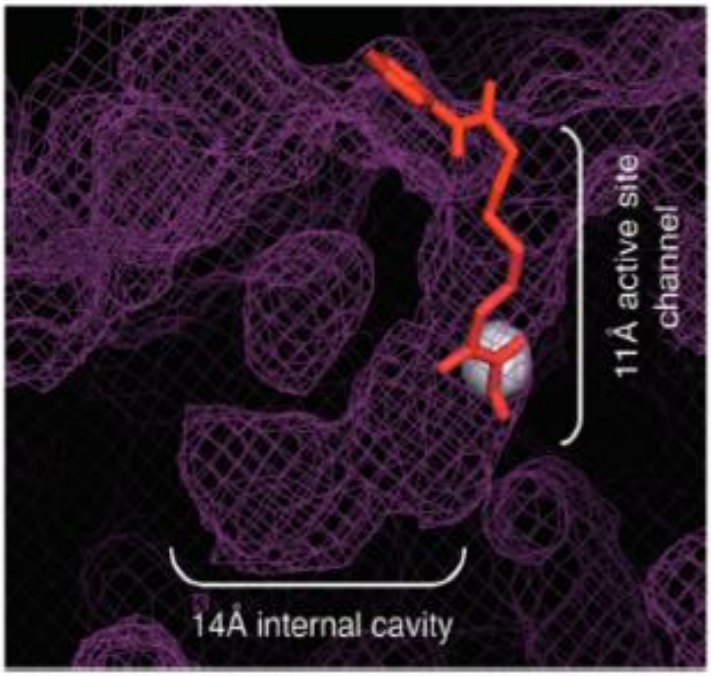


**Figure 1.5 – Crystal structure of HDAC1.** Vorinostat or SAHA (shown as ball and stick in red color) is docked into the crystal structure of HDAC1 (purple mesh; PDB-4BKX). The 11 Å active site channel and 14 Å internal cavity are labeled, where the Zn metal is shown as a grey sphere. Copyright permission was obtained from Wambua. M. K. *et al. J Med. Chem* 2014, 57 (37).

The first crystal structure of HDAC1 was resolved in 2013 with a resolution of 3.0 Å (29). HDAC1 was complexed with MTA1, a subunit of the NuRD corepressor complex. The structure revealed that inositol tetraphosphate [Ins-(1,4,5,6)-$P_4$] was sandwiched between the HDAC1 and MTA1 proteins. Another crystal structure of HDAC1:MTA1 was resolved in 2016 with 3.3 Å resolution (35). In this case, inositol-6-phosphate was sandwiched between HDAC1 and MTA1, and a novel peptide-based inhibitor derived from histone H4 was bound to the active site (Figure 1.6). The structure shed insights into the substrate recognition and allosteric regulation of HDAC activity. For example, the D99 residue at the surface of the active site undergoes a conformational change upon binding

to the inhibitor peptide. Structural information further suggests that inositol phosphates are conserved modules that regulate class I HDAC activity.

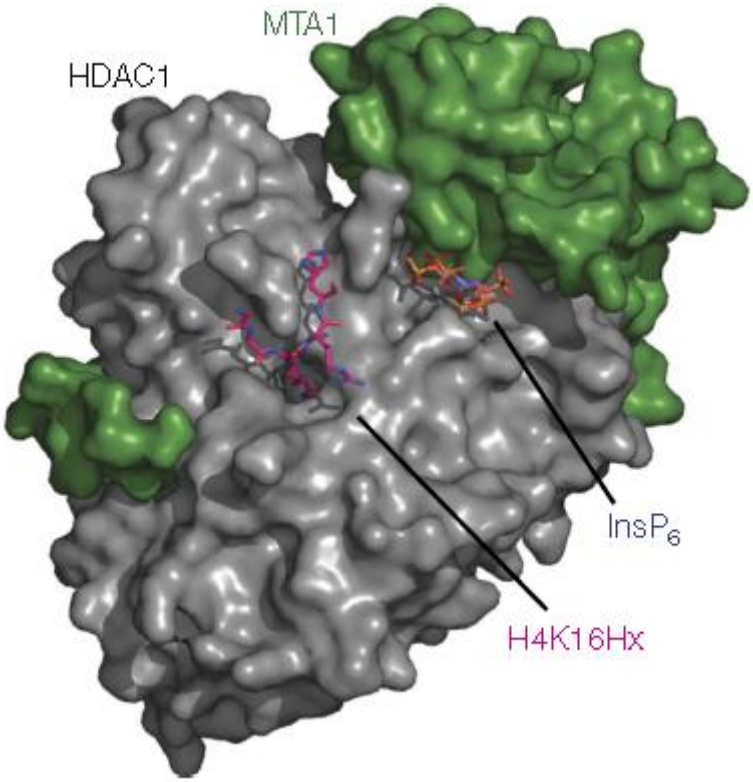


**Figure 1.6 – Crystal structure of HDAC1:MTA bound to the inhibitor peptide H4K16Hx and inositol hexaphosphate.** HDAC1 surface is shown in gray color and MTA1 corepressor is in green color. Inositol hexaphosphate (orange ball and stick) is sandwiched between HDAC1 and MTA1. Inhibitor peptide H4K16Hx (pink ball and stick) is bound to the 11 Å channel of HDAC1. Copyright permission was obtained from Watson P *et al. Nature communications*, 2016, 7 (35).

### 1.5.3 Mechanism of HDACs

Class I, II and IV HDACs share a similar mechanism and require a metal ion for catalytic activity (16) . Among the class I HDACs, the HDAC8 mechanism has been studied in the greatest detail (28,39). A general acid-base-mediated deacetylation

mechanism was reported in 2016 (40). Two catalytic dyads composed of His-Asp residues are involved in the mechanism of HDAC deacetylation. The active site of HDAC8 contains a Zn metal, a water molecule, Y306, and the two catalytic dyads: H142-D176 and H143-D183 (Figure 1.7). The Zn metal is coordinated by the oxygen atoms of water, D267, and D178 along with the backbone nitrogen from D267. The acetylated lysine in the substrate also interacts with the Zn metal and Y306 (Scheme 1.2B). H143 acts as the general base and abstracts a proton from the water to increase its nucleophilicity. The activated water then attacks the carbonyl carbon of the acetylated lysine in the substrate to form a tetrahedral intermediate. The oxyanion of the tetrahedral intermediate is stabilized by the Zn ion and Y306. The protonated H143 acts as a general acid and donates a proton to the amine of the substrate during hydrolysis of the amide bond, yielding lysine and the acetate byproduct. H142 remains protonated throughout the deacetylation reaction and serves as an electrostatic catalyst (Scheme 1.2C and D). The majority of the active site residues are conserved among HDAC isoforms. Class II HDACs, HDAC4, HDAC5 and HDAC7 contain histidine instead of Y306, which is consistent with the reduced enzymatic activity of class II HDACs compared to class I.

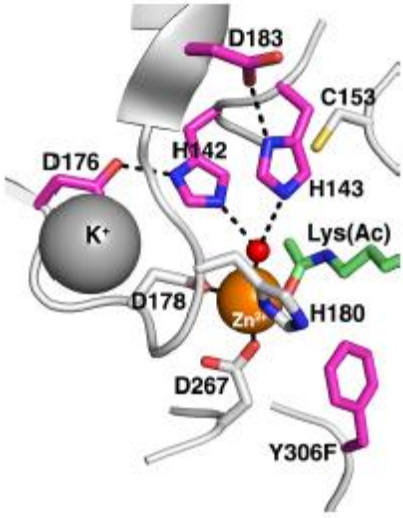


**Figure 1.7 – Active site residues of HDAC8 involved in catalysis.** $Zn^{2+}$ and $K^{+}$ metals are shown in orange and gray spheres, respectively. The oxygen atom of the water molecule is depicted as a red sphere. The $Zn^{2+}$ metal is flanked by D267, D178, and H180 whereas the oxygen of water is stabilized by the two His-Asp catalytic dyads made up of H142-D176 and H143-D183. Copyright permission was obtained from Lucy, S.M. *et al*. *Biochemistry,* 2016, 55 (40).

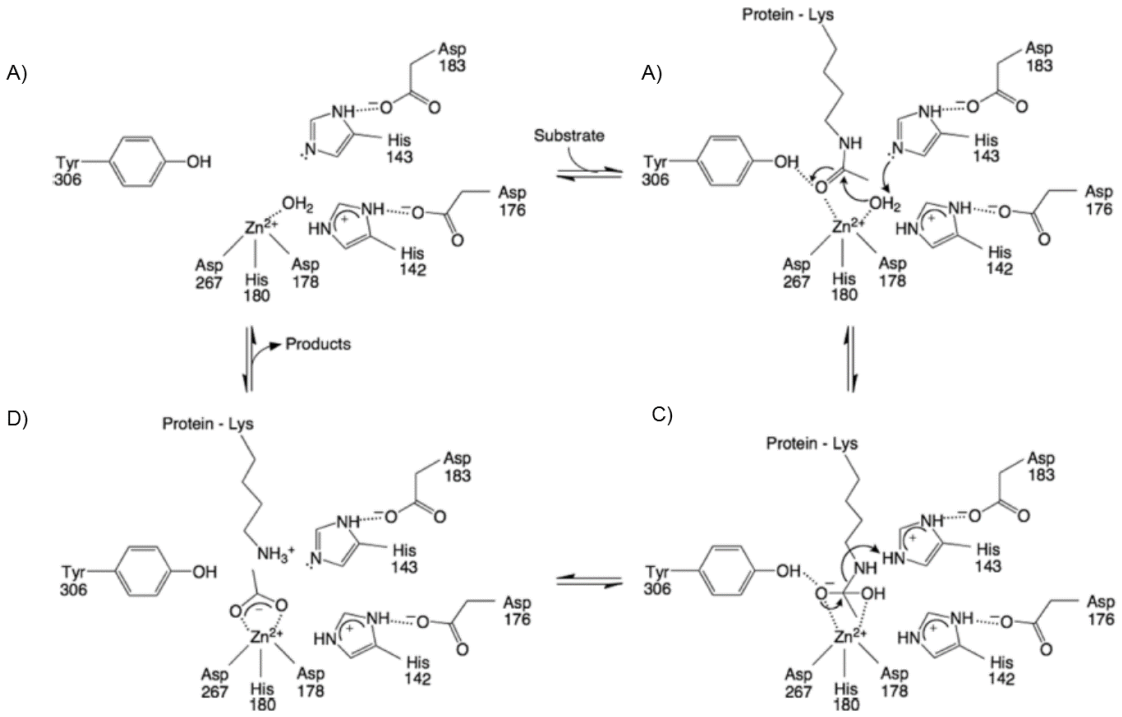


**Scheme 1.2 – The proposed catalytic mechanism of HDAC8.** A) Active site residues are shown prior to the entry of the substrate. B) The carbonyl oxygen of the acetyl lysine substrate interacts with the $Zn^{2+}$ metal and the hydroxyl group of Y306. H143 acts as the general base and activates water for the nucleophilic attack. Water attacks the carbonyl carbon to form the intermediate. C) The oxyanion intermediate is stabilized by hydrogen bonding to Y306 and the $Zn^{2+}$ metal. H143 acts as a general acid by donating a proton to form the acetic acid byproduct and substrate lysine. D) The substrate lysine abstracts a proton from the acetic acid to form protonated lysine and acetate byproduct. Upon exit of the products, the enzyme is ready for another round of catalysis. Copyright permission was obtained from Lucy, S.M. *et al*. *Biochemistry,* 2016, 55 (40).

### 1.5.4 HDAC associated complexes

HDAC proteins do not interact with the nucleosome directly. Instead, interacting proteins are required for physiological function and enzymatic activity (41). Previous studies have shown that associated proteins augment HDAC enzymatic activity. Class I HDAC proteins typically exist in multiprotein complexes (Figure 1.8) (42,43). For instance, HDAC1 and 2 are found in the Sin3, NuRD (Nucleosome Remodelling and Deacetylation) and CoREST (Corepressor for element 1-silencing transcription factor) complexes, whereas HDAC3 is found in the NCOR/SMRT (nuclear receptor co-repressor/silencing mediator of retinoid and thyroid receptor) complex. The corepressor complexes contain both DNA binding and histone binding subunits, which interact with the nucleosomes of the target genes and recruit HDACs to the promoter regions to deacetylate histones. These complexes possess different functions. Mi2 in the NuRD complex exhibits helicase activity to remodel chromatin and facilitate deacetylation by HDACs. Lysine specific demethylase1 (LSD1) in the CoREST complex demethylates histones to further condense chromatin. In this case, the combinatorial effect of deacetylation and demethylation represses gene transcription.

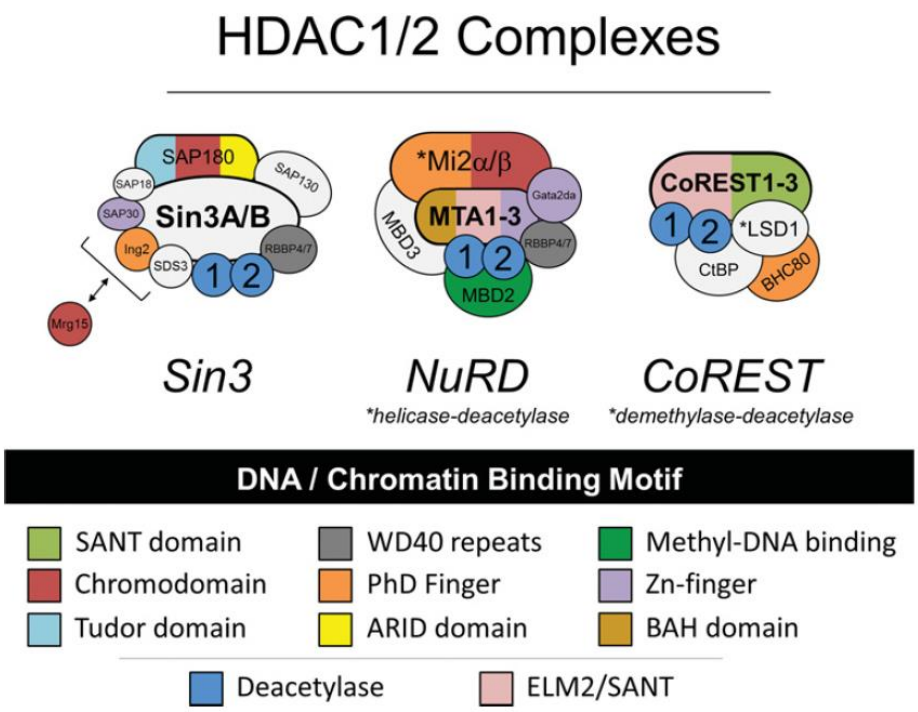


**Figure 1.8 – Multi protein complexes associated with HDAC1 and HDAC2.** Each complex contains multiple subunits. The function of each subunit is color coded and labeled. The subunit involved in binding to HDAC1 and HDAC2 is marked in bold letters- Sin3A/B, MTA 1-3, CoREST 1-3. Copyright permission was obtained from Kelly R.D. *et al., Biochem Society Transactions*, 2013, 41 (43).

### 1.6 HDAC functions and Cancer

HDAC proteins play important roles in a variety of cellular processes, such as proliferation, differentiation, cell cycle arrest and apoptosis. (Figure 1.9) (44). HDAC proteins repress genes involved in cell cycle progression by deacetylation of histone proteins. For example, HDAC decreases the expression of important tumor suppressor proteins, such as p53 and p21, which are crucial for cell cycle regulation (45). p53 is a transcription factor that mediates cell cycle arrest and apoptosis via binding to the promoter region of important cell cycle regulator genes, including p21 and p27. Both p21

and p27 block cell proliferation by inhibiting cyclin-dependent kinases (CDKs). HDAC1-deficient embryonic stem cells show high levels of p21 and p27 expression, suggesting HDAC proteins play a key role in cell cycle regulation (46). p21 and p27 expression also increased upon HDAC inhibitor treatment, leading to cell cycle arrest, differentiation and apoptosis. This topic will be discussed further in section 1.7.

The unregulated activities of HDAC proteins are associated with a variety of diseases, such as asthma, arthritis, schizophrenia, and cancer (15). HDACs are overexpressed in multiple cancer types. Previous studies have reported the overexpression of HDAC1, 2 and 3 in gastric, colorectal, and renal cell carcinoma (47). HDAC3 and HDAC6 are upregulated in colon and breast cancer (48,49). Overexpression of HDAC1-3 and HDAC8 is implicated in prostate cancer (50) . HDAC8 overexpression is associated with childhood neuroblastoma and promotes disease progression (51). Knockdown of HDAC8 in neuroblastoma cells lead to inhibition of cell growth and induction of cell cycle arrest. A truncating mutation of HDAC2 leads to loss of function in human epithelial cancers harboring microsatellite instability (52). In a panel of mesenchymal tumors, HDAC2 was overexpressed compared to HDAC1 (53). Knockdown of HDAC1, 2 and 3 in multiple cancer cell lines resulted in an inhibition of cell proliferation (47,54). Knockdown of HDAC1 in liver cancer cells inhibited cell growth, induced apoptosis, and increased the expression of p21 and p27 genes (55).

Class II HDACs are also upregulated in multiple cancer types (56). For instance, HDAC7 and HDAC9 are overexpressed in pancreatic and cervical cancer, respectively. Overexpression of HDAC6 is also found in several cancers (57). Given the involvement

of HDAC proteins in disease formation, they have emerged as important therapeutic targets for drug development.

**1.7 HDAC inhibitors as anti-cancer therapeutics**

Many HDAC inhibitors are in clinical trials as anti-cancer drugs (44). Currently, four HDAC inhibitors have been approved by the FDA as cancer therapeutics (Scheme 1.3). Vorinostat (SAHA, Suberoyl Anilide Hydroxamic Acid, Zolinza®) and romidepsin (Depsipeptide, FK-228, Istodax®) are approved for the treatment of cutaneous T-cell lymphoma, whereas belinostat (PXD101, Beleodaq®) and panabinostat (LBH-589, Farydak®) are approved to treat peripheral T-cell lymphoma and multiple myeloma, respectively (58-61). Importantly, HDAC inhibitors cause cell cycle progression defects and apoptosis in cancer cells (62), suggesting that HDAC activity is critical for cell growth. As a consequence, HDAC inhibitor mechanism of action is thought to involve in anti-cancer drugs. HDAC inhibitor-induced cell cycle arrest has been primarily attributed to the expression of the p21 (waf1/cip1) and p27 (kip1) proteins after histone hyperacetylation and transcriptional upregulation. All four FDA approved HDAC inhibitors are pan HDAC inhibitors.

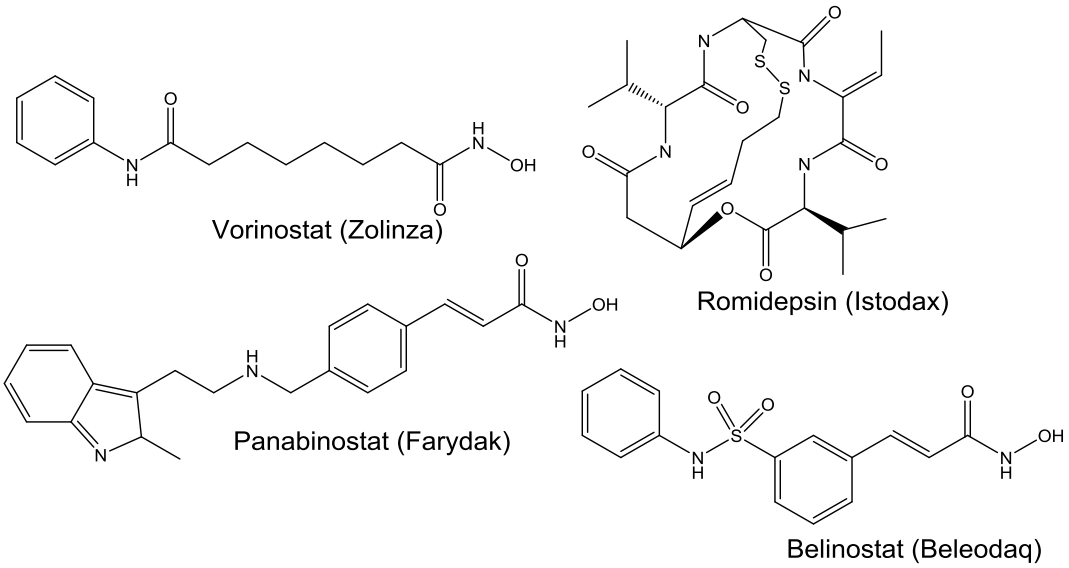


**Scheme 1.3 – Chemical structures of the HDAC inhibitors approved by FDA.**

Pan HDAC inhibitors affect all or most metal-dependent HDAC isoforms due to the high similarity between active sites (63). A disadvantage associated with pan inhibitors is that they exhibit side effects such as fatigue, nausea and vomiting. But the pan inhibitors are useful in studying the function of all HDAC proteins in the cell. On the other hand, selective inhibitors are needed to target specific HDACs deregulated in various types of cancer. Highly selective HDAC3, HDAC6, and HDAC8 inhibitors have been reported (64-66). Unfortunately, a strictly HDAC1 selective inhibitor is not currently available. Development of selective inhibitors will assist in deciphering the role of individual HDACs in the cell as well as discovering novel substrates of HDAC isoforms.

**1.8 Non-histone substrates of HDACs**

Identifying novel substrates is an effective way to reveal new functions of any enzyme. Histones are widely considered as predominant substrates of HDACs (67). The role of HDAC1 in transcriptional regulation has been well characterized through changes in histone acetylation. As discussed earlier, the anti-cancer activities of HDAC inhibitors

are widely thought to result from the altered gene expression due to histone acetylation (62). However, HDAC inhibitor-mediated cell cycle arrest, particularly mitotic arrest, does not always correlate with changes in histone acetylation or protein expression (57,68), suggesting that non-histone proteins may play a role in HDAC inhibitor anti-cancer activity.

Beyond histones, the large and growing list of acetylated proteins (69) implicates non-histones proteins as substrates of HDAC enzymes. Multiple acetylated proteins are present in the cell, including transcription factors, chaperones, structural proteins, DNA repair enzymes, and viral proteins (Figure 1.9) (70). Given that acetylation can regulate protein activity, stability, and interactions (70), identifying novel substrates will reveal the full spectrum of HDAC functions in the cell. In fact several non-histone substrates have been identified for HDAC6 and HDAC8 (Table 1.1) (44,71-73).

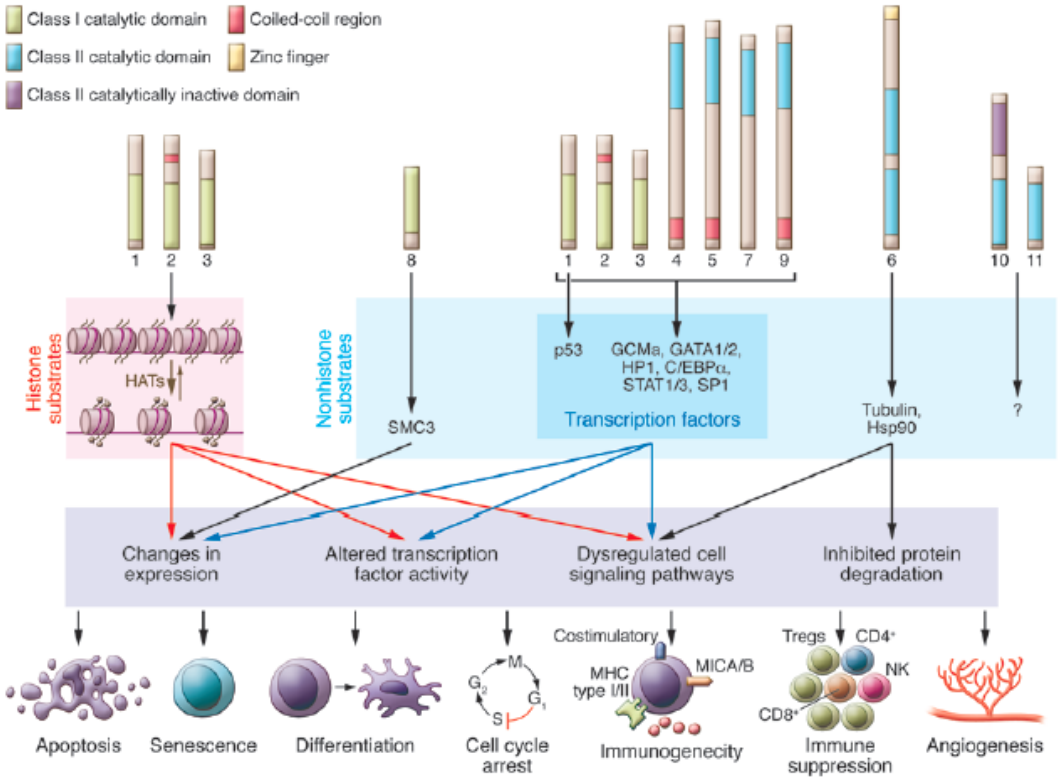


**Figure 1.9 – Key processes regulated by HDACs.** HDACs mediate multiple key processes by deacetylating both histone and non-histone substrates. Apart from histones, HDAC deacetylates several non-histone substrates such as tubulin, HSP90 and p53. As a consequence, HDAC mediates key processes including apoptosis, differentiation and cell cycle arrest. Copyright permission was obtained from West, A. *et al*. *J of Clini. Invest.*, 2014,124, (44).

**Table 1.1 – Non-histone substrates of HDAC1, HDAC6 and HDAC8.**

| HDAC1 | HDAC6 | HDAC8 |
|---|---|---|
| p53 (73) | α-tubulin (74) | p53 (75) |
| E2F1 (76) | HSP90 (77,78) | SMC3 (79) |
| | Cortactin (80) | ERRα (81) |
| | Tat (82) | ARID1A (69) |
| | Ku70 (83) | Cortactin (84) |
| | β-catenin (85) | Inv(16) fusion protein (86) |
| | Peroxiredoxins (87) | RAI1 (69) |
| | Survivin (88) | THRAP3 (69) |
| | p38 (MAPK) (89) | ZRANB2 (69) |
| | MSH2 (90) | NCOA3 (69) |
| | HSPA5 (91) | |
| | GRP78 (92) | |
| | MST1 (93) | |
| | RIG1 (94) | |
| | HMGN2 (95) | |

HDAC6 is a cytoplasmic deacetylase, suggesting the nucleosomal histones located in the nucleus are not their main substrate. Multiple non-histone substrates have been identified for HDAC6. α-Tubulin is a cytoskeletal protein that exists in stable or dynamic microtubule states (74). Dynamic microtubules contain low levels of acetylation compared to stable microtubules. HDAC6 deacetylates α-tubulin and promotes depolymerization of microtubules to augment cell motility. Hsp-90 is another known substrate of HDAC6 (75,76). Hsp-90 is a molecular chaperone involved in protein folding. Acetylation of Hsp90 inhibits its chaperone function, hence affect correct folding of proteins. For instance, HDAC6 deacetylates Hsp90 and promotes its chaperone function.

Identifying α-tubulin and Hsp90 as non-histone substrates of HDAC6 revealed new functions for HDAC6 in cell migration and protein folding.

However, only a few validated substrates of HDAC1 have been reported, including p53 and E2F1 (77,78). Acetylation of p53 enhances its stability and DNA binding ability. HDAC1-mediated deacetylation reduces the stability and activity of p53. Overexpression of HDAC1 is implicated in many diseases, which could be partly explained by the inactivation of the impotant tumor suppresor p53 by HDAC1-mediated deacetylation. The second known non-histone substrate of HDAC1 is E2F1. E2F1 is a transcription factor involved in cell cycle regulation. E2F1 undergoes acetylation upon dissociation from retinoblastoma (Rb) protein. Acetylation enhances its activity and DNA binding ability. Rb bound HDAC1 was responsible for E2F1 deacetylation. Substrate identification is an effective tool to fully understand the function of HDAC1 in normal and disease settings. New methods are needed to discover non-histone substrates to broaden our understanding of HDAC function and assist in deciphering the HDAC inhibitor mechanism of action.

**1.9 Available methods for substrate identification**

Few methods are available for HDAC substrate identification. For example, proteomic analysis after treatment with isoform-selective HDAC inhibitors has been effective to identify possible substrates of HDAC6 and HDAC8 (44,71). In the case of HDAC8, MCF7 cells were treated with or without HDAC8 selective inhibitor-PCI-34051 for 24h in media containing stable isotope labeled amino acids (Figure 1.10). After lysis and trypsin digestion, acetylated proteins were immunoprecipitated and subjected to quantitative LC-MS/MS analysis to compare global changes in acetylation. Five hits were

identified (SMC3, RAI1, ZRANB2, NCOA3 and THRAP3) as possible substrates of HDAC8. These five candidate proteins were validated as substrates using peptide deacetylation assays. Selective inhibitor treatment combined with MS analysis served as a versatile method to identify substrates of HDAC8.

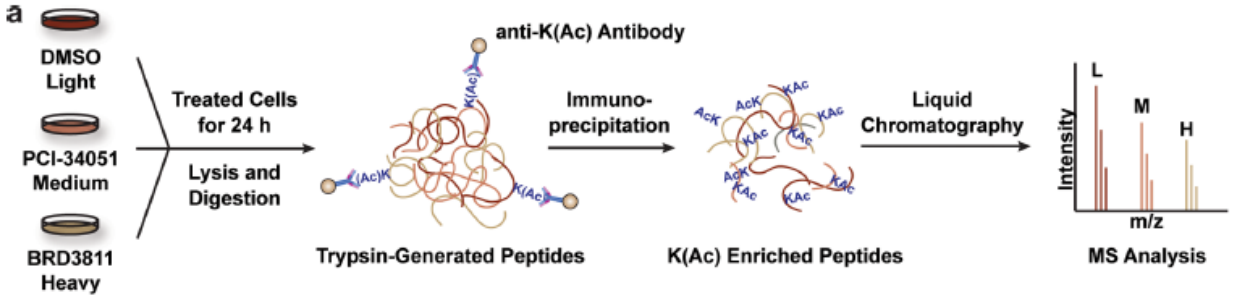


**Figure 1.10 – Work flow for the HDAC8 substrate identification strategy.** Cell were grown in heavy, medium and light isotope containing media and treated with or without HDAC8 selective inhibitor for 24 h. Cells were lysed, digested with trypsin and immunoprecipitated with acetyl lysine antibody to enrich acetylated peptides, which was then analysed by MS. Copyright permission was obtained from Olson D.E *et al. ACS Chem Biol*, 2014, 9. (44).

Multiple HDAC inhibitors have been used in a large scale quantitative proteomic study to study acetylation site specificity *in cellulo (71)*. HeLa cells were treated with pan HDAC inhibitors, Class I selective HDAC inhibitors, sirtuin inhibitors, and HDAC6 and HDAC8 selective inhibitors; and the global changes in acetylation were analysed using SILAC based LC-MS/MS. More than 8000 acetylation sites were dynamically changed upon inhibitor treatment. Most of the HDAC inhibitors affected only a small fraction of the targets suggesting they have distinct set of substrates. Selective inhibitor treatment coupled to MS is a high throughput method to study lysine acetylation regulated by

multiple HDACs in the cell. The method also proves the value of developing selective inhibitors to understand the function of individual HDAC in the cell.

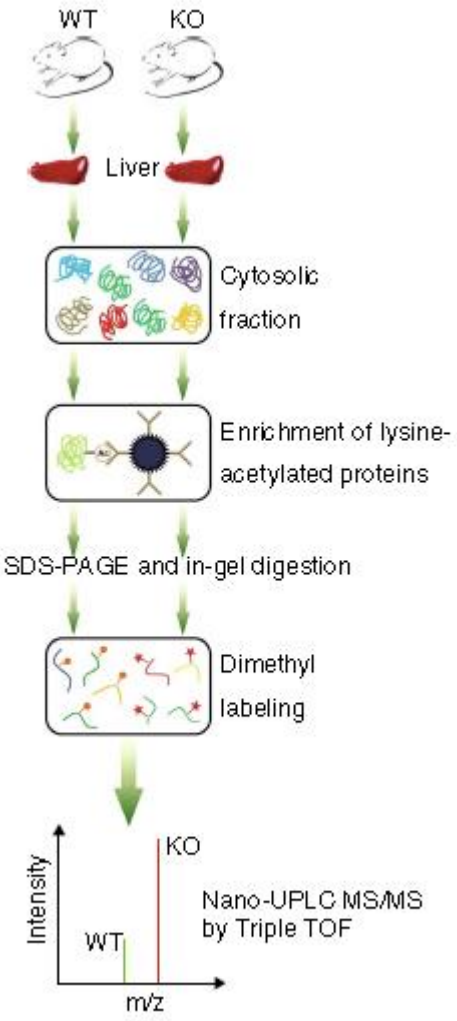


**Figure 1.11 – Workflow for the HDAC6 substrate identification method.** Copyright permission was obtained from Zhang L. *et al*. *Protein & cell*, 2015, 6 (72).

HDAC6 knockout mice have also been used to identify novel substrates of HDAC6 (72). The acetylated proteins of wild type or HDAC6 knockout mice cells from liver tissue were immunoprecipitated with a pan acetyl-lysine antibody, digested with trypsin, followed by dimethyl labeling and quantitative mass spectrometry to identify HDAC6 substrates

(Figure 1.11). The method identified 107 acetylated proteins in the HDAC6 knockout mice compared to wild type. Among these, three hits (MYH9, Hsc70 and DNAJA1) were thorougly validated as cellular substrates of HDAC6.

Unfortunately, HDAC1 substrate identification has been hampered by limitations in these available methods. For example, genetic and pharmacological methods have been ineffective with HDAC1. One reason is the ability of HDAC2 to compensate in the absence of HDAC1, which makes genetic knockdown methods unreliable. The second reason is the lack of HDAC1-selective inhibitors, which makes the mass spectrometric based methods unavailable. Given the steadily growing list of acetylated proteins, HDAC1 is likely to have multiple non-histone substrates. New strategies to identify HDAC1 substrates are needed to characterize the full biological activiites of HDAC1 in physiological as well as pathological conditions.

**1.10 Prior work in the Pflum lab**

To develop a new method to identify HDAC1 substrates, we took advantage of the many mutants generated in the Pflum lab. Previous work in the Pflum lab focused on characterizing the residues in both the 11 Å and 14 Å cavity in HDAC1 (37,38). Acetylated substrates or HDAC inhibitors were known to bind through the 11 Å active site channel (Figure 1.12). Alanine scanning mutagenesis of H28, P29, D99, G149, F150, Y204, F205 and L271 located in the 11 Å active site channel, showed significant reduction in deacetylase activity (Figure 1.13) (38). Reduced activity of the mutants suggests that the residues are important for maintaining enzymatic activity. Among these residues, F150 and F205 were shown to be critical for maintaining the 11 Å active site conformation. The data also showed that F150, which is highly conserved among all the HDAC isoforms

(Figure 1.12B), is critical to maintain HDAC activity. Kinetic characterization of the F150A mutant indicated that the reduced activity of F150A was not due to loss of substrate binding. These studies shed insight towards the role of 11 Å residues in substrate and inhibitor binding.

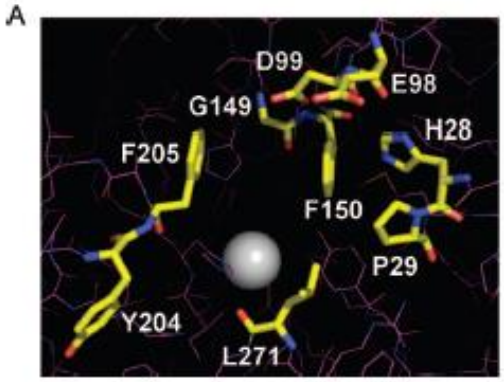


B

| | H28 P29 | E98 D99 | G149 F150 | Y204 F205 | L271 |
|---|---|---|---|---|---|
| HDAC1 | HP | ED | GF | YF | L |
| HDAC2 | HP | ED | GF | YF | L |
| HDAC3 | HP | DD | GF | FF | L |
| HDAC4 | HP | SD | GF | FF | L |
| HDAC5 | HP | SD | GF | FF | V |
| HDAC6a | FP | YD | GY | FW | A |
| HDAC6b | HP | FD | GF | FF | V |
| HDAC7 | HP | TD | GF | FF | V |
| HDAC8 | LA | YD | GF | FF | M |
| HDAC9 | HP | SD | GF | FF | V |
| HDAC10 | EI | FD | GF | FW | A |
| HDAC11 | HP | PN | GF | TY | I |

**Figure 1.12 – Residues in the 11 Å active site of HDAC1**. A) Amino acids lining the substrate binding cavity of HDAC1 homology model. Zn metal is shown as a gray sphere. B) Sequence alignment of metal dependent HDACs. Less conserved residues are highlighted in red. Copyright permission was obtained from Weerasinghe, S.V. *et al, J. Med. Chem., 2008, 51.* (38).

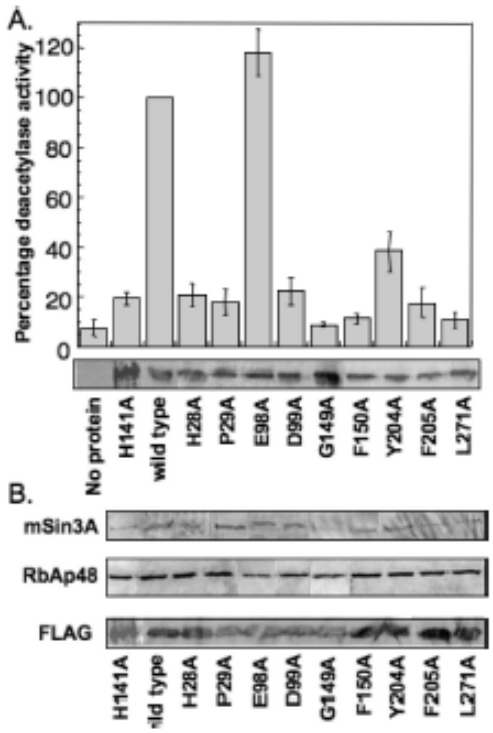


**Figure 1.13 – Residues in the 11 Å active site channel are important for HDAC1 deacetylase activity.** A) Wild type or mutant HDAC proteins were expressed in Jurkat cells, immunoprecipitated using anti-FLAG agarose beads and tested in deacetylation assay and SDS-PAGE analysis. B) Association of immunoprecipitated HDAC1 with mSin3A and RbAp48 was also analyzed. Copyright permission was obtained from Weerasinghe, S.V. *et al, J. Med. Chem., 2008, 51* (38).

Previous work also focused on studying the role of residues lining the 14 Å internal cavity using alanine scan mutagenesis (Figure 1.14) (37). Based on speculations from computational and biochemical studies, the acetate byproduct of deacetylation was believed to exit through the 14 Å cavity. The, polar and charged residues Y23, Y24, R36 and C151 were mutated to study their effects on enzymatic activity and acetate binding (Figure 1.15). All four mutants displayed reduced activity and affected acetate binding. The data is consistent with the hypothesis that the 14 Å internal cavity residues are

involved in stabilizing the acetate byproduct. Both the F150A and C151A mutants will be discussed in great detail in Chapter 2 section 2.2.

A.

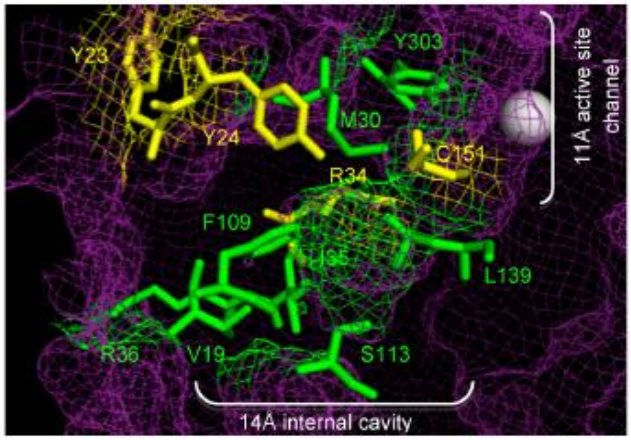


B.

| | V19 | Y23 | Y24 | M30 | R34 | I35 | R36 | F109 | S113 | L139 | C151 | Y303 |
|---|---|---|---|---|---|---|---|---|---|---|---|---|
| HDAC1 | V | Y | Y | M | R | I | R | F | S | L | C | Y |
| HDAC2 | I | Y | Y | M | R | I | R | F | S | L | C | Y |
| HDAC3 | V | H | Y | M | R | L | A | F | Y | L | C | Y |
| HDAC4 | K | T | C | E | R | I | Q | A | A | G | C | H |
| HDAC5 | K | M | C | E | R | I | Q | A | A | G | C | H |
| HDAC6a | E | L | W | E | R | L | H | C | A | G | C | Y |
| HDAC6b | N | L | W | E | R | I | L | C | A | G | C | Y |
| HDAC7 | K | S | C | E | R | I | Q | A | A | G | C | H |
| HDAC8 | P | S | M | K | R | A | S | Y | I | W | C | Y |
| HDAC9 | K | V | C | E | R | I | Q | A | A | G | C | H |
| HDAC10 | A | L | W | E | R | L | T | C | A | G | C | Y |
| HDAC11 | Y | F | M | F | K | W | G | L | T | F | C | Y |

**Figure 1.14 – Residues in the 14 Å internal cavity of HDAC1**. A) Amino acids lining the internal cavity of HDAC1 crystal structure (4BKX). The Zn metal is shown as a gray sphere. B) Sequence alignment of metal dependent HDACs. Less conserved residues are highlighted in red. Copyright permission was obtained from Wambua, M. K. *et al. J. Med. Chem.,* 2014, 57. (37).

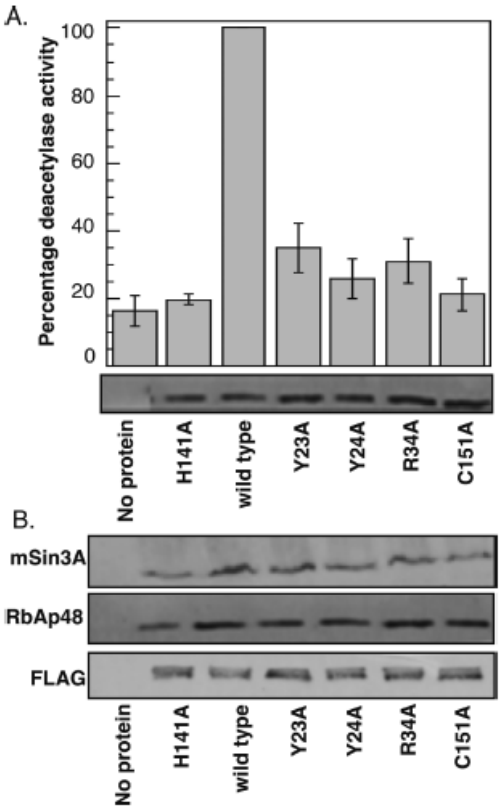


**Figure 1.15 – Residues in the 14 Å internal cavity affect HDAC1 deacetylase activity.** A) Wild type or mutant HDAC proteins were expressed in Jurkat cells, immunoprecipitated using anti-FLAG agarose beads and subjected to deacetylation assays and SDS-PAGE analysis. B) Association of immunoprecipitated HDAC1 with mSin3A and RbAp48 was also analyzed. Copyright permission was obtained from Wambua, M. K. *et al. J. Med. Chem.,* 2014, 57 (37).

### 1.11 Dissertation work

To fully characterize the function of HDAC1, new methods are needed to identify cellular substrates. While some non-histone substrates have been identified (Table 1.1), the list of verified HDAC substrates remains considerably shorter than the long list of acetylated proteins. Understanding the biological function of individual HDAC proteins has been hampered by the lack of systemic tools for substrate discovery. **The long term**

**goal of this project is to develop a simple tool to discover and validate substrates of HDAC proteins, which will lead to a detailed understanding of HDAC related biology in normal and disease settings**.

We employed a substrate trapping strategy to identify novel substrates of HDAC1. In the trapping strategy, catalytically active wild type enzyme binds to substrates transiently, whereas inactive mutants bind more stably. In prior work, more than seventy inactive mutants were generated to study the structure and function of HDAC1 (37,38). The majority of these mutants were inactive, making them possible substrate traps. We selected few conserved residues from three different regions for trapping studies. Studies showed that these mutants act as potential substrate traps by identifying Eg5/Kinesin5 as a HDAC substrate from Jurkat cells (Chapter 2). Eg5 also colocalized with HDAC1 during the prophase of mitosis, which reveals a previously unknown role for HDAC1 in cell cycle regulation.

We next successfully extended the trapping strategy to the HEK293 cell line (Chapter 3) and established that trapping is applicable to other cell lines as well. A few new substrates were identified, and LSD1 was further characterized as a HDAC1 substrate using secondary experiments. HDAC1 regulated the acetylation of LSD1, altered histone H3 substrate binding, and affected gene repression by LSD1. This study uncovered a novel mechanism of HDAC inhibitor-mediated derepression of target genes through LSD1. This work highlights the importance of identifying non-histone substrates to understand the full activity of HDAC1 in physiological and pathological conditions, which will assist in deciphering the HDAC inhibitor mechanism of action.

The fourth chapter of this dissertation describes a study related to the effect of HDAC1 single nucleotide polymorphisms (SNP) on expression, activity, and post translational regulation. Although the aberrant activities of HDACs are implicated in many cancers, the mechanism leading to HDAC deregulation is not very well studied. **The goal of this project was to understand the link between SNPs and HDAC associated carcinogenesis.** The unregulated expression of multiple genes related to cancer are linked to the presence of a SNP. Cancer-related HDAC SNPs have been used as biomarkers to predict disease susceptibility and drug sensitivity. Based on the involvement of HDAC1 in cancer, we hypothesized that an exonic SNP of HDAC1 identified in collaboration with the Cisneros lab could affect expression, activity, and post-translational modifications. We performed a mutational analysis of non-synonymous HDAC1 exonic SNP-F437C to understand the HDAC1-related carcinogenesis. These studies shed light on the molecular mechanism leading to HDAC deregulation and cancer onset, which may enable the creation of new diagnostics and cancer treatment options.

# CHAPTER 2. IDENTIFICATION OF EG5 AS A HDAC1 SUBSTRATE USING TRAPPING MUTANTS

(Portions of the text in this chapter are adapted from Nalawansha, D. A. *et al*. 2016, Cell Chemical Biology, *in revision*)

## 2.1 INTRODUCTION

Substrate identification is an effective means of uncovering the functions of any enzyme. In the case of HDAC1, histones are widely considered its predominant substrates (67). By studying histone acetylation, the role of HDAC1 in transcriptional regulation has been characterized. In fact, the anti-cancer activities of HDAC inhibitors are widely thought to result from the altered gene expression due to histone acetylation (62). However, HDAC inhibitor-mediated cell cycle arrest, particularly mitotic arrest, does not always correlate with changes in histone acetylation or protein expression (57,68), suggesting that non-histone proteins may play a role in HDAC inhibitor anti-cancer activity. Outside of histones, only a few additional validated substrates of HDAC1 have been reported, including p53 and E2F1 (20,79). Yet, a wide variety of acetylated proteins have been identified in proteomic analyses (69,80), suggesting that many acetylated non-histone substrates are present in the cell.

Unfortunately, identification of non-histone substrates of HDAC1 has been largely serendipitous because facile methods to systematically discover cellular targets are lacking. For example, proteomic analysis after treatement with isoform-selective HDAC inhibitors has been effective to identify possible substrates of HDAC6 and HDAC8 (44,71). However, no strictly HDAC1-selective inhibitor is known, making HDAC1 substrate identification challenging. To fully characterize the function of HDAC1 and the

anti-cancer activities of drugs targeting HDAC1, new methods are needed to identify cellular substrates.

Substrate trapping is a method used widely to identify the substrates of protein tyrosine phosphatases using catalytically inactive mutants (20,41,81-84). Two commonly used trapping mutants of protein tyrosine phosphatase 1B (PTP1B) were created by mutating a nucleophilic residue in the active site (C215S) or a residue that acts as a general acid (D181A) during catalysis (41). These mutants were characterized as substrate trapping mutants because they displayed a 500 to 100,000-fold reduction in catalytic efficiency, while exhibiting similar substrate binding properties as the wild type enzyme. The C/S and D/A double mutant also displayed efficient substrate trapping properties (85). Mutation of these catalytic amino acids produced inactive enzymes that were used to purify novel substrates. Given the success with phosphatases, we extended the trapping strategy to HDAC1 with the aim of identifying physiological substrates.

## 2.2 RESULTS

### 2.2.1 HDAC1 substrate trapping strategy

Inactive mutants can bind substrates more stably than the wild type protein, allowing the purification of typically transiently bound substrates (Figure 2.1A and 2.1B). The crystal structure of HDAC1 revealed that the active site has a deep, narrow 11 Å channel and a 14 Å internal cavity (Figure 2.1C) (29). Previously, residues in the 11 Å and 14 Å channels of HDAC1 were mutated to alanine to study structure and function (37,38). The majority of these mutants were catalytically inactive, making them potential substrate traps. Among these mutants, we chose three (H141A, F150A and C151A) where the mutated residues are located in the various active site regions (Figure 2.1C)

and conserved among the HDAC family. H141 acts as a general base during catalysis (67). F150 lies within the 11 Å channel active site near the substrate binding region (86,87). C151 is present in the 14 Å internal cavity and is involved in acetate byproduct escape during deacetylation (37). Thus, these three mutants are inactive by different mechanisms and may offer differing abilities to trap substrates.

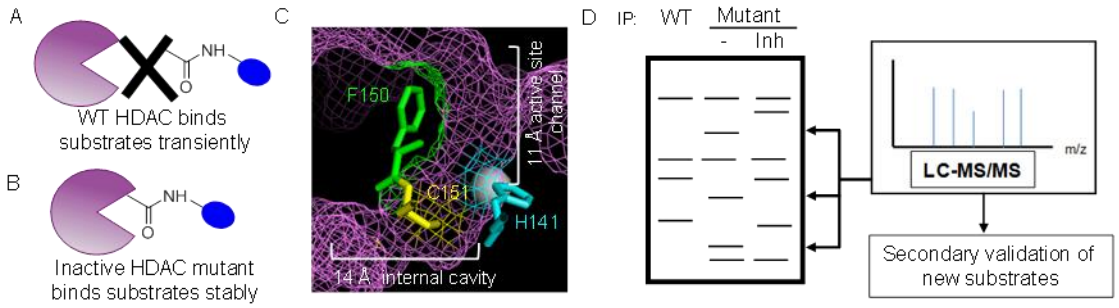


**Figure 2.1 - The Substrate Trapping Strategy.** (A) Catalytically active wild type (WT) HDAC enzyme binds substrates transiently. (B) Inactive HDAC mutant enzyme binds substrates more stably, which allows trapped substrates to be isolated by immunoprecipitation. (C) Amino acid residues that were mutated in this study are shown as ball and stick structures in the HDAC1 crystal structure (shown as purple mesh, PBD: 4BKX). The metal ion required for catalysis is shown as a gray sphere. D) Workflow for the substrate trapping study with initial gel analysis of wild type and mutant HDAC1 immunoprecipitates to identify candidate protein bands. An HDAC inhibitor (Inh) was included in a control immunoprecipitate to distinguish associated proteins from substrates by competing for active site binding. Candidate proteins present in only the mutant immunoprecipitate were excised from the gel and identified by liquid chromatography-tandem mass spectrometry (LC-MS/MS). Substrates were then confirmed using a series of secondary experiments.

### 2.2.2 Substrate trapping with inactive HDAC1 mutants to identify candidate substrates

Substrate trapping was performed with three inactive mutants of HDAC1 (H141A, F150A and C151A) to identify new substrates. Wild type or mutant HDAC1-FLAG proteins were overexpressed and immunoprecipitated in the absence or presence of competitive active site inhibitor, SAHA. This active site inhibitor provided a helpful control by distinguishing substrates bound to the active site from associated proteins bound to HDAC1 via interactions outside of the active site. Bound proteins were separated by SDS-PAGE and visualized with Sypro ruby total protein stain. Proteins present in the mutant but not wild type or SAHA treated immunoprecipitates were putative new substrates (Figure 2.1D), which were identified using liquid chromatography-tandem mass spectrometry (LC-MS/MS) analysis.

All mutants were able to immunoprecipitate histones (Figure 2.2B, lanes 2-4 or Figure A2.1B) and other proteins (Figure 2.2A and B, lanes 2-4 or Figure A2.1A, p45, p95 and p130), consistent with their substrate trapping abilities. The immunoprecipitation of histones and several protein bands (p45, p95 and p130) were decreased upon SAHA treatment (Figure 2.2A and 2.2B or Figure A2.1A and A2.1B, compare lanes 2-4 to lanes 6-8), suggesting that these new proteins interact directly with the active site of HDAC1 and could be substrates. The data further confirm that inactive HDAC1 mutants display substrate trapping abilities appropriate for substrate identification.

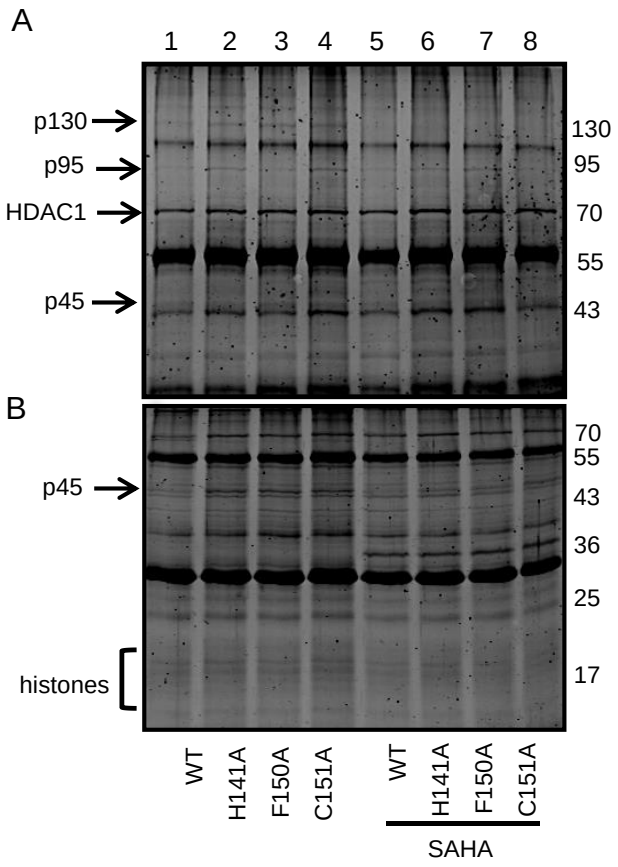


**Figure 2.2 - Substrate trapping by HDAC1 mutants.** Wild type (WT) and mutant HDAC1 (indicated below each lane) were expressed as Flag-tagged proteins in T-Ag Jurkat cells, immunoprecipitated with anti-Flag agarose, separated by 12% (A) or 16 % (B) SDS-PAGE, and visualized with SyproRuby total protein stain. Arrows indicate immunoprecipitated HDAC1 or possible substrates (p130, p95, p45, or histones) observed in the absence but not presence of competitive active site inhibitor SAHA (0.8 mM). Repetitive trials are shown in Figure A2.1.

To identify the proteins interacting with the HDAC1 trapping mutants in a SAHA-dependent manner, gel bands were excised, trypsin digested, and subjected to LC-MS/MS analysis. With high confidence, p45 and p130 were identified as γ-actin and Eg5 (also known as Kinesin like protein 11, KIF11), respectively (Table 2.1 and Figures A.2.2-

A.2.5). The protein corresponding to p95 was not identified with high confidence by MS analysis. Prior work reported that HDAC1 interacts with filamentous actin (F-actin), which comprises γ-actin, during mitosis (88). However, a connection between Eg5 and HDAC1 had not been documented previously. Peptides corresponding to Eg5 were observed in all three mutant pull downs, but not in wild type (Table 2.1). Eg5 plays an important role in protein transport and formation of the bipolar spindle during the prophase of mitosis (89). Mitotic defects leading to apoptosis are associated with the anti-cancer activities of HDAC inhibitor drugs (57,68,90-92), although the mechanism accounting for mitotic arrest is poorly understood. To possibly gain insight into HDAC inhibitor drug action, Eg5 was further studied as an HDAC1 substrate.

**Table 2.1 - Proteins identified after trapping by mass spectrometry (MS)**

| Protein band | Protein name (Accession) | MW (kDa) | Sample | Unique peptide count[a] | Unique spectral Count[b] | % Coverage[c] |
|---|---|---|---|---|---|---|
| p130 | Kinesin like protein 11(KIF11)/Eg5 (KIF11_HUMAN) | 120 | HDAC1 (WT) | ND[d] | ND[d] | ND[d] |
| | | | H141A | 1 | 1 | 1 |
| | | | F150A | 2 | 2 | 3 |
| | | | C151A | 2 | 2 | 2 |
| p45 | Actin cytoplasmic 2 (ACTG_HUMAN) | 42 | HDAC1 (WT) | 8 | 11 | 32 |
| | | | H141A | 11 | 15 | 49 |
| | | | F150A | 5 | 7 | 29 |
| | | | C151A | ND[d] | ND[d] | ND[d] |

[a] **Unique Peptide count -** Number of different amino acid sequences that are associated with a protein. [b] **Unique Spectral count –** Number of unique spectra that identified each unique peptide including modifications. [c]% Coverage – the percentage of the protein amino acid sequence that was identified. [d] ND- Not Detected (No peptide ID observed by MS analysis after immunoprecipitation with the indicated HDAC1 protein). The data are shown from one trial.

### 2.2.3 Co-immunoprecipitation of HDAC1 and Eg5

To confirm that p130 is Eg5 in the trapping experiment, immunoblotting was performed with an Eg5 antibody after trapping. Wild type and C151A mutant HDAC1 immunoprecipitated Eg5 in a SAHA-dependent manner (Figure 2.3A, top gel, compare lanes 2 and 3 to lane 4, Figure A2.6A), consistent with the MS characterization of p130 as Eg5. In addition, Eg5 acetylation was elevated in immunoprecipitates with the inactive C151A mutant compared to wild type (Figure 2.3A, middle gel, compare lane 3 to 2),

suggesting that Eg5 is a cellular substrate of HDAC1. The elevated levels of acetylation with the mutant also indicate stable binding between acetylated Eg5 and C151A HDAC1, consistent with earlier substrate trapping studies (Figure 2.2).

To further confirm the association of HDAC1 with Eg5 *in cellulo,* a co-immunoprecipitation experiment was performed. Endogenous Eg5 and HDAC1 were immunoprecipitated separately from T-Ag Jurkat cells and probed for the presence of the interaction by Western blot. Eg5 was immunoprecipitated with HDAC1 (Figure 2.3B, lane 2), and vice versa (Figure 2.3B, lane 3). The data confirm that HDAC1 and Eg5 interact *in cellulo*. However, the quantities of co-immunoprecipitated proteins were low, which suggests that the interaction between wild type HDAC1 and Eg5 is of low affinity or occurs transiently under cellular conditions.

To determine whether the Eg5–HDAC1 interaction is cell type specific, HDAC1-FLAG and Eg5-myc were cotransfected into HEK293 cells and immunoprecipitated using FLAG and myc antibodies. The Eg5–HDAC1 interaction was also observed in HEK293 cells (Figure 2.3C, lanes 2 and 3), confirming that the interaction extends beyond Jurkat cells. Similar to the T-Ag Jurkat study, the low quantities of coimmunoprecipitated proteins suggest that the HDAC1–Eg5 interaction is transient or occurring under specific cellular conditions.

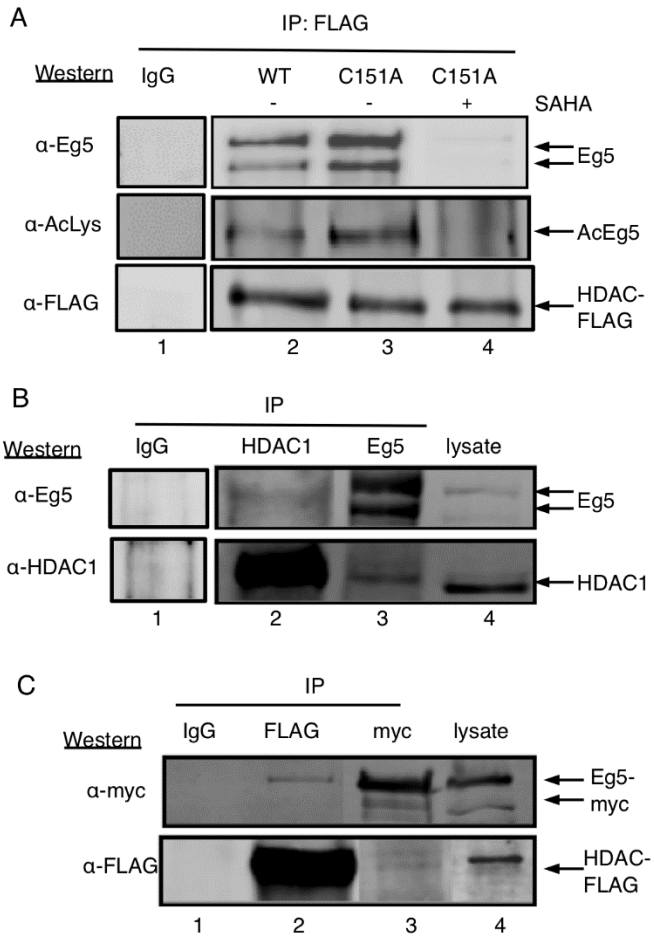


**Figure 2.3 - Eg5 interacts with HDAC1.** A) Wild type (WT) or C151A HDAC1 were expressed as FLAG-tagged proteins in T-Ag Jurkat cells, immunoprecipitated (IP) with anti-Flag agarose in the absence (lanes 2 and 3) or presence (lane 4) of SAHA (3 mM), separated by SDS-PAGE, and Western blotted with Eg5 (top), acetyl-lysine (AcLys, middle), or Flag (bottom) antibodies. Repetitive trials are shown in Figure A2.6A. B) Endogenous HD1 and Eg5 were immunoprecipitated (IP) separately from T-Ag Jurkat cells, separated by SDS-PAGE, and Western blotted with Eg5 (top) or HDAC1 (bottom) antibodies. Repetitive trials are shown in Figure A2.6B. C) HDAC1-Flag and Eg5-myc were coexpressed in HEK293 cells, immunoprecipitated (IP) separately with either Flag or myc antibodies, separated by SDS-PAGE, and Western blotted with myc (top) or Flag

(bottom) antibodies. Agarose beads without bound antibodies were used as an immunoprecipitation controls (lane 1). Repetitive trials are shown in Figure A2.6C. For all gels, arrows indicate the position of Eg5 and HDAC1 in the gels.

**2.2.4 Eg5 is a substrate of HDAC1**

To validate that Eg5 is a substrate of HDAC1 *in cellulo*, we performed *in vitro* deacetylation assays. First, experiments were performed using recombinant Eg5 and HDAC1. Eg5 was expressed and purified from bacteria (Figure 2.4, lane 6-10). Purified bacterial Eg5 was chemically acetylated by varying concentrations of acetic anhydride and incubation time (Figure 2.5, lanes 2-4 and 6-8). Based on the optimal results, Eg5 was acetylated by incubating with 0.2 mM acetic anhydride for 1h (Figure 2.5, lane 6) for use in *in vitro* deacetylation assays. Acetylated Eg5 was incubated with or without recombinant HDAC1. Eg5 acetylation was significantly reduced in the presence of HDAC1 (Figure 2.6A, top gel, compare lanes 2 and 1). In the presence of the HDAC inhibitor SAHA, acetylation of Eg5 remained (Figure 2.6A, top gel, compare lanes 2 and 3), confirming that deacetylation is HDAC dependent. Quantification also confirmed that HDAC1 deacetylated Eg5 (Figure 2.6B and Figure A.2.7, Figure A.2.8, Table A.2.1 and Table A.2.2).

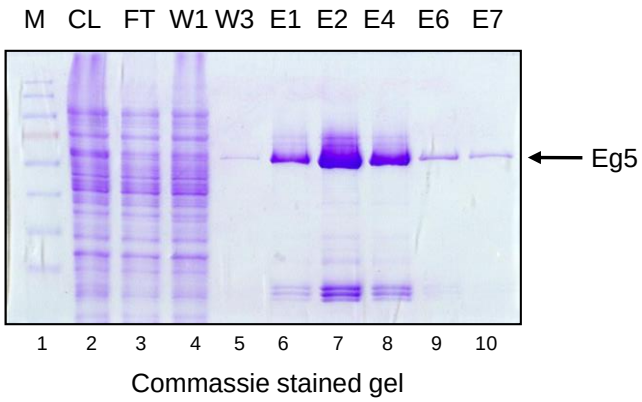


**Figure 2.4 – SDS-PAGE analysis of bacterial expressed Eg5.** His-tagged Eg5 was expressed in bacteria and purified using Ni-NTA beads. Different fractions (CL– crude lysate, FT– flowthrough, W– washing, E– elutions) were separated by SDS-PAGE and subjected to coommassie staining.

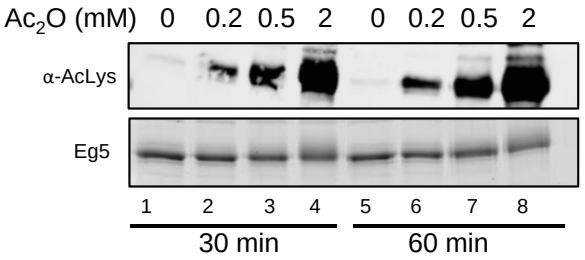


**Figure 2.5 – Optimization of *in vitro* acetylation of recombinant Eg5.** Eg5 (0.5 µg) was incubated with varying concentrations of acetic anhydride for 30min or 1h. Then the reaction was concentrated using a speedvac concentrator and separated by 10% SDS-PAGE, and analysed by Sypro Ruby stain (for total Eg5) or acetyl lysine antibody.

To further validate that HDAC1 can deacetylate Eg5, we performed *in vitro* deacetylation assays using cellular Eg5 and HDAC1. Eg5 was immunoprecipitated from T-Ag Jurkat cells and incubated with immunoprecipitated HDAC1 in the absence or presence of SAHA. Similar to results with recombinant proteins, Eg5 acetylation was

significantly reduced in the presence of HDAC1 (Figure 2.6C, top gel, compare lanes 2 and 1), indicating that HDAC1 is able to deacetylate Eg5. SAHA inhibited HDAC1-mediated deacetylation of Eg5 (Figure 2.6C, top gel, compare lanes 2 and 3). Quantification confirmed reproducible HDAC1-dependent Eg5 deacetylation (Figure 2.6D, Figure A.2.9, Table A.2.4, Table A.2.5 and Figure A.2.10). Combined with the fact that Eg5 acetylation was elevated in immunoprecipitates with the inactive C151A mutant compared to wild type (Figure 2.3A), these studies substantiate that Eg5 is a substrate of HDAC1.

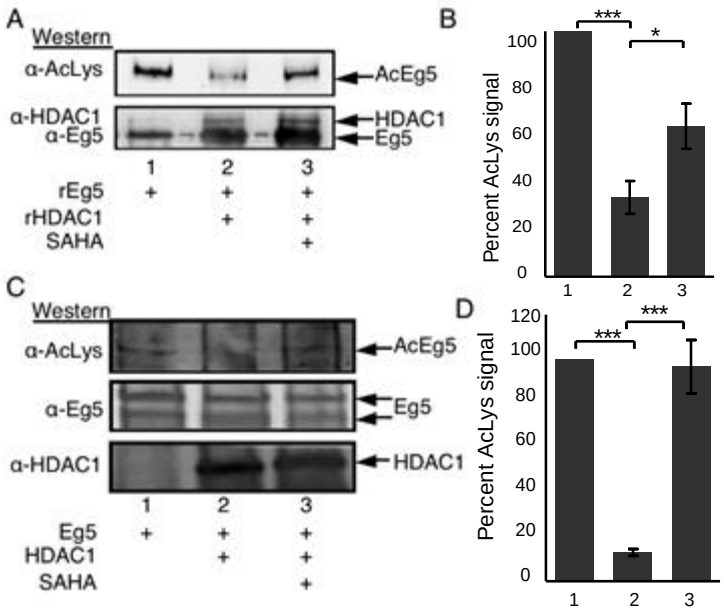


**Figure 2.6 - Eg5 is deacetylated by HDAC1.** A) Bacterially-expressed and chemically acetylated Eg5 was incubated in the absence or presence of recombinant HDAC1 and SAHA for 2h at 37 °C and analyzed by SDS-PAGE and western blotting with acetyl lysine (top) and a combination of Eg5 and HDAC1 (bottom) antibodies. B) Quantification of the Ac-Lys western blot from part A. Mean and standard error of three independent trials are shown (Figure A.2.7 and Table A2.1). Quantification of the Eg5 blot as a load control is

shown in Figure A.2.8 and Table A2.2. One way ANOVA test: *p<0.05, ***p<0.0005 C) *In vitro* deacetylase assay: Eg5 was immunoprecipitated from T-Ag Jurkat cells (lane 1) and incubated with immunoprecipitated HDAC1 in the presence (lane 3) or absence of 3 mM SAHA (lane 2) for 1 h at 30°C, followed by SDS-PAGE separation and immunoblotting with acetyl lysine (top), Eg5 (middle), and HDAC1 (bottom) antibodies. D) Quantification of the Ac-Lys western blot from part C. Mean and standard error of three independent trials are shown (Figure A.2.9 and Table A2.3). Quantification of the Eg5 blot as a load control is shown in Figure A.2.10 and Table A2.4. One way ANOVA test; *p<0.05, ***p<0.0002

**2.2.5 HDAC1 deacetylates K890 of Eg5**

To date only one Eg5 acetylation site (K146) has been identified in a global proteomics study (80). To understand if acetylated K146 is the predominant site for HDAC1 mediated deacetylation, we created a K146A mutant using the full length myc-tagged Eg5 construct (89). First, we studied the acetylation state of K146A to assess if K146 is a dominant acetylated lysine in Eg5. Wild type Eg5 and K146A were transfected into HEK293 cells, followed by immunoprecipitation and immunoblotting with an acetyl lysine antibody to detect acetylation. The level of acetylation of the K146A mutant was comparable to that of wild type Eg5 (Figure 2.7A), suggesting that other acetylation sites are present in Eg5. In addition, immunoprecipitation of the wild type or K146A mutant Eg5 by HDAC1 was similar (Figure 2.7B), indicating that K146 is not the dominant acetylation site for HDAC1. Taken together, the data indicate that a site other than K146 is the predominant site for HDAC1-mediated deacetylation on Eg5.

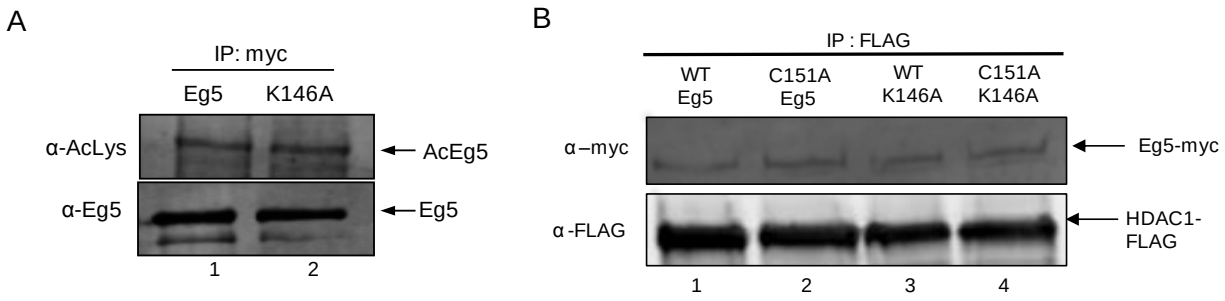


**Figure 2.7 – K146 is not a predominant Eg5 acetylation site regulated by HDAC1.** A) Myc-tagged wild type or K146A mutant Eg5 were transfected into HEK293 cells, treated with SAHA for 24h, and immunoprecipitated with a myc antibody. SDS-PAGE separation and immunoblotting was performed with acetyl lysine (top) or myc (bottom) antibodies. No change in the acetylation levels of the wild type and mutant proteins were observed (top gel), which indicates that K146 is not a predominant acetylation site on Eg5. Repetitive trials are shown in Figure A2.11A. B) FLAG-tagged wild type (WT) or C151A mutant HDAC1 were cotransfected with myc-tagged wild type or K146A mutant Eg5 into HEK293 cells. The wild type and C151A mutant HDAC1 were immunoprecipitated using anti-FLAG agarose beads, separated by SDS-PAGE, and immunoblotted with myc (top) or FLAG (bottom) antibodies. No changes in the levels of immunoprecipitated Eg5 were observed with either wild type or mutant proteins (top gel), which indicates that K146 is not a site bound and regulated by HDAC1. Repetitive trials are shown in Figure A2.11B.

We used a mass spectrometry-based approach to identify the putative acetylation sites in Eg5 regulated by HDAC1. Myc-tagged Eg5 was transfected into HEK293 cells in the absence or presence of wild type HDAC1. After 48h, cells were treated with or without HDAC inhibitors for 24h. The broad spectrum inhibitor SAHA was used, in addition to the HDAC1/2 selective inhibitor SHI-1:2. After harvesting, immunoprecipitation, and SDS-

PAGE separation, protein bands corresponding to Eg5 were excised from the gel, trypsin digested, and subjected to LC-MS/MS analysis. The HDAC 1/2 selective inhibitor SHI-1:2 enhanced acetylation of Eg5 at K890 compared to untreated sample (Table 2.2 and Figure A.2.12). The site was not acetylated when Eg5 was cotransfected with HDAC1, suggesting that K890 is the target site for HDAC1-mediated deacetylation (Figure A.2.12G-H).

To probe the acetylation status of Eg5 at K890, we created a K890R mutant using the full length myc-tagged Eg5 construct. Following transfection of wild type and K890R Eg5 into HEK293 cells, Eg5 was immunoprecipitated and immunoblotted with an acetyl lysine antibody to detect acetylation. Interestingly, the level of acetylation of K890R was significantly reduced compared that of wild type Eg5 (Figure 2.8A, compare lanes 2 and 3, top gel). Quantification of the acetylated Eg5 signal clearly showed that mutation of K890 leads to a significant reduction of acetylation of Eg5 (Figure 2.8B, Figure A.2.13, Table A.2.5, Table A.2.6). These data further suggest that K890 is a major acetylation site on Eg5.

**Table 2.2 – MS analysis of K890 in Eg5**

| Protein name/ Accession | Trials | Sample | % Coverage | Unique # of acetylated peptides |
|---|---|---|---|---|
| Kinesin like protein 11(KIF11)/Eg5 (KIF11_HUMAN) | 1 | Eg5+DMSO | 71 | 0 |
| | | Eg5+SHI-1:2 | 72 | 1 |
| | | Eg5+SAHA | 82 | 0 |
| | | Eg5+HDAC1 | 73 | 0 |
| | 2 | Eg5+DMSO | 80 | 0 |
| | | Eg5+SHI-1:2 | 69 | 1 |
| | | Eg5+SAHA | 75 | 0 |
| | | Eg5+HDAC1 | 83 | 0 |

**Unique # of acetylated Peptides-** Number of different amino acid sequences containing an acetylated lysine residue that are associated with a protein. % Coverage – the percentage of the protein amino acid sequence that was identified.

To further determine whether K890 is involved in the interaction between Eg5 and HDAC1, wild type or K890R mutant myc-tagged Eg5 were cotransfected with either wild type or C151A mutant Flag-tagged HDAC1 into HEK293 cells, followed by immunoprecipitation of HDAC1 using a Flag antibody. The amount of K890R mutant coimmunoprecipitated with wild type or C151A mutant HDAC1 was significantly reduced compared to that of wild type Eg5 (Figure 2.8C, compare lanes 4 and 5 to 2 and 3, top gel), indicating that K890 is essential for the binding of Eg5 to HDAC1. The data again support that Eg5 is acetylated predominantly at K890, and K890 is a target site for HDAC1.

### 2.2.6 Acetylation at K890 affects ATPase activity of Eg5

We next study the effect of acetylation on ATPase activity of Eg5. Myc-tagged wild type or K890R mutant Eg5 were transfected into HEK293 cells, treated with HDAC1/2 selective inhibitor (SHI-1:2) for 24h, and immunoprecipitated with a myc antibody. Following immunoprecipitation, Eg5 protein was eluted and subjected to ATPase reaction. The ATPase activity of wild type is significantly reduced compared to K890R mutant (Figure 2.8E, histogram compare column 2 and 3). The data indicate that HDAC1 mediated deacetylation is critical for Eg5 motor activity.

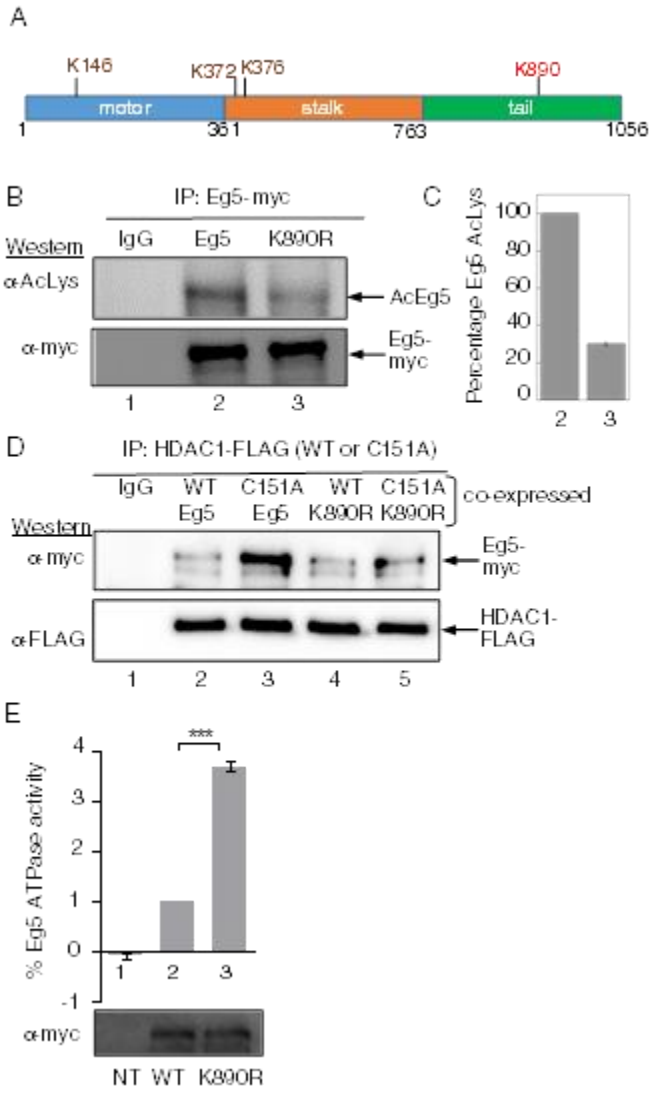

**Figure 2.8** - **Eg5 is deacetylated by HDAC1 at K890**. A) Myc-tagged wild type or K890R mutant Eg5 were transfected into HEK293 cells, treated with HDAC1/2 selective inhibitor (SHI-1:2) for 24h, and immunoprecipitated with a myc antibody. SDS-PAGE separation and immunoblotting was performed with acetyl lysine (top) and myc (bottom) antibodies. Repetitive trials are shown in Figure A2.13A. B) Quantification of the Ac-Lys western blot from part A. Mean and standard error of four independent trials are shown (Figure A.2.13, Table A2.5). Quantification of the myc blot as a load control is shown in Figure A.2.14 and Table A2.6 Student t–test, *p<0.05, ***p<0.0001. C) FLAG-tagged wild type (WT) or C151A mutant HDAC1 were cotransfected with myc-tagged wild type or K890R mutant Eg5 into HEK293 cells. Wild type and C151A mutant HDAC1 were immunoprecipitated using anti-FLAG agarose beads, separated by SDS-PAGE, and immunoblotted with myc (top) and FLAG (bottom) antibodies. Repetitive trials are shown in Figure A2.15. . E) Myc-tagged wild type or K890R mutant Eg5 were transfected into HEK293 cells, treated with HDAC1/2 selective inhibitor (SHI-1:2) for 24h, and immunoprecipitated with a myc antibody. Half of the immunoprecipitate was used for ATPase assay and other half was was separated by SDS-PAGE and immunoblotted with myc antibody. Mean and standard error is shown from at least three independent trials (Table S3). NT – non transfected. ***p<0.0001.

### 2.2.7 Eg5 colocalized with HDAC1 during mitosis

For HDAC1 to deacetylate Eg5 *in vivo*, both proteins must colocalize together *in cellulo*. HDAC1 is predominantly present in the nucleus (93), whereas Eg5 is in the cytoplasm (94). We first analyzed the HDAC1-Flag fusion protein by microscopy to confirm that the Flag tag does not affect HDAC1 localization to the nucleus. HEK293 cells

expressing Flag-tagged wild type HDAC1 were grown on glass cover slips, fixed, and blocked with bovine serum albumin (BSA), followed by visualization of the Flag tag. As expected (93,94), HDAC1-Flag was predominantly nuclear, whereas Eg5 was cytoplasmic in interphase cells (Figure 2.9 or Figure A2.16). These data indicate that the HDAC1-FLAG fusion protein maintains the same nuclear localization as endogenous HDAC1.

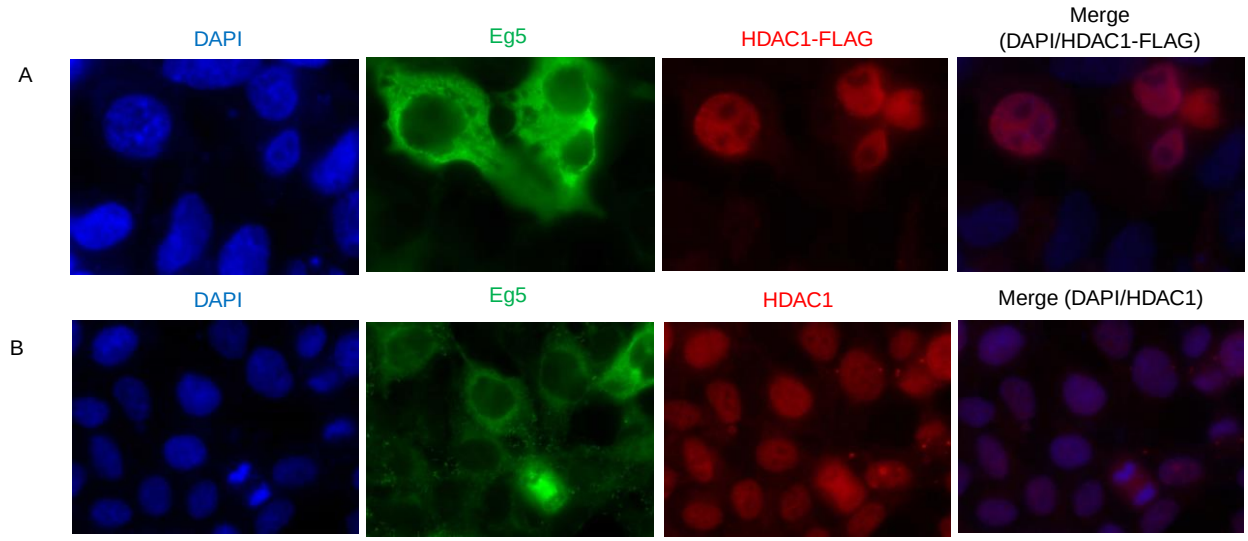


**Figure 2.9 – Endogenous and overexpressed HDAC1 localizes to the nucleus**. HEK293 cells expressing FLAG tagged HDAC1 (A) or HEK293 cells alone (B) were fixed and stained with FLAG (A) or HDAC1 (B) antibodies (red). Cells were counterstained with DAPI (blue) and visualized using fluorescence microscopy. Both endogenous and overexpressed HDAC1 were predominantly nuclear. The data suggests that the FLAG tag does not affect the localization of HDAC1-FLAG. Repetitive trials are shown in Figure A2.16.

Eg5 plays a critical role in bipolar spindle formation during mitosis (89). Given that nuclear envelope breakdown occurs during mitosis, we hypothesized that HDAC1 interacts with Eg5 after the initiation of mitosis. To determine the subcellular localization

of endogenous HDAC1 and Eg5 under mitotic conditions, HEK293 cells were seeded onto glass cover slips, fixed, and blocked with BSA, followed by visualization of HDAC1 and Eg5 in cells undergoing mitosis. In prophase, the first stage of mitosis, Eg5 was localized to the separating centromeres (Figure 2.10B), consistent with its role in spindle formation. While HDAC1 was localized with DNA in prophase, the merged image showed that a population of HDAC1 colocalized with Eg5 (Figure 2.10B). In contrast, Eg5 and HDAC1 did not colocalize during metaphase, anaphase, or telophase; in these cases, HDAC1 was associated with the DNA, which was located between the Eg5-bound spindle poles (Figure 2.10C-E). In interphase cells, HDAC1 was predominantly nuclear, whereas Eg5 was in the cytoplasm (Figure 2.10A), as expected (93,94)**.** These results indicate that HDAC1 colocalized with Eg5 specifically during prophase, which suggests that HDAC1-mediated deacetylation of Eg5 occurs at the earliest stages of mitosis.

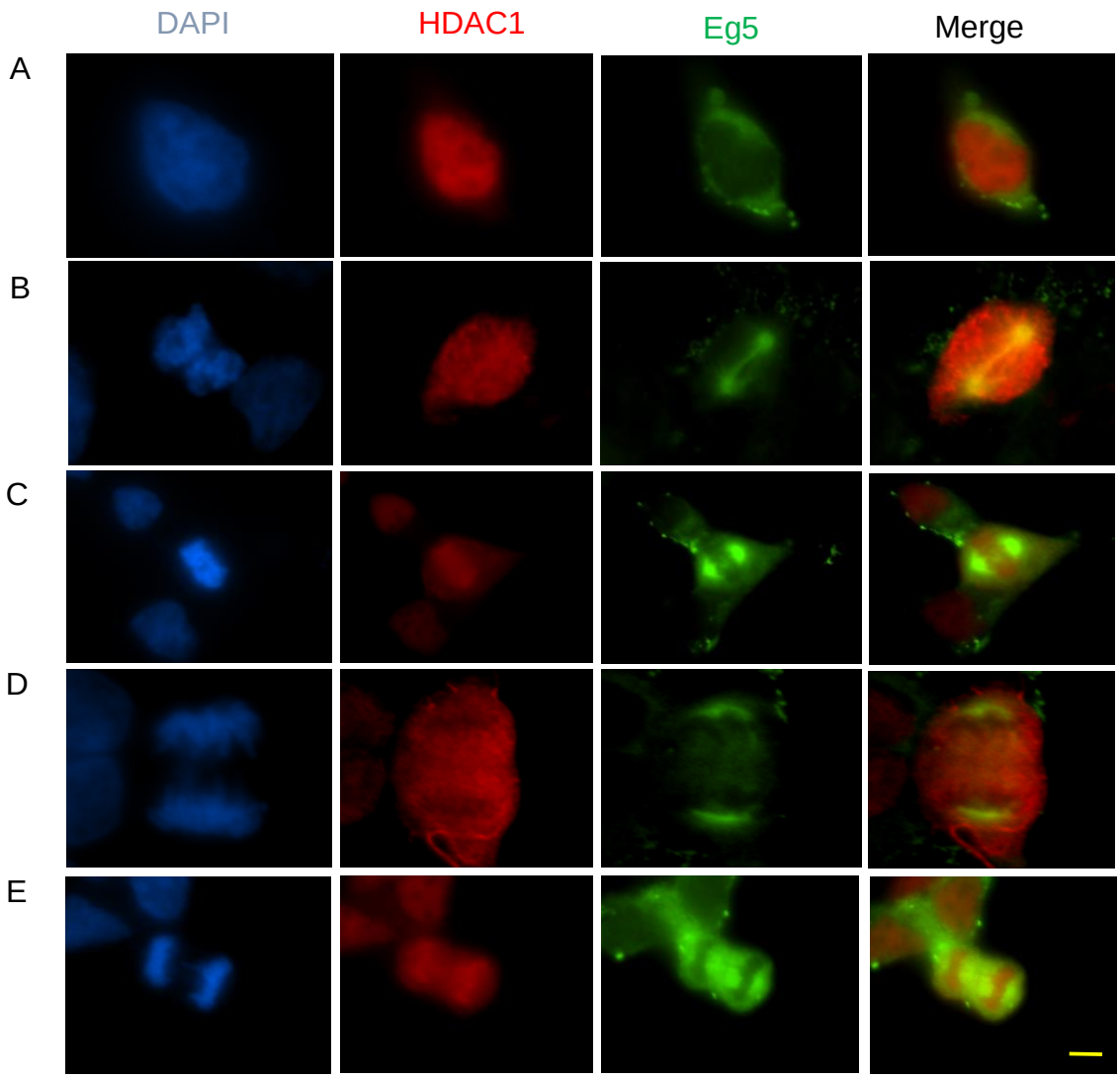


**Figure 2.10 - Eg5 colocalized with HDAC1 during prophase**. HEK293 cells were fixed and stained with HDAC1 (red) and Eg5 (green) antibodies. Cells were counterstained with DAPI (blue). Fluorescence microscopy was used to visualize HDAC1 and Eg5 in each cell. Cells in interphase (A), prophase (B), metaphase (C), anaphase (D), and telophase (E) are shown. HDAC1 (red) and Eg5 (green) images were used to generate merged images (yellow). Yellow indicates colocalization. Repetitive trials are shown in Figure A2.17.

### 2.2.8 HDAC inhibitors promote monopolar spindle formation

Previous studies have shown that HDAC inhibitors arrests cell cycle at G1/G0 and G2/M phases (95,96). To understand the role of HDAC1 in cell cycle progression, HEK293 cells were treated with Eg5 inhibitor or HDAC1 and 2 selective inhibitor (SHI-1:2) for 48h, before analyzing by flow cytometer. The data clearly showed that both Eg5 inhibitor and SHI-1:2 inhibitor arrested cells at mitosis (Figure 2.11A, Table S3). The data indicate that HDAC1 and 2 play a key role in mitotic progression. Prior work has shown that S-trityl-L-cysteine (STLC) is a specific and potent inhibitor of Eg5 (97). STLC arrests cells specifically at mitotic phase by affecting Eg5 function, which leads to the formation of monopolar spindles. Therefore, we looked at the spindle formation after treating the HEK293 cells with STLC or SHI-1:2 for 48h. Interestingly, monopolar spindles were observed with both STLC and SHI-1:2 treated cells (Figure 2.11B and 2.11C, Table S4). In the DMSO treated cells, monopolar spindles were not visible. This is also consistent with prior work showing the effect of HDAC1 and HDAC2 in mitosis (98). Mitotic defects including monopolar spindles were observed in the embryonic stem cells with double conditional knockout of HDAC1 and HDAC2. Here, we show that HDAC mediated deacetylation of Eg5 affects bipolar spindle formation, causing mitotic arrest. The interaction between Eg5 and HDAC1 during mitosis could be a key mechanism that regulates cell cycle progression. Given that HDAC1 and 2 selective inhibitor produces less monopolar spindles (53%) compared to Eg5 inhibitor (100%), suggests that HDAC1 and 2 act on more than one target in the cell to cause cell cycle arrest. This could also be rationalized by the involvement of another HDAC, such as HDAC3 to fully inhibit the function of Eg5 during cell cycle arrest.

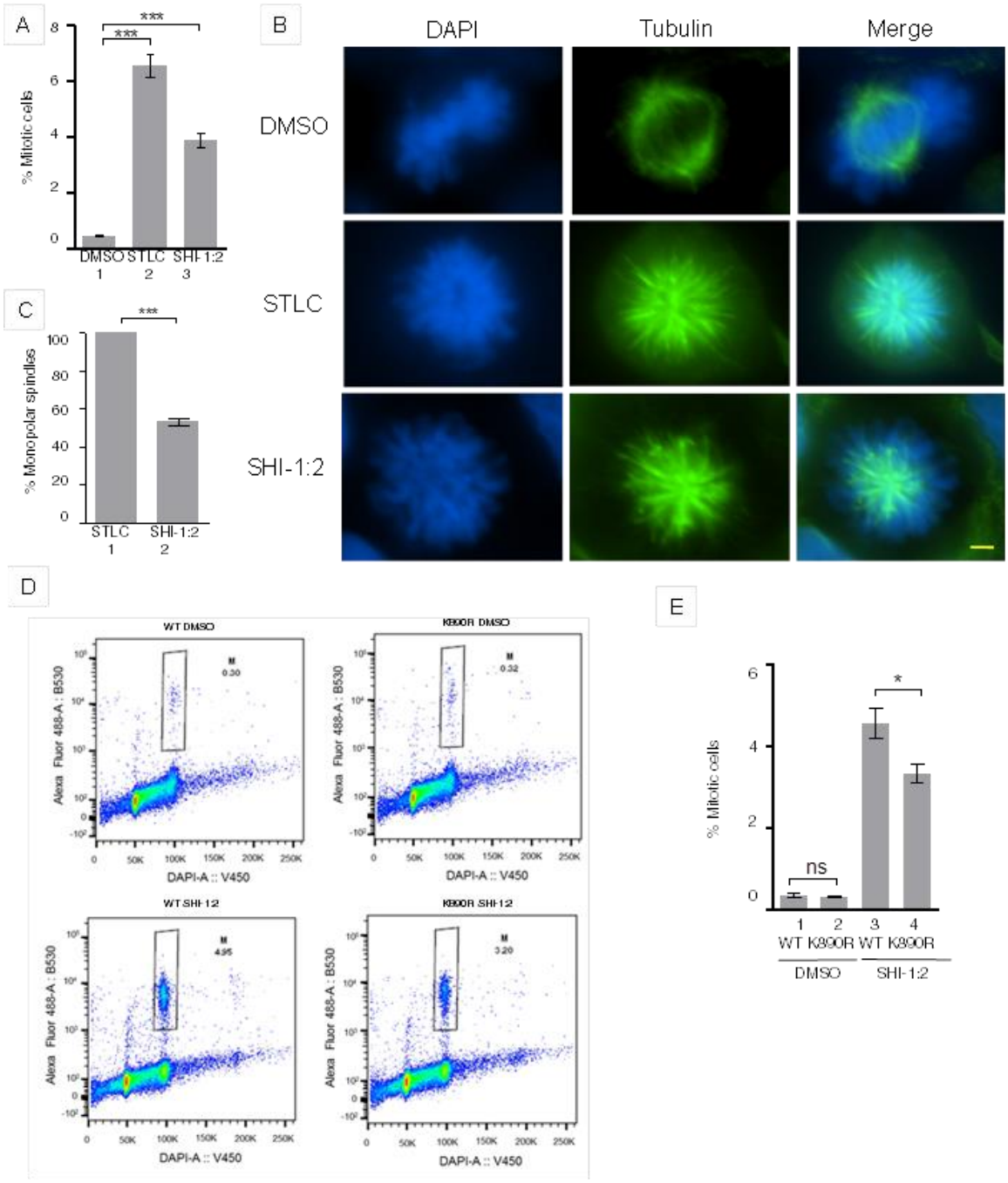


**Figure 2.11 – Acetylation of Eg5 partially contributes to HDAC1 and 2 selective inhibitor induced mitotic arrest.** A) HEK293 cells were treated with DMSO, STLC (10 μM) or SHI-1:2 (10 μM) for 48h followed by fixing and staining with Alexa fluoro®488 conjugated phospho-histone H3 (Ser10) antibody and DAPI. Samples were analyzed by

flow cytometry and percent mitotic cells were plotted. ***p<0.0001. B) HEK293 cells were treated with DMSO, STLC (10 μM) or SHI-1:2 (10 μM) for 48h followed by fixing and staining with α-tubulin (green) and DAPI (blue). Fluorescence microscopy was used to visualize tubulin and DAPI in each cell. C) Quantitative analysis of monopolar spindles present in STLC and SHI-1:2 treated cells. Monopolar spindles were counted from at least 100 mitotic cells from four independent experiments. ***p<0.002. Scale bar – 10 μM. D) Flow cytometry analysis of cells transfected with wild type and mutant Eg5. Myc-tagged wild type or K890R mutant Eg5 were transfected into HEK293 cells, treated with HDAC1/2 selective inhibitor (SHI-1:2) for 48h and subjected to staining with Alexa fluoro®488 conjugated phospho-histone H3 (Ser10) antibody and DAPI prior to flow cytometric analysis. Percent cells in the mitosis (M) is shown near the square containing mitotic cells. E) Quantification of the mitotic cells is shown as a histogram. *p<0.05.

### 2.2.9 Acetylation at K890 partially contributes to cell cycle arrest caused by HDAC inhibitors

To further gain insights into the mechanistic link between Eg5 and HDAC1, we looked at the cell cycle arrest caused by wild type Eg5 and K890R mutant Eg5. HEK293 cells were transfected with wild type and K890R mutant Eg5 and cells were treated with SHI-1:2 for 48h to induce acetylation, before analyzing by flow cytometer. K890R mutant transfected cells showed reduction in cell cycle arrest compared to wild type Eg5 transfected cells (Figure 2.11D and 2.11E). The partial effect of K890R mutant could also be due to the dominant function of endogenous Eg5. In line with these data, we speculate that Eg5 deacetylation is one of many mechanisms that leads to HDAC inhibitor-mediated cell cycle arrest.

## 2.3 Discussion

Aberrant expression of HDAC1 is implicated in multiple diseases, including cancer. Currently, four HDAC inhibitors are approved as anti-cancer therapies, and multiple HDAC inhibitors are in the clinic. HDAC inhibitors influence proliferation due to perturbed cell cycle progression, which ultimately leads to apoptosis. The model that has emerged to account for HDAC inhibitor-mediated cell death centers on altered histone acetylation and gene expression (62). However, several studies have found that mitotic arrest in the presence of HDAC inhibitors does not correlate with changes in histone acetylation or protein expression (57,68), which suggests that non-histone targets may be influenced by HDAC inhibitors. Identifying non-histone substrates that play a role in HDAC inhibitor-mediated cell death is critical to guide the development of more effective and selective anti-cancer drugs.

Here, we explored use of inactive HDAC1 mutants as tools to trap and identify unknown substrates. Using the trapping strategy, we provide the first evidence that Eg5 is an HDAC1 substrate. HDAC1 deacetylated Eg5 *in vitro* using both recombinant and cell-derived proteins (Figure 2.6), which confirm that Eg5 is a substrate for HDAC1. Mass spectrometric analysis identified a new acetylation site on Eg5, K890. Studies with the K890R mutant indicated that K890 is a major Eg5 acetylation site regulated by HDAC1 and is critical for binding to HDAC1 (Figure 2.8). Further, we show that deacetylation at K890 is critical for maintaining ATPase activity of Eg5. Eg5 interacted with HDAC1 in both T-Ag Jurkat and HEK293 cells, although the low levels of coimmunoprecipitated protein implicated that the interaction is cell condition dependent. Importantly, Eg5 colocalized with HDAC1 only during the prophase stage of mitosis. The mitosis-specific interaction is

consistent with the low level of coimmunopreciptiation observed in asynchronous cells (Figure 2.3B and 2.3C) and the need for nuclear envelope breakdown to allow HDAC1 and Eg5 to exist in the same cellular location. Further, HDAC1 and 2 selective inhibitor caused mitotic arrest and promoted monopolar spindle formation (Figure 2.11A and B). Acetylation of Eg5 at K890 partially contributed to the HDAC inhibitor-mediated cell cycle arrest (Figure 2.11D). From these data, we hypothesize that HDAC1-mediated deacetylation of Eg5 during prophase is an essential step in mitotic progression. The model that emerges suggests that Eg5 is acetylated prior to mitosis (Figure 2.12A). Upon entering the prophase of mitosis, the nuclear envelope breaks down to allow HDAC1 to colocalize with Eg5 and catalyze deacetylation (Figure 2.12B). Then, deacetylated Eg5 completes centromere separation and formation of the bipolar spindle to promote the cells into the later stages of mitosis (Figure 2.12C).

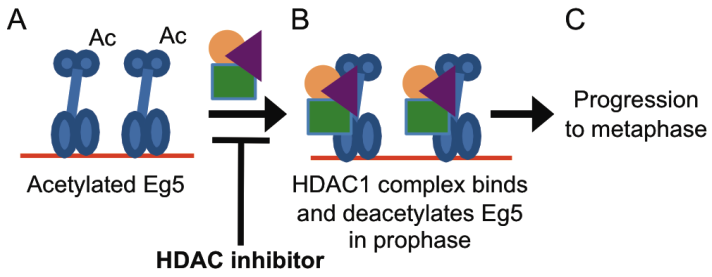


**Figure 2.12 - Model of the role of HDAC1 in Eg5-mediated mitotic progression**. A) Eg5 (blue) is acetylated (Ac) prior to entry into mitosis. B) Upon entering the prophase of mitosis, HDAC1 (magenta) interacts with Eg5 after nuclear envelope breakdown, which results in Eg5 deacetylation. Associated proteins (yellow and green) may be involved in the interaction. HDAC inhibitors would prevent deacetylation and cell progression, resulting in mitotic arrest. C) Eg5 deacetylation promotes centromere separation and bipolar spindle formation, leading to metaphase progression and complete cell division.

HDAC1 is recruited to gene-specific histone targets to regulate transcription through multiprotein complexes, such as Sin3, NuRD and CoREST (43). Based on this prior work, we speculate further that associated proteins are required for HDAC1-mediated Eg5 interaction and deacetylation during prophase (Figure 2.12B). A recent study showed that HDAC1 is displaced from chromatin during mitosis to interact with filamentous actin (F-actin)(88), which also localizes to the mitotic spindles (99). Consistent with this prior data, the trapping mutants studied here also bound γ-actin, a component of F-actin. Given the role of Eg5 in bipolar spindle formation, we hypothesize that HDAC1 interacts with F-actin to facilitate Eg5 deacetylation during mitosis. Eg5 also interacts with NCOR1 (nuclear receptor corepressor 1) (100) and NCOR1 is known to associate with HDAC1 via the mSin3a complex (88). We speculate that Eg5 deacetylation may also be mediated by the mSin3a/NCOR complex. Given the key role of associated proteins in regulating HDAC activity in gene expression, the proposed model also includes associated proteins as players in mediating Eg5 deacetylation (Figure 2.12B).

Previous work reported that HDAC inhibitors block mitotic progression beyond prometaphase (57,68,90-92). Maximal mitotic arrest was observed when HDAC inhibitors were present prior to the start of mitosis (90). These earlier results with HDAC inhibitors are consistent with the proposed model (Figure 2.12) where Eg5 deacetylation occurs in the earliest stage of mitosis, before complete centromere separation. Prior work also reported that HDAC inhibitor-treated cells failed to progress to metaphase partially due to inefficient localization of various centromeric proteins (90,92). However, HDAC inhibitor treatment did not influence the quantities of centromeric proteins, although Eg5 was not tested (90-92). The influence of HDAC inhibitors on centromeric protein

localization is consistent with the proposed model where HDAC1-mediated Eg5 deacetylation is critical for mitotic progression (Figure 2.12). Moreover, the model provides a compelling mechanistic hypothesis proposing that HDAC inhibitors induce mitotic arrest through disruption of Eg5 acetylation and bipolar spindle formation (Figure 2.12B).

An embryonic stem cell line harboring double conditional knockoout of HDAC1 and HDAC2 led to increased monopolar spindles and chromosomal segregation defects, clearly suggesting that HDAC1 and 2 plays an essential role during mitotic progression (98). Here, we show for the first time that HDAC1 and 2 selective inhibitor causes mitotic arrest and promotes monopolar spindle formation, confirming that HDAC affects Eg5 function similar to an Eg5 inhibitor. Moreover, the model provides a compelling mechanistic hypothesis proposing that HDAC inhibitors induce mitotic arrest through disruption of Eg5 acetylation, reduction of ATPase activity and monopolar spindle formation (Figure 2.8E and Figure 2.11B).

HDAC inhibitor-induced cell cycle arrest has been primarily attributed to the expression of the p21 (waf1/cip1) and p27 (kip1) proteins after histone hyperacetylation and transcriptional upregulation (101). However, arrest due to mitotic defects were observed rapidly after inhibitor treatment and in the absence of transcription (68,102), suggesting a histone acetylation independent mechanism. Previous studies implicated HDAC3 in mitotic defects (57,68). HDAC3 knockdown reproduced the mitotic defects observed with HDAC inhibitor treatment, with spindle instability and prometaphase arrest (68). Like HDAC1, a population of HDAC3 localized to the mitotic spindle during prophase (57). HDAC3 was associated with stable corepressor complex containing NCOR1

throughout mitosis, suggesting it is in an activated form during mitosis (57). HDAC3 deacetylates NudC (nuclear distribution protein C) (103), which is critical for kinetochore-microtubulin attachment via dynein/dynactin. Taken together, HDAC1 and HDAC3 may function together during mitosis to regulate proper centromere separation and spindle formation.

Prior work documented a clear role for post-translational modifications in regulating Eg5 activity in mitosis. Phosphorylation at T937 promotes Eg5 localization to the spindle (94). Eg5 is also phosphorylated at T927 to enhance binding to centrosomes during bipolar spindle formation (89). Based on this earlier work on phosphorylation, acetylation may also have an impact on Eg5 activity and/or binding during mitosis. With only a single acetylated site on Eg5 (K146) previously identified in a large proteomic study (80), the effect of acetylation on Eg5 function during mitosis has not yet been fully characterized. Here, we identified K890 as a predominant acetylated site on Eg5 and the target site for HDAC1-mediated deacetylation. The acetylation of K890 also regulates the affinity of Eg5 to HDAC1. The work here with HDAC1 suggest that Eg5 acetylation at K890 is dynamic and may play an important role in mitotic progression.

Since HDAC1 substrate identification suffers from a lack of discovery tools, the substrate trapping strategy developed here will assist in identifying physiological substrates of HDAC1. In this work, we discovered that several HDAC1 mutants (HDAC1 F150A and C151A) act as efficient subtrate traps. The F150 and C151 residues are conserved among all HDAC isoforms (37,38), suggesting that the method can be applied to identify cellular substrates of other HDAC isoforms. Given the role of HDAC proteins in cancer formation and use of HDAC inhibitor drugs in anti-cancer therapy, these studies

will have a direct impact on cancer biology studies and drug design efforts by revealing new functional roles of HDAC proteins in cellular events.

**2.4 Expermental procedure**

**2.4.1 Antibodies and reagents**

HDAC1 (catalog number – H3284), FLAG (catalog number – F3165), and myc (catalog number – C3956) antibodies, as well as anti-FLAG agarose beads (catalog number – A2220 ), were purchased from Sigma. The polyclonal Eg5 antibody (catalog number – NB500-181) was purchased from Novus. Monoclonal HDAC1 (for immunofluorescence; catalog number - 5356P), acetyl histone H3 (catalog number – 9649P) and polyclonal acetyl lysine (catalog number – 9681S) antibodies were purchased from Cell signaling. Protein A/G plus agarose beads were purchased from Santa Cruz. ProLong gold antifade mounting solution was purchased from Life Technologies. Secondary rabbit (Alexa fluoro 488; catalog number – A11008) and mouse (Alexa Fluoro 647; catalog number – A21235) antibodies were obtained from Molecular Probes. Recombinant HDAC1 (catalog number - 50051) was purchased from BPS biosciences.

**2.4.2 Expression plasmids and mutagenesis**

HDAC1 single point mutants were created using the pBJ5HDAC1-FLAG expression plasmid, as previously described (38). Myc-tagged pRcCMV-Eg5 was a generous gift from Dr. Anne Blangy (Centre de Recherche de Biochimie Macromoléculaire) (89). The Eg5-K146A and K890R mutants were constructed by Quickchange site directed mutagenesis (Agilent) using pRcCMV-Eg5 (K146A Forward primer- 5’ CCA CGT ACC CTT CAT CAA ATT TTT GAG GCA CTT ACT GAT AAT GGT ACT G 3’ and K146A Reverse primer- 5’ C AGT ACC ATT ATC AGT AAG TGC CTC AAA

AAT TTG ATG AAG GGT ACG TGG 3', K890R Forward primer- 5' CTT GAT CAG ATG ACT ATT GAT GAA GAT AGA TTG ATA GCA CAA AAT CTA GAA C 3' and K890R Reverse primer 5' G TTC TAG ATT TTG TGC TAT CAA TCT ATC TTC ATC AAT AGT CAT CTG ATC AAG 3'). The mutagenesis was performed as described by the manufacturer. Then, mutation was confirmed by DNA sequencing.

**2.4.3 Cell culture and transient transfections**

Human T-Ag Jurkat cells were grown in RPMI 1640 (Life technologies) supplemented with 10% fetal bovine serum (FBS; Life Technologies) and 1% antibiotic/anti-mycotic (Hyclone) at 37 °C in a 5% $CO_2$ environment. HEK293 cells were maintained in Dulbecco's modified Eagle's medium (Life technologies) supplemented with 10% FBS and 1% antibiotic/anti-mycotic at 37 °C in a 5% $CO_2$ environment.

**2.4.4 Starting a new cell culture**

Pre-warmed media supplemented with 10% FBS (Life Technologies) and 1% antibiotic/anti-mycotic (Hyclone) (10 mL) were added to a T75 flask (Biolite) and placed in a $CO_2$ incubator for 10 min. A vial containing banked cells (1 mL, $10X10^6$ cells) was taken from the liquid nitrogen tank and placed in a floater and thawed quickly in a 37 °C incubator. The contents were transferred to a 15 mL centrifuge tube, and complete media (5 mL: media containing 10% FBS and 1% antibiotic/anti-mycotic) was added before centrifugation. Cells were collected by centrifugation at 1000 rpm for 5 min. The supernatant was removed by aspiration, and cells were resuspended in complete media (1 mL) and transferred to the T75 flask containing pre-warmed media. Cells were maintained at 37 °C in a 5% $CO_2$ environment.

### 2.4.5 Long term storage of mammalian cells

Cells (10 X $10^6$ in 1 mL) were stored in a liquid nitrogen tank for future use. Confluent cells (50 mL;1 X $10^6$ cells per mL) were spun down at 1000 rpm for 5 min and media was removed by aspiration. A cell pellet was resuspended in complete media containing 10% FBS, 1% antibiotic/anti-mycotic, and 5% DMSO (5 mL) and transferred into five labeled cryo tubes (1 mL, Cell line,date banked, 10 X $10^6$ cells, person's name). The cryo tubes were wrapped in styrofoam and first stored at -20 $^0$C for a day, then -80 $^0$C for a second day, and transferred to a liquid nitrogen tank for long term storage.

### 2.4.6 Long term storage of bacterial cells

Bacterial cells (DH5α; a single colony) transformed with plasmids (wid type or mutants) were grown overnight (12-16h) in LB medium (5 mL; 1% bacto tryptone, 0.5% yeast extract, 1% NaCl) at 37 $^0$C with rocking at 250 rpm in a bacterial incubator to a cell density of 3-4 X $10^9$/mL. Without harvesting, the overnight grown cultures (750 µL) were tranferred to 1.5 mL eppendorf tubes and mixed with 60% glycerol (250 µL). The culture and glycerol were mixed by vortexing and stored in -80 $^0$C for future use.

### 2.4.7 Bacterial transformations

DH5α competent cells (Chapter 4, section 4.4.7) were used for transformation. DH5α competent cells (100 µL) were thawed on ice and mixed with wild type or mutant HDAC1 DNA (100-500 ng), and incubated on ice for 20 min. Then, a heat shock was applied to the cells by incubating at 42 $^0$C for 45-60s followed by incubation on ice for 2 min. LB medium (500 µL) was then added to the cells and incubated at 37 $^0$C for 1.5 h with shaking at 250 rpm. Cells were collected by centrifuging at 13.2 X $10^3$ rpm for 10 min. After centrifugation, the soluble fraction (400 µL) was removed and the cell pellet was

resuspended in the remaining medium and plated on LB-agar plates (1% bacto tryptone, 0.5% yeast extract, 1% NaCl, 2% agar) containing ampicillin (100 µg/mL). Plates were inverted and incubated at 37 $^0$C overnight.

**2.4.8 Plasmid isolation (Miniprep and Midiprep)**

A single colony from a bacterial transformation or a small clump of a glycerol stock containing plasmid DNA was inoculated in 5 mL (for miniprep) or 200 mL (for midiprep) LB medium containing ampicillin (100 µg/mL) and grown at 37 $^0$C overnight with shaking at 250 rpm. For a miniprep, cells were harvested by spining at 4000 rpm for 10 min at 4 $^0$C and resuspended in cold P1 buffer (300 µL ; 50 mM Tris-Cl, pH 8.0, 10 mM EDTA, 100 µg/mL RNAse A). After resuspension, P2 buffer (300 µL; 200 mM sodium hydroxide, 1% SDS) was added, mixed by inverting tube gently, incubated at room temperature for 5 min, and neutralized by adding cold P3 buffer (300 µL; 3.0 M potassium acetate, pH 5.5). The contents were transferred to an eppendorf tube and incubated on ice for 10 min, followed by centrifugation at 13.2 X $10^3$ rpm for 10 min. The soluble fraction was transferred to a new tube and re-centrifuged to get rid of any particles left from the first spin. The cleared fraction was mixed with isopropanol (540 µL), and plasmid DNA was collected by centrifugation at 13.2 X $10^3$ rpm for 10 min. The pellet was air dried and dissolved in deionized water (20 µL) and stored at -20 $^0$C until further use. Midipreps were performed by using the Qiagen tip-100 kit, according to the Qiagen plasmid midiprep procedure. Midiprep DNA was used in mammalian cell transfection.

### 2.4.9 Transfection of DNA into T-Ag Jurkat cells

T-Ag Jurkat cells (40 X $10^6$ cells; 1 X $10^6$ /mL) were harvested by centrifugation at 1000 rpm for 5 min. The medium was removed by aspiration and cells were resuspended in phenol red-free RPMI media containing no FBS or antibiotics (20 mL). Cells were then centrifuged again at 1000 rpm for 5 min, the medium was removed, and the cell pellet was resuspended in RPMI medium without phenol red (800 µL). The resuspended solution was then transferred to a 1.5 mL microcentrifuge tube, mixed with plasmid DNA (20 µg; from midiprep) and incubated at room temperature for 10 min. The contents were transferred to a BTX 4 mm electroporation cuvette (Fisher Biotech) and transfection of DNA into T-Ag Jurkat cells (40 X $10^6$) was performed by electroporation using a BTX electro cell manipulator (For 10 X $10^6$ cells S= 250 V, T = 500V/capacitance and resistance, C = 800 µF and R= 129 Ohms). After electroporation, cuvettes were incubated at room temperature for 10 min. Meanwhile, RPMI medium with 10% FBS and 1% antibiotic/antimycotic (40 mL) was added to T75 flasks and maintained at 37 $^0$C in an incubator. After the 10 min incubation period, the transfected cells were added to the T75 flasks containing warm medium (40 mL) and maintained for 48 h in a $CO_2$ incubator. Cells were collected by spinning at 1000 rpm for 5 min at 4 $^0$C. The cell pellet was washed with ice cold DPBS (1 mL; HyClone; 137 mM NaCl, 2.7 mM KCl, 4.3 mM $Na_2HPO_4$, 1.4 mM $KH_2PO_4$, pH = 7.4), centrifuged, and the DPBS was removed by aspiration. The cell pellet was immediately subjected to lysis or stored at -80 $^0$C until further use.

### 2.4.10 Transfection of DNA into HEK293 cells

Transfection of DNA into HEK293 cells (at 60% confluency, 20 X $10^6$) was performed with Jetprime transfection reagent (VWR) according to the manufacturer's

instructions. Briefly, cells were seeded to achieve 60% confluency after 24 h. The following day, Jetprime buffer (500 µL) was mixed with plasmid DNA (5 µg from a midiprep), vortexed, centrifuged briefly, and then mixed with Jetprime transfection reagent (10 µL per 5 µg transfection). The mixture was vortexed, centrifuged briefly, and incubated at room temperature for 10 min. The DNA:jetprime mixture was added to the growth media of the cells and incubated in a 37 °C incubator with a 5% $CO_2$ environment. After 4h, the transfection mixure containing medium was replaced with fresh medium containing 10% FBS and 1% antibiotic/antimycotic and grown for 48 h. After a 48 h growth period, the transfected cells were trypsinized, harvested by centrifugation at 1000 rpm, washed once with DPBS (Hyclone), and either used immediately or stored at -80 $^0$C as a pellet.

**2.4.11 Cell lysis**

A microcentrifuge tube containing the cell pellet was taken from the -80 $^0$C freezer or used fresh, and put on ice prior to lysis. Protease inhibitor cocktail (GenDepot-P3100-005; 5 µL of 100X) was added to the cell pellet to a final concentration of 1X and the cell pellet was resuspended in ice cold Jurkat Lysis Buffer (500 µL; JLB; 50 mM Tris pH 8, 150 mM NaCl, 10% (v/v) glycerol, 0.5 % (v/v) Triton X-100). Cell lysis was performed by incubating at 4 $^0$C for 30 min with rotation and the cell debris was removed by centrifugation at 13.2 X $10^3$ rpm for 14 min at 4 $^0$C. The supernatant was tranferred to a new eppendorf tube and used immediately or stored at -80 $^0$C until further use.

**2.4.12 Immunoprecipitation**

Cell lysates were taken from -80 $^0$C and thawed on ice. Anti-FLAG agarose beads (20 µL of bead slurry; Sigma) were used to pull down overexpressed wild type or mutant

HDAC1 proteins from cell lysates. Beads were washed two times with cold TBS (500 µL; Tris buffered saline; 50 mM Tris-Cl, 150 mM NaCl) by spinning at 5 rcf for 1min. Lysates (2 mg) were mixed with the pre-washed anti-FLAG agarose beads and incubated overnight with rotation at 4 $^0$C. After incubation, beads were washed three times with JLB (1 mL) by spining at 5 rcf for 1 min. The bound proteins were eluted by adding 2X SDS loading dye (25 µL; 100 mM Tris-Cl pH 6.8, 4% SDS, 20% glycerol, 0.008% bromophenol blue) and boiling for 5 min at 95 $^0$C. After a short spin, β-mercaptoethanol (10% v/v) was added, heated at 95 $^0$C for 1 min, and cooled on ice prior to SDS-PAGE. For immunoprecipitation of endogenous proteins, protein A/G plus agarose beads (Santa Cruz; 20 µL bead slurry) were used. Beads were washed similar to anti-FLAG agarose beads. First, lysates were incuabted with the respective antibody for 1 h at 4 $^0$C with rotation. After 1 h, the antibody:lysate mixture was incubated with the pre-washed agarose beads overnight at 4 $^0$C with rotation. The washing and elution was performed similar to FLAG immunoprecipitation.

**2.4.13 Co-Immunoprecipitation**

T-Ag Jurkat lysates (2 mg) were incubated with either HDAC1 (1 µL; 1 µg/µL) or Eg5 (1 µL; dilution-1:300) antibodies at 4 °C for 1 h and then further incubated with prewashed protein A/G plus agarose beads (20 µL bead slurry) overnight at 4 °C to immunoprecipitate each protein. For co-immunoprecipitation of overexpressed proteins, HDAC1-FLAG and Eg5-myc DNA were cotransfected into HEK293 cells, as described, and the myc-tagged Eg5 proteins were immunoprecipitated by incubating lysates (2 mg) with myc antibody (2 µL; dilution-1:150) for 1 h at 4°C. Then, the immunocomplex was further incubated with prewashed protein A/G plus agarose beads (20 µL bead slurry) at

4 °C overnight. FLAG-tagged HDAC1 protein in the lysate (2 mg) was immunoprecipitated using prewashed anti-FLAG agarose beads (20 µL bead slurry; Sigma) by incubating at 4 °C overnight with rocking. Bound beads were washed three times with JLB (1 mL). Bound proteins were eluted by adding 2X SDS loading dye (25 µL), separated by 10% SDS-PAGE, transferred to PVDF membrane (Immobilon P), and immunoblotted with their respective antibodies.

**2.4.14 Sodium Dodecyl Sulfate Polyacrylamide Gel Electrophoresis (SDS-PAGE)**

Prior to pouring the gel, gel plates (1.5 mm; BioRad) were washed well with distilled water and dried using a paper towel. Gel plates were assembled into the gel set up (BioRad) and checked for any leakage using water. If the set up was not leaking, water was removed and dried well using a Kimwipe (KIMTECH). To pour the separating layer of a 10% gel, 2 mL of 4X Tris/SDS separating buffer (0.4% SDS, 1.5 M Tris, 0.24 M HCl; pH 8.8), 2 mL of 40% acrylamide (Omnipur; 37:1), 3.92 mL of double distilled water, 80 µL of 10% (w/v) ammonium persulfate (freshly prepared APS) and 8 µL of N, N, N', N'-tetramethylthylenediamine (TEMED; ACROS) were mixed well, and poured in between glass plates up to ¾ height. Methanol was slowly added on top of the separating layer to create a smooth surface and the gel was allowed to set for 2 h. After 2 h, the methanol was removed and the gel surface was dried well using a Kimwipe. A 5% stacking layer was prepared by mixing 1 mL of 4X Tris/SDS buffer (0.4% SDS, 1.5 M Tris, 0.24 M HCl; pH 6.8), 0.5 mL 40% acrylamide, 2.48 mL double distilled water, 20 µL 10% (w/v) ammonium persulfate, and 4 µL TEMED. The stacking layer was poured on top of the separating layer and a 10 well comb was placed slowly without forming any air bubbles. The gel was allowed to polymerize for 2 h and then immersed in a tank (Biorad) filled with

SDS-running buffer (1X; 0.5% SDS; 0.025 M Tris; 0.05 M glycine). Samples were slowly loaded into the wells along with the pre-stained molecular weight marker (Fisher) as a standard. The gel was first run for 10 min at 120V and then run at 200V for 1 h. After electrophoresis, the gel was subjected to Sypro Ruby staining or western blotting.

**2.4.15 Sypro Ruby staining**

After SDS-PAGE, the gel was removed from the gel plates, rinsed with water, and incubated with fixing solution (40 mL, 50% methanol and 7% acetic acid) at room temperature for 30 min in a rocking platform. Then, the fixing solution was removed and Sypro Ruby total protein stain (Invitrogen) was added. The gel chamber was covered with a foil, and incubated overnight at room temperature on a rocking platform. After removing the staining solution, the gel was immersed in destaining solution (40 mL; 10% methanol and 7% acetic acid) for 30 min at room temperature while rocking. Then, the destaining solution was removed and the gel was washed with distilled water three times (25 mL) to remove remaining acid. The stained gel was scanned using a Typhoon 9210 variable mode imager (Excitation – 450 nm, Emission – 610 nm).

**2.4.16 Western blotting**

Proteins in the gel were transferred to a PVDF membrane (Immobilin P). First, the gel was washed with water (25 mL) and then transfer buffer (1X; 3-[Cyclohexylamino]-1-propanesulfonic acid (CAPS); 900 mL of 1X CAPS and 10% methanol, pH=10.6). Separately, the PVDF membrane was soaked in methanol and then soaked in transfer buffer. Sponges and filter papers were also soaked in the transfer buffer. The gel and membrane were sandwiched between filter papers, and then covered with sponges from two sides. The complete set was immersed in the western blot apparatus (Biorad)

containing transfer buffer and then electrotransferred at 90 V for 2 h. An ice block was inserted from one side to avoid melting of the gel. The whole apparatus was covered with ice to make the transfer efficient. Following electrotransfer, the PVDF membrane was removed, allowed to air dry for a few minutes, wet with methanol briefly, and then soaked in PBST (1X phosphate buffered saline with tween-20; 8 mM $Na_2HPO_4$, 150 mM NaCl, 2 mM $KH_2PO_4$, 3 mM KCl, 0.1% Tween-20). The membrane was blocked with blocking solution overnight at room temperature (10 mL; 5% w/v milk in PBST). Then, the blocking solution was removed, the membrane was washed briefly with PBST, and the membrane was incubated with primary antibody (10 mL; 5% w/v BSA in PBST containing FLAG (1:10000 dilution) or Eg5 (1:1000 dilution), or HDAC1 (1:10000 dilution), or Acetyl lysine (1:1000 dilution), or myc (1:1000 dilution) for 2 h at room temperature or overnight at 4 $^0$C on a rocking platform. The antibody solution was removed and the membrane was washed three times 5 min each with PBST (10 mL). The seconday antibody solution was added, which contained 5% w/v milk in PBST and Alexa fluoro 488 anti-rabbit (1:1000), or Alexa Fluoro 647 anti-mouse (1:1000), or HRP-conjugated anti-rabbit (1:2000), and incubated for 1 h at room temperature on a rocking platform. The solution was removed and the membrane was washed three times 5 min each with PBST (10 mL). The fluorescent signal was observed using a Typhoon 9210 variable mode imager (excitation - 650 nm and emission – 670 nm). The HRP-mediated chemiluminiscence was visualized using a Fluorochem Imager (Alpha Innotech) using the HRP substrate (Pierce; 400 µL).

**2.4.17 Bacterial expression and purification of Eg5**

The bacterial expression plasmid (pRSET) for Eg5 was a generous gift from Dr. Susan Gilbert (104). The bacterial expression construct (pRSET) for Eg5-His was

transformed into *E. coli* BL21 (DE3) (Chapter 2; section 2.4.7). Transformed cells were grown in LB media (5 mL) containing 100 µg/mL ampicillin overnight at 37 $^{0}$C, diluted 200X into fresh LB medium (500 mL) containing 100 µg/mL ampicillin, and incubated at 37 $^{0}$C until the $OD_{600nm}$ reached 0.6. Protein expression was then induced with 0.5 mM isopropyl-1-thio-β-D-galactopyranoside (IPTG) at 30 °C. After 20h of protein production at 30 °C with 250 rpm shaking, cells were harvested by centrifugation at 4000 rpm for 20 min at 4 $^{0}$C. Cells were resuspended in lysis buffer (20 mL; 50 mM Tris-HCl pH 8.3, 300 mM NaCl and 10 mM imidazole) and lysed by double passage through a chilled French press at 1,000 psi. Cell debris was removed by centrifugation at 14,000 rpm for 30 min at 4 $^{0}$C. Ni-NTA beads (Pierce; 2 mL bead slurry) were washed two times with cold TBS (5 mL; Tris buffered saline; 50 mM Tris-Cl, pH 7.4, 150 mM NaCl,) by spining at 5000 rcf for 1 min. The cleared lysate was incubated with prewashed Ni-NTA beads for 2 h at 4 °C. The loaded Ni-NTA beads were washed three times (10 mL) with wash buffer (50 mM Tris-HCl, pH 8.3, 300 mM NaCl, and 25 mM imidazole). His-tagged Eg5 protein was eluted using elution buffer (1 mL each repeated seven times (E1-E7); 50 mM Tris-HCl pH 8.3, 300 mM NaCl, and 300 mM imidazole). Fractions (E1-E7) containing Eg5 were collected and dialyzed overnight against dialysis buffer (50 mM Tris buffer pH 7.4, 10% glycerol and 1 mM DTT). Then, the protein was concentrated using a 10 kDa molecular weight cutoff centrifugal filter device (Millipore). A bradford assay (Bio-Rad) was used to quantify protein concentration using bovine serum albumin as the standard. All the fractions (crude lysate, flowthrough, washes and elutions) were analysed by SDS-PAGE (Figure 2.4).

### 2.4.18 Acetylation of bacterial Eg5 using acetic anhydride

*In vitro* acetylation of Eg5 was first optimized to find the appropriate concentration of acetic anhydride and incubation time. Eg5 (0.5 µg) was incubated with varying amounts of acetic anhydride (0.2 mM, 0.5 mM and 2 mM) in ammonium bicarbonate buffer and 0.002% methanol (50 mM, pH 7) for 30 min or 1 h at room temperature in a volume of 100 µL and analysed by acetyl lysine antibody (Figure 2.5). Incubation of Eg5 with 0.2 mM acetic anhydride for 1 h was selected as the best condition for acetylation. For *in vitro* deacetylation assays, bacterially expressed Eg5 (20 µg) was acetylated by incubating with acetic anhydride (0.2 mM) in ammonium bicarbonate buffer and 0.002% methanol (50 mM, pH 7) for 1 h at room temperature in a volume of 100 µL. Excess acetic anhydride was removed using a 3 kDa molecular weight cutoff centriprep column (Sigma Aldrich Amicon Ultra). Acetylated Eg5 was aliquoted and stored at -80 $^{0}$C until further use.

### 2.4.19 Gel image quantification

Gel bands were quantified using ImageQuant version 5.1. Squares with similar area were drawn around gel bands and the bands in each lane were separately background corrected. The raw value for the control reaction (Ex: Eg5 acetylation without HDAC1) was set to 100% and the percentage signal for other lanes was calculated compared to the control. The percentages of the acetyl lysine signal were divided by the percentage of the total immunoprecipitated protein to get the final percentage value. The average percentages from at least three independent trials are shown in Figures 2.6 and 2.8, with mean and standard error shown in Tables A.2.1, A.2.3 and A.2.5.

### 2.4.20 Substrate trapping and SAHA competition experiments

Following transfection and harvesting as described earlier (Chapter 2; section 2.4.9), cells were lysed as described (section 2.4.11). Immunoprecipitation of HDAC1-FLAG wild type or mutant proteins was performed as described earlier (Chapter 2; section 2.4.12). For SAHA competition reactions, SAHA (final concentration of 0.8 mM) was added during immunoprecipitation. After immunoprecipitation, more stringent washing condtions were used to reduce non-specific binding partners. Bound proteins were washed three times with high salt JLB (1 mL; 50 mM Tris pH 8, 500 mM NaCl, 10% (v/v) glycerol, 0.5 % (v/v) Triton X-100). Bound proteins were separated by SDS-PAGE (Section 2.4.14) and visualized with Sypro Ruby total protein stain (Section 2.4.15)

### 2.4.21 Mass spectrometry analysis

Gel slices containing protein bands were excised from the Sypro Ruby stained gel, washed with destaining buffer (50 µL; 1:1 (v/v) acetonitrile: 50 mM ammonium bicarbonate) for 15 min at room temperature, and dehydrated in acetonitrile (50 µL). The gel pieces were rehydrated with 50 mM ammonium bicarbonate (50 µL) for 5 min and then an equal volume of acetonitrile was added. After incubating at room temperature for 15 min, the gel slices were dehydrated again in acetonitrile (50 µL). After removal of the acetonitrile, the gel slices were dried using a speedvac concentrator (ThermoSavant). Gel slices were swelled with reducing buffer (100 µL; 50 mM TCEP in 25 mM ammonium bicarbonate) for 10 min at 37 °C, followed by incubation with alkylation buffer (100 µL; 55 mM iodoacetamide in 25 mM ammonium bicarbonate) for 1 h at room temperature in the dark while shaking. Then, gel pieces were washed 2 times with destaining buffer (50 µL) for 5 min at room temperature, dehydrated with acetonitrile (50 µL), and dried. To digest

the gel-bound proteins, gel slices were incubated with digestion buffer (50 µL; 20 ng/µL trypsin in 40 mM ammonium bicarbonate and 9% acetonitrile) overnight at 37 °C. The resultant digest solution was collected and the gel pieces were extracted using extraction buffer (50 µL; 50% acetonitrile and 0.2% formic acid (ProteoChem). The combined digestion and extraction solutions were dried and stored at -20 °C in preparation for MS analysis at the Wayne State University and Karmanos Cancer Center Proteomics Core facility.

For MS analysis, dried peptide digests were resuspended in a solution of 5% acetonitrile, 0.1% formic acid, and 0.005% trifluoroacetic acid. Samples were separated by ultra high pressure reverse phase chromatography using an Acclaim PepMap RSLC column and an Easy nLC 1000 UHPLC system (Thermo). Peptides were analyzed with a Q-Exactive mass spectrometer (Thermo) with a 70,000 resolution MS1 scan over 375-1600 m/z, followed by 17,500 resolution MS2 scans using a 1.6 m/z window and 30% normalized collision energy for HCD. Peak lists were generated with Proteome Discoverer (ver 1.4; Thermo), and peptides scored using Mascot (ver 2.4; Matrix Science). The search parameters included parent and fragment ion tolerances of 15 ppm and 0.02 Da, respectively, fixed modification of +57 on C (carbamidomethylation), variable modifications of +16 on M (oxidation), +42 on K and N-termini (acetylation), +80 on STY (phosphorylation), and a tryptic digest with up to 1 missed cleavage. MS2 spectra were searched against a consensus human protein database from SwissProt, and simultaneously against a scrambled database to calculate the false discovery rate (FDR). Results were imported into Scaffold (ver 4.3; Proteome Software) and a subset database search was performed with X!Tandem using slightly wider search parameters (up to 2

missed cleavages; additional variable modifications of -18 and -17 on N-termini (ammonia loss or conversion to pyro-glutamic acid). Protein identification was considered to be positive if at least 1 unique peptide was scored as ≤1% FDR, and the protein threshold was ≤1% FDR (Table 2.1).

### 2.4.22 *In vitro* deacetylation assays

Endogenous HDAC1 and Eg5 were immunoprecipitated separately from T-Ag Jurkat cells using their respective antibodies. Briefly, HDAC1 (1 µL; 1 µg/µL) or Eg5 (1 µL; dilution-1:300) were incubated separately with lysates (2 mg) at 4 °C for 1 h. Then, each lysate was separately added to prewashed Protein A/G agarose beads (20 µL bead slurry, Santa Cruz), incubated overnight at 4 °C, and washed three times with JLB (1 mL). Immunoprecipitated HDAC1 on the beads was resuspended in HDAC assay buffer (100 µL; 50 mM Tris-Cl, pH 8.0, 137 mM NaCl, 2.7 mM KCl, 1 mM $MgCl_2$) and preincubated in the absence (1.2 % DMSO) or presence of SAHA (3 mM in 1.2% DMSO) for 15 min at 30 °C while shaking at 750 rpm. Immunoprecipitated Eg5 on the beads was resuspended in HDAC assay buffer (50 µL), mixed with the preincubated HDAC1 immunoprecipitate, and then incubated at 30 °C for 1 h while shaking at 750 rpm. After incubation, beads were collected by centrifugation and bound proteins were eluted from the beads using SDS loading dye (25 µL; 100 mM Tris-Cl pH 6.8, 4% SDS, 20% glycerol, 0.008% bromophenol blue), resolved by 10% SDS-PAGE (Section 2.4.14), transferred to PVDF membrane (Immobilon P), and immunoblotted with acetyl lysine, HDAC1, or Eg5 antibodies (section 2.4.16).

For the *in vitro* deacetylation assay, recombinant HDAC1 (4 µg, BPS Biosciences) was resuspended in HDAC assay buffer (50 µL; 50 mM Tris-Cl, pH 8.0, 137 mM NaCl,

2.7 mM KCl, 1 mM $MgCl_2$) and preincubated in the absence (2% DMSO) or presence of SAHA (2 mM in 2% DMSO) for 30 min at 37 °C while shaking at 750 rpm. Acetylated Eg5 (1 µg) (Section 2.4.18) was then added and the reaction was incubated at 37 °C for 2 h while shaking at 750 rpm. After incubation, the reaction was stopped by adding 5X SDS loading dye (10 µL; 100 mM Tris-Cl pH 6.8, 4% SDS, 20% glycerol, 0.008% bromophenol blue). The protein products were resolved by SDS-PAGE (10%) (Section 2.4.14), transferred to PVDF membrane (Immobilon P), and immunoblotted with acetyllysine, HDAC1, or Eg5 antibodies (Section 2.4.16).

**2.4.23 Identification of acetylated lysines in Eg5**

To identify the target site of Eg5 regulated by HDAC1, HEK293 cells (at 60% confluency) were transfected with myc-tagged Eg5 plasmid alone or cotransfected with FLAG-tagged wild type HDAC1 and allowed to recover under normal growth conditions for 48 h (section 2.4.10). After the 48 h recovery period, cells were treated without (2% DMSO in growth medium) or with SHI-1:2 (10 µM in 2% DMSO in growth medium) or SAHA (10 µM in 2% DMSO in growth medium) for an additional 24 h before harvesting and washing, as described. Cells were lysed (Section 2.4.11) and Eg5 was immunoprecipitated with myc antibody (Section 2.4.12), separated on a SDS-PAGE gel (10%) (Section 2.4.14), and visualized by Sypro Ruby total protein stain (Molecular Probes) according to the manufacturer's instructions (Section 2.4.15). Bands corresponding to Eg5 were excised from the gel and subjected to in gel digestion and mass spectrometry as described above (Section 2.4.21).

### 2.4.24 ATPase assays

For *in vitro* ATPase assay, HEK293 cells (at 60% confluency) were transfected with myc-tagged wild type or mutant Eg5 plasmid and allowed to recover under normal growth conditions for 48 h. After the 48 h recovery period, cells were treated with SHI-1:2 (10 µM in 2% DMSO in growth media) for an additional 24 h before harvesting and washing, as described. Cells were lysed and Eg5 was immunoprecipitated with myc antibody and bound myc-tagged protein was eluted using myc peptide by incubating at 4 °C for 30 min. Eluted wild type or K890R mutant protein was used in the ATPase assay. ADP-Glo assay was used to measure the amount of ADP produced according to manufacturer's instructions. First, ATPase reaction (20 µL: 0.5 mM ATP, 2 µL from the immunoprecipitated protein) was performed at 37 °C for 30 min in the ATPase reaction buffer (25 mM triethanolamine, 13 mM Magnesium acetate, 1.8 mM DTT). Next, the components were transferred to 96 well plate, glo reagent (20 uL) was added, and incubated at room temperature for 40 min, followed by the addition of kinase detection reagent (40 µL). After 30 min incubation at room temperature, chemiluminiscence readings were taken using the GeNiOS plate reader and the reaction containing no enzyme was used as the background correction. Readings of the wild type Eg5 was set to 1 and the IgG control and K890R activity was calculated relative to wild type.

### 2.4.25 Indirect Immunofluorescence

For endogenous HDAC1 and Eg5 immunofluorescence experiments, HEK293 cells were grown on glass cover slips in 6 well plates (Corning). At 40% confluency, cells were fixed with ice-cold methanol for 15 min at -20 °C, washed three times with PBS (2 mL; 10 mM $Na_2HPO_4$, 1.8 mM $KH_2PO_4$, 137 mM NaCl, 2.7 mM KCl, pH 7.4), and blocked

with 1% bovine serum albumin (GenDEPOT) in PBST (2 mL; PBS containing 0.1% tween-20) for 1 h at room temperature. After blocking, cells were incubated with a mixture of primary antibodies to HDAC1 (1:6000) and Eg5 (1:1000) in PBST overnight at 4 °C (1 mL). After washing 3 times with PBS (2 mL), cells were incubated with a mixture of secondary antibodies in PBST (1 mL; Alexa fluor 488 rabbit antibody and Alexa fluor 647 mouse antibody; 1:500) for 1 h at room temperature. Then, cells were washed three times with PBS (2 mL) and stained with DAPI (1 µg/µL) for 5 min and washed three times with PBS. Glass coverslips were mounted onto slides using ProLong gold antifade mounting solution and stored at 4 °C until use. The slides were visualized using an Olympus inverted IX81 fluorescence microscope (magnification 100X).

For HDAC1-FLAG and Eg5 colocalization experiments, the same procedure was followed except transiently transfected HEK293 cells were fixed with 4% paraformaldehyde (2 mL) for 15 min at room temperature instead of methanol. After fixation, cells were washed three times with PBS (2 mL) and permeabilized by incubating with 0.3% triton X-100 (2 mL) for 10 min at room temperature. After washing three times with PBS, cells were blocked for 1 h at room temperature in PBS containing 5% BSA and 0.3% triton X-100. 1% BSA and 0.3% triton X-100 was used in place of 0.1% tween-20 in the PBST buffer to prepare antibody dilution buffer as well.

To count monopolar spindles, HEK293 cells were treated with DMSO, STLC (10 uM) or SHI-1:2 (10 uM) for 48h. Then, cells were washed with PBS briefly, fixed with 4% paraformaldehyde for 15 min at room temperature, followed by permeabilizing with 0.3% triton-X-100 for 10 min at room temperature. Cells were washed three times with PBS, and blocked with 1% bovine serum albumin (GenDEPOT) in PBST (2 mL; PBS containing

0.3% triton-X-100) for 1 h at room temperature. After blocking, cells were incubated with a primary antibody to α-tubulin overnight at 4 °C, followed by secondary antibody in PBST (1 mL; Alexa fluoro488 rabbit antibody) for 1 h. Then, cells were washed three times with PBS (2 mL) and mounted onto slides using ProLong gold antifade mounting solution. The slides were visualized using an Nikon Eclipse Ni-U Microscope with motorized epifluorescence. Monopolar spindles were counted from atleast 100 mitotic cells and presented as a percentage. Monopolar spindles seen in STLC treated samples were set to 100% and monopolar spindles seen with SHI-1:2 was presented relative to STLC.

**2.4.26 Cell cycle analysis using Flow Cytometry**

HEK293 cells were treated with DMSO, STLC (10 uM) or SHI-1:2 (10 uM) for 48 h, harvested and washed with PBS twice. Cells (2 X $10^6$) were fixed with 70% ethanol overnight at 4 °C and proceed to staining. Fixed cells were washed once with cold PBS (500 uL) and permeabilized with 0.25% Triton X-100 (in PBS) for 15 min on ice followed by incubation with the antibody to phospho histone H3 (S10) conjugated to Alexa Fluor 488 (100 uL) for 1 h. After washing with PBS once, cells were stained with DAPI (1 µg/mL) overnight at 4 °C. Flow cytometry analysis was performed at Microscopy, Imaging and Cytometry resources core at the Karmanos Cancer Institute, Wayne State University. Samples were run on BD LSR II analytical flow cytometer (BD Biosciences, San Jose, CA) and analyzed by ModFit LT v4.0 (Verity Software House, Topsham, ME) and FlowJo v10 (FlowJo, LLC, Ashland, OR) software.

To study the effect of wild type and mutant Eg5 on cell cycle arrest, HEK293 cells (at 60% confluency) were transfected with myc-tagged wild type or mutant Eg5 plasmid and allowed to recover under normal growth conditions for 48 h. After the 48 h recovery

period, cells were treated without (2% DMSO) or with SHI-1:2 (10 µM in 2% DMSO in growth media) for an additional 48 h. Cells were harvested, washed and fixed overnight at 4 °C with 70% ethanol. Staining of phospho histone H3 and DAPI was performed and analyzed by flow cytometry as described in the above paragraph.

# CHAPTER 3. HDAC1- MEDIATED DEACETYLATION OF LSD1 AFFECTS SUBSTRATE BINDING AND GENE EXPRESSION

(A portion of this chapter is reprinted or adapted from Nalawansha, D. A. *et al.* 2016, LSD1 substrate binding and gene expression are affected by HDAC1-mediated deacetylation, *ACS Chem. Biol*., *in revision*)

## 3.1 Introduction

In Chapter 2, a substrate trapping mutant strategy was performed with HDAC1 to identify Eg5/Kinesin 5 as a novel HDAC1 substrate in Jurkat cells (105). Given the significance of identifying non-histone substrates to explore the role of HDAC1 in the cell, we extended this HDAC1 trapping strategy to HEK293 cells. In this chapter, lysine specific histone demethylase 1 (LSD1) was identified as a novel substrate of HDAC1 using trapping mutants to reveal a previously unidentified crosstalk between HDAC1 and LSD1.

## 3.2 Results

### 3.2.1 Substrate trapping identifies novel substrates of HDAC1 in HEK293 cells

For HEK293 trapping, wild type and mutant HDAC1 were overexpressed in HEK293 cells, and then cells were treated with SAHA to induce robust acetylation. SAHA treatment increases the number of acetylated proteins in the cell to augment the ability to trap HDAC substrates. Wild type and mutant HDAC1 were immunoprecipitated in the presence or absence of SHI-1:2 as an active site inhibitor. This active site inhibitor competes with bound substrates and assists in distinguishing substrates from interacting proteins. Bound substrates present in the mutant but not wild type or inhibitor immunoprecipitate were visualized using gel methods. Among the several inactive HDAC1 mutants screened (H141A, F150A and C151A), C151A HDAC1 displayed good

substrate trapping properties in HEK293 cells (Figure 3.1, lane 3). Therefore, the C151A mutant was selected for further trapping studies.

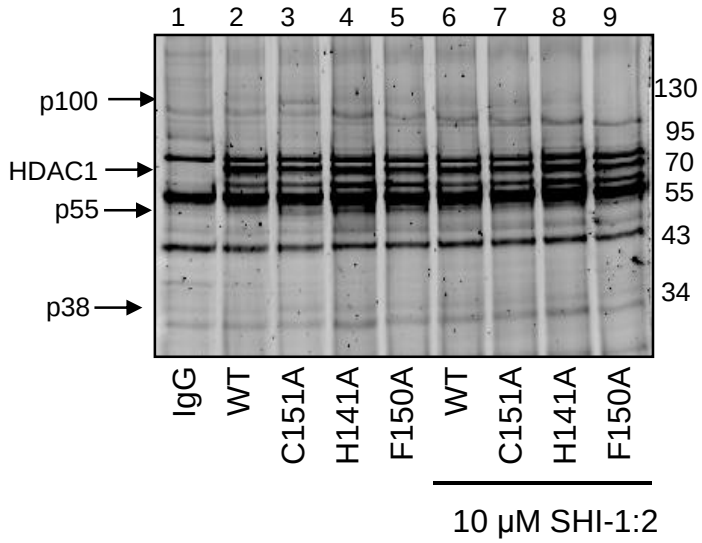


**Figure 3.1– Screening inactive mutants in HEK293 cells**. Wild type (WT) or mutant HDAC1 (indicated below each lane) were expressed as Flag-tagged proteins in HEK293 cells and then cells were treated with 10 μM SAHA for 24 h to induce robust protein acetylation. Cells were lysed and proteins were immunoprecipitated with anti-Flag agarose in the presence or absence of 10 μM SHI-1:2. Bound proteins were separated by SDS-PAGE, and stained with Sypro Ruby total protein stain. Arrows point to HDAC1 or possible substrates (p100, p55, p38) present in mutant but not WT or inhibitor treated samples. Repetitive trials are shown in Figure A.3.1.

Three new bands (p100, p55 and p38) appeared only in the C151A mutant, but not in the wild type immunoprecipitates (Figure 3.2A, compare lanes 1 and 2). The p100, p55 and p38 bands disappeared when SAHA (Figure 3.2A, compare lanes 2 and 4) or HDAC1 and 2-selective inhibitor (SHI-1:2) (Figure 3.2B, compare lanes 2 and 4) was used

as an active site competitor, suggesting that these proteins interact directly with the active site of HDAC1 and could be potential substrates.

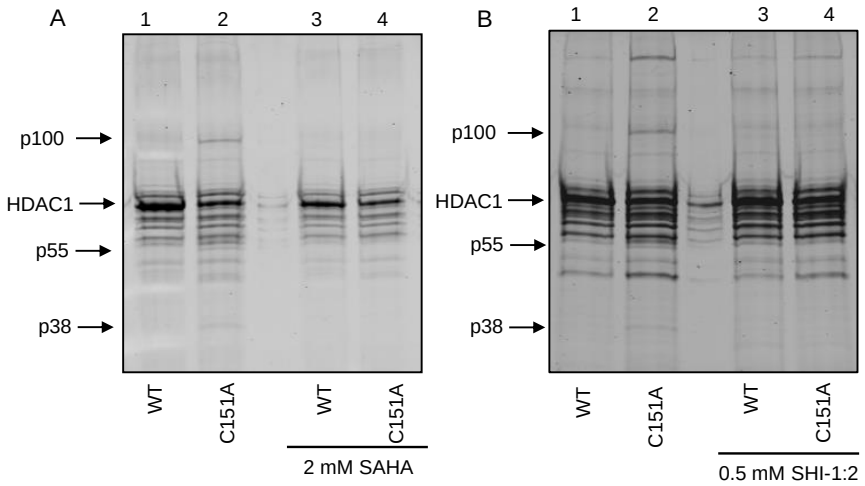


**Figure 3.2–Substrate trapping in HEK293 cells**. Wild type (WT) or mutant HDAC1 (indicated below each lane) were expressed as Flag-tagged proteins in HEK293 cells and then cells were treated with 10 µM SAHA for 24 h to induce robust protein acetylation. Cells were lysed and proteins were immunoprecipitated with anti-Flag agarose in the presence or absence of A) 2 mM SAHA, or B) 0.5 mM SHI-1:2. Bound proteins were separated by SDS-PAGE, and stained with sypro ruby total protein stain. Arrows point to HDAC1 or possible substrates (p100, p55, p38) present in mutant but not WT or inhibitor treated samples. Repetitive trials are shown in Figure A.3.2.

To confirm the selectivity of bound substrates, we used HDAC1 and 2-selective inhibitor (SHI-1:2) and HDAC6-selective inhibitor (tubastatin) as competitors (Figure 3.3). The p100, p55 and p38 bands were observed only in the presence of tubastatin, suggesting that they are substrates of HDAC1 (Figure 3.3, compare lanes 2 to 3 and 4).

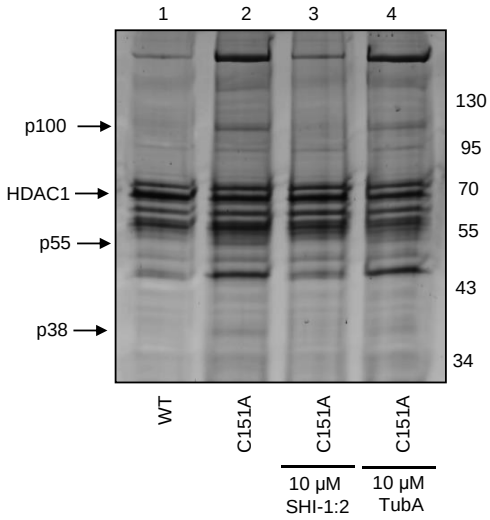


**Figure 3.3– Substrate trapping with inhibitor competition in HEK293 cells**. Wild type (WT) or mutant HDAC1 (indicated above each lane) were expressed as Flag-tagged proteins in HEK293 cells and then cells were treated with 10 μM SAHA for 24 h to induce robust protein acetylation. Cells were lysed and proteins were immunoprecipitated with anti-Flag agarose in the presence or absence of 10 μM SHI-1:2 or 10 μM tubastatin. Bound proteins were separated by SDS-PAGE, and stained with sypro ruby total protein stain. Arrows point to HDAC1 or possible substrates (p100, p55, p38) present in mutant but not WT or inhibitor treated samples. Repetitive trials are shown in Figure A.3.2.

To identify the p100, p55, and p38 proteins interacting with C151A HDAC1, the gel bands were excised, trypsin digested, and subjected to LC-MS/MS analysis. With high confidence, p38, p55 and p100 were identified as rRNA 2'-O-methyltransferase fibrillarin (histone-glutamine methyltransferase), RuvB-like 2 (reptin 52), and lysine specific histone demethylase 1 (LSD1 or KDM1A), respectively (Table 3.1, Figures A.3.3-A.3.8). For all three hits, sequence coverage was higher in the mutant compared to wild type, suggesting effective trapping by the mutant.

**Table 3.1- Mass spectrometric analysis of p100, p55 and p38***

| Protein band | Protein name (Accession) | MW (kDa) | Sample | Unique peptide count* | Unique spectral count# | % Coverage€ |
|---|---|---|---|---|---|---|
| p100 | Lysine specific histone demethylase 1A (LSD1) (KDM1A_HUMAN) | 93 | HDAC1 (WT) | 6 | 6 | 11 |
| | | | C151A | 26 | 31 | 43 |
| p55 | RuvB- like 2 (RUVB2_HUMAN) | 51 | HDAC1 (WT) | 3 | 3 | 8 |
| | | | C151A | 10 | 13 | 25 |
| p38 | rRNA 2'-O-methyltransferase fibrillarin (FBRL_HUMAN) | 34 | HDAC1 (WT) | 1 | 1 | 3 |
| | | | C151A | 6 | 7 | 26 |

***Unique peptide count** – Number of different amino acid sequences that are associated with a protein. #**Unique spectral count** – Number of unique spectra that identified each unique peptide including modifications. €**% Coverage** – the percentage of the protein amino acid sequence was identified.

rRNA 2'-O-methyltransferase fibrillarin is capable of methylating RNA and proteins (106,107). Fibrillarin mediates the methylation of glutamine 104 in histone H2A and disrupts its interaction with the FACT (Facilitator of chromatin transcription) complex involved in transcription. RuvB-like 2 is a component of the NuA4 histone acetyltransferase complex that mediates the acetylation of histone H2A and H4 (108). RuvB-like 2 protein also possesses ATP-dependent DNA helicase activity (109) and is found in a complex with the INO80 chromatin remodeling complex (110). LSD1 is a histone lysine demethylase, typically found in association with HDAC1/2 and CoREST to mediate H3K4 demethylation and regulate gene expression (Figure 3.4) (111). The fact that LSD1 and HDAC1 are found in the same complex in cells is consistent with a possible substrate relationship. We selected the LSD1 protein for further validation due to its

important role in gene expression regulation, as well as implications in diseases such as cancer (12,112).

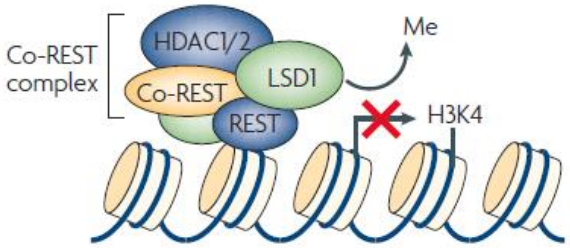


**Figure 3.4 - LSD1 mediates the demethylation of lysine 4 of histone H3.** LSD1 is typically found in complex with HDAC1, HDAC2 and CoREST to mediate the demethylation (Me) of lysine 4 of Histone H3 (H3K4), which leads to gene repression. Copyright permission obtained from *Klose, R. J. et al. Nat. Rev. Mol. Cell. Biol*. 2007, 8 (113).

### 3.2.2 Validation of p100 as LSD1

I confirmed that the p100 protein is in fact LSD1 using substrate trapping. Wild type and mutant HDAC1 were overexpressed in HEK293 cells, immunoprecipitated in the presence or absence of SHI-1:2, and the bound p100 was analysed by western blotting (Figure 3.5). Consistent with the MS data, LSD1 was trapped only by the C151A mutant, but not by the WT HDAC1 (Figure 3.5, top, compare lanes 2 and 3). SHI-1:2 treatment decreased LSD1 trapping (Figure 3.5, top, compare lanes 3 and 5), suggesting that LSD1 interacts with the active site of HDAC1. This LSD1 Western blot analysis confirmed that LSD1 is trapped by HDAC1 mutants.

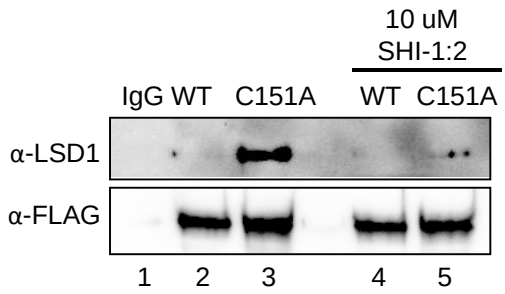


**Figure 3.5 – Validation of p100 as LSD1.** Wild type (WT) or C151A HDAC1 were expressed as Flag-tagged proteins in HEK293 cells, and cells were treated with 10 μM SAHA for 24 h prior to harvesting. FLAG-tagged wild type and mutant HDAC1 were immunoprecipitated with anti-Flag agarose in the presence or absence of 10 μM SHI-1:2, separated by SDS-PAGE, and immunoblotted with LSD1 and FLAG antibodies. Repetitive trials are shown in Figure A.3.9.

### 3.2.3 HDAC inhibitors regulate LSD1 acetylation

Since LSD1 must be acetylated to act as an HDAC1 substrate, we analyzed the acetylation status of LSD1. FLAG-tagged LSD1 was transfected into HEK293 cells and cells were treated with HDAC1 and 2-selective inhibitor (SHI-1:2), as well as broad spectrum HDAC inhibitor-SAHA, to induce acetylation prior to harvesting. FLAG-tagged LSD1 was immunoprecipitated with anti-FLAG agarose beads and immunoprecipitates were analyzed by FLAG and acetyl lysine antibodies. The pan HDAC inhibitor SAHA enhanced LSD1 acetylation (Figure 3.6, top, compare lanes 2 vs 4), confirming that HDAC proteins regulate acetylation of LSD1. Interestingly, the HDAC1 and 2-selective inhibitor (SHI-1:2) was also capable of inducing LSD1 acetylation (Figure 3.6, top, compare lanes 2 vs 3), consistent with the hypothesis that LSD1 is an HDAC1 substrate.

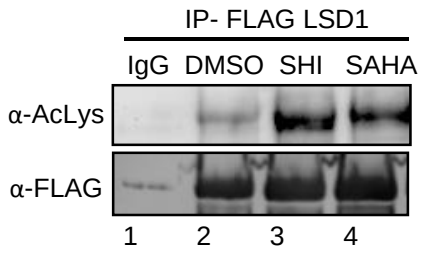


**Figure 3.6 – HDAC inhibitors regulate LSD1 acetylation**. HEK293 cells were transfected with FLAG-LSD1 and grown for 48 h. Then 10 μM SHI-1:2 and 10 μM SAHA were added for another 24 h. Cells were harvested and FLAG-LSD1 was immunoprecipitated with anti-FLAG agarose beads. Immunoprecipitates were analyzed by western blotting with FLAG and acetyl lysine antibodies. Repetitive trials are shown in Figure A.3.10.

### 3.2.4 LSD1 is a substrate of HDAC1

To confirm that HDAC1 deacetylates LSD1, we performed an *in vitro* deacetylation assay using recombinant LSD1 (rLSD1: a gift of Dr. Ryuji Hamamoto) and recombinant HDAC1 (rHDAC1). rLSD1 was chemically acetylated using acetic anhydride. Acetylated rLSD1 was incubated in the absence or presence of rHDAC1. As a control, rHDAC1 was pre-incubated with or without SAHA prior to the incubation with acetylated rLSD1. Acetylation of rLSD1 was significantly reduced in the presence of rHDAC1 (Figure 3.7A, top, compare lanes 1 and 2), but not SAHA-treated rHDAC1 (Figure 3.7A, top, compare lanes 2 and 3), suggesting that HDAC1 deacetylates LSD1. Quantification of acetylated LSD1 also confirmed that HDAC1 significantly reduces LSD1 acetylation (Figure 3.7B and Figure A.3.12A). These data indicate that LSD1 is a substrate of HDAC1.

To validate that LSD1 is a substrate of HDAC1 *in cellulo*, we performed deacetylation assays using cellular LSD1 and HDAC1. FLAG-tagged LSD1 was

overexpressed in the absence or presence of wild type or C151A mutant HDAC1. LSD1 was immunoprecipitated from HEK293 cells, separated by SDS-PAGE, and analyzed by Western blotting with acetyl lysine antibodies. Acetylation of LSD1 was markedly reduced in the presence of WT HDAC1 (Figure 3.7C, top, compare lanes 2 and 3), but not with the catalytically inactive mutant (Figure 3.7C, top, compare lanes 2 and 4). Quantification of acetylated LSD1 also confirmed that HDAC1 significantly reduces LSD1 acetylation (Figure 3.7D and Figure A.3.14A). The fact that LSD1 acetylation depended on the presence of active HDAC1 supports the conclusion that LSD1 is a substrate of HDAC1.

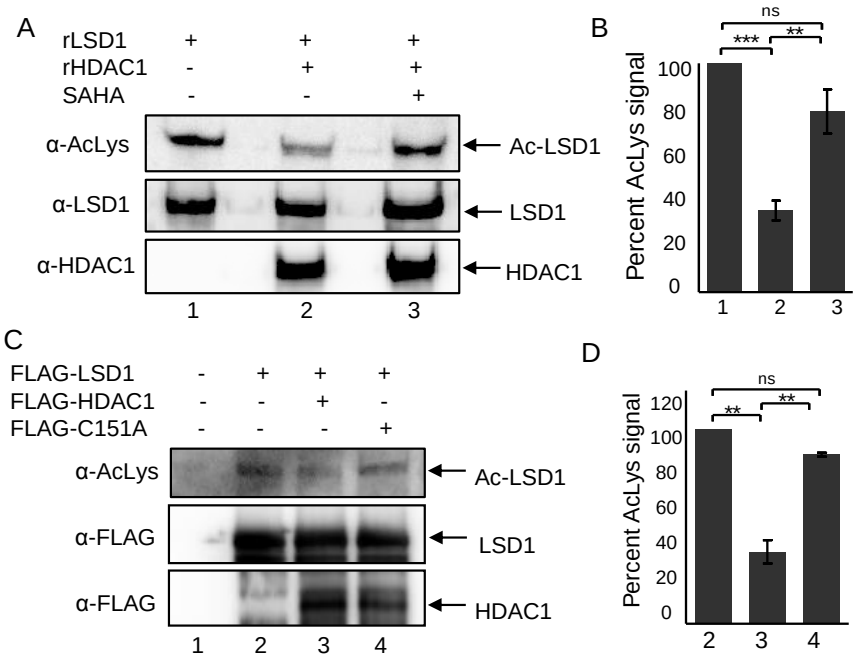


**Figure 3.7 – LSD1 is a substrate of HDAC1.** A) Acetylated recombinant LSD1 was incubated with or without recombinant HDAC1 and SAHA for 2.5 h at 37 °C and separated by SDS-PAGE and analysed by AcLys, HDAC1, and LSD1 antibodies. Repetitive trials are shown in Figure A.3.11. B) Quantification of AcLys LSD1 signal from part A. Three independent trials are shown as mean ± standard error in Figure A.3.12A. LSD1 blot was used as a loading control and quantification is shown in Figure A.3.12B and C. **p<0.01,

***p<0.001, ns-not significant. C) FLAG-tagged wild type (WT) or C151A mutant HDAC1 were cotransfected with FLAG-tagged wild type LSD1 into HEK293 cells. FLAG tagged proteins were immunoprecipitated using anti-FLAG agarose beads, separated by SDS-PAGE, and immunoblotted with acetyl lysine (AcLys) and FLAG antibodies. Repetitive trials are shown in Figure A.3.13. D) Quantification of AcLys LSD1 signal from part C. Three independent trials are shown as mean ± standard error in Figure A.3.14A. LSD1 blot was used as a loading control and quantification is shown in Figure A.3.14B and C. **p<0.01, ns-not significant.

### 3.2.5 HDAC inhibitors affected LSD1 activity *in cellulo*

Acetylation has been demonstrated to regulate protein activity, stability, and interactions (70). As a first step to understand the role of acetylation on LSD1, we studied the effect of HDAC-mediated acetylation on LSD1 demethylation activity. FLAG-tagged LSD1 was overexpressed in HEK293 cells, and cells were treated with HDAC inhibitors to induce robust acetylation prior to harvesting. FLAG-LSD1 was immunoprecipitated with anti-FLAG agarose beads before use as the enzyme source in demethylation assays. LSD1 activity was comparable in SHI-1:2 or SAHA-treated samples and DMSO samples (Figure 3.8). These data indicate that acetylation of LSD1 does not significantly alter its *in vitro* demethylation activity.

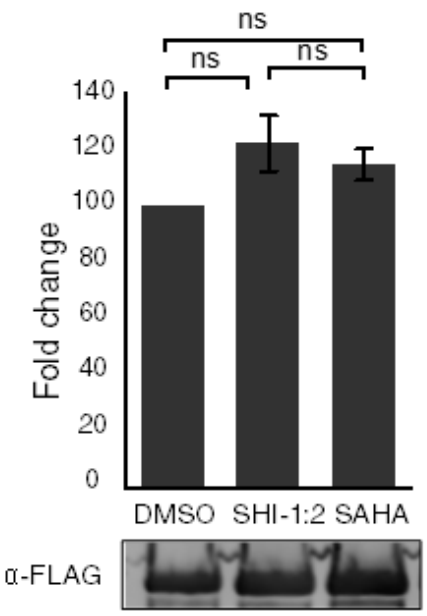


**Figure 3.8 - *In-vitro* demethylation assay of LSD1**. HEK293 cells were transfected with FLAG-LSD1 and grown for 48 h. Then 10 µM SHI-1:2 or 10 µM SAHA was added for another 24 h, cells were harvested and proteins were immunoprecipitated with anti-FLAG agarose beads. Half of the immunoprecipitate was subjected to LSD1 activity assay (histogram); the other half was analyzed by western blotting with FLAG antibody (gel image). The fluorescence signal was background corrected using a reaction with all the components except the LSD1 enzyme. The background corrected signal of each sample was normalized to DMSO treated LSD1 enzyme (set to 1). The mean and the standard error from at least three independent trials are shown. ns – not significant. Percent demethylation activity, mean and standard error for independent trials are shown in the Table A.3.1.

In addition to the *in vitro* demethylation assay, which utilizes a histone H3 peptide substrate, we analysed LSD1 demethylase activity *in cellulo* by monitoring dimethylated histone H3 (H3K4me2) protein in different cell lines. HeLa, MCF-7, or HEK293 cells were treated with SHI-1:2 or SAHA to promote robust acetylation. Cell lysates were then

analysed for methylated H3 using gel methods (H3K4me2) (Figure 3.9). Consistent with previous work (114), HDAC inhibitors enhanced H3K4me2 levels in the three cell lines (Figure 3.9A and 3.9B, H3K4me2 blot, compare lanes 1 to 2 and 3, Figure 3.9C, H3K4me2 blot, compare lanes 2 to 3 and 4), suggesting reduced demethylase activity upon inhibitor treatment. These results suggest that HDAC proteins do have a direct impact on LSD1 activity, albeit not through alteration of its catalytic function. In addition to H3K4me2 mark, we also analyzed the effect of HDAC inhibitors on H3K9me2, which is also regulated by LSD1. In contrast, the effect of HDAC inhibitors on dimethylated lysine 9 of H3 (H3K9me2) was inconsistent (Figure 3.9A and B, H3K9me2 blots), although H3K9 acetylation was consistently elevated (Figure 3.9, H3K9ac blots). Given that LSD1 mainly target H3K4me2 mark when it is in complex with HDAC1 and 2, we did not study H3K9me2 mark further.

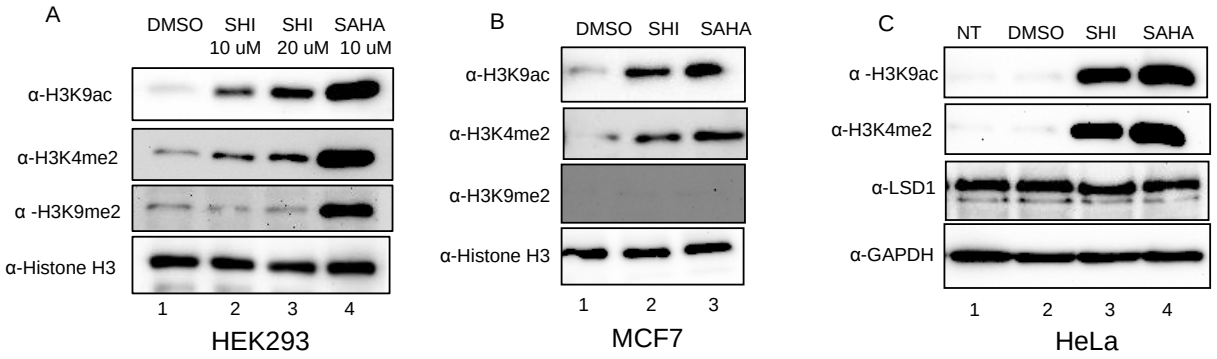


**Figure 3.9 – HDAC inhibitors increase methylation of H3K4 in lysates**. A) HEK293, B) MCF7, or C) HeLa cells were untreated (NT) or treated with DMSO, 10 µM SHI-1:2, or 10 µM SAHA for 24 h, harvested, lysed and proteins were separated by SDS-PAGE followed by immunoblotting with LSD1, histone H3, Histone H3K4me2, histone H3K9ac and GAPDH antibodies. Repetitive trials are shown in Figure A.3.15.

### 3.2.6 LSD1 acetylation altered histone H3 binding ability

*In cellulo* demethylation assays suggested that acetylation of LSD1 affects its enzymatic activity (Figure 3.9) whereas *in vitro* assays showed that acetylated LSD1 retains robust catalytic activity (Figure 3.8). Acetylation of a protein may also affect protein-protein interactions or substrate binding (70). LSD1 activity is regulated by binding to the CoREST protein (111)**.** To assess if LSD1 activity is reduced due to changes in protein-protein associations, coimmunoprecipitation studies were performed. FLAG-tagged LSD1 was overexpressed in HEK293, and cells were treated with HDAC inhibitors to induce acetylation. Cells were harvested and FLAG-LSD1 was immunoprecipitated with anti-FLAG agarose beads. Proteins were separated by SDS-PAGE and immunoblotted with antibodies to CoREST, in addition to the H3 substrate as a control (Figure 3.10). Acetylation did not affect the LSD1/CoREST interaction (Figure 3.10A, CoREST blot, compare lane 2 to 3 and 4). In contrast, HDAC inhibitors altered the interaction between LSD1 and its cellular substrate histone H3 (Figure 3.10A, Histone H3 blot, compare lane 2 to 3 and 4). These data indicated that HDAC inhibitor-mediated acetylation of LSD1 has a direct effect on the interaction between LSD1 and Histone H3. Further, co-immunoprecipitated H3 in SHI-1:2 and SAHA treated cells displayed elevated methylation at lysine 4 compared to DMSO control (Figure 3.10A, H3K4me2 blot, compare lane 2 to 3 and 4), suggesting a loss of LSD1 enzyme function. These data revealed that acetylation alters the substrate binding ability of LSD1, which diminishes its demethylation activity.

To further study acetylation-dependent LSD1/H3 binding, we analyzed the effect of HDAC inhibitors on the H3 interaction with endogenous LSD1. Endogenous LSD1 was immunoprecipitated from HDAC inhibitor treated HEK293 or HeLa cell lysates and analyzed

by Western blot (Figure 3.10B and C). Similar to overexpressed LSD1, endogenous LSD1 interacted more robustly with H3 and methylated H3K4 upon HDAC inhibitor treatment (Figure 3.10B and C, H3 and H3K4me2 blots, compare lane 2 with lanes 3 and 4). These data are consistent with the hypothesis that LSD1 acetylation alters its interaction with H3 and thus the methylation of H3K4. In addition, the similar results obtained with both HEK293 and HeLa cells showed that the acetylation-dependence of H3 binding and methylation is general.

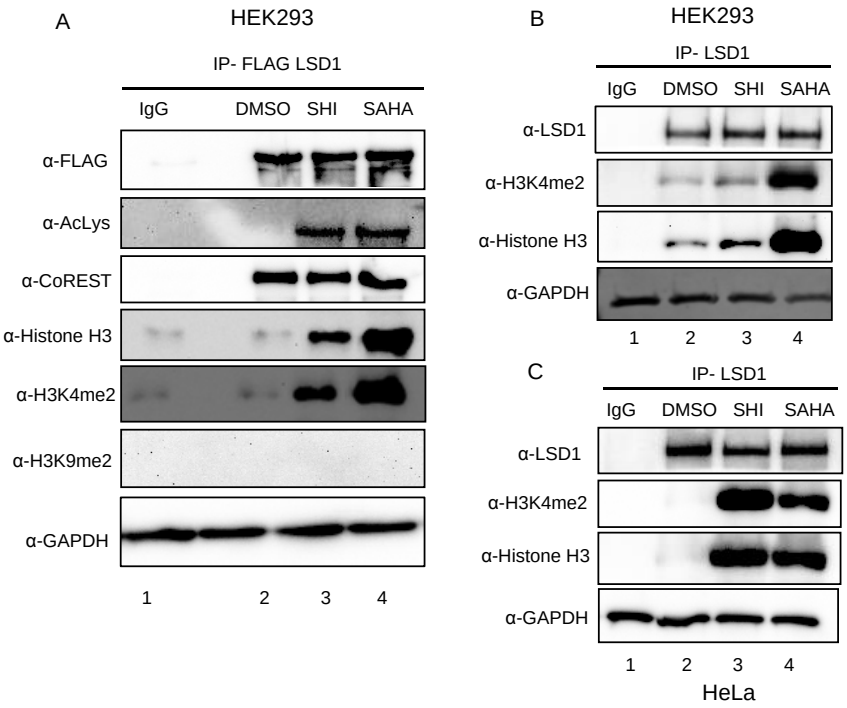


**Figure 3.10 – Acetylation of LSD1 induces LSD1-H3 interaction**. A) FLAG-LSD1 was overexpressed in HEK293 and cells were untreated (IgG) or treated with DMSO or HDAC inhibitors to induce acetylation. Cells were harvested and proteins were immunoprecipitated with anti-FLAG agarose beads. Immunoprecipitates were analyzed by Western blotting with FLAG, acetyl lysine, histone H3, histone H3K4me2, histone H3K9me2, and CoREST antibodies. B) HEK293 cells or C) HeLa cells were treated with HDAC inhibitors, harvested,

and endogenous LSD1 was immunoprecipitated. Western blotting was performed with LSD1, histone H3, and histone H3K4me2 antibodies. GAPDH was used as a loading control. Repetitive trials are shown in Figures A.3.16 and A.3.17.

### 3.2.7 Acetylation of LSD1 at K374 affects histone H3 binding

To fully understand the effect of LSD1 acetylation on Histone H3 binding, we utilized a mass spectrometric based approach to identify acetylated lysines on LSD1. FLAG-tagged LSD1 was transfected into HEK293 cells and cells were then treated with or without HDAC inhibitors. After lysis, immunoprecipitation, and SDS-PAGE separation, protein bands corresponding to LSD1 were excised from the gel, trypsin digested, and subjected to mass spectrometric (MS) analysis. Both SAHA and SHI-1:2 enhanced acetylation of LSD1 at K374 compared to untreated samples, suggesting that K374 is the target site for HDAC1 mediated deacetylation (Table 3.2, Figure A.3.18). K374 is a solvent exposed amino acid which lies in an α-helix (Sα1) in the substrate binding lobe of LSD1 (Figure 3.11A). Previous studies have shown the involvement of this α-helix in histone H3 binding (115-118).

**Table 3.2- MS analysis of LSD1 acetylation***

| Protein name/ Accession | Trials | Sample | % Coverage | Unique # of acetylated peptides |
|---|---|---|---|---|
| Lysine Specific histone demethylase 1 (LSD1) (KDM1A_HUMAN) | 1 | LSD1+DMSO | 90 | 3 (K6, K268, K280) (K374 covered, but no acetylation) |
| | | LSD1+SHI-1:2 | 94 | 6 (K6, K268, K280, K374, K404, K503, K507) |
| | | LSD1+SAHA | 59 | 0 (K374 not covered) |
| | 2 | LSD1+DMSO | 71 | 0 (K374 covered, but no acetylation) |
| | | LSD1+SHI-1:2 | 84 | 3 (K268, K374, K404) |
| | | LSD1+SAHA | 75 | 0 (K374 covered, but no acetylation) |
| | 3 | LSD1+DMSO | 75 | 0 (K374 covered, but no acetylation) |
| | | LSD1+SAHA | 79 | 1 (K374) |

***% Coverage** – the percentage of the protein amino acid sequence was identified. Unique # of acetylated peptides - number of different amino acid sequences containing acetylated lysines. Red color represents the acetylated lysines identified reproducibly only in HDAC inhibitor treated samples. Spectra shown in Figure A.3.18.

To study whether acetylation at K374 is a major site regulated by HDACs, we created a K374R mutant using the full length FLAG-tagged LSD1 construct. Following transfection of wild type LSD1 and K374R into HEK293 cells, HDAC inhibitors were added to induce LSD1 acetylation in cells. Then, LSD1 was immunoprecipitated and immunoblotted with an acetyl lysine antibody to detect acetylation. As anticipated, the level of acetylation of K374R was significantly reduced after HDAC inhibitor treatment, compared to that of wild type LSD1 (Figure 3.11B, top, compare lanes 3 and 4 to 6 and 7). These data suggest that K374 is a major HDAC-dependent acetylation site on LSD1.

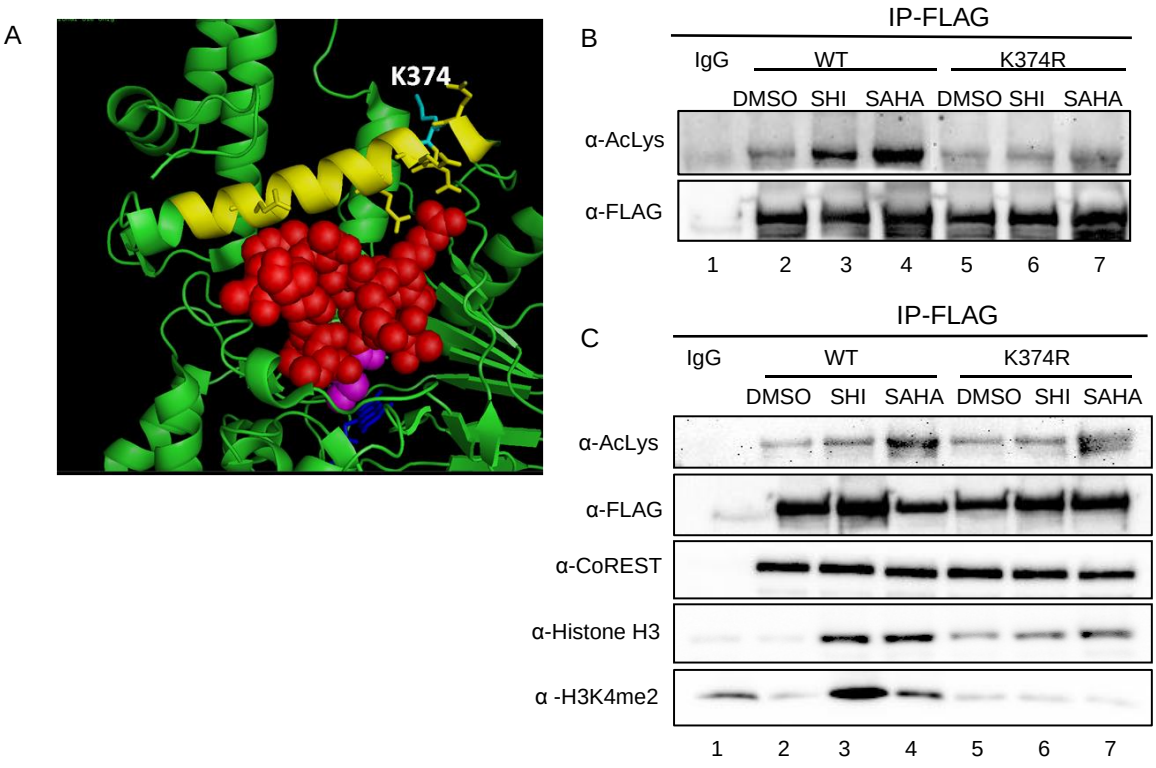


**Figure 3.11 – Acetylation at K374 alters LSD1/H3 interaction.** A) **A** crystal structure of LSD1 (2V1D-green) bound to histone H3 (red spheres) and FAD (dark blue). K374 (light blue) is solvent exposed and present in the Sα1 helix (yellow) of the substrate binding lobe. B) and C) FLAG-tagged wild type or K374R mutant LSD1 were transfected into HEK293

cells, and cells were treated with HDAC1/2 selective inhibitor (SHI-1:2) or SAHA. FLAG-LSD1 was immunoprecipitated with FLAG antibody, subjected to SDS-PAGE separation, and immunoblotting with the indicated antibodies. Repetitive trials are shown in Figures A.3.16 and A.3.19.

To test the effect of acetylation at K374 on LSD1/H3 interaction, HEK293 cells were transfected with WT or K374R mutant FLAG-LSD1, treated with SHI-1:2 or SAHA, and harvested, before LSD1 was immunoprecipitated and analyzed by western blotting (Figure 3.11C). Consistent with the hypothesis, the K374R LSD1 mutant coimmunoprecipitated reduced histone H3 compared to wild type (WT) (Figure 3.11C, Histone H3 blot, compare lanes 3 and 4 to 6 and 7). Methylated lysine 4 of histone H3 (H3K4me2) is higher in HDAC inhibitor treated WT compared to that of mutant LSD1 (Figure 3.11C, H3K4me2 blot, compare lanes 3 and 6) suggesting loss of LSD1 activity. The data indicate that K374 acetylation of LSD1 is critical for altered histone H3 binding. Given the placement of K374 in the histone H3 binding Sα1 helix (Figure 3.11A, yellow helix), we hypothesize that K374 acetylation results in non-productive binding between LSD1 and histone H3, thereby leading to elevated H3 methylation.

### 3.2.8 Acetylation of LSD1 at K374 reactivates expression of LSD1 target genes

LSD1 represses target genes through demethylation of lysine 4 in histone H3. Based on the altered LSD1 binding and consequent methylation of histone H3 at lysine 4 of the K374R mutant, we hypothesize that acetylation of LSD1 affects the expression of downstream target genes. Because SCN3A and SCN2A are two known target genes of LSD1 (111,112), we analyzed their expression using real time-PCR (RT-PCR). HEK293 cells were transfected with WT or K374R mutant FLAG-LSD1, treated with SHI-1:2, and

harvested; then RNA was isolated, converted to cDNA, and used as the template in PCR reactions using gene specific primers. Consistent with the hypothesis, SHI-1:2 treatment resulted in increased expression of both SCN2A (5.4 ± 1 fold) and SCN3A (2.4 ± 0.1 fold) compared to the DMSO control with the wild type LSD1 (Figure 3.12A and B). In contrast, SHI-1:2 treatment showed values comparable to the DMSO control in the presence of the K374R mutant LSD1 (Figure 3.12B, column 4). These data suggest that K374 is critical for efficient HDAC inhibitor-dependent LSD1 gene regulation. Taken together with earlier co-immunprecipitation studies, we hypothesize that LSD1 acetylation at K374 alters LSD1/H3 binding, augments the active chromatin mark H3K4me2, and reactivates the expression of LSD1 target genes.

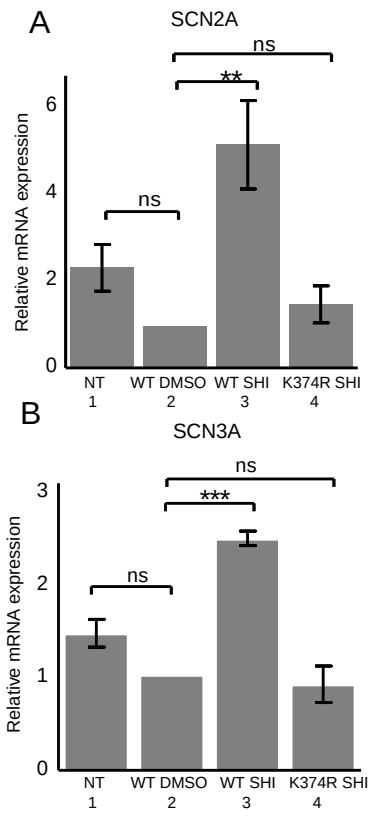


**Figure 3.12- Acetylation of LSD1 at K374 reactivates expression of LSD1 target genes.** HEK293 cells were transfected with WT or K374R mutant FLAG-LSD1, treated with SHI-1:2, and harvested, before RNA was isolated from cells, converted to cDNA, and then used as the template in PCR reactions using gene specific primers for SCN2A (A), SCN3A (B) and GAPDH genes. Fold change was calculated compared to DMSO treated WT LSD1 transfected sample, which is normalized to 1 (column 2). Relative mRNA expression was calculated from four independent trials with mean and standard error shown in Table S3. **p<0.01, ***p<0.001, ns-not significant. Data summarized in Table A.3.2 and A.3.3.

### 3.3 Discussion

Aberrant expression of HDAC1 is implicated in multiple diseases, which have made HDAC1 an interesting drug target (119). Substrate identification is important to unravel new functions of HDAC1 in the cell, and to reveal the mechanism of action of HDAC

inhibitor drugs. We employed a substrate trapping strategy with HDAC1 in HEK293 cells and discovered that LSD1 is a substrate of HDAC1. LSD1 was the first identified histone demethylase and mediates the removal of methylation on H3K4 and H3K9 to regulate gene expression (112). Given that both HDAC1 and LSD1 are overexpressed in multiple cancers (119-122), uncovering the mechanistic link between HDAC1 and LSD1 will lead to a better understanding of the functions of these epigenetic enzymes in normal and disease settings.

LSD1 is typically found in association with HDAC1, HDAC2, BRAF35 and CoREST (111). Previous reports indicated that LSD1 activity and substrate specificity can be regulated by its interacting proteins (111,123,124). CoREST is important for maintaining LSD1 activity and protects LSD1 from proteasomal degradation. HDAC5 also interacts with LSD1 and protect LSD1 from proteasomal degradation to promote breast cancer progression (125). Further, HDAC5 deacetylates LSD1 *in vitro*, but failed to do so *in cellulo*, suggesting LSD1 acetylation might be regulated by other deacetylases. In this report, HDAC1 was able to deacetylate LSD1 both *in vitro* and *in cellulo,* suggesting that HDAC1 is the deacetylase responsible for regulating LSD1 activity. Further, we show for the first time that LSD1 is acetylated at K374 and leads to non-productive binding between histone H3 and LSD1. Altered H3 binding is accompanied with reduced LSD1 demethylation of H3, which leads to a derepression of LSD1 target genes. Based on our data, we hypothesize that HDAC1 regulates LSD1 activity through deacetylation of K374 (Figure 3.13A). Deacetylated LSD1 binds to histone H3 in a productive conformation and allows the demethylation and repression of LSD1 target genes, including tumor suppressors to promote cancer progression (Figure 3.13A). The combined activity of HDAC1 and LSD1 enhances H3K4 demethylation, and H3K9 and K14 deacetylation to mediate gene

repression (126). The mechanism of HDAC inhibitors is based on promoting acetylation of H3K9 and K14 to mediate gene reactivation. Here, we uncovered a secondary mechanism of HDAC inhibitors, which enhance LSD1 acetylation and inhibit demethylation of H3K4me2 from target gene promoters (Figure 3.13B). Accumulation of active chromatin marks by inhibition of HDAC and LSD1 activities, leads to derepression of important tumor suppressors, which inhibits cancer progression. The present study reveals a functional relationship between HDAC1 and LSD1 in regulating gene expression.

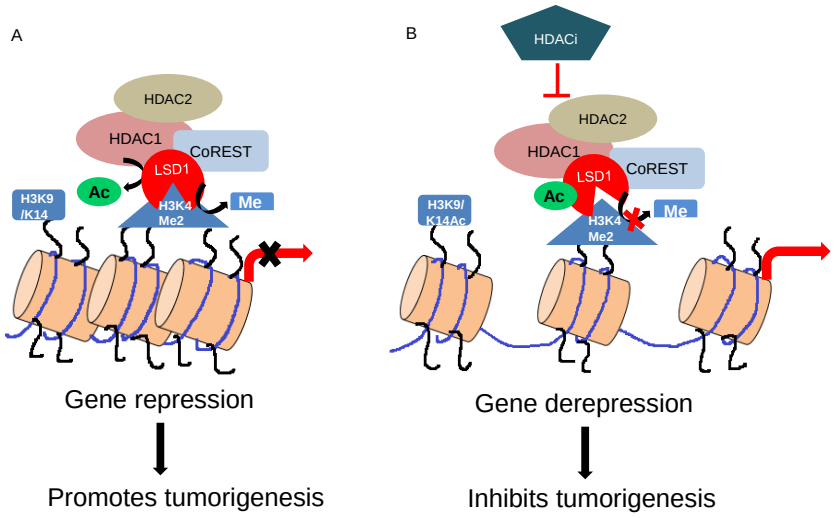


**Figure 3.13 - Schematic model depicting the combined activities of HDAC1 and LSD1 on gene expression and tumorigenesis.** A) HDAC1-mediated deacetylation of LSD1 allows proper binding of methylated lysine of Histone H3, hence LSD1 catalyzes the demethylation and repression of target genes to promote tumorigenesis. HDAC1 also mediates gene repression through deacetylation of H3K9 and K14. B) HDAC inhibitors enhance LSD1 acetylation, and reduce histone H3 binding, leading to reduced LSD1 activity, elevated H3 methylation, and derepression of target genes to inhibit tumorigenesis. HDAC inhibitors promote acetylation of K9 and K14 to reactivate gene expression.

HDAC inhibitors such as Trichostatin A reactivate LSD1 target genes, however the mechanism of this reactivation was not understood (111). Previous groups have shown that HDAC inhibitors enhance the H3K4me2 mark, which is the target site for LSD1 demethylation (114). Consistent with the previous findings, HDAC1 and 2 selective inhibitor (SHI-1:2) as well as the pan inhibitor-SAHA induce methylation of H3K4. These results also confirm that HDAC1 works upstream of LSD1 and regulates its activity through acetylation. Here, we uncovered a new mechanism where HDAC1 regulates the repression of LSD1 target genes through deacetytation of LSD1.

LSD1 consists of three domains: the SWIRM, amine oxidase (AOD), and tower domains. The AOD comprises the FAD binding and substrate binding lobes (127). There are two alpha helices (Sα1 and Sα3) rich in acidic residues in the substrate binding lobe, which form tight interactions with the basic residues of histone H3 and positions the methylated lysine correctly for LSD1-mediated demethylation (Figure 3.14) (115,118). The Sα1 helix (372-394 residues) is also believed to undergo a conformational change upon H3 binding (116). Our data suggest that acetylation of LSD1 at K374, which lies in the Sα1 helix, leads to altered binding between LSD1 and H3. Based on our data, we hypothesize that acetylation of K374 induces a conformational change that affects the interactions between LSD1 and H3, thereby leading to non-productive binding of H3. This altered binding leads to incorrect positioning of methylated lysine (H3K4me2) in the catalytic center, which is consistent with our data showing loss of LSD1 enzymatic activity. Our hypothesis is further supported by a recent report that documents the effect of three disease related mutations of LSD1 (E379K, D556G, Y761H) (128). Among these, E379, which also lies in the Sα1 helix (Figure 3.14), is important for Histone H3 binding. The

E379K LSD1 mutant displayed reduced $V_{max}$ and altered $K_m$, suggesting that amino acids in the Sα1 helix are critical for substrate binding.

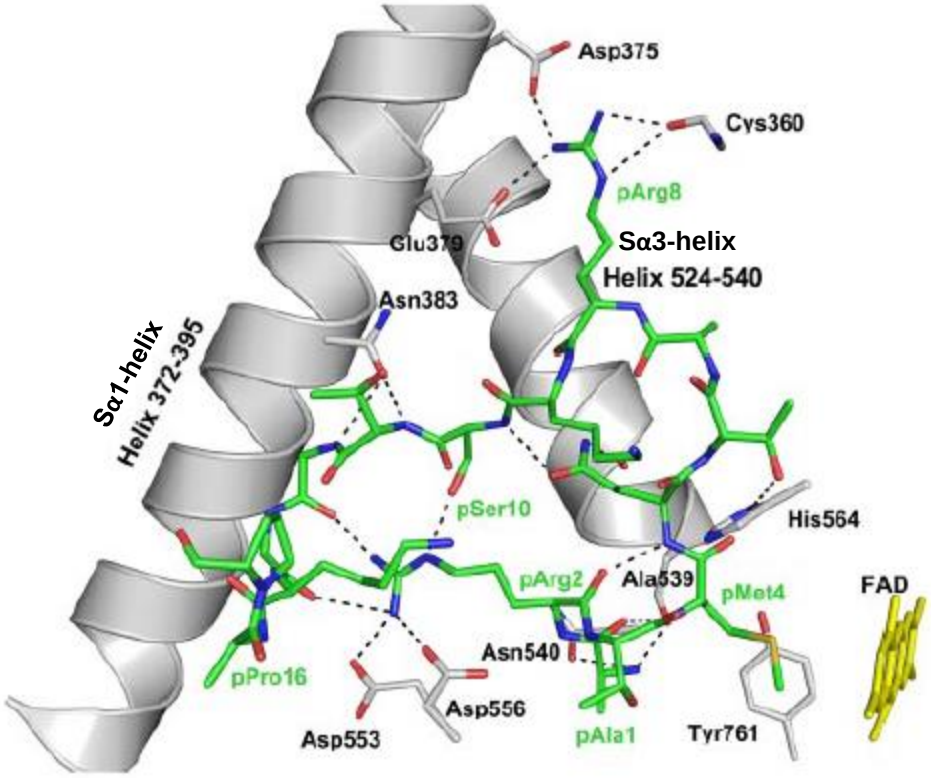


**Figure 3.14 – Substrate binding lobe of LSD1.** A closer view of the interactions between the histone H3 peptide (residues are shown in green) and LSD1 (residues and alpha helices are shown in gray). The Sα1 helix and Sα3 helix are shown in gray and form multiple interactions with histone H3. The FAD cofactor is shown in yellow. Adapted from (115).

In contrast to *in cellulo* data, results from the *in vitro* demethylation assay showed that HDAC inhibitors have no significant effect on LSD1 activity. The utilization of histone H3 peptide as a substrate in the *in vitro* assay may not accurately reflect the activity with the native nucleosome. We speculate that LSD1 acetylation-mediated altered H3 binding is a structural phenomenon that requires a nucleosomal substrate rather than a peptide

substrate (129). However, further structural characterization is needed to fully uncover the acetylation-mediated interaction of LSD1 and H3.

A recent paper documented that LSD1 acetylation suppressed epithelial to mesenchymal transition (EMT) (129). Male absent on the first (MOF) acetyltranferase was responsible for the acetylation of LSD1 in epithelial cells, whereas acetylation was not observed in mesenchymal cells. Acetylation of LSD1 disrupted nucleosomal binding, inhibited demethylation activity, and reactivated LSD1 target genes, which is consistent with our hypothesis. Three lysines in the tower domain of LSD1 (K432, K433 and K436) were identified using *in silico* analysis and global proteomics data from phosphosite. Although these lysines could be possible sites for MOF-mediated acetylation, we speculate that acetylation of LSD1 at K374, may also contribute to the LSD1 activity observed. Further studies are needed to identify the acetyltransferase responsible for mediating K374 acetylation in LSD1. Altogether, the data from both studies suggest that acetylation of LSD1 affects histone H3 binding, impairs demethylase activity, and mediates derepression of target genes involved in important processes, such as cell cycle and EMT. Given that HDAC1 is highly expressed in cancer cells, HDAC1 might compete with MOF to deacetylate LSD1 and promote tumor progression. The data from this recent report also showed that LSD1 was not acetylated in mesenchymal cells and this could be partly or completely due to the overexpression of HDAC1 (129).

Here, we provide a mechanistic basis for HDAC inhibitor-mediated histone methylation through discovering LSD1 as a substrate of HDAC1 (Figure 3.13B). Our findings demonstrate the significance of discovering novel substrates of specific HDACs towards understanding the full activities of these enzymes in the cell. Despite a growing

list of acetylated proteins, the HDACs involved in regulating these proteins have not been well studied mainly due to the lack of substrate discovery tools. Our substrate trapping strategy is a simple method which could be applied to other HDAC isoforms as well. Here, we uncovered a previously unknown functional link between HDAC1 and LSD1 using trapping mutants. Given the involvement of HDAC1 and LSD1 in cancer formation, and the use of HDAC inhibitors as promising anti-cancer drugs, these studies will broaden the understanding of diverse functional roles of HDAC1 in pathological conditions and assist in deciphering HDAC inhibitor mechanisms of action.

### 3.4 Experimental procedure

#### 3.4.1 Antibodies and Reagents

FLAG (catalog number – F3165) and LSD1 (catalog number – L4418) antibodies, as well as anti-FLAG agarose beads (catalog number – A2220), were purchased from Sigma. Acetyl lysine (catalog number – 9814S), acetyl histone H3 (catalog number – 9649P), histone H3 (catalog number – 4499), H3K4me2 (catalog number – 9725P), H3K9me2 (catalog number – 4658P), GAPDH (catalog number – 5174P) and secondary HRP conjugated rabbit (catalog number – 7074) antibodies were purchased from Cell Signaling. CoREST antibody was obtained from Bethyl Laboratories (catalog number – A300-130A-T). Protein A/G plus agarose beads were purchased from Santa Cruz. Secondary rabbit (Alexa fluor 488; catalog number – A11008) and mouse (Alexa Fluor 647; catalog number – A21235) antibodies were obtained from Molecular Probes. Recombinant HDAC1 (catalog number - 50051) was purchased from BPS Biosciences. First strand cDNA synthesis kit was purchased from New England Biolabs and Trizol plus RNA Easy Kit was purchased from Invitrogen. Fast Sybr green master mix (catalog

number - 4385612) and the 96 well PCR reaction plates (catalog number - 4360954) were purchased from Applied Biosystems. Proteomic grade Trypsin was purchased from Sigma aldrich (catalog number – T6567). The LSD1 Fluorometric Drug Discovery Kit was purchased from Enzo Life Sciences (catalog number – BML-AK544-0001).

### 3.4.2 Expression plasmids

HDAC1 single point mutants were previously described (38). FLAG tagged pCAGGs-LSD1 was a generous gift from Dr. Ryuji Hamamoto (University of Chicago) (130). The pCAGGs-LSD1 K374R mutant was created by Quickchange site directed mutagenesis (Agilent) using pCAGGS-LSD1 as a template using the following primers (K374R Forward primer: 5' GGA CAA GCT GTT CCT AAA GAG AGA GAT GAA ATG GTA GAG CAA GAG 3', K374R Reverse primer: 5' CTC TTG CTC TAC CAT TTC ATC TCT CTC TTT AGG AAC AGC TTG TCC 3'). The mutation was confirmed by DNA sequencing.

### 3.4.3 Cell culture

HEK293 cells were grown in Dulbecco's modified Eagle's medium (DMEM; Life Technologies) supplemented with 10% Fetal Bovine Serum (FBS; Life Technologies) and 1% antibiotic/anti-mycotic (Hyclone) at 37 $^{0}$C in a 5% $CO_2$ incubator. HeLa cells were grown in Ham's F12 media (Life Technologies) supplemented with 10% (FBS and 1% antibiotic/anti-mycotic (Hyclone) at 37 $^{0}$C in a 5% $CO_2$ incubator. MCF7 cells were maintained in Eagle's minimum essential medium (EMEM: ATCC) supplemented with 10% FBS at 37$^{0}$C in a 5% $CO_2$ environment. For inhibitor treatments, cells were grown in the presence of an inhibitor for an additional 24 h after the 48 h growth period.

### 3.4.4 Transient transfections of DNA into HEK293 cells

Transfection was carried out as described in Chapter 2, section 2.4.10.

### 3.4.5 Cell Lysis

This procedure is described in Chapter 2, section 2.4.11.

### 3.4.6 Immunoprecipitation

This procedure is described in Chapter 2, section 2.4.12.

### 3.4.7 Co-Immunoprecipitation

For co-immunoprecipitation experiments using overexpressed LSD1 protein, FLAG-tagged LSD1 was transfected into HEK293 cells and grown for 48 h as described. Cells were subsequently treated with SHI-1:2 (10 µM in growth medium) or SAHA (10 µM in growth medium) for an additional 24 h. Cells were lysed as described (section 3.4.5) and proteins were immunoprecipitated from the lysates using pre-washed anti-FLAG agarose beads (20 µL bead slurry) (section 3.4.6) overnight at 4 °C with rocking. For endogenous LSD1 co-immunoprecipitation experiments, HEK293 or HeLa cells were treated with SHI-1:2 (10 µM in growth medium) or SAHA (10 µM in growth medium) for 24 h before harvesting and lysis (section 3.4.5). Cell lysates were incubated with LSD1 antibody (5 µg) at 4 °C for 1 h and then further incubated with pre-washed protein A/G plus agarose beads (20 µL bead slurry) (Chapter 2, section 2.4.13) overnight at 4 °C. Bound proteins were washed three times with Jurkat Lysis Buffer (JLB; 1 mL) and eluted using SDS loading dye (25 µL; 100 mM Tris-Cl pH 6.8, 4% SDS, 20% glycerol, 0.008% bromophenol blue), separated by 10% SDS-PAGE (Chapter 2, section 2.4.14), transferred to PVDF membrane (Immobilon P), and immunoblotted with the indicated antibodies (Chapter 2, section 2.4.16).

### 3.4.8 Elution of FLAG-tagged proteins using FLAG peptide

After immunoprecipitation, beads were washed three times with JLB (1 mL) and bound proteins were eluted by incubating for 30 min at 4 °C using 3X FLAG peptide (APEXBIO; 50 µL; 0.25 mg/mL in Tris-buffered saline; 20 mM Tris-Cl pH 8.0, 150 mM NaCl). After incubation, beads were separated by centifuging at 5 X $10^3$ rcf (x g) for 1 min at 4 °C. The supernatant (50 µL) was transferred to a new eppendorf tube, mixed with SDS-loading dye (10 µL from 5X) and β-mecaptoethanol (10% v/v) prior to SDS-PAGE.

### 3.4.9 SDS-PAGE and Western blot

This protocol was described in Chapter 2, section 2.4.14 and 2.4.16. After Western blotting, chemiluminiscence signal was measured using a Fluorochem SP (Alpha Innotech) imager. Fluorescence signal was scanned using the Typhoon 9210 variable mode imager.

### 3.4.10 Sypro Ruby staining

The staining procedure is described in Chapter 2, section 2.4.15.

### 3.4.11 Acetylation of recombinant LSD1 using acetic anhydride

Baculovirus expressed LSD1 was a kind gift from Dr. Ryuji Hamamoto (University of Chicago)(130). For acetylation of recombinant LSD1, the same procedure was used as described in Chapter 2, section 2.4.18.

### 3.4.12 Gel image quantification

Gels scanned using the Fluorochem SP (Alpha Innotech) imager were quantified using the AlphaEase®FC software (version 6.0.0). Squares with exact area were drawn around each gel band and each lane was separately background corrected. The percentages of the background corrected acetyl lysine signal was divided by the

percentage of the background corrected total immunoprecipitated protein from the same gel. The average percentages from at least three independent trials were shown in Figure 3.7 with mean and standard error shown in Figure A.3.12 and Figure A.3.14.

### 3.4.13 Substrate trapping and inhibitor competition

Following transfection of HEK293 cells with pBJ5-HDAC1 or pBJ5-HDAC1 mutant plasmids, cells were grown for 48 h and then subsequently treated with SAHA (10 µM in growth medium containing DMEM, 10% FBS, and 1% antibiotic/anti-mycotic) for another 24 h before harvesting. Cells (20 X $10^6$) were lysed in JLB (500 µL; 50 mM Tris-Cl pH 8.0, 150 mM NaCl, 10% glycerol and 0.5% triton-X100) containing 1X protease inhibitor cocktail (GenDEPOT) at 4 °C for 30 min with rotation. The supernatant was collected by centrifugation at 13.2 X $10^3$ rpm for 10 min at 4 °C. Wild type or mutant HDAC proteins were immunoprecipitated using pre-washed anti-FLAG agarose beads (20 µL bead slurry) by incubating at 4 °C overnight with rotation. For inhibitor competition experiments, SHI-1:2 (10 µM in JLB) or tubastatin (10 µM in JLB) was added during immunoprecipitation. After immunoprecipitation, beads were washed three times with JLB (1 mL) and bound proteins were eluted using 3X FLAG peptide (section 3.4.8). The eluted proteins were mixed with SDS loading dye (25 µL; 100 mM Tris-Cl pH 6.8, 4% SDS, 20% glycerol, 0.008% bromophenol blue), separated by 10% SDS-PAGE, and visualized with Sypro Ruby total protein stain.

### 3.4.14 Mass Spectrometry

To identify the proteins bound to the HDAC1 mutant, mass spectrometry analysis was used (Chapter 2, Section 2.4.21). Instead of Jurkat cells (Chapter 2), wild type or mutant HDAC1 proteins were expressed in HEK293 cells.

### 3.4.15 LSD1 validation

For LSD1 validation studies, trapping experiments were performed as described above (section 3.4.13) and SHI-1:2 was used as the competitor. The eluted proteins were separated by 10% SDS-PAGE, transferred to a PVDF membrane (Immobilin P), and immunoblotted with LSD1 and FLAG antibodies.

### 3.4.16 LSD1 acetylation assessment

FLAG-tagged LSD1 was transfected into HEK293 cells (20 X $10^6$) and grown for 48 h. After 48 h, cells were incubated with SHI-1:2 (10 µM in growth medium) or SAHA (10 µM in growth medium) for another 24 h, harvested and lysed as described earlier. FLAG-tagged LSD1 protein was immunoprecipitated using anti-FLAG agarose beads (20 µL bead slurry) at 4 °C overnight with rocking. After immunoprecipitation, beads were washed three times with JLB (1 mL). Bound proteins were eluted using SDS loading dye (25 µL), separated by 10% SDS-PAGE, transferred to PVDF membrane (Immobilon P), and immunoblotted with the FLAG and acetyl lysine antibodies.

### 3.4.17 *In vitro* deacetylation assays

For *in vitro* deacetylation assay, recombinant LSD1 was subjected to chemical acetylation using acetic anhydride (section 3.4.11). Prior to the addition of LSD1, recombinant HDAC1 (4 µg, BPS Biosciences) was first incubated with or without SAHA (1 mM in DMSO) in the HDAC assay buffer (48 µL; 50 mM Tris-Cl pH 8.0, 137 mM NaCl, 2.7 mM KCl, 1 mM $MgCl_2$) for 1 h at 37 °C while shaking at 400 rpm. After the preincubation period, acetylated recombinant LSD1 (1 µg) was incubated with or without HDAC1 for another 2.5 h at 37 °C while shaking at 400 rpm. The reaction was stopped by adding 4X SDS loading dye (final concentration 1X), and the reaction mixture was

separated by 10% SDS-PAGE, transferred to PVDF membrane (Immobilin P), and immunoblotted with acetyl lysine, LSD1 and HDAC1 antibodies.

### 3.4.18 *In cellulo* deacetylation assay

For *in cellulo* deacetylation assays, pBJ5 expression constructs of wild type or C151A mutant HDAC1 were cotransfected with the pCAGGs construct of FLAG-tagged LSD1 into HEK293 cells, and grown for 48 h. After 48 h, cells were incubated with SAHA (10 µM in growth medium) for another 24 h, before harvesting and lysis as described (section 3.4.5). FLAG-tagged HDAC1 and LSD1 proteins were immunoprecipitated using pre-washed anti-FLAG agarose beads (25 µL bead slurry) at 4 °C overnight with rocking. Bound beads were washed three times with JLB (1 mL) and bound proteins were eluted using 3X FLAG peptide, as described (section 3.4.8), separated on a 10% SDS-PAGE, transferred to PVDF membrane (Immobilin P), and immunoblotted with acetyl lysine and FLAG antibodies.

### 3.4.19 *In vitro* demethylation assay

FLAG-tagged LSD1 was transfected into HEK293 cells (20 X $10^6$) and grown for 48 h. After 48 h, cells were incubated with SHI-1:2 (10 µM in growth medium) or SAHA (10 µM in growth medium) for another 24 h, harvested, and lysed as described earlier (section 3.4.5). FLAG-tagged LSD1 protein was immunoprecipitated using pre-washed anti-FLAG agarose beads (20 µL bead slurry) at 4 °C overnight with rocking. After washing three times with JLB (1 mL), beads were divided into two halves. One half of the immunoprecipitate was used for *in vitro* demethylation assays according to the manufacturer's instructions (Enzo Life Sciences). The other half was eluted using 2X SDS loading dye, separated by 10% SDS-PAGE, and immunoblotted with FLAG antibody. The

fluorescence signal from the demethylation assay was background corrected using a reaction with all the components except the LSD1 enzyme. Then the signal of each sample was normalized to LSD1 immunoprecipitated from untreated cells (set to 1). The mean and the standard error from at least three independent trials are provided in Table A.3.1.

### 3.4.20 *In cellulo* demethylation assay

HEK293, HeLa, and MCF7 cells were treated with HDAC inhibitors for 24 h. For HEK293 and HeLa, SHI-1:2 and SAHA was used at a 10 µM concentration, whereas for MCF7, 5 µM HDAC inhibitors were used. After 24 h, cells were harvested and lysed; lysates (50 µg) were mixed with SDS loading dye (1X) and β-mercaptoethanol (10% v/v), separated by 12% SDS-PAGE, transferred to PVDF membrane (Immobilon P), and immunoblotted with the indicated antibodies.

### 3.4.21 Identification of putative acetylated lysines in LSD1

To identify acetylated lysines in LSD1that are regulated by HDAC1, FLAG-tagged LSD1 was overexpressed in HEK293 cells (20 X $10^6$) and the cells were allowed to grow for 48 h. After a 48 h recovery period, cells were treated with 2% DMSO or SHI-1:2 (10 µM in growth mediun) or SAHA (10 µM in growth medium) for another 24 h. Following harvesting and lysis, LSD1 was immunoprecipitated using pre-washed anti-FLAG agarose beads (25 µL bead slurry), separated by SDS-PAGE (10%) and visualized by Sypro Ruby total protein stain. LSD1 bands were excised from the Sypro Ruby stained gel and subjected to in gel digestion and mass spectrometry (Chapter 2, section 2.4.21)

### 3.4.22 Real Time PCR (RT-PCR)

#### 3.4.22.1 RNA isolation and purification

FLAG-tagged wild type or K374R mutant LSD1 was transfected into HEK293 cells (5 X $10^6$) and grown for 48 h. After 48 h, cells were incubated with SHI-1:2 (10 µM in growth medium) for another 24 h and harvested. After washing cells with cold PBS, RNA was isolated according to manufacturer's instructions (Ambion). Briefly, cells (1 X $10^6$) were lysed by adding the TRIzol® reagent (1 mL) and pipetting up and down. The lysate with the TRIzol® reagent was incubated at room temperature for 5 min to completely dissociate the nucleoprotein complex. Chloroform (200 µL/mL TRIzol®) was added, mixed well, and incubated at room temperature for another 2-3 min. The tubes were centrifuged at 12 X $10^3$ rcf (X g) for 15 min at 4 °C. After centrifugation, the mixture had separated into three layers: colorless upper phase containing RNA, an interphase containing DNA, and the lower red colored layer with cell debris. The upper layer with RNA (~400 µL) was carefully transferred to a new microcentrifuge tube and an equal volume of 70% ethanol was added. The tubes were inverted and everything was transferred into the spin cartridge. The RNA was purified according to the PureLink™ RNA mini kit instructions (Ambion). The concentration and the purity of the RNA were measured using a Nanodrop 2000 UV-vis spectrophotometer.

#### 3.4.22.2 cDNA synthesis

cDNA synthesis was performed according to the manufacturer's instructions (New England Biolabs). RNA (1 µg) was first incubated with oligo dT primer (2 µL from 50 µM) at 65°C for 5 min in a 8 µL reaction volume. After 5 min, the microcentrifuge tubes were spun briefly and put on ice. Then, Protoscript II Reaction Mix (10 µL from 2X) and

Protoscript II Enzyme Mix (2 µL from 10X) were added to the tubes containing RNA and oligo dT and incubated at 42 °C for 1 h. After 1 h, tubes were incubated at 80 °C for 5 min to inactivate the enzyme. The cDNA was then used immediately or stored at -20 °C.

**3.4.22.3 PCR reaction**

Real time PCR reaction (20 µL) included cDNA (50 ng), forward and reverse primers (1 µL from 10 µM primer; final 0.5 mM), RNAse free water and SYBR green reagent (1X). PCR was performed on a FAST 7500 instrument (Applied Biosystems). Each reaction was done in triplicate from four independent RNA isolations. For each sample, an average was taken from the expression values ($C_t$) of triplicates. Average expression values were normalized to the GAPDH control and fold change was calculated compared to DMSO treated wild type LSD1, which was set to 1. The mean and the standard error from at least four independent trials are shown in Table A.3.2 and Table A.3.3. The PCR cycle included 3 steps; 1) 95°C, 20s, 1 cycle 2) 95°C, 3s, 45 cycles 3) 60°C, 30s. Gene specific primers for SCN2A, SCN3A, and GAPDH were (SCN2A forward primer: 5'-GAT GAG GAT GAT GAA AAT GGC-3'; SCN2A reverse primer: 5'-CTA ATT TTC TAA TAG GGT TGA AGG G-3'; SCN3A forward primer: 5'-CAC CAC TTC CTA CTT TAA TGG CA-3'; SCN3A reverse primer: 5'-AAA TAG AGA CAG GAA AGC CCA G-3'; GAPDH forward primer: 5'-GAA GGT GAA GGT CGG AGT C-3'; GAPDH reverse primer: 5'-GAA GAT GGT GAT GGG ATT TC-3' (112).

**3.4.14 Statistical analysis**

All data were presented as mean±standard error from at least three independent trials. One way ANOVA test was used to compare the data sets using GraphPad Prism software (version 5.01). $p<0.05$ was considered statistically significant.

# CHAPTER 4. AN HDAC1 SNP REVEALS CROSSTALK BETWEEN ACETYLATION AND PHOSPHORYLATION

## 4.1 Introduction

The unregulated expression of genes related to cancer is often linked to the presence of a Single Nucleotide Polymorphism (SNP). A SNP is a naturally occurring variation at a particular site in the DNA that occurs between individuals. Cancer-related HDAC SNPs have been used as biomarkers to predict disease susceptibility and drug sensitivity (131,132). A few studies have shown an association of HDAC3 and HDAC4 SNPs with schizophrenia and HDAC3 SNPs with diabetes mellitus (133-135). A SNP in the promoter region of HDAC10 was associated with increased expression and development of hepatocellular carcinoma (136). A recent study showed that an HDAC1 SNP affects patient response to corticosteroids in asthmatics (137). These prior reports clearly suggest a link between HDAC SNPs and disease formation (138).

To gain insights into the regulation of HDAC1, we focused on studying the effect of HDAC1 SNPs found in cancer**.** This project was initiated in collaboration with Andres Cisneros lab. The Cisneros lab created an algorithm named “Hypothesis Driven-SNP-Search (HyDn-SNP-S)” to search SNPs in cancer genotyping studies stored in the database of Genotypes and Phenotypes (dbGAP) at NCBI (139). Using this HyDn-SNP-S algorithm, Rebecca Swett in the Cisneros lab identified 66 cancer-related SNPs in HDAC 1, 3 and 6 (40 intronic SNPs and 26 exonic SNPs) (Table 4.1). Based on the involvement of HDAC1 in cancer, we hypothesized that a SNP of HDAC1 identified through Hypothesis driven SNP-search (HyDn-SNP-S) could affect its expression, activity and post-translational modifications. Here we performed a mutational analysis of non-

synonymous HDAC1 exonic SNP-F437C to understand its HDAC1-related carcinogenesis. Our data suggest that the F437C SNP affects a crosstalk between acetylation and phosphorylation of HDAC1. These studies shed insights on the the molecular mechanism leading to HDAC deregulation and cancer onset, which may forge the creation of new diagnostics and cancer treatment options.

**Table 4.1- SNPs in HDAC 1, 3, 6 identified by using HyDn-SNP-S***

| HDAC isoform | # of Exonic SNPs | # of Intronic SNPs | Exonic SNPs | Phenotypes |
|---|---|---|---|---|
| HDAC1 | 8 | 16 | F437C | Prostate,Melanoma,Lung |
| HDAC3 | 8 | 18 | Q55Q, R265P,N411S | Prostate,Melanoma,Lung |
| HDAC6 | 10 | 6 | G1083D, V701A | Prostate,Melanoma,Lung |

*Table is provided by Dr. Rebecca Swett from the Cisneros lab.

## 4.2 Results

### 4.2.1 Effect of F437 mutation on HDAC1 expression, activity, and migration

The presence of a SNP in a gene can affect activity, stability, expression, or post translational modifications. First, we created the HDAC1 F437C mutant and analyzed its effect on HDAC deacetylase activity and expression. Wild type or F437C mutant HDAC1 was overexpressed in T-Ag Jurkat cells, immunoprecipitated using anti-FLAG agarose beads, and subjected to HDAC activity assays and gel analysis. The F437C mutant had a modestly reduced enzymatic activity (73±3%) compared to wild type (100%) (Figure 4.1, lanes 2 and 4). The expression level of the F437C mutant was similar to wild type HDAC1 (Figure 4.1, compare lanes 2 and 4), which suggested that the F437C SNP did not affect the expression of HDAC1.

The enzymatic activity of HDAC1 is affected by the presence of associated proteins (41). The reduced enzymatic activity could be accompanied by a change in

associated proteins caused by the HDAC1 exonic SNP. Infact, F437C lies in the C terminus of HDAC1, which is known to interact with associated proteins, such as mSIN3A and RbAp48. Binding of HDAC1 to mSin3a and RbAp48 can influence activity (67). We analysed the effect of F437 HDAC1 substitution mutants on association with RbAp48 (Figure 4.1, bottom western blot, lanes 2-8). The data showed that mutation of F437 had no effect on RbAp48 association compared to wild type.

Enzymatic activity can also be affected by post translational modifications (PTMs) (140). Because PTMs can lead to a change in migration through SDS-PAGE, we next analyzed the migration of wild type and mutant HDAC1. Interestingly, the F437C HDAC1 mutant exhibited faster migration by SDS-PAGE compared to wild type HDAC1. Based on the initial gel analysis of F437C mutant, we hypothesized that the F437C SNP influenced a post-translational modification of HDAC1, which affects its migration.

To study the effect of polarity or sterics at the 437 position on HDAC activity and migration, four additional mutants (F437L, F437A, F437S, F437Y) were created. Phenylalanine at 437 was mutated to serine and tyrosine to study the effect of polarity on HDAC activity and migration. F437 was mutated to leucine and alanine to study the effect of sterics. The F437 mutants displayed 73-97% remaining deacetylase activity compared to WT HDAC1 (Figure 1, lanes 5-8), suggesting that smaller or polar residues at the 437 position also have an effect on HDAC activity. Interestingly, F437C, F437S and F437A migrated faster and F437L and F437Y migrate at an intermediate rate compared to WT HDAC1 (Figure 1, Western blot, compare lanes 4, 6, 7 vs 5, 8) suggesting polar or smaller residues at 437 position also affected HDAC1 modification. Non polar (F437L) or polar bulky (F437Y) residues at 437 position affect migration to a lesser extent compared to

F437C (Figure 1, Western blot, compare lanes 4 to 5 and 8). Overall, the altered migration of F437C is consistent with the hypothesis that a SNP at the F437 position is affecting a post-translational modification, and polarity at this position is also an important determinant.

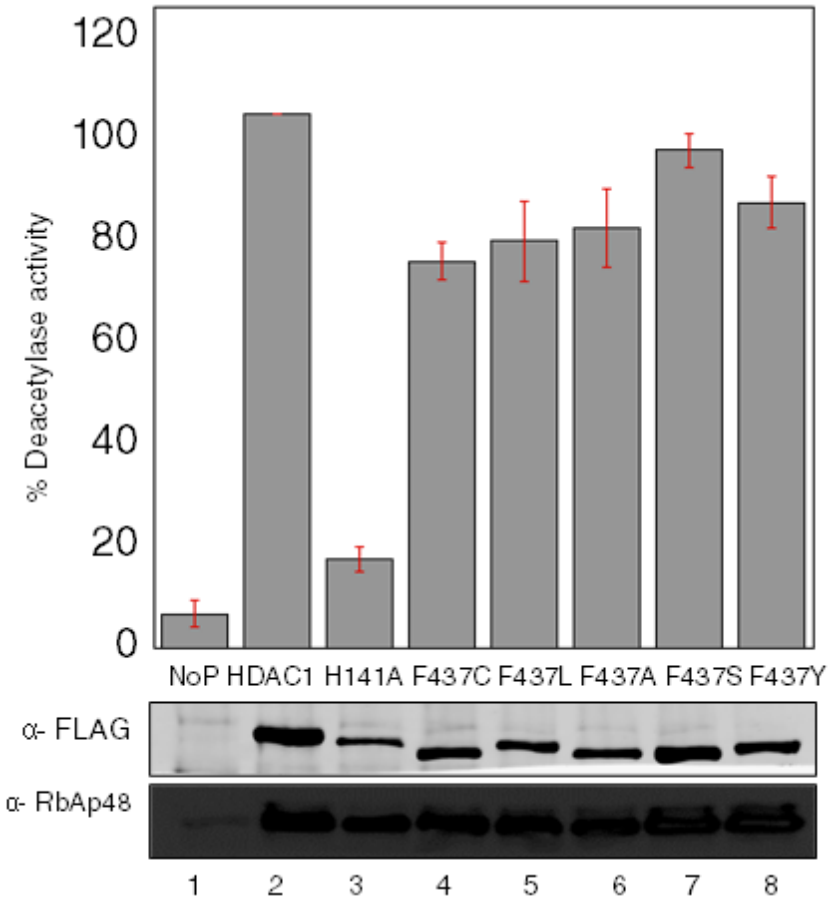


**Figure 4.1 – Effect of HDAC1 F437 mutant on activity, expression and migration.** Wild type or mutant HDAC1 proteins was expressed as FLAG-tagged proteins in T-Ag Jurkat cells and immunoprecipitated with anti-FLAG agarose beads. Catalytic activity was measured using an *in vitro* fluorescence assay (histogram). Proteins were separated by SDS-PAGE and immunoblotted with FLAG antibody (gel image, α-FLAG) to assess protein levels or RbAp48 binding (gel image, α-RbAp48**)**. The histogram represents the

mean percent activity of at least three independent trials (wild type is set to 100%, Table A. 4.1). The standard error is shown as error bars. Repetitive trials are shown Figure A.4.1.

### 4.2.2 Characterizing the gel shift in F437C mutant

HDAC1 undergoes several post translational modifications, including phosphorylation, sumoylation, ubiquitination, and acetylation, which affect its activity, stability and subcellular localization (Figure 4.2)(141). HDAC1 is phosphorylated at S393, S421 and S423 and phosphorylation is important for HDAC deacetylase activity (137). Acetylation of HDAC1 occurs at K432, K438, K439 and K441, which reduces its enzymatic activity (142). Since the cancer-related HDAC1 SNP lies near sites of acetylation, we hypothesized that the F437C mutation might affect HDAC1 acetylation, which leads to a change in migration and enzymatic activity. We expect that wild type HDAC1 is unacetylated whereas F437C promotes acetylation of HDAC1. To test the hypothesis, we used the gel analysis of multiple mutants as an indication of modification.

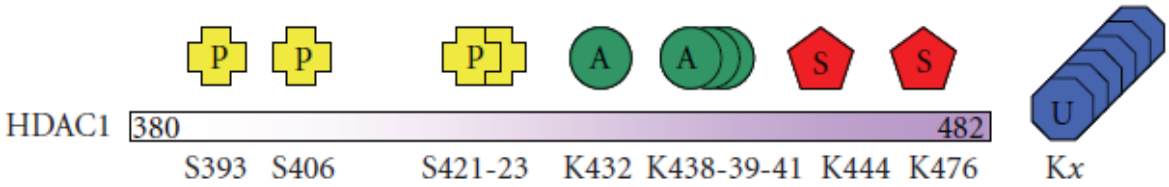


**Figure 4.2 – Post-translational modifications of HDAC1.** Only the C-terminal region of HDAC1 (380-482) is shown, because it is rich in PTMs. P-phosphorylation, A- acetylation, S-sumoylation, U – ubiquitination (143).

To initially characterize whether the observed gel shift of F437C in gel analysis is due to acetylation, the four lysine residues known to be acetylated (K432, K438, K439, K441) were mutated to arginines (4R) using site directed mutagenesis. A previous study

reported lysine to arginine mutations as a means to mimic the deacetylated form of HDAC1, as arginines cannot undergo acetylation and maintains the positively charged state of lysine (142). Also, the 4R+F437C mutant was created to confirm that the gel shift observed with the F437C mutant is in fact due to acetylation. If the shift of HDAC1 F437C is due to acetylation at K432, K438, K439 and K441, we should not see a shift in either the 4R or the 4R+F437C HDAC1 mutants compared to wild type, as they lack lysines that can undergo acetylation. As expected, the 4R HDAC1 and 4R+F437C HDAC1 mutants migrated slower than HDAC1 F437C (Figure 4.3A, compare lanes 2 to 4 and 5). These data are consistent with the hypothesis that the faster migration of F437C was due to acetylation of HDAC1 at K432, K438, K439 and K441.

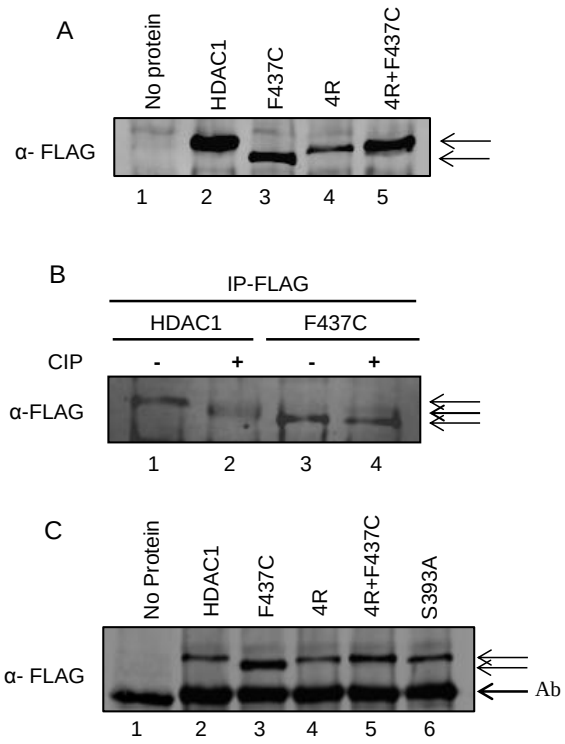


**Figure 4.3 – The F437C mutant affects acetylation and phosphorylation.** A) Wild type or mutant HDAC1 proteins were expressed as FLAG-tagged proteins in T-Ag Jurkat cells, immunoprecipitated with anti-FLAG agarose beads, separated by SDS-PAGE, and

immunoblotted with FLAG antibody. Arrows indicate migration of F437C and deacetylated mimic mutants. Repetitive trials are shown in Figure A.4.2. B) Wild type or mutant HDAC1 proteins were expressed as FLAG-tagged proteins in T-Ag Jurkat cells, immunoprecipitated with anti-FLAG agarose beads, and subjected to *in vitro* dephosphorylation using CIP (calf intestinal phosphate). Then, proteins were separated by SDS-PAGE and immunoblotted with the FLAG antibody. Repetitive trials are shown in Figure A.4.10. C) Wild type or mutant HDAC1 proteins were expressed as FLAG-tagged proteins in T-Ag Jurkat cells, immunoprecipitated with anti-FLAG agarose beads and bound proteins were separated by SDS-PAGE, and immunoblotted with FLAG antibody. Arrows indicate the migration of deacetylated and unphosphorylated mutants compared to F437C. Repetitive trials are shown in Figure A.4.11.

**4.2.3 Characterizing the PTM of F437C mutant**

To study acetylation of the F437C HDAC1 mutant, we utilized a mass spectrometric- based approach. Due to the high abundance of lysine (amino acid residues 430-441 including the sites of acetylated lysines), acetylated lysines were not covered after trypsin digestion. Instead of acetylation, phosphorylation of WT HDAC1 at S393 was observed from the mass spectrometric analysis (Figure A.4.3-4.6). Although a peptide containing S393 was identified in the F437C mutant, S393 was unphosphorylated (Figure A.4.7-4.9). The data suggests that the F437C mutant negatively affected phosphorylation at S393.

To confirm the phosphorylation of wild type HDAC1 that was observed by MS, we performed *in vitro* dephosphorylation assays using calf intestinal phosphatase (CIP). Wild type or mutant HDAC1 was overexpressed in T-Ag Jurkat cells and immunoprecipitated

using anti-FLAG agarose beads. The immunoprecipitated proteins were incubated with or without CIP and analysed by Western blotting. Interestingly, CIP-treated HDAC1 migrated more quickly compared to untreated WT, suggesting that HDAC1 is phosphorylated (Figure 4.3B, compare lane 1 and 2). In contrast, migration of F437C did not change upon CIP treatment (Figure 4.3B, compare lane 3 and 4), suggesting it is not phosphorylated. The data is consistent with the phosphorylation of S393 observed with the mass spectrometric data. Interestingly, the migration pattern of F437C was not similar to CIP-treated wild type HDAC1 (Figure 4.3B, compare lanes 2 and 3), which suggests that F437C may have multiple PTM.

To observe the migration pattern of dephosphorylated or deacetylated HDAC1, the migration of different deacetylated mimic mutants (4R and 4R+F437C) compared to the phosphomutant (S393A) (144) were analysed using gel electrophoresis (Figure 4.3C). According to MS data, wild type HDAC1 is phosphorylated and we hypothesized that would not be acetylated. In contrast, F437C is acetylated and not phosphorylated. Interestingly, the migration of deacetylated mimic 4R and 4R+F437C mutants were comparable to unphosphorylated S393A migration (Figure 4.3C, compare lanes 4, 5 and 6). Like the 4R and 4R+F437C mutants, the migration of the S393A mutant is intermediate compared to F437C and wild type and is consistent with the migration observed with CIP-treated wild type HDAC1 (Figure 4.3B, compare lanes 2 and 4). From the results of both *in vitro* dephosphorylation and migration analysis, we speculate that the faster migration of F437C is due to acetylation at K432, K438, K439 and K441 and lack of phosphorylation at S393.

### 4.2.4 F437C mutant affects acetylation of HDAC1 at K432

Given the hypothesis that faster migration of F437C is due to acetylation, we generated additional mutants, including a phophomimetic (S393E), an acetylmimetic (4Q: K432Q, K438Q, K439Q and K441Q), and a phosphomutant/acetylmimetic (S393A/4Q) to further characterize the acetylation of F437C mutant. The expectation is the wild type would migrate similarly to the phosphomimetic S393E, if both are phosphorylated. As expected, migration of wild type HDAC1 was comparable to S393E, suggesting wild type HDAC1 is phosphorylated (Figure 4A, compare lanes 2 and 3). If acetylated at all four lysines (K432, K438, K439 and K441), the HDAC1 F437C mutant should migrate similar to the acetylated mimic mutants 4Q or S393A/4Q. The reason for comparing S393A/4Q to 4Q was to observe any effect due to S393 phosphorylation on acetylation. Interestingly, the HDAC1 4Q and S393A/4Q mutants migrated further than the F437C mutant (Figure 4.4A, compare lanes 7 to 8 and 9). The migration pattern of 4Q was comparable to S393A/4Q suggesting that phosphorylation at S393 does not regulate acetylation (Figure 4.4A, compare lanes 8 and 9). The different migrations observed for F437C and 4Q could be due to the fact that not all four lysines are modified in the F437C mutant HDAC1.

Prior work has shown that acetylation of K432 is critical for HDAC1 activity, where K438, K439 and K441 has very little effect on activity (142)**.** To test whether F437C is acetylated only at a single lysine, the K432Q single mutant was generated and analyzed by western blotting. The K432Q mutant migrated similarly to the F437C mutant (Figure 4.4B, compare lanes 2 and 4). The data indicated that the F437C mutant likely affected acetylation at a single lysine of HDAC1.

To further confirm which lysine is acetylated in the F437C mutant, we created the deacetylated mimic K432R/F437C mutant and analyzed by Western blotting (Figure 4.4C). If F437C is acetylated at the K432 residue, the migration of K432R/F437C mutant should be slower than that of F437C, due to a lack of acetylation at the K432 position in the K432R/F437C mutant. As expected, the K432R/F437C mutant migrated more slowly compared to the F437C mutant (Figure 4.4C, compare lanes 3 and 5), suggesting that the F437C mutant was specifically acetylated at K432.

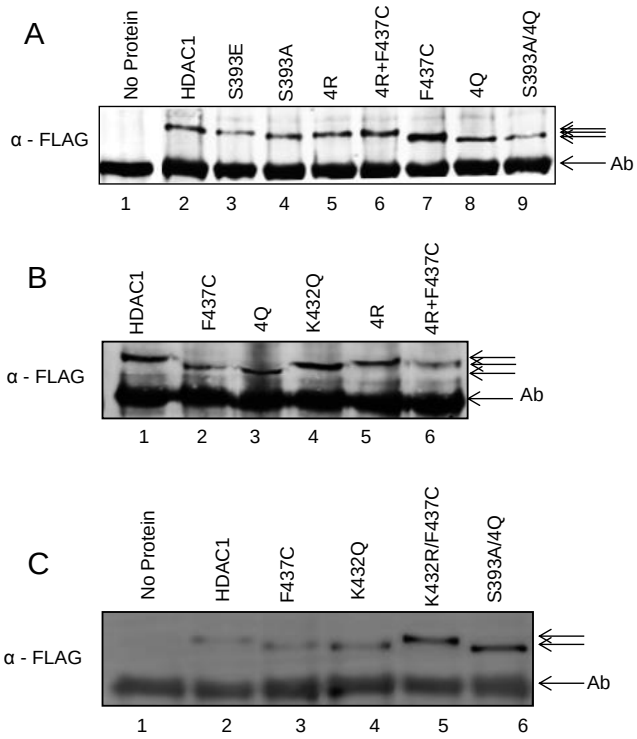


**Figure 4.4 – The F437C mutant affects acetylation at K432.** Wild type or mutant HDAC1 proteins were expressed as FLAG-tagged proteins in T-Ag Jurkat cells, immunoprecipitated with anti-FLAG agarose beads, separated by SDS-PAGE and immunoblotted with FLAG antibody. Repetitive trials are shown in Figure A.4.12.

### 4.3 Discussion

The aberrant activity of HDAC proteins is implicated in multiple diseases, including cancer (47,145). As a consequence, HDAC proteins have emerged as anti-cancer targets. Multiple HDAC inhibitors are in clinical trials, with four HDAC inhibitors approved as anti-cancer therapeutics (58-61). Despite the importance of HDAC proteins in cancer, the mechanisms leading to deregulation of HDAC activity are poorly understood. The presence of SNPs is well known to affect disease susceptibility, drug sensitivity, splicing, and post-translational modifications (131,132). SNPs are also known to cause changes in gene expression and protein interactions. SNPs on HDAC proteins are now gaining attention due to their correlation with diseases.

Here we identified a new HDAC1 exonic SNP (F437C) using HyDN-SNP-S and performed a mutational analysis to understand the influence of this mutation on PTMs. The HDAC1 F437C SNP lies in the C terminal domain of HDAC1, which is known to bind to associated proteins. Also, HDAC1 is highly post-translationally modified in its C-terminus (141). Phosphorylation of HDAC1 occurs at S393, S421 and S423. Phosphorylation was shown to be important for activity and complex formation (137). Acetylation of HDAC1 occurs at six residues (K218, K220, K432, K438, K439, and K441) and loss of acetylation abrogates deacetylase activity to affect gene transcription (142). For example, acetylation of HDAC1 at K432 is critical for its deacetylase activity. Acetylation of HDAC1 is regulated by the p300 and Sirt1 enzymes during differentiation and cellular stress (146). Regulation of HDAC activity by acetylation in different cancer models is still not fully understood.

According to our data, an HDAC1 exonic SNP at F437 resulted in reduced enzymatic activity compared to wild type HDAC1, but had no effect on HDAC expression. Interestingly, gel migration of HDAC1 SNP-F437C was faster than wild type, suggesting that F437C affects a PTM of HDAC1. Further, our data indicated that the presence of the HDAC1 SNP promoted acetylation at K432. HDAC1 SNP negatively affected the phosphorylation of HDAC1 at S393. A similar type of crosstalk between acetylation and phosphorylation was observed with histone H3, HDAC2, and p53 previously (20,44,147,148).

According to the data, we hypothesized that wild type HDAC1 is phosphorylated at S393 and deacetylated at K432 (Figure 4A), whereas the F437C mutant is dephosphorylated at S393 and acetylated at K432 (Figure 4B). Due to these modifications, wild type HDAC1 is active and is capable of regulating gene expression. In contrast, the reduced activity of acetylated F437C mutant would lead to altered gene expression. The hypothetical model (Figure 4) explains that the reduced activity of the F437C mutant HDAC1 can be related to altered gene expression in various types of cancer, and could be used as a biomarker in different cancer models (75,149). Therefore, studying the details of the regulation of HDAC1 in cancer will assist in revealing mechanism of HDAC1-mediated cancer progression.

HDAC overexpression shows a positive correlation with cancer initiation and progression (150). But several studies have found that a lower expression level of HDACs is also associated with cancer (75,151,152). A truncating mutation of HDAC2 in colon cancer causes loss of protein expression and activity (52). Presence of a SNP in HDAC10 led to an increase in expression in hepatocellular carcinoma (136). HDAC3 and HDAC4

SNPs have been identified in diabetes mellitus and schizophrenia (133-135). An HDAC1 SNP was found to be important for response to corticosteroids (138). Here, we show that presence of an exonic SNP in HDAC1 protein leads to a reduction in activity, which might lead to the activation of oncogenes to promote carcinogenesis.

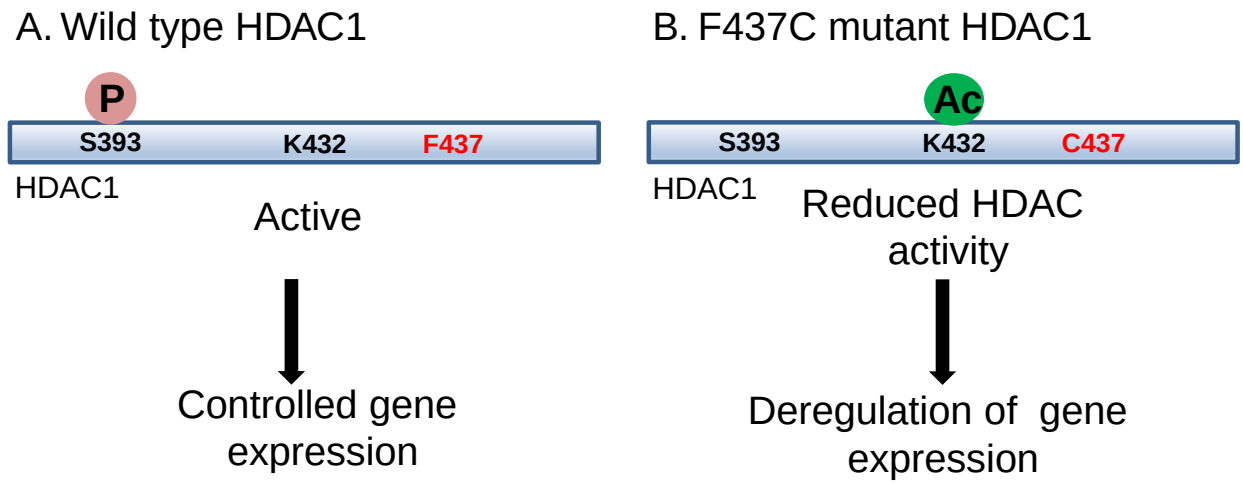


**Figure 4.5 – Hypothetical model.** A) Wild type HDAC1 is phosphorylated at S393, but not acetylated at K432. Wild type HDAC1 is active and gene expression is controlled. B) The HDAC1 SNP at F437C inhibits phosphorylation at S393 and induces acetylation at K432, which leads to a reduction in enzymatic activity, to presumably affect gene expression controlled by HDAC1.

Given the importance of HDAC proteins in disease formation and the use of HDAC inhibitor drugs in anti-cancer therapy, understanding the mechanisms leading to HDAC deregulation will have a direct impact on cancer biology studies and drug design efforts. A detailed understanding of the role of HDAC1 SNPs in different diseases will assist in finding new treatments in a personalized manner.

## 4.4 Experimental procedure

### 4.4.1 Antibodies and Reagents

FLAG (catalog number – F3165) and RbAp48 (catalog number R3654) antibodies and as well as anti-FLAG agarose beads (catalog number – A2220), were purchased from Sigma. Secondary mouse (Alexa Fluoro 647; catalog number – A21235) and secondary rabbit (Alexa Fluoro 488; catalog number – A11008) antibodies were obtained from Molecular Probes. Calf intestinal phosphatase (CIP) was purchased from New England BioLabs (NEB). Proteomic grade trypsin was purchased from Sigma and a FLUOR DE LYS® HDAC fluorometric activity assay kit (BML-AK500-0001) was purchased from Enzo Life Sciences.

### 4.4.2 Expression plasmids

Single point mutants of HDAC1 were created using the pBJ5HDAC1-FLAG expression plasmid, as previously described (38) and described in sections 4.4.3.

### 4.4.3 Polymerase Chain Reaction (PCR)

Two step (touchdown PCR program) site directed mutagenesis was used to create HDAC1 mutants using the primers described in Table 4.2 (mutated bases are underlined). The PCR reactions included water, 10X Pfu buffer (5 µL of 200 mM Tris, 100 mM $(NH4)_2SO_4$, 100 mM KCl, 1% TritonX-100, 20 mM $MgSO_4$, 1 mg/mL BSA, pH 8.8), DMSO (5 µL), plasmid template (1 µL from 100 ng/uL stock), forward and reverse primers (1 µL from 25 pmol/µL stocks), and dNTPs (2µL of 10 mM; 2.5 mM of each base). The final volume of the PCR reaction was 49 µL, without the Pfu enzyme. The PCR reaction was mixed well, briefly spun, and incubated for 1 minute at 95 °C in the thermocycler (Eppendorf Mastercycler Gradient). After 1 min, Pfu enzyme (1 µL) was added to the

tubes, and mixed well by pipetting up and down, before the program was run for 5h. The final concentration of reaction components are as follows, plasmid template (2ug/mL), dNTP (0.4mM), forward and reverse primers (0.5 pmol/uL). The first half of the PCR cycle included 9 cycles of denaturing time of 95 °C for 1 min, annealing time of 1 min where the temperature decreased by 1°C per cycle from 60°C to 50°C, and extension time of 72 °C for 6 min. The second half included 15 cycles of denaturing time of 95 °C for 1 min, annealing step at 50 °C for 2 min, and extension time of 72 °C for 6 min. The final extension step was performed at 72°C for 10 min. PCR products were separated by 1 % agarose gel (section 4.4.4) and used for subsequent steps.

PCR fragments amplified from the first PCR reaction were used as the template for the second PCR reaction. The same touch down PCR program was used for the amplification of full length HDAC1 gene, which was then used in homologous recombination (section 4.4.6).

**Table 4.2 – List of primers used in mutagenesis***

| Primer | Sequence (5'-3') |
|---|---|
| HD100-For | GCC AGA ATG CGG CCG CAT GGC GCA G |
| pBJ5-153 Rev | TAT CAT GTC TGG ATC CGG |
| F437C for | GG GGC CGC AAG AAC TCT TCC AAC TGC AAA AAA GCC AAG AGA GTC |
| F437 rev | GAC TCT CTT GGC TTT TTT GCA GTT GGA AGA GTT CTT GCG |
| F437L for | GG GGC CGC AAG AAC TCT TCC AAC TTA AAA AAA GCC AAG AGA GTC |
| F437A for | GG GGC CGC AAG AAC TCT TCC AAC GCC AAA AAA GCC AAG AGA GTC |
| F437S for | GG GGC CGC AAG AAC TCT TCC AAC TCC AAA AAA GCC AAG AGA GTC |
| F437Y for | GG GGC CGC AAG AAC TCT TCC AAC TAC AAA AAA GCC AAG AGA GTC |
| 4R for | GAG GGA GAG GGG GGC CGC AGG AAC TCT TCC AAC TTC AGA AGA GCC AGG AGA GTC AAA ACA GAG GAT G |
| 4R,Q,A rev | GCG GCC CCC CTC TCC CTC CTC TTC AG |
| 4R+F437C | GAG GGA GAG GGG GGC CGC AGG AAC TCT TCC AAC TGC AGA AGA GCC AGG AGA GTC AAA ACA GAG GAT G |
| 4Q for | GAG GGA GAG GGG GGC CGC CAG AAC TCT TCC AAC TTC CAA CAA GCC CAG AGA GTC AAA ACA GAG GAT G |
| K432Q for | GAG GGA GAG GGG GGC CGC CAG AAC TCT TCC AAC TTC AAA AAA GC |
| K432R for | GAG GGA GAG GGG GGC CGC AGG AAC TCT TCC AAC TTC AAA AAA GC |
| K432R/F437C for | GAG GGA GAG GGG GGC CGC AGG AAC TCT TCC AAC TGC AAA AAA GCC AAG AG |

* Underlined residues represents the mutations introduced.

### 4.4.4 DNA agarose gel electrophoresis

PCR reaction products (50uL; section 4.4.3) or digested products (20uL;section 4.4.5) were mixed with 6X DNA gel loading dye (10 µL; 15% Ficoll®-400, 66 mM EDTA,19.8 mM Tris-HCl, 0.102% SDS, 0.09% bromophenol blue, pH 8.0) and separated by 1% agarose gel by running at 120 V for 1 h in 1X tris acetate EDTA buffer (1X TAE; 40 mM Tris, 1 mM EDTA, 2.3 mL glacial acetic acid). Gel bands were excised from the gel using a razor blade, and purified using the QIAgen gel extraction kit (cat # 28704) and then used for homologous recombination.

### 4.4.5 Restriction digestion

pBj5-HDAC1 (67) plasmid was digested with *Not1* (Promega) and *EcoR1* (Promega) enzymes by incubating at 37 °C for 2 h while shaking at 250 rpm. The restriction digestion reaction mixture contained pBH5HDAC1 plasmid (1 µL of 1 µg/µL), buffer H (2 µL; Promega), BSA (1 µL of 2 mg/mL), *Not1* and *EcoRI* (1 µL each 10 U/µL) and water (14 µL). The final concentration of all components were as follows, pBH5HDAC1 plasmid (50 µg/mL), buffer H (1X), BSA (0.1 mg/mL), *Not1* and *EcoRI* (0.5 U). After incubation, the digested products were separated by agarose gel electrophoresis (section 4.4.4) and desired band (3.3 kb) was excised and purified from the gel using the QIAgen gel extraction kit (cat # 28704).

### 4.4.6 Homologous recombination

To combine the *Not1* and *EcoRI* digested plasmid (section 4.4.5) with the mutant HDAC1 PCR product (section 4.4.3), homologous recombination was used. KC8 cells (50 µL, section 4.4.7) were thawed on ice and mixed with purified PCR insert (5 µL; section 4.4.3), digested pBJ5 plasmid (5 µL; section 4.4.5), KCM buffer (10 µL of 0.1 M KCl, 30 mM $CaCl_2$, 50 mM $MgCl_2$) and 30 µL of water. The final concentration of the buffer was 0.01 M KCl, 3 mM $CaCl_2$, 5 mM $MgCl_2$ in a 100 µL total volume. The mixture was incubated on ice for 20 min before heat shock was given at 42 °C for 60s. Cells were then incubated on ice for 2 min and LB media (500 µL; 1% peptone, 0.5% yeast extract and 1% NaCl) was then added. The mixture was incubated at 37 °C for 1.5 h while shaking at 250 rpm. The cells were harvested by centrifuging at $13.2X10^3$ for 10 min and 400 uL of the supernatant was removed. The remaining cells were resuspended in the remaining media (200 uL), and plated on LB-agar plates containing ampicillin (100ug/mL). The

plates were incubated overnight (12-16 h) at 37 °C and observed for the presence of colonies that contained the pBJ5-HDAC1 plasmid. Single colonies were inoculated in LB media containing ampicillin (5 mL), grown overnight at 37 °C with shaking at 250 rpm, and subjected to miniprep or midiprep plasmid purification (Chapter 2; section 2.4.8). After verification for the presence of the HDAC1 insert by restriction digestion (section 4.4.5), the mutation was confirmed by DNA sequencing (University of Michigan DNA Sequencing Core).

**4.4.7 Competent cell preparation**

KC8 cells were a kind gift from Finley lab at Wayne State University. A single colony from an LB agar plate with ampicillin antibiotic (100 µg/mL) was inoculated in LB media (5 mL) and grown overnight at 37 °C while shaking at 250 rpm. The following day, the overnight culture was diluted 200-fold (1 mL of overnight grown culture was added to 200 mL of new LB media) and grown for a few hours (typically 3-4 h) until the $OD_{600}$ reached 0.3-0.5. Once the $OD_{600}$ was 0.5, cells were harvested by spinning at 4000 rpm for 10 min at 4 °C. Cells were resuspended in a cold $CaCl_2$ solution (250 mL; 50 mM), and incubated on ice for 30 min, followed by centrifugation at 4000 rpm for 10 min. The cell pellet was resuspended in cold $CaCl_2$ (10 mL; 50 mM) containing glycerol (10%) and incubated 1 h on ice. Following incubation on ice, cells were aliquoted (200 uL) into microcentrifuge tubes and stored at -80 °C until further use.

### 4.4.8 Bacterial Transformation

The protocol was described in Chapter 2, section 2.4.7. The protocol is described for DH5α and it is also same for KC8 cells.

### 4.4.9 Plasmid isolation (Miniprep and midiprep)

The protocol was described in Chapter 2, section 2.4.8.

### 4.4.10 Cell culture

The protocol was described in Chapter 2, section 2.4.3.

### 4.4.11 Transient transfections

The protocol was described in Chapter 2, section 2.4.9.

### 4.4.12 Cell lysis

The protocol was described in Chapter 2, section 2.4.11.

### 4.4.13 Immunoprecipitation

The protocol was described in Chapter 2, section 2.4.12.

### 4.4.14 Co-Immunoprecipitation

For co-immunoprecipitation of overexpressed proteins, wild type or mutant HDAC1-FLAG was transfected into T-Ag Jurkat cells (section 4.4.11). After lysis as described (section 4.4.12), FLAG-tagged HDAC1 in the lysates (2 mg) was immunoprecipitated using pre-washed anti-FLAG agarose beads (20 µL bead slurry) by incubating at 4 °C overnight with rocking. Bound beads were washed three times with Jurkat Lysis Buffer (JLB; 1 mL; 50 mM Tris-Cl pH 8.0, 150 mM NaCl, 10% glycerol, and 0.5% triton-X100) and bound proteins were eluted with 2X SDS loading dye (25 µL: 50 mM Tris-Cl pH 6.8, 2% SDS, 10% glycerol, 0.004% bromophenol blue), separated by

10% SDS-PAGE (section 4.4.15), transferred to PVDF membrane (Immobilon P), and immunoblotted with FLAG and RbAp48 antibodies (section 4.4.15).

**4.4.15 SDS-PAGE and western blot**

The protocol was described in Chapter 2, section 2.4.14 and 2.4.16.

**4.4.16 HDAC activity assay**

HDAC activity assays were performed using the Fluoro de Lys™ Fluorometric Activity Assay kit (Enzo Life Sciences). Following transfection of FLAG-tagged wild type or mutant HDAC1 plasmids (section 4.4.11), cells were lysed in JLB (500 µL) containing 1X protease inhibitor cocktail (GenDEPOT) at 4 °C for 30 min with rotation (section 4.4.12). Protein concentration of the lysates were measured by Bradford assay. Wild type or mutant HDAC1 was immunoprecipitated from the T-Ag Jurkat lysates (2 mg) using pre-washed anti-FLAG agarose beads (20 µL bead slurry) by incubating overnight at 4 °C with rotation. The immunoprecipitates were washed three times with JLB (1 mL) and divided into two halves. One half was used in the HDAC activity assay, whereas the second half was used for the gel analysis. For the activity assay, immunoprecipitated HDAC1 on bead was resuspended in the HDAC assay buffer (25 µL; 50 mM Tris-Cl, pH 8.0, 137 mM NaCl, 2.7 mM KCl, 1 mM $MgCl_2$) and incubated with the Fluoro de Lys substrate (25 µL of 100 uM) at 37 $^0$C for 45 min with shaking (750 rpm). Next, the developer (50 µL of a 1X solution) was added and incubated for another 10 min, with readings (fluorescence; ex: 360 nm, em: 450 nm) taken using the GENios Plus plate reader (Tecan). The fluorescence signal was background corrected using a reaction with all the components except the HDAC enzyme. Then, the signal of each mutant was normalized to wild type HDAC1 (set to 100%). The means and the standard errors from

at least three independent trials are shown in Figure 4.1. For the gel analysis, bound proteins were eluted using 2X SDS loading dye (25 µL; 50 mM Tris-Cl pH 6.8, 2% SDS, 10% glycerol, 0.004% bromophenol blue), separated by 10% SDS-PAGE, transferred to a PVDF membrane (Immobilin-P) and immunoblotted with FLAG antibody.

**4.4.17 Mass Spectrometric analysis**

To identify the possible post-translational modifications on wild type and F437C mutant HDAC1, FLAG-tagged wild type or F437C mutant HDAC1 were overexpressed in T-Ag Jurkat cells (section 4.4.11). Following harvesting and lysis (section 4.4.12), wild type or F437C mutant HDAC1 were immunoprecipitated using pre-washed anti-FLAG agarose beads (20 µL bead slurry) by incubating overnight at 4 °C with rocking (section 4.4.13). Bound proteins were washed three times with JLB (1 mL), eluted using 2X SDS loading dye (25 µL; 50 mM Tris-Cl pH 6.8, 2% SDS, 10% glycerol, 0.004% bromophenol blue), separated by 10% SDS-PAGE, and stained with Sypro Ruby total protein stain. Gel slices containing the HDAC1 proteins were excised from the Sypro Ruby stained gel, trypsin digested, and subjected to MS analysis, as described in chapter 2, section 2.4.21 (105).

**4.4.18 *In vitro* dephosphorylation assays**

For *in vitro* dephosphorylation assays, wild type or mutant HDAC1-FLAG were transfected into T-Ag Jurkat cells, as described (section 4.4.11). FLAG-tagged HDAC1 protein in the lysates (2 mg) were immunoprecipitated using pre-washed anti-FLAG agarose beads (20 µL bead slurry) by incubating at 4 °C overnight with rocking (section 4.4.13). Bound beads were washed three times with JLB (1 mL), and beads were resuspended in NEB buffer 3.1 (20 µL; 100 mM NaCl, 50 mM Tris-HCl, 10 mM $MgCl_2$,

100 µg/mL BSA, pH 7.9; New England Biolabs), and incubated at 37 $^{o}$C for 1 h in the absence or presence of Calf Intetinal Phosphatase (CIP; NEB; 100 U). Then, the reaction was stopped by adding 2X SDS loading dye (10 µL) and proteins were separated by 10% SDS-PAGE, transferred to PVDF membrane (Immobilon P), and immunoblotted with FLAG antibody.

# CHAPTER 5 - CONCLUSIONS AND FUTURE DIRECTIONS

HDAC proteins regulates key cellular processes such as proliferation, differentiation and apoptosis. As a consequence, dysregulation of HDAC activity and expression is associated with multiple diseases, including cancer. Substrate identification is an effective approach to fully understand the function of individual HDACs in physiological processes as well as in diseases. Despite the growing list of acetylated proteins, very few non-histone substrates have been identified for HDAC1 due to the lack of substrate discovery tools.

The main goal of my first dissertation project was to develop a method to identify substrates of HDAC1. By applying a substrate trapping strategy to HDAC1, few new substrates have been identified. Among these hits, Eg5 or Kinesin like protein 11 and Lysine specific histone demethylase (LSD1) were fully characterized as novel substrates of HDAC1.

Three inactive mutants (H141A, F150A and C151A) were selected from HDAC1 active site and screened for substrate trapping ability in jurkat cells. All three mutants were able to bind to Eg5, suggesting that Eg5 could be a potential substrate of HDAC1. The results indicated that HDAC1 deacetylates Eg5 at K890 which affects ATPase activity of Eg5. HDAC1 colocalized with Eg5 during prophase in mitosis. HDAC1 and 2 selective inhibitor increased cell cycle arrest at mitotic phase. Further mechanistic studies proved that mitotic arrest phenotype observed with HDAC1 and 2 selective inhibitor was mainly due to inactivation of Eg5 and formation of monopolar spindles. The study clearly uncovered a previously unknown function of HDAC1 during mitosis and the mechanism of HDAC1 and 2 selective inhibitor induced mitotic arrest.

The substrate trapping strategy was extended to HEK293 cells to confirm that this method can be applied to multiple cell lines to discover non-histone substrates of HDAC1. The C151A mutant displayed good trapping ability compared to other mutants tested. Three new substrates were identified using mass spectrometry. Among these three hits, LSD1 was further validated using secondary assays to understand the functional link between HDAC1 and LSD1. The data indicated that HDAC1 deacetylates LSD1 at K374. Acetylation of LSD1 at K374 affected the histone H3 binding and target gene expression. The study revealed a crosstalk between two epigenetic enzymes as well as a secondary mechanism of HDAC inhibitors on LSD1 activity. Overall, identification of two non-histone substrates of HDAC1 revealed new functions of HDAC1 and the mechanism of action of HDAC inhibitors.

The substrate trapping strategy seems an effective tool to identify substrates of HDAC1. The method can be applied to other HDAC isoforms as well. This project could be directed to multiple directions in the future. As initial studies were performed with three strictly conserved active site residues, multiple mutants can be screened from the 11 A and 14 A channels to find the optimal substrate trapping mutant. Most importantly, the trapping strategy could be applied to compare the substrate profile of HDAC1 in physiological conditions and pathological conditions using respective cell lines. Further, the strategy can be applied to class II HDAC isoform, HDAC6. Given that HDAC6 has two deacetylase domains, this method can be applied to distinguish between substrate specificities among the two domains. In conclusion, this method holds a great promise to broaden the substrate profile and regulation of HDAC1 in normal and disease conditions in the future.

The second project of my dissertation focused on undersdanding the effect of HDAC1 SNP on expression, activity and post-translational modifications. Presence of HDAC1 exonic SNP-F437C, reduced the deacetylase activity, increased acetylation at K432. Further, presence of F437C negatively affected the phosphorylation of HDAC1 at S393. These studies are helpful in understanding how mutations could affect enzymatic activity or modifications in disease conditions. Detailed understanding of the role of HDAC1 SNPs in different diseases will assist in finding new treatments in a personalized a manner.

## APPENDIX A – CHAPTER 2 REPRODUCIBLE TRIALS

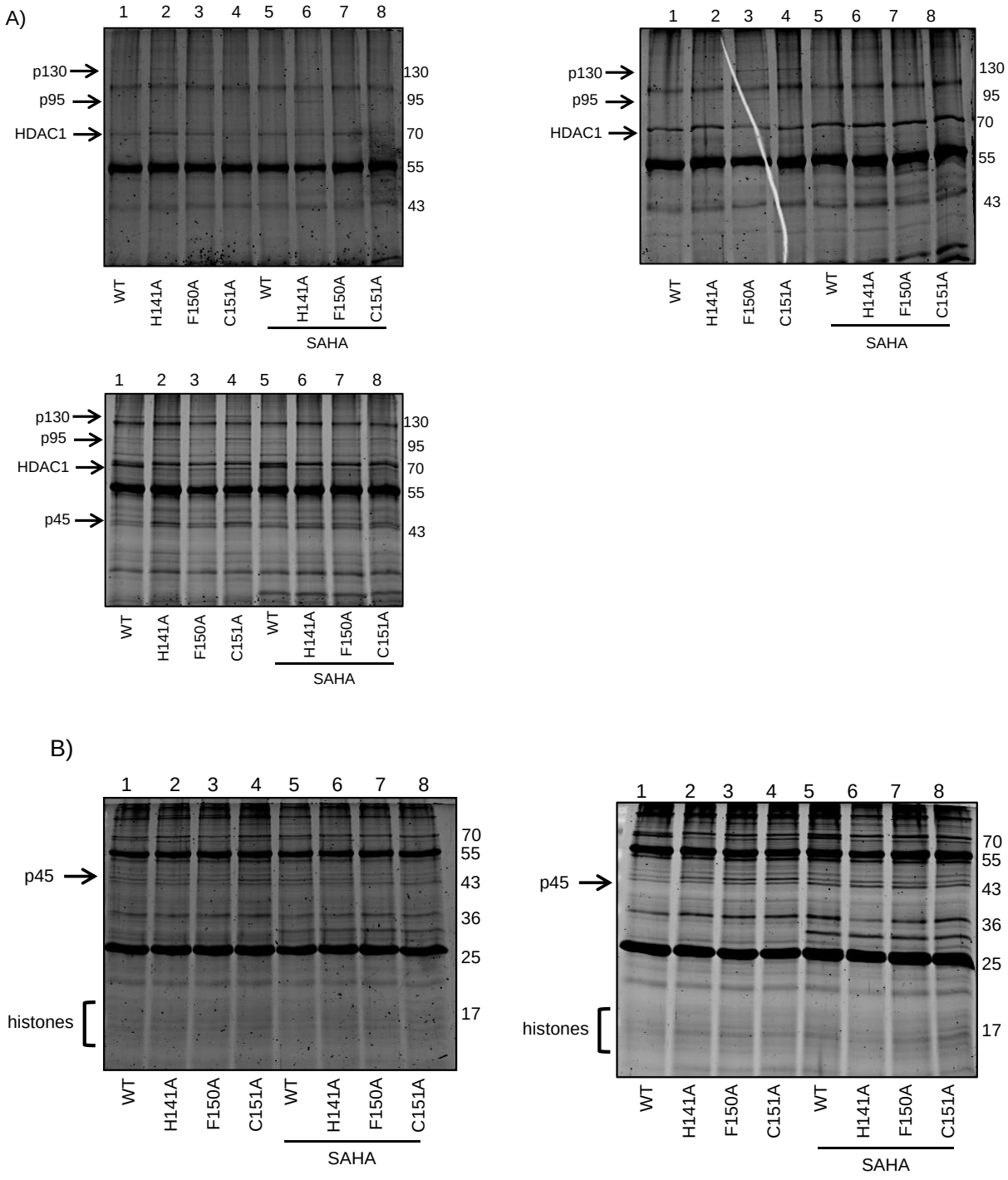


**Figure A 2.1 - Substrate trapping by HDAC1 mutants.** Wild type (WT) and mutant HDAC1 (indicated below each lane) were expressed as Flag-tagged proteins in T-Ag Jurkat cells, immunoprecipitated with anti-Flag agarose, separated by 12% (A) or 16 %

(B) SDS-PAGE, and visualized with SyproRuby total protein stain. Arrows indicate immunoprecipitated HDAC1 or possible substrates (p130, p95, p45, or histones) observed in the absence but not presence of competitive active site inhibitor SAHA (0.8 mM). Repetitive trials are shown in Figure 2.2.

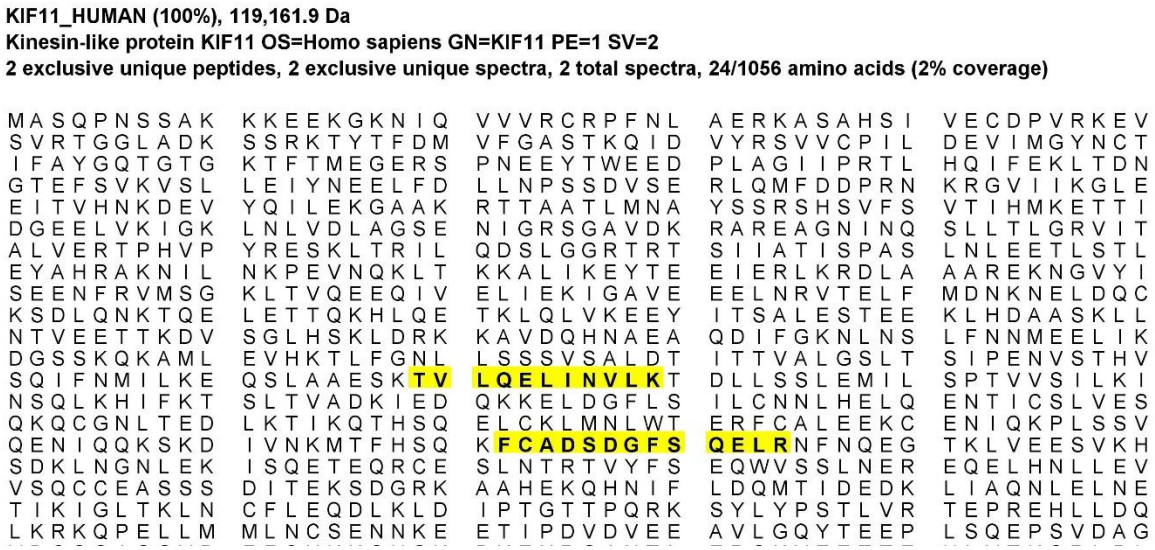


**Figure A.2.2 - Peptides of Eg5 (KIF11) observed in the substrate trapping experiment.** Primary sequence of Eg5 (KIF11), which was identified in the substrate trapping experiment as p130. Peptides observed in the MS/MS analysis are highlighted in yellow. The parameters were set to protein threshold 95%, peptide threshold 99% with minimum number of peptides set to 2.

A) Peptide sequence- TVLQELINVLK

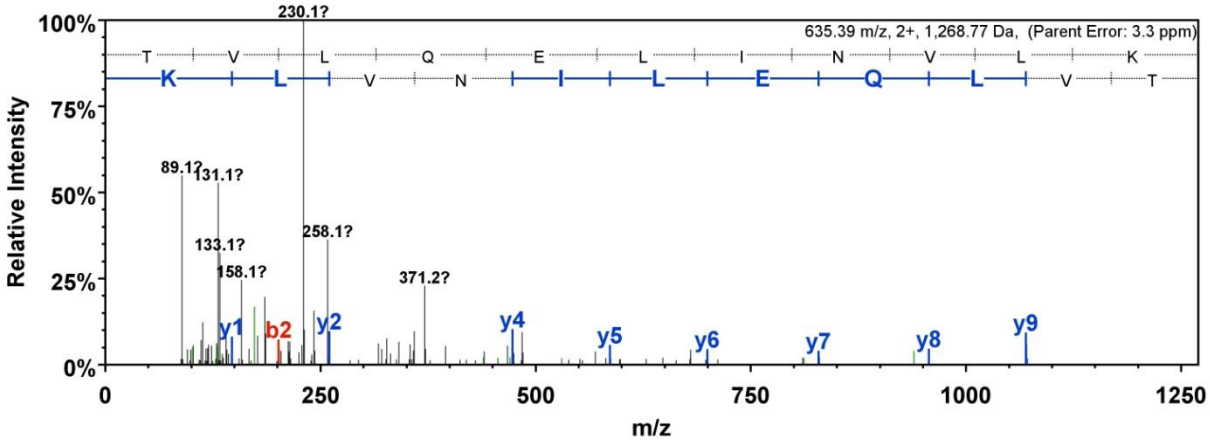


B) Peptide sequence- FCADSDGFSQELR

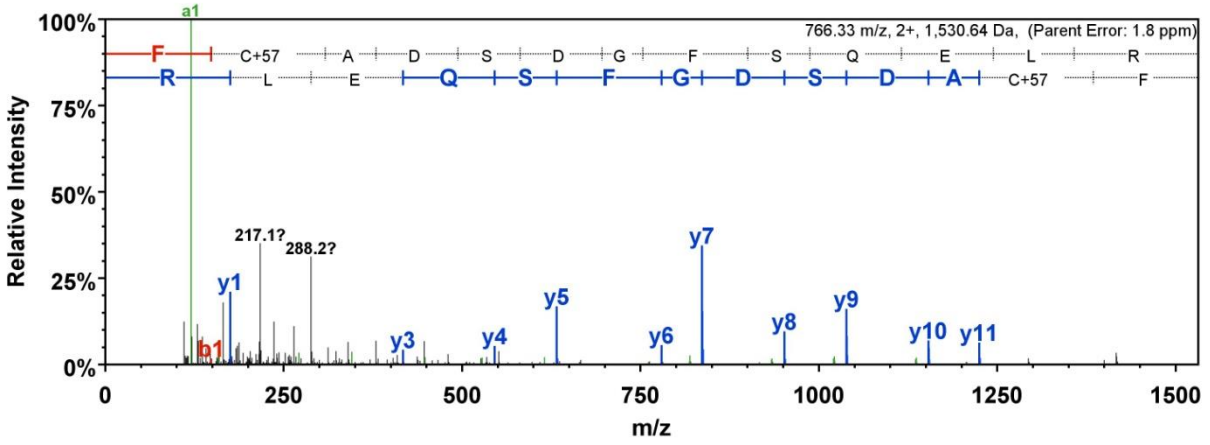


**Figure A.2.3** – **Spectra of Eg5 (KIF11) peptides identified by MS/MS analysis**. The annotated spectra of Eg5 (KIF11) peptides identified by MS/MS analysis (Figure 2.2). Each spectrum represents the different peptides identified from Eg5.

**ACTG_HUMAN (100%), 41,793.9 Da**
**Actin, cytoplasmic 2 OS=Homo sapiens GN=ACTG1 PE=1 SV=1**
**8 exclusive unique peptides, 11 exclusive unique spectra, 15 total spectra, 120/375 amino acids (32% coverage)**

MEEEIAALVI DNGSGMCKAG FAGDDAPRAV FPSIVGRPRH QGVMVGMGQK
DSYVGDEAQS KRGILTLKYP IEHGIVTNWD DMEKIWHHTF YNELRVAPEE
HPVLLTEAPL NPKANREKMT QIMFETFNTP AMYVAIQAVL SLYASGRTTG
IVMDSGDGVT HTVPIYEGYA LPHAILRLDL AGRDLTDYLM KILTERGYSF
TTTAEREIVR DIKEKLCYVA LDFEQEMATA ASSSSLEKSY ELPDGQVITI
GNERFRCPEA LFQPSFLGME SCGIHETTFN SIMKCDVDIR KDLYANTVLS
GGTTMYPGIA DRMQKEITAL APSTMKIKII APPERKYSVW IGGSILASLS
TFQQMWISKQ EYDESGPSIV HRKCF

**Figure A.2.4 - Peptides of actin observed in the substrate trapping experiment.**

Primary sequence of cytoplasmic actin identified in the substrate trapping experiment as p45. Peptide sequences observed in the MS/MS analysis are highlighted in yellow, while modified amino acids are in green. The parameters were set to protein threshold 95%, peptide threshold 99% with minimum number of peptides set to 2.

Peptide sequence- AVFPSIVGRPR

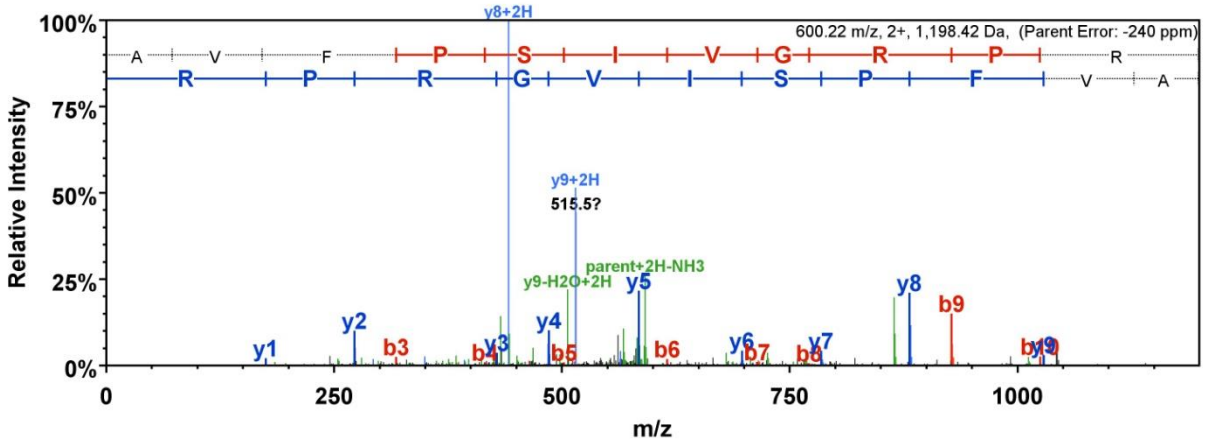


**Figure A.2.5– Spectrum of actin peptide identified by MS/MS analysis.** The annotated spectrum of one of the cytoplasmic actin peptides identified by MS/MS analysis.

A

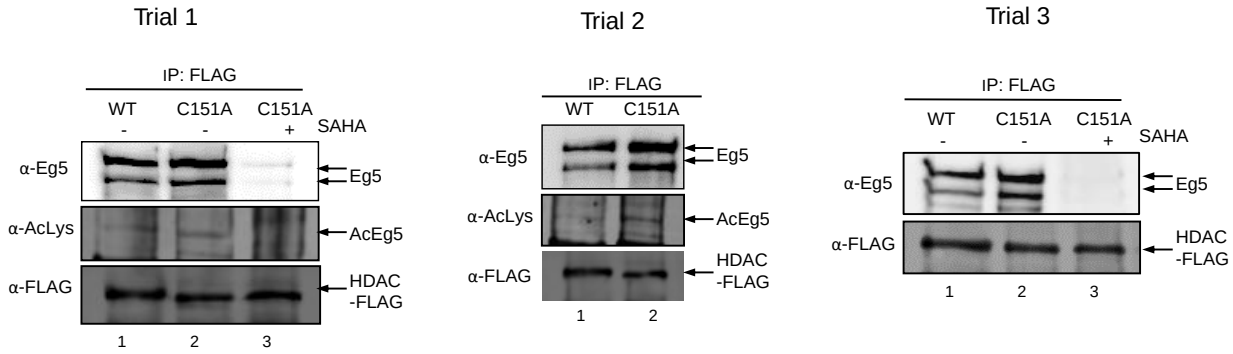

B

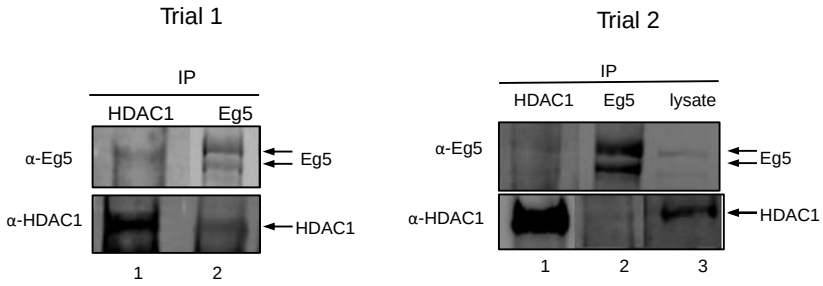


C

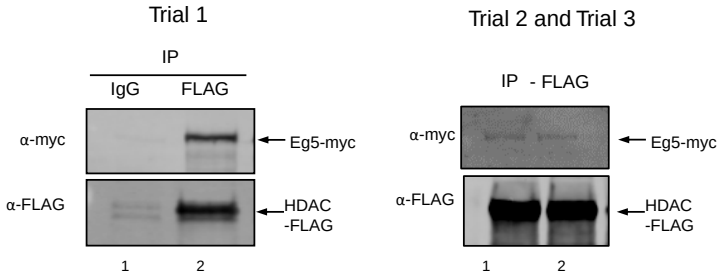


**Figure A.2.6 - Eg5 interacts with HDAC1.** A) Wild type (WT) or C151A HDAC1 were expressed as FLAG-tagged proteins in T-Ag Jurkat cells, immunoprecipitated (IP) with anti-Flag agarose in the absence (lanes 1 and 2) or presence (lane 3) of SAHA (3 mM), separated by SDS-PAGE, and Western blotted with Eg5 (top), acetyl-lysine (AcLys, middle), or Flag (bottom) antibodies. Three trials are shown here with a fourth shown in Figure 2.3A. B) Endogenous HD1 and Eg5 were immunoprecipitated (IP) separately from T-Ag Jurkat cells, separated by SDS-PAGE, and Western blotted with Eg5 (top) or HDAC1 (bottom) antibodies. Two trials are shown here with a third shown in the Figure 2.3B. C) HDAC1-Flag and Eg5-myc were coexpressed in HEK293 cells, immunoprecipitated (IP) separately with Flag antibody, separated by SDS-PAGE, and Western blotted with myc (top) or Flag (bottom) antibodies. Agarose beads without bound antibodies were used as an immunoprecipitation controls (Figure A 2.6C-lane 1). Three

trials are shown here with a fourth shown in Figure 2.3C. For all gels, arrows indicate the position of Eg5 and HDAC1 in the gels.

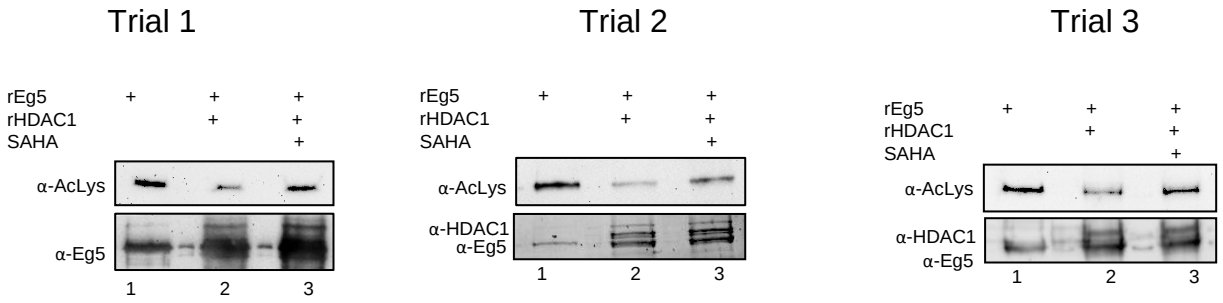


**Figure A.2.7 – Independent trials used for quantification of *in vitro* assay with recombinant HDAC1.** Western blot analyses from three independent trials (first trial is shown in Figure 2.6A). These blots were quantified with the raw data shown as a Table A.2.1 or a histogram (Figure 2.6B). To assure equal protein loading, the Eg5 bands in the Eg5 Western blot were quantified with the data shown in Table A.2.2.

**Table A.2.1 – Quantification of AcLys signal from *in vitro* deacetylation assay**

| | Trial | Trial | Trial | Mean | Standard |
|---|---|---|---|---|---|
| rEg5 Ac-Lys | 100 | 100 | 100 | 100 | 0.0 |
| rEg5 Ac-Lys + rHDAC1 | 39 | 19 | 39 | 32 | 7 |
| rEg5 Ac-Lys + rHDAC1 + | 70 | 43 | 71 | 61 | 9 |

*Data shown in Figure 2.6B.

**Table A.2.2 - Quantification of Total Eg5 signal from *in vitro* deacetylation assay**

| | Trial 1 | Trial 2 | Trial 3 | Mean | Standard Error |
|---|---|---|---|---|---|
| Eg5 | 100 | 100 | 100 | 100 | 0.0 |
| rEg5 + rHDAC1 | 106 | 116 | 127 | 115 | 5 |
| rEg5 + rHDAC1 + SAHA | 98 | 127 | 118 | 114 | 9 |

*Data shown in Figure A.2.8

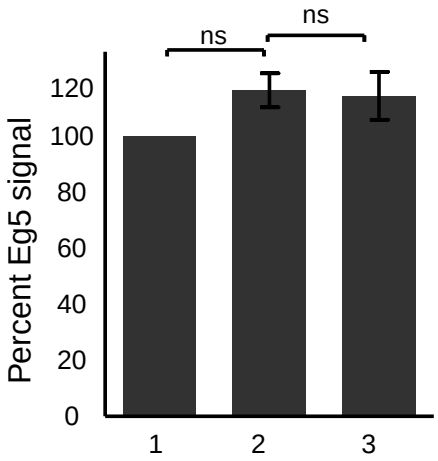


**Figure A.2.8 – Quantification of total Eg5 protein.** Raw data is shown in the table A.2.2. ns- not significant.

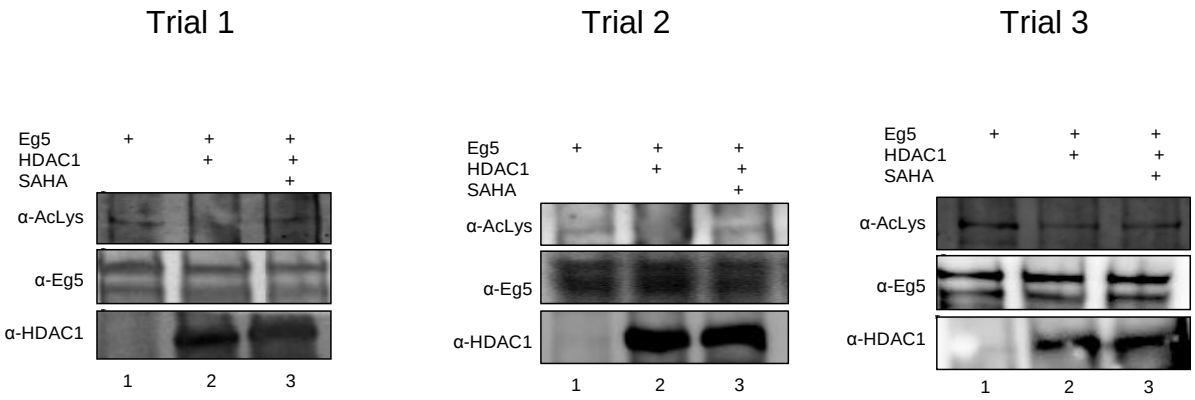


**Figure A.2.9 – Independent trials used for quantification of deacetylation with cellular HDAC1.** Western blots from three independent trials (Trial 1 is shown in Figure 2.6C) were quantified with the raw data shown in Table A.2.3 or histogram (Figure 2.6D). To assure equal protein loading, the Eg5 bands in the Eg5 Western blot were quantified with the data shown as a Table A.2.4.

**Table A.2.3 – Quantification of AcLys signal from *in cellulo* deacetylation assay**

| | Trial | Trial | Trial | Mean | Standard |
|---|---|---|---|---|---|
| Eg5 Ac-Lys | 100 | 100 | 100 | 100 | 0.0 |
| Eg5 Ac-Lys + HDAC1 | 12 | 11 | 16 | 13 | 2 |
| Eg5 Ac-Lys + HDAC1 + | 90 | 120 | 80 | 97 | 12 |

*Data shown in Figure 2.6D.

**Table A.2.4 – Quantification of Eg5 signal from *in cellulo* deacetylation assay**

| | Trial 1 | Trial 2 | Trial 3 | Mean | Standard Error |
|---|---|---|---|---|---|
| Eg5 | 100 | 100 | 100 | 100 | 0.0 |
| Eg5 + HDAC1 | 97 | 90 | 110 | 99 | 6 |
| Eg5 + HDAC1 + SAHA | 96 | 110 | 90 | 92 | 2 |

*Data shown in Figure A.2.10.

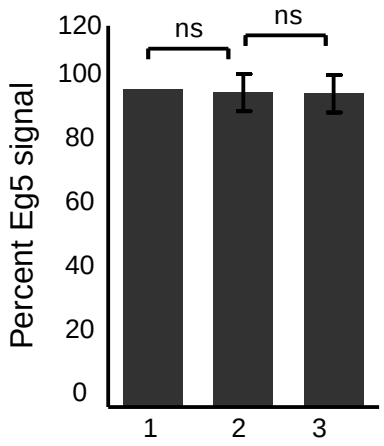


**Figure A.2.10** – **Quantification of total Eg5 protein.** Raw data is shown in Table A.2.4. ns- not significant

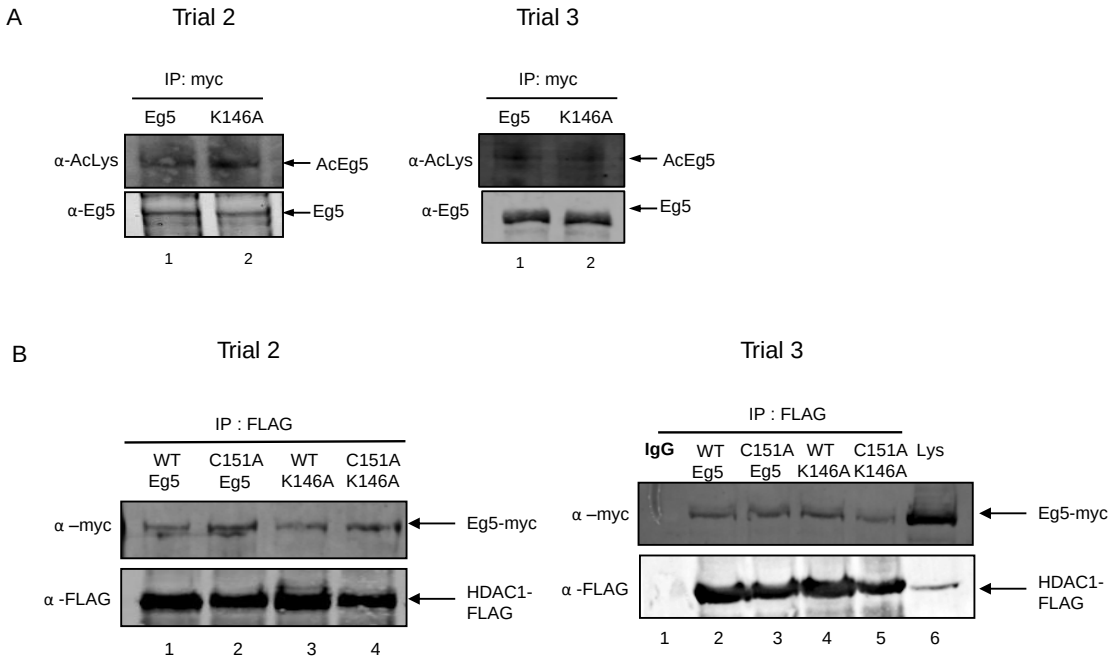


**Figure A 2.11 – K146 is not a predominant Eg5 acetylation site regulated by HDAC1.** A) Myc-tagged wild type or K146A mutant Eg5 were transfected into HEK293 cells, treated with SAHA for 24 h, and immunoprecipitated with a myc antibody. SDS-PAGE separation and immunoblotting were performed with acetyl lysine (top) and myc (bottom) antibodies. No change in the acetylation levels of the wild type and mutant proteins were observed (top gel), which indicated that K146 is not a predominant acetylation site on Eg5. Two trials are shown here with a third shown in Figure 2.7A. B) FLAG-tagged wild type (WT) or C151A mutant HDAC1 were cotransfected with myc-tagged wild type or K146A mutant Eg5 into HEK293 cells. Wild type and C151A mutant HDAC1 were immunoprecipitated using anti-FLAG agarose beads, separated by SDS-PAGE, and immunoblotted with myc (top) and FLAG (bottom) antibodies. No changes in the levels of immunoprecipitated Eg5 were observed with either wild type or mutant proteins (top gel), which indicated that K146 is not a site bound and regulated by HDAC1. Two trials are shown here with a third shown in Figure 2.7B.

## A. Eg5 + DMSO sample - sequence converage

**KIF11_HUMAN (100%), 119,161.9 Da**
**Kinesin-like protein KIF11 OS=Homo sapiens GN=KIF11 PE=1 SV=2**
**89 exclusive unique peptides, 177 exclusive unique spectra, 438 total spectra, 745/1056 amino acids (71% coverage)**

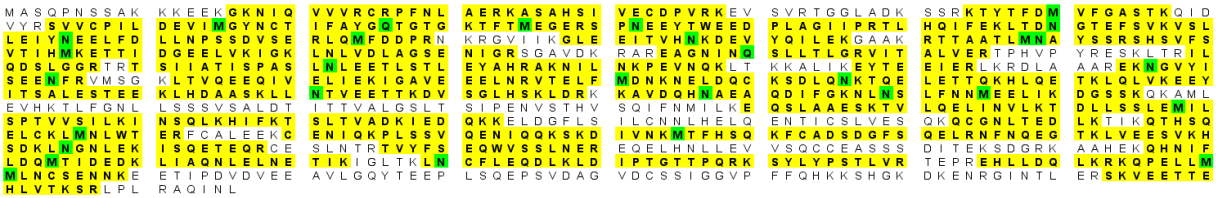

## B. Eg5 + DMSO sample - peptide identified

Peptide sequence- (K)QHNIFLDQMTIDEDKLIAQNLELNETIK(I)

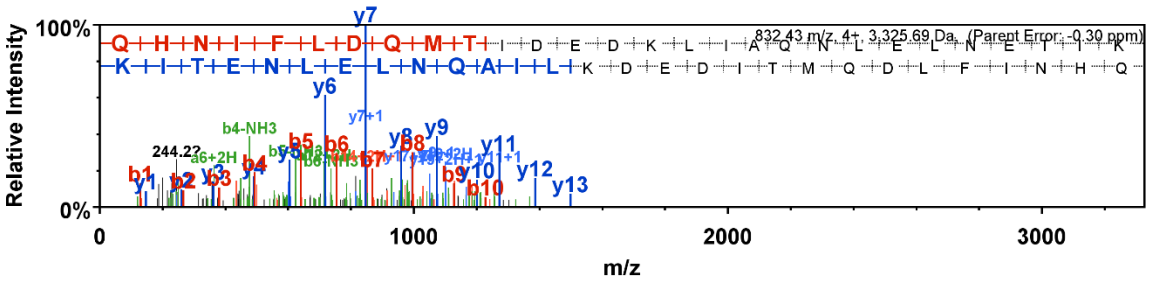

## C. Eg5 + SHI-1:2 sample - sequence coverage

KIF11_HUMAN (100%), 119,161.9 Da
Kinesin-like protein KIF11 OS=Homo sapiens GN=KIF11 PE=1 SV=2
80 exclusive unique peptides, 178 exclusive unique spectra, 584 total spectra, 763/1056 amino acids (72% coverage)

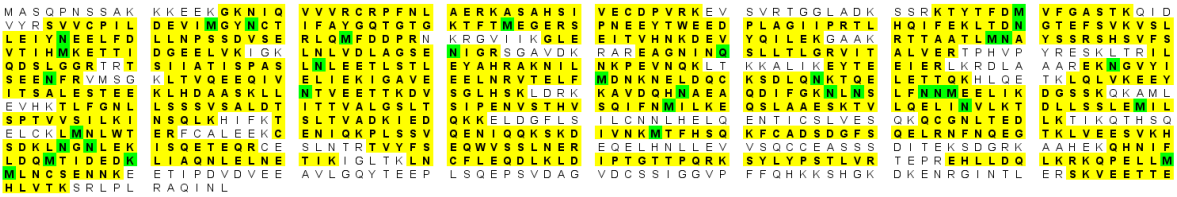

## D. Eg5 + SHI-1:2 sample - peptide identified

Peptide sequence- (K)QHNIFLDQMTIDEDKAcLIAQNLELNETIK(I)

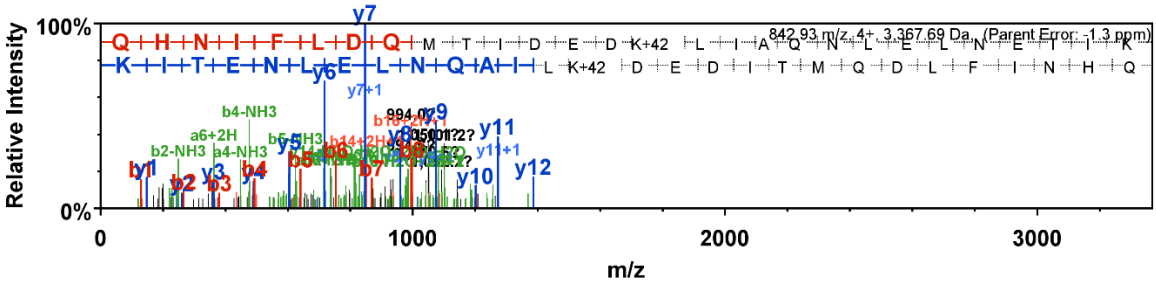

## E. Eg5 + SAHA sample - sequence coverage

KIF11_HUMAN (100%), 119,161.9 Da
Kinesin-like protein KIF11 OS=Homo sapiens GN=KIF11 PE=1 SV=2
100 exclusive unique peptides, 211 exclusive unique spectra, 794 total spectra, 866/1056 amino acids (82% coverage)

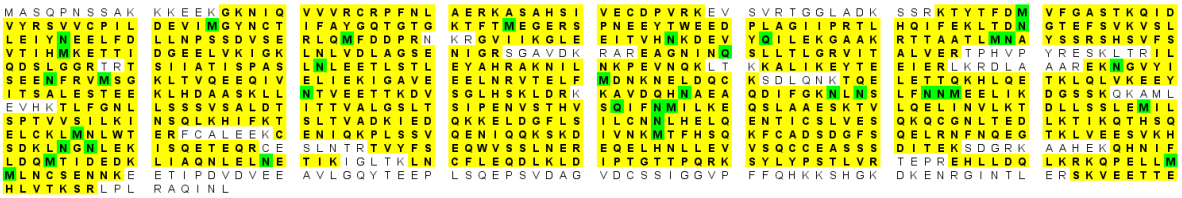

## F. Eg5 + SAHA sample - peptide identified

Peptide sequence- (K)QHNIFLDQMTIDEDKLIAQNLELNETIK(I)

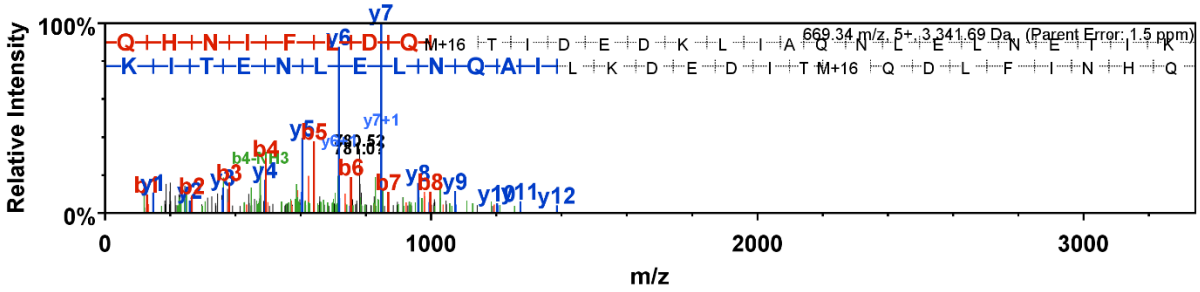

## G. Eg5 + overexpressed HDAC1 sample - sequence coverage

KIF11_HUMAN (100%), 119,161.9 Da
Kinesin-like protein KIF11 OS=Homo sapiens GN=KIF11 PE=1 SV=2
91 exclusive unique peptides, 206 exclusive unique spectra, 723 total spectra, 773/1056 amino acids (73% coverage)

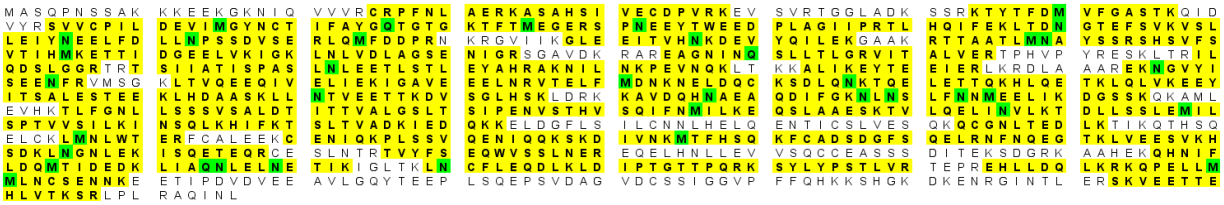

## H. Eg5 + overexpressed HDAC1 sample - peptide identified

Peptide sequence- (K)QHNIFLDQMTIDEDKLIAQNLELNETIK(I)

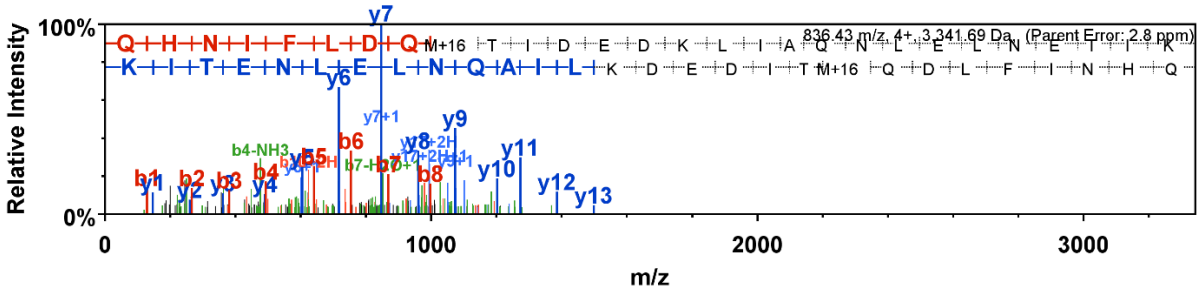


**Figure A.2.12- MS analysis of K890.** A) Primary sequence of Eg5 (KIF11) identified in the control DMSO-treated sample. Peptides observed in the MS/MS analysis are highlighted in yellow. The parameters were set to protein threshold 95%, peptide threshold 99% with minimum number of peptides set to 2 for all samples discussed here. B) Spectrum of the Eg5 peptide containing K890 from control DMSO-treated sample identified by MS/MS analysis (unacetylated K890 shown in red). C) Primary sequence of Eg5 (KIF11) identified in the SHI-1:2-treated sample. Peptides observed in the MS/MS analysis are highlighted in yellow. D) Spectrum of Eg5 peptide containing acetylated K890 from the SHI-1:2-treated sample identified by MS/MS analysis (acetylated K890 shown in red). E) Primary sequence of Eg5 (KIF11) identified in the SAHA-treated

sample. Peptides observed in the MS/MS analysis are highlighted in yellow. F) Spectrum of Eg5 peptide containing K890 from SAHA treated sample identified by MS/MS analysis (unacetylated K890 shown in red). G) Primary sequence of Eg5 (KIF11) identified in the Eg5 sample where HDAC1 was overexpressed. Peptides observed in the MS/MS analysis are highlighted in yellow. D) Spectra of Eg5 peptide containing K890 from Eg5 where HDAC1 was overexpressed identified by MS/MS analysis (unacetylated K890 shown in red).

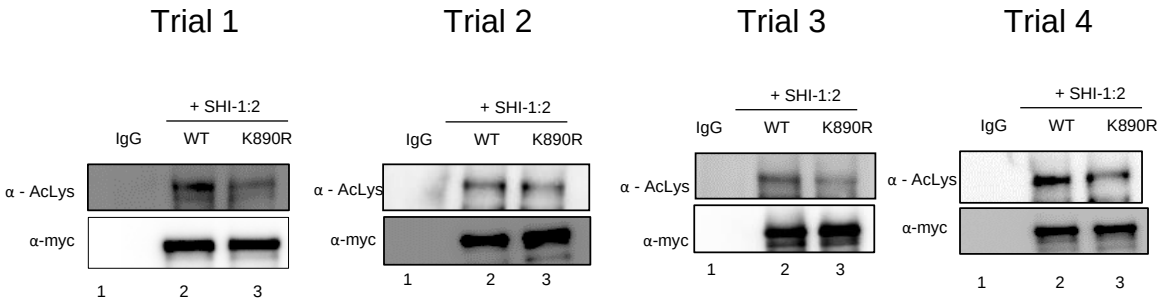


**Figure A.2.13** – **Independent trials used for quantification of K890R aceylation**. A-D) Western blots from four independent trials (Trial 3 is shown in Figure 2.8A) were quantified with the raw data shown in Table A.2.5 or as a histogram (Figure 2.8B). To assure equal protein loading, the Eg5-myc bands in the myc Western blot were quantified with the data shown as a Table A.2.6 or histogram (Figure A.2.14)

**Table A.2.5 – Quantification of AcLys signal from WT and K890R mutant**

| | Trial 1 | Trial 2 | Trial 3 | Trial 4 | Mean | Standard Error |
|---|---|---|---|---|---|---|
| Eg5 AcLys | 100 | 100 | 100 | 100 | 100 | 0.0 |
| K890R AcLys | 31 | 28 | 29 | 32 | 30 | 1 |

*Data shown in Figure 2.8B.

**Table A.2.6 – Quantification of myc signal from WT and K890R mutant**

| | Trial 1 | Trial 2 | Trial 3 | Trial 4 | Mean | Standard Error |
|---|---|---|---|---|---|---|
| Eg5-myc | 100 | 100 | 100 | 100 | 100 | 0.0 |
| K890R myc | 100 | 104 | 102 | 104 | 103 | 1 |

*Data shown in Figure A.2.14.

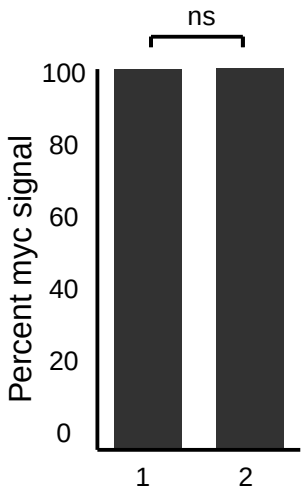


**Figure A.2.14** – **Quantification of myc signal from WT and K890R mutant.** Raw data is shown in the table A.2.6. ns - not significant

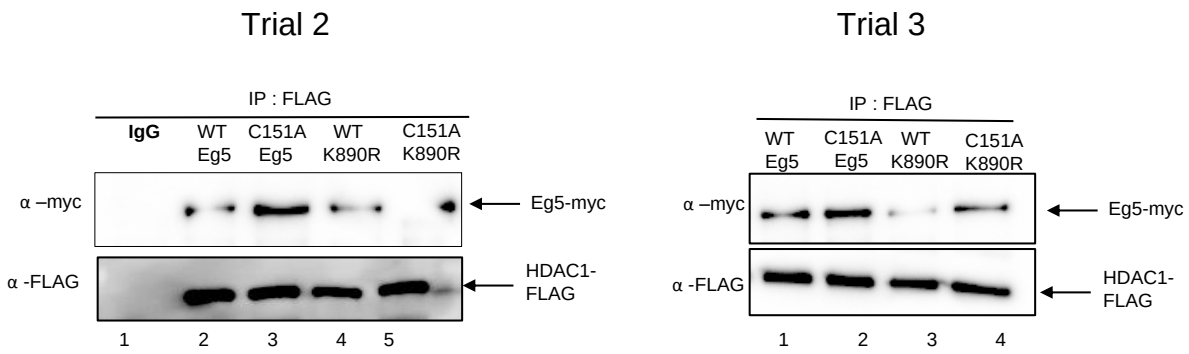


**Figure A.2.15 – Acetylation of Eg5 at K890 mediates the interaction between Eg5 and HDAC1.** FLAG-tagged wild type (WT) or C151A mutant HDAC1 were cotransfected with myc-tagged wild type or K890R mutant Eg5 into HEK293 cells. Wild type and C151A mutant HDAC1 were immunoprecipitated using anti-FLAG agarose beads, separated by SDS-PAGE, and immunoblotted with myc (top) and FLAG (bottom) antibodies. Two trials are shown here with a third shown in the Figure 2.8.C.

Trial 2

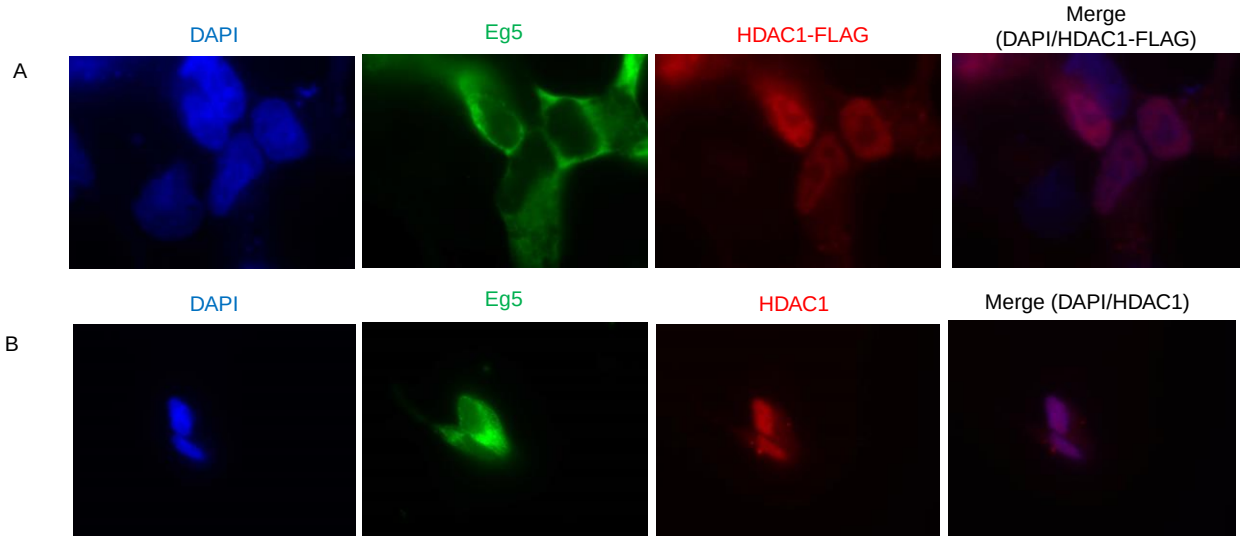

Trial 3

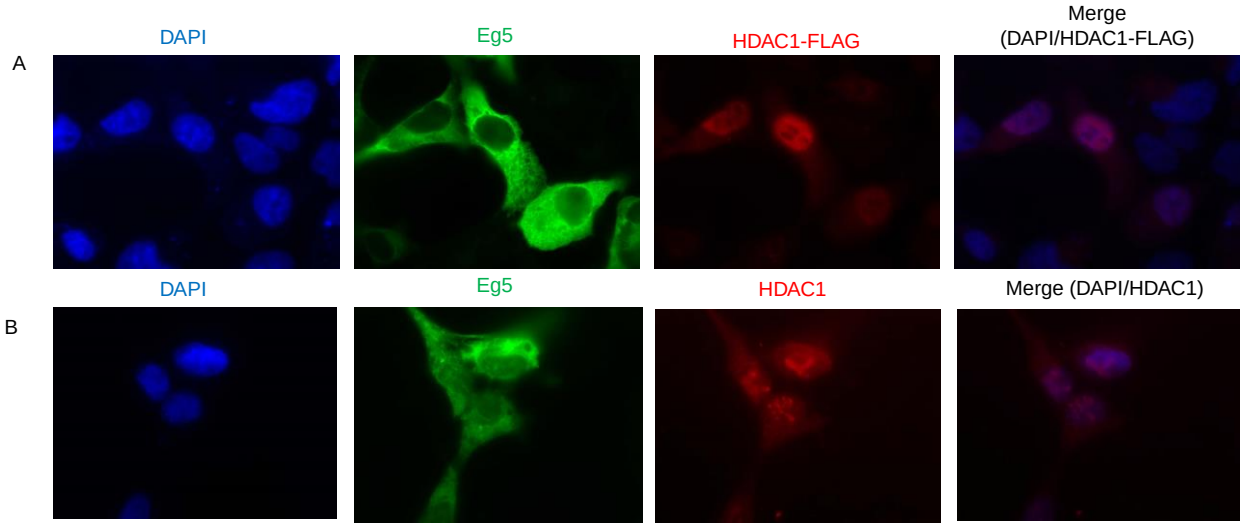


**Figure A.2.16 – Repetitive trials for endogenous and overexpressed HDAC1 localization in the nucleus**. HEK293 cells expressing FLAG-tagged HDAC1 (A) or HEK293 cells alone (B) were fixed and stained with FLAG (A) or HDAC1 (B) antibodies (red). Cells were counterstained with DAPI (blue) and visualized using fluorescence microscopy. Both endogenous and overexpressed HDAC1 were predominantly nuclear. The data suggests that the FLAG tag does not affect the localization of HDAC1-FLAG. Two trials are shown here with the third shown in Figure 2.9.

A) INTERPHASE

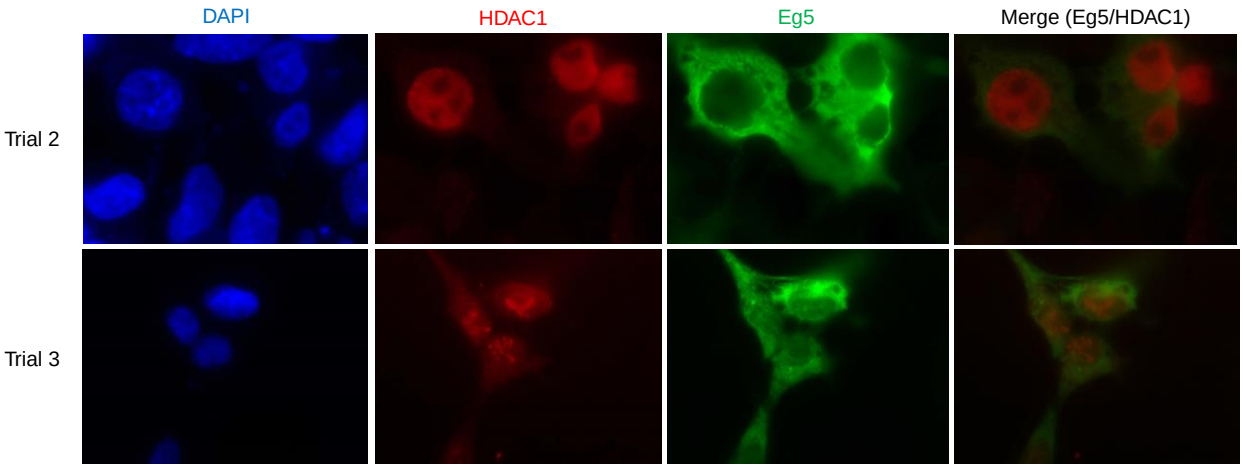


B) PROPHASE

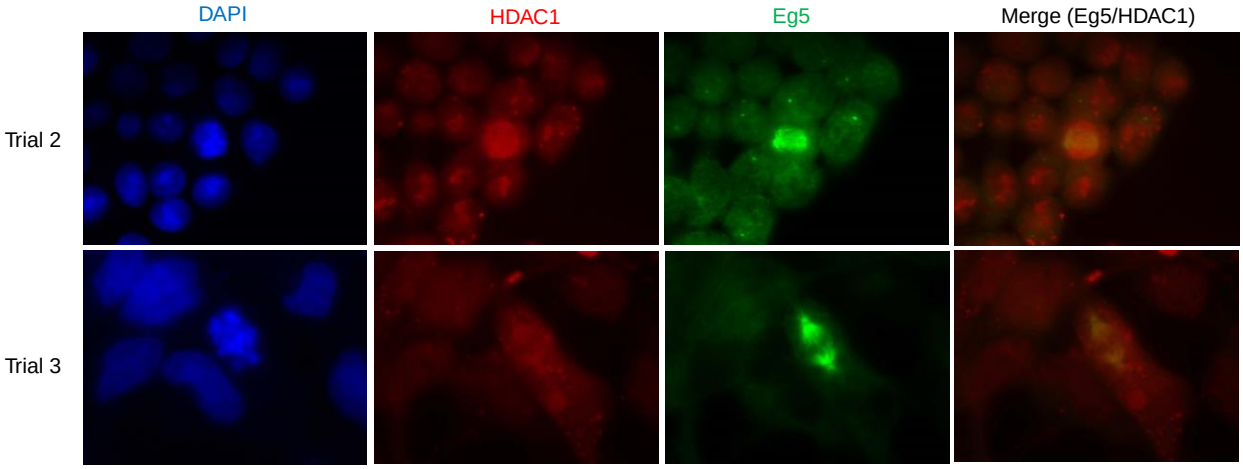


C) METAPHASE

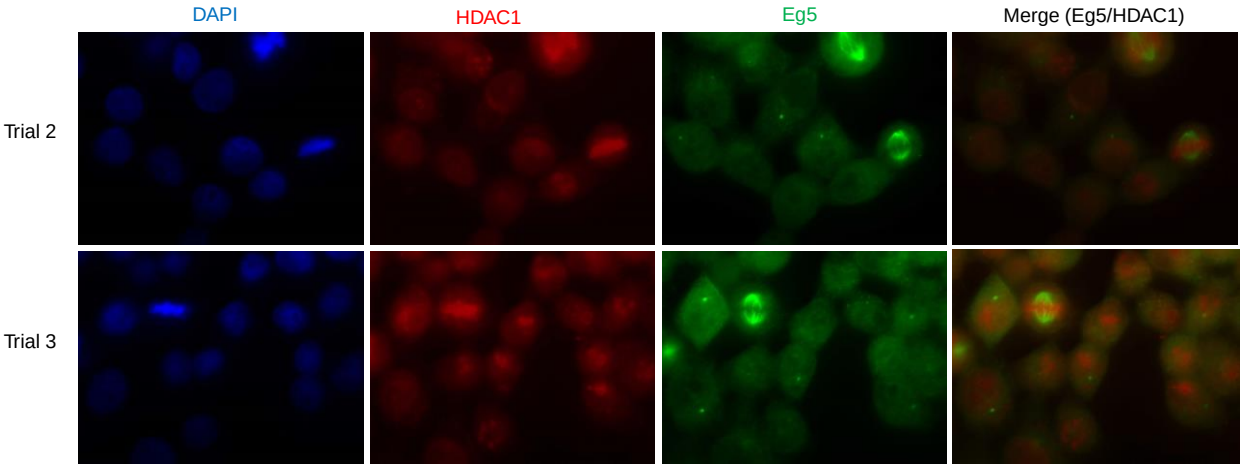

D) ANAPHASE

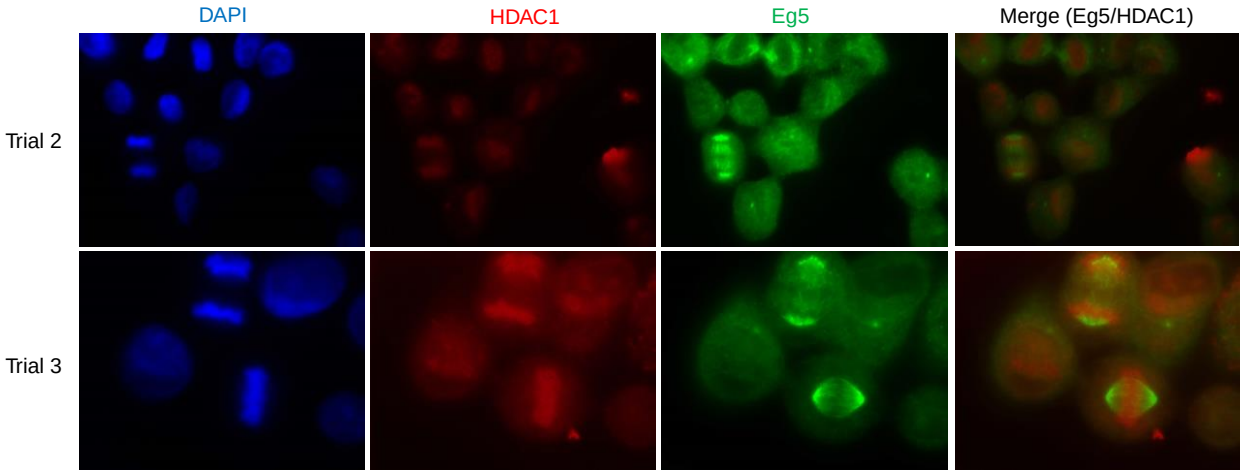

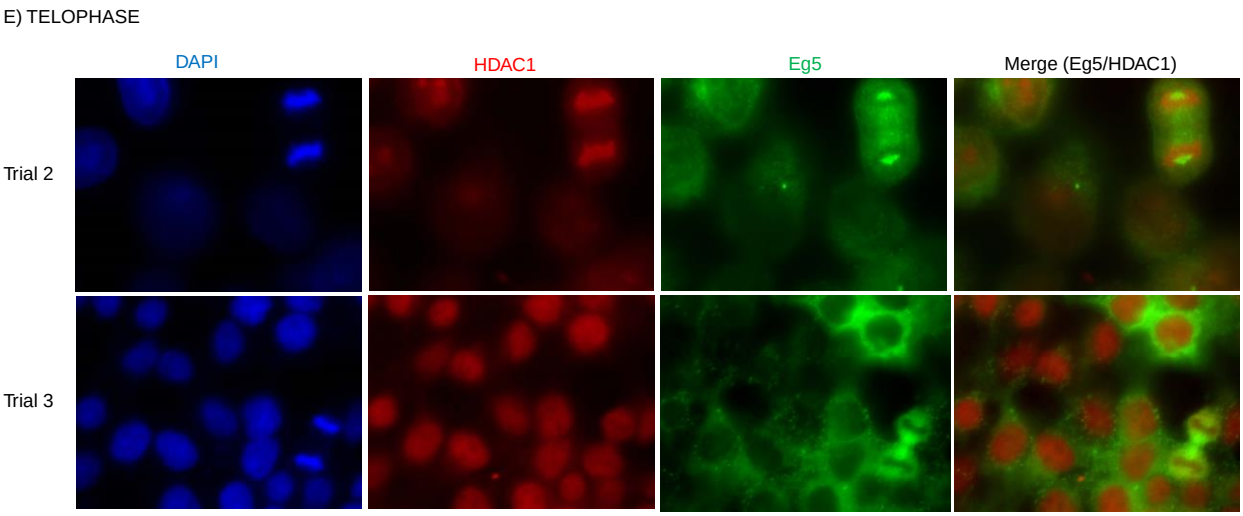


**Figure A.2.17 – Repetitive trials for Eg5 and HDAC1 localization in mitotic phases.** HEK293 cells were fixed and stained with HDAC1 (red) and Eg5 (green) antibodies. Cells were counterstained with DAPI (blue). Fluorescence microscopy was used to visualize HDAC1 and Eg5 in each cell. Cells in interphase (A), prophase (B), metaphase (C), anaphase (D), and telophase (E) are shown. HDAC1 (red) and Eg5 (green) images were used to generate merged images (yellow). Two trials are shown here with the third shown in Figure 2.10.

## APPENDIX B – CHAPTER 3 REPRODUCIBLE TRIALS

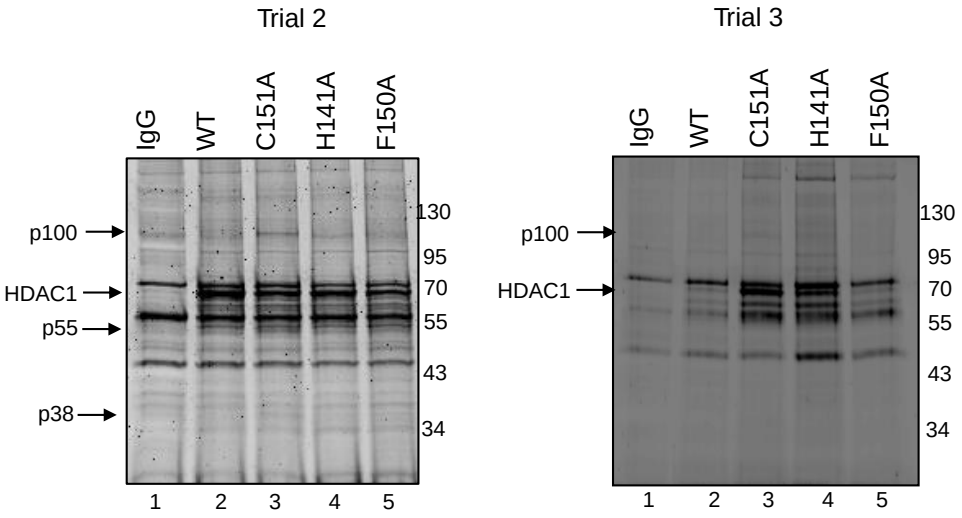


**Figure A.3.1–Repetitive trials for substrate trapping in HEK293 cells**. Wild type (WT) or mutant HDAC1 (indicated above each lane) were expressed as Flag-tagged proteins in HEK293 cells and then cells were treated with 10 μM SAHA for 24 h to induce robust protein acetylation. Cells were lysed and proteins were immunoprecipitated with anti-Flag agarose in the presence or absence of 10 μM SHI-1:2. Bound proteins were separated by SDS-PAGE, and stained with Sypro Ruby total protein stain. Arrows point to HDAC1 or possible substrates (p100, p55, p38) present in mutant but not WT or inhibitor treated samples. Two trials are shown here, with the third shown in the Figure 3.1

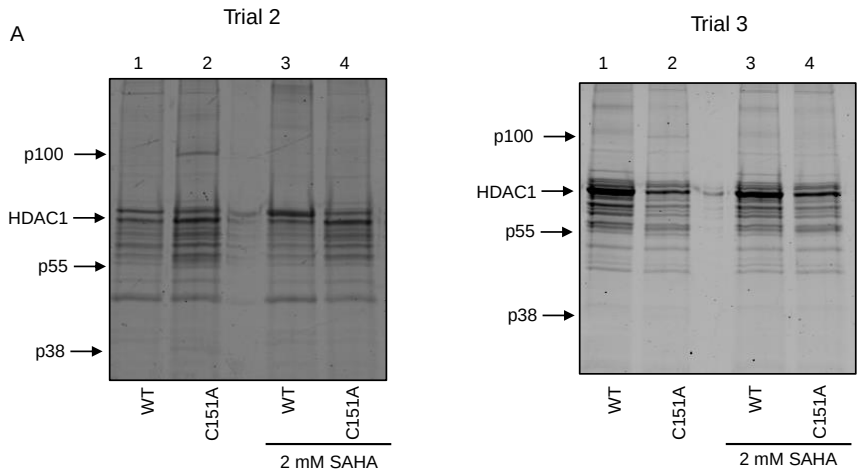

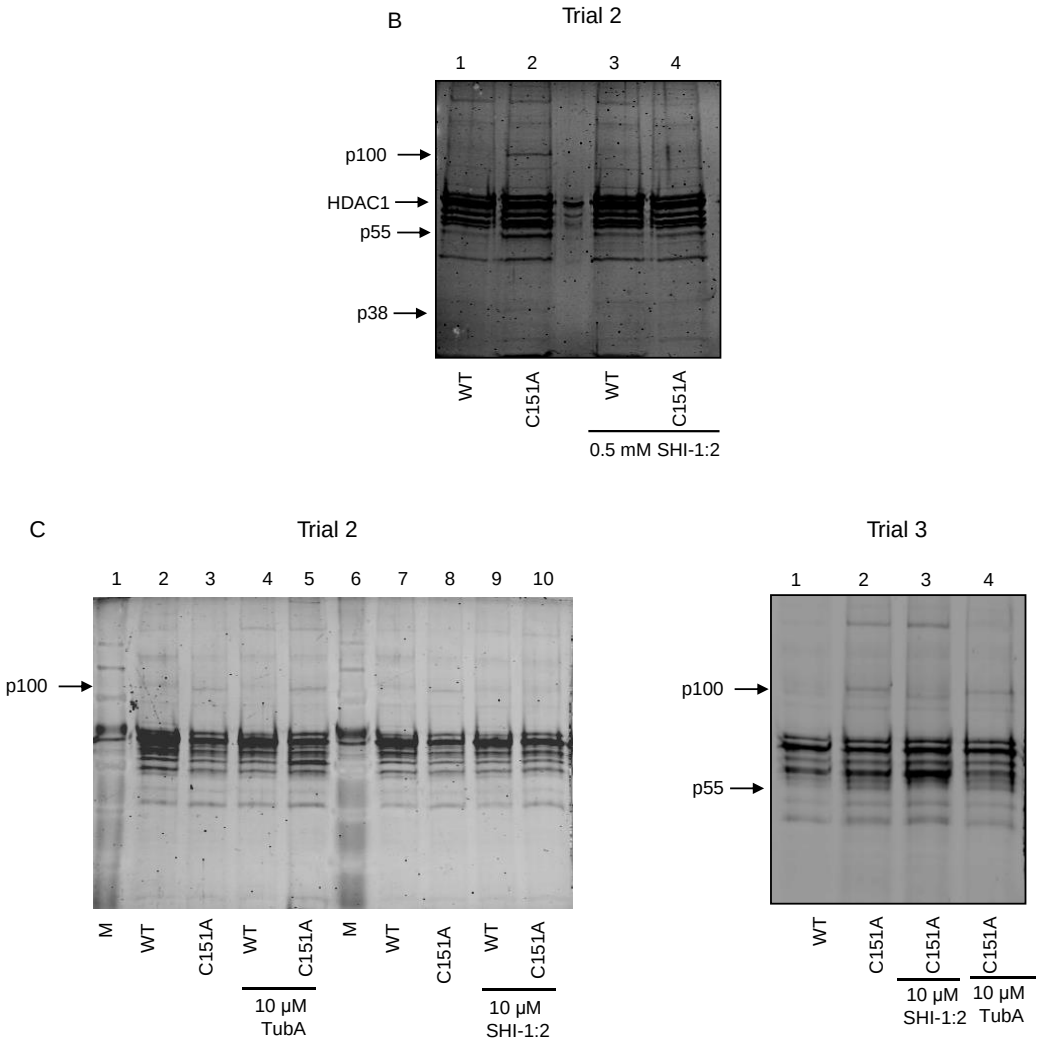


**Figure A.3.2–Repetitive trials for substrate trapping and inhibitor competition**. Wild type (WT) or mutant HDAC1 (indicated below each lane) were expressed as Flag-tagged proteins in HEK293 cells and then cells were treated with 10 µM SAHA for 24h to induce robust protein acetylation. Cells were lysed and proteins were immunoprecipitated with anti-Flag agarose in the presence or absence of A) 2 mM SAHA, B) 0.5 mM SHI-1:2, C) 10 µM SHI-1:2, and 10 µM Tubastatin (TubA) . Bound proteins were separated by SDS-PAGE, and stained with Sypro Ruby total protein stain. Arrows point to HDAC1 or possible substrates (p100, p55, p38) present in mutant but not WT or inhibitor treated samples. Several trials are shown here, with an additional trial shown in Figure 3.2 and 3.3.

A

KDM1A_HUMAN (100%), 92,903.4 Da
Lysine-specific histone demethylase 1A OS=Homo sapiens GN=KDM1A PE=1 SV=2
7 exclusive unique peptides, 7 exclusive unique spectra, 7 total spectra, 102/852 amino acids (12% coverage)

MLSGKKAAAAA AAAAAAAATG TEAGPGTAGG SENGSEVAAQ PAGLSGPAEV GPGAVGERTP RKKEPPRASP PGGLAEPPGS
AGPQAGPTVV PGSATPMETG IAETPEGRRT SRRKRAKVEY REMDESLANL SEDEYYSEEE RNAKAEKEKK LPPPPPQAPP
EEENESEPEE PSGVEGAAFQ SRLPHDRMTS QEAACFPDII SGPQQTQKVF LFIRNRTLQL WLDNPKIQLT FEATLQQLEA
PYNSDTVLVH RVHSYLERHG LINFGIYKRI KPLPTKKTGK VIIIGSGVSG LAAARQLQSF GMDVTLLEAR DRVGGRVATF
RKGNYVADLG AMVVTGLGGN PMAVVSKQVN MELAKIKQKC PLYEANGQAV PKEKDEMVEQ EFNRLLEATS YLSHQLDFNV
LNNKPVSLGQ ALEVVIQLQE KHVKDEQIEH WKKIVKTQEE LKELLNKMVN LKEKIKELHQ QYKEASEVKP PRDITAEFLV
KSKHRDLTAL CKEYDELAET QGKLEEKLQE LEANPPSDVY LSSRDRQILD WHFANLEFAN ATPLSTLSLK HWDQDDDFEF
TGSHLTVRNG YSCVPVALAE GLDIKLNTAV RQVRYTASGC EVIAVNTRST SQTFIYKCDA VLCTLPLGVL KQQPPAVQFV
PPLPEWKTSA VQRMGFGNLN KVVLCFDRVF WDPSVNLFGH VGSTTASRGE LFLFWNLYKA PILLALVAGE AAGIMENISD
DVIVGRCLAI LKGIFGSSAV PQPKETVVSR WRADPWARGS YSYVAAGSSG NDYDLMAQPI TPGPSIPGAP QPIPRLFFAG
EHTIRNYPAT VHGALLSGLR EAGRIADQFL GAMYTLPRQA TPGVPAQQSP SM

B

Peptide sequence - (K)APILLALVAGEAAGImENISDDVIVGR(C)

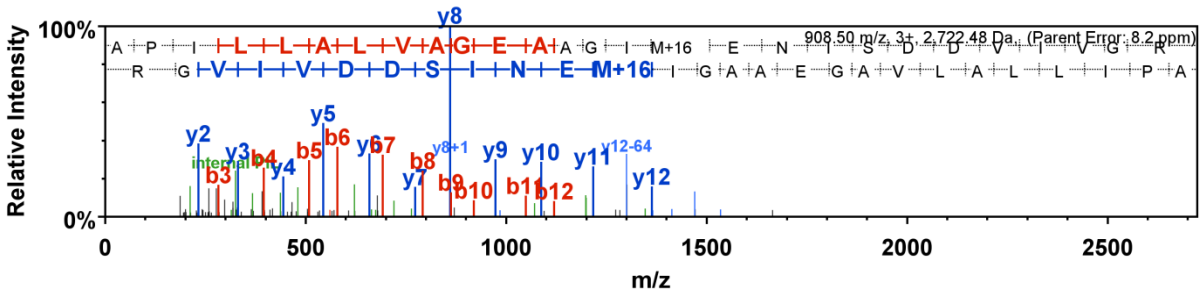


**Figure A.3.3 – Peptides of LSD1 observed in the wild type HDAC1 substrate trapping experiment.** A) Primary sequence of LSD1, which was identified in the substrate trapping experiment as p100. Peptides observed in the MS/MS analysis are highlighted in yellow. Green color represents the oxidation of methionine. The parameters were set to protein threshold 95%, peptide threshold 99% with minimum number of peptides set to 2. B) Spectrum of one representative peptide from LSD1 identified by MS/MS analysis after trapping with wild type HDAC1 is shown below the sequence.

A

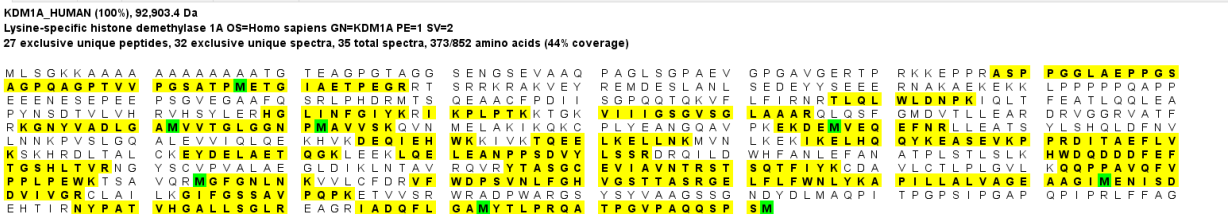


B

Peptide sequence - (K)EKDEmVEQEFNR(L)

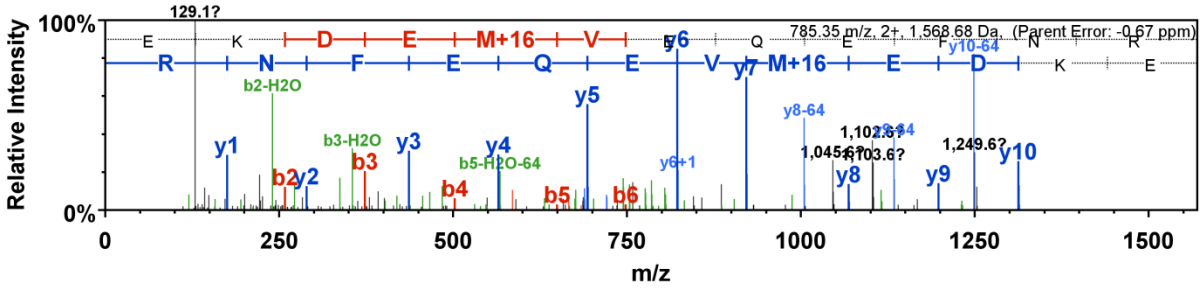


**Figure A.3.4 – Peptides of LSD1 observed in the HDAC1 C151A mutant substrate trapping experiment.** A) Primary sequence of LSD1, which was identified in the substrate trapping experiment as p100. Peptides observed in the MS/MS analysis are highlighted in yellow. Green color represents the oxidation of methionine. The parameters were set to protein threshold 95%, peptide threshold 99% with minimum number of peptides set to 2. B) Spectrum of one representative peptide from LSD1 identified by MS/MS analysis after trapping with C151A HDAC1 is shown below the sequence.

A

RUVB2_HUMAN (100%), 51,158.1 Da
RuvB-like 2 OS=Homo sapiens GN=RUVBL2 PE=1 SV=3
3 exclusive unique peptides, 3 exclusive unique spectra, 3 total spectra, 36/463 amino acids (8% coverage)

MATVTATTKV PEIRDVTRIE RIGAHSHIRG LGLDDALEPR QASQGMVGQL AARRAAGVVL EMIREGKIAG RAVLIAGQPG TGKTAIAMGM
AQALGPDTPF TAIAGSEIFS LEMSKTEALT QAFRRSIGVR IKEETEIIEG EVVEIQIDRP ATGTGSKVGK LTLKTTEMET IYDLGTKMIE
SLTKDKVQAG DVITIDKATG KISKLGRSFT RARDYDAMGS QTKFVQCPDG ELQKRKEVVH TVSLHEIDVI NSRTQGFLAL FSGDTGEIKS
EVREQINAKV AEWREEGKAE IIPGVLFIDE VHMLDIESFS FLNRALESDM APVLIMATNR GITRIRGTSY QSPHGIPIDL LDRLLIVSTT
PYSEKDTKQI LRIRCEEEDV EMSEDAYTVL TRIGLETSLR YAIQLITAAS LVCRKRKGTE VQVDDIKRVY SLFLDESRST QYMKEYQDAF
LFNELKGETM DTS

B

Peptide sequence - (R)QASQGmVGQLAAR(R)

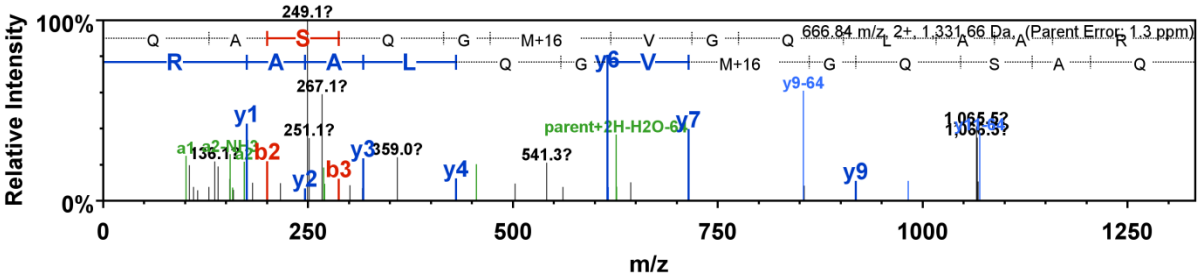


**Figure A.3.5 - Peptides of RuvB like 2 observed in the wild type HDAC1 substrate trapping experiment.** A) Primary sequence of RuvB like 2, which was identified in the substrate trapping experiment as p55. Peptides observed in the MS/MS analysis are highlighted in yellow. Green color represents the oxidation of methionine. The parameters were set to protein threshold 95%, peptide threshold 99% with minimum number of peptides set to 2. B) The annotated spectrum of one representative RuvB like 2 peptides identified by MS/MS analysis after trapping with wild type HDAC1 is shown below the sequence.

A

RUVB2_HUMAN (100%), 51,158.1 Da
RuvB-like 2 OS=Homo sapiens GN=RUVBL2 PE=1 SV=3
10 exclusive unique peptides, 13 exclusive unique spectra, 14 total spectra, 117/463 amino acids (25% coverage)

MATVTATTKV PEIRDVTRIE RIGAHSHIRG LGLDDALEPR QASQGMVGQL AARRAAGVVL EMIREGKIAG RAVLIAGQPG TGKTAIAMGM
AQALGPDTPF TAIAGSEIFS LEMSKTEALT QAFRRSIGVR IKEETEIIEG EVVEIQIDRP ATGTGSKVGK LTLKTTEMET IYDLGTKMIE
SLTKDKVQAG DVITIDKATG KISKLGRSFT RARDYDAMGS QTKFVQCPDG ELQKRKEVVH TVSLHEIDVI NSRTQGFLAL FSGDTGEIKS
EVREQINAKV AEWREEGKAE IIPGVLFIDE VHMLDIESFS FLNRALESDM APVLIMATNR GITRIRGTSY QSPHGIPIDL LDRLLIVSTT
PYSEKDTKQI LRIRCEEEDV EMSEDAYTVL TRIGLETSLR YAIQLITAAS LVCRKRKGTE VQVDDIKRVY SLFLDESRST QYMKEYQDAF
LFNELKGETM DTS

B

Peptide sequence - (K)GTEVQVDDIKR(V)

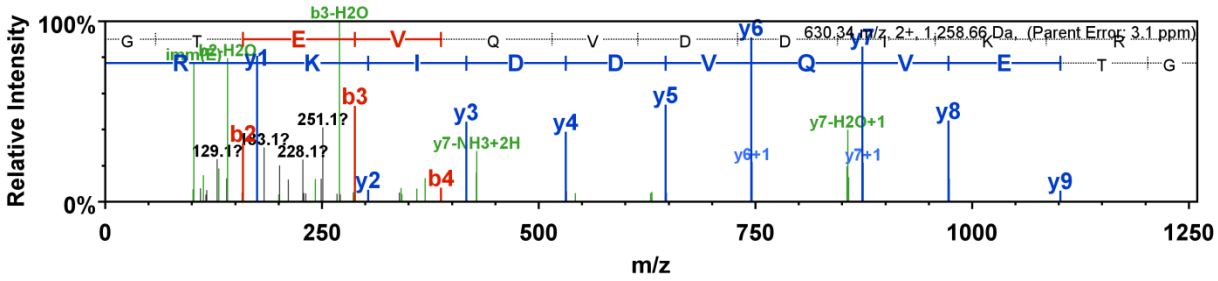


**Figure A.3.6 - Peptides of RuvB like 2 observed in the HDAC1 C151A mutant substrate trapping experiment.** A) Primary sequence of RuvB like 2, which was identified in the substrate trapping experiment as p55. Peptides observed in the MS/MS analysis are highlighted in yellow. Green color represents the oxidation of methionine. The parameters were set to protein threshold 95%, peptide threshold 99% with minimum number of peptides set to 2. B) The annotated spectrum of one representative RuvB like 2 peptide identified by MS/MS analysis after trapping with C151A HDAC1 mutant.

A

FBRL_HUMAN (43%), 33,784.1 Da
rRNA 2'-O-methyltransferase fibrillarin OS=Homo sapiens GN=FBL PE=1 SV=2
1 exclusive unique peptides, 1 exclusive unique spectra, 1 total spectra, 9/321 amino acids (3% coverage)

MKPGFSPRGG GFGGRGGFGD RGGRGGRGGF GGGRGRGGGF RGRGRGGGGG GGGGGGGGRG GGGFHSGGNR GRGRGGKRGN
QSGKNVMVEP HRHEGVFICR **GKEDALVTK**N LVPGESVYGE KRVSISEGDD KIEYRAWNPF RSKLAAAILG GVDQIHIKPG
AKVLYLGAAS GTTVSHVSDI VGPDGLVYAV EFSHRSGRDL INLAKKRTNI IPVIEDARHP HKYRMLIAMV DVIFADVAQP
DQTRIVALNA HTFLRNGGHF VISIKANCID STASAEAVFA SEVKKMQQEN MKPQEQLTLE PYERDHAVVV GVYRPPPKVK
N

B

Peptide sequence - (R)GKEDALVTK(N)

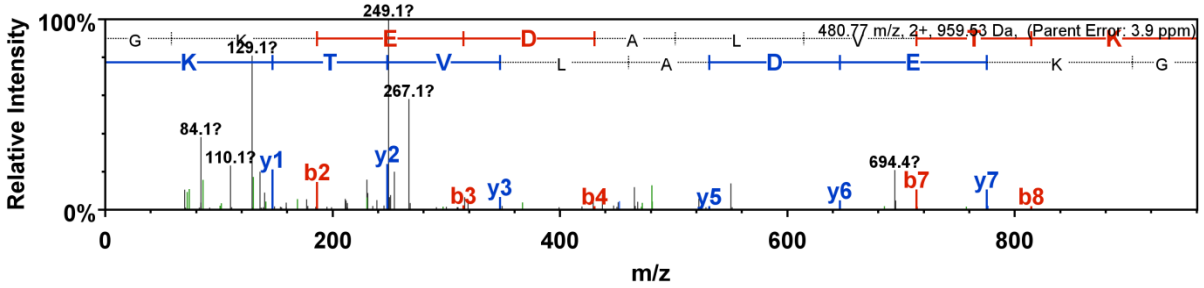


**Figure A.3.7 - Peptides of rRNA-2'-O-methyltransferases fibirllarin (FBRL) observed in the wild type HDAC1 substrate trapping experiment.** A) Primary sequence of FBRL, which was identified in the substrate trapping experiment as p38. Peptides observed in the MS/MS analysis are highlighted in yellow. The parameters were set to protein threshold 95%, peptide threshold 99% with minimum number of peptides set to 2. B) The annotated spectrum of one representative FBRL peptides identified by MS/MS analysis after trapping with wild type HDAC1 is shown below the sequence.

A

FBRL_HUMAN (100%), 33,784.1 Da
rRNA 2'-O-methyltransferase fibrillarin OS=Homo sapiens GN=FBL PE=1 SV=2
6 exclusive unique peptides, 7 exclusive unique spectra, 7 total spectra, 91/321 amino acids (28% coverage)

MKPGFSPRGG GFGGRGGFGD RGGRGGRGGF GGGRGRGGGF RGRGRGGGGG GGGGGGGGRG GGGFHSGGNR GRGRGGKRGN
QSGKNVMVEP HRHEGVFICR GKEDALVTKN LVPGESVYGE KRVSISEGDD KIEYRAWNPF RSKLAAAILG GVDQIHIKPG
AKVLYLGAAS GTTVSHVSDI VGPDGLVYAV EFSHRSGRDL INLAKKRTNI IPVIEDARHP HKYRMLIAMV DVIFADVAQP
DQTRIVALNA HTFLRNGGHF VISIKANCID STASAEAVFA SEVKKMQQEN MKPQEQLTLE PYERDHAVVV GVYRPPPK VK
N

B

Peptide sequence - (R)DHAVVVGVYRPPPK(V)

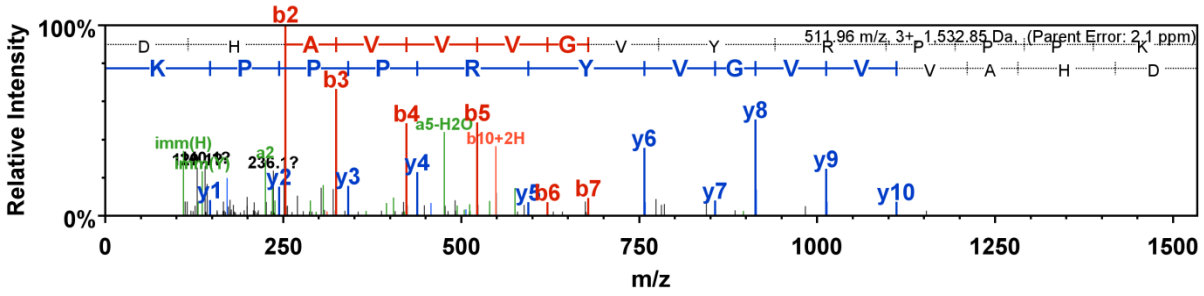


**Figure A.3.8 - Peptides of rRNA-2'-O-methyltransferases fibirllarin (FBRL) observed in the C151A substrate trapping experiment.** A) Primary sequence of FBRL, which was identified in the substrate trapping experiment as p38. Peptides observed in the MS/MS analysis are highlighted in yellow. Green color represents the oxidation of methionine. The parameters were set to protein threshold 95%, peptide threshold 99% with minimum number of peptides set to 2. B) The annotated spectrum of one representative FBRL peptides identified by MS/MS analysis after trapping with C151A HDAC1 mutant.

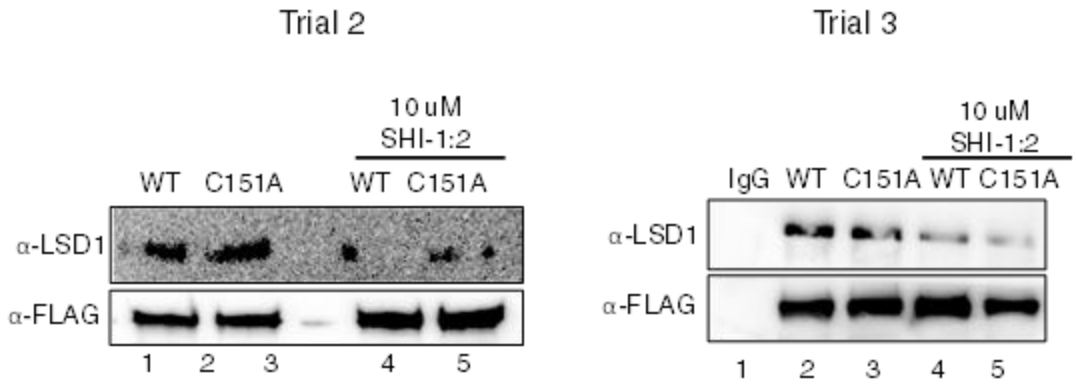


**Figure A.3.9 – Repetitive trials for validation of p100 as LSD1.** Wild type (WT) or C151A HDAC1 were expressed as Flag-tagged proteins in HEK293 cells, and cells were treated with 10 μM SAHA for 24 h prior to harvesting. FLAG-tagged wild type and mutant HDAC1 were immunoprecipitated with anti-Flag agarose in the presence or absence of 10 μM SHI-1:2, separated by SDS-PAGE, and immunoblotted with LSD1 and FLAG antibodies. Two trials are shown here, with the third shown in Figure 3.5.

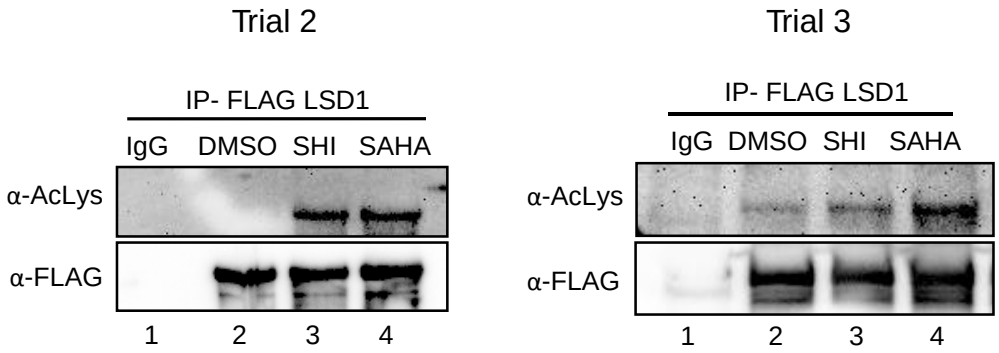


**Figure A.3.10 – HDAC inhibitors regulate LSD1 acetylation**. HEK293 cells were transfected with FLAG-LSD1 and grown for 48 h. Then 10 μM SHI-1:2 or 10 μM SAHA was added for another 24 h. Cells were harvested and FLAG-LSD1 was immunoprecipitated with anti-FLAG agarose beads. Immunoprecipitates were analyzed by Western blotting with FLAG and acetyl lysine antibodies. Two trials are shown here, with the third shown in Figure 3.6.

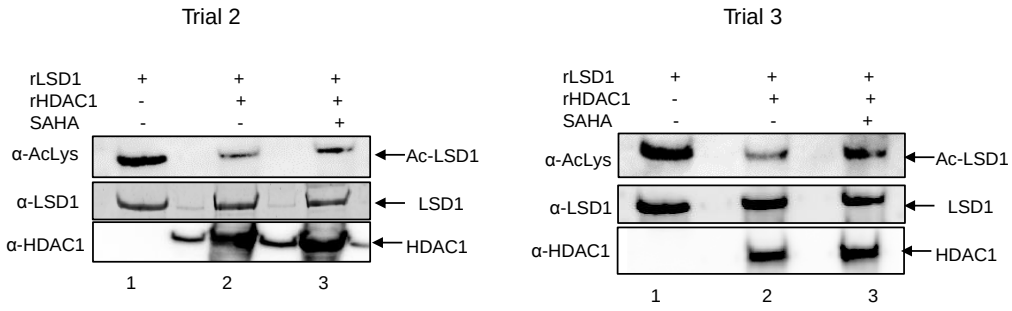


**Figure A.3.11 – Repetitive trials for *in vitro* deacetylation using recombinant LSD1 and recombinant HDAC1.** Acetylated recombinant LSD1 was incubated with or without recombinant HDAC1 and SAHA for 2.5 h at 37 °C and separated by SDS-PAGE and analysed by AcLys, HDAC1 and LSD1 antibodies. Two trials are shown here, with the third shown in Figure 3.7A.

A

| | Trial 1 | Trial 2 | Trial 3 | Mean | Standard Error |
|---|---|---|---|---|---|
| rLSd1 Ac-Lys | 100 | 100 | 100 | 100 | 0.0 |
| rLSD1 Ac-Lys + rHDAC1 | 43 | 28 | 36 | 36 | 4 |
| rLSD1 Ac-Lys + rHDAC1 + SAHA | 97 | 64 | 76 | 79 | 10 |

B

| | Trial 1 | Trial 2 | Trial 3 | Mean | Standard Error |
|---|---|---|---|---|---|
| LSD1 | 100 | 100 | 100 | 100 | 0.0 |
| rLSD1 + rHDAC1 | 106 | 96 | 102 | 99 | 2 |
| rLSD1 + rHDAC1 + SAHA | 92 | 95 | 94 | 94 | 1 |

C

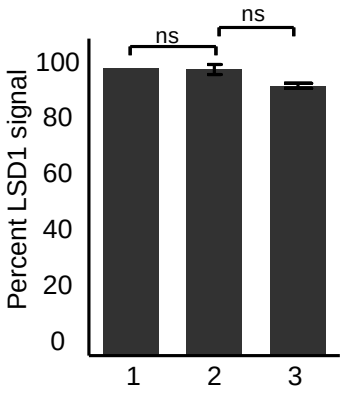


**Figure A.3.12- Quantification of *in vitro* deacetylation assay.** Percent AcLys signal of rLSD1 was quantified from Western blots using three independent trials and raw data are shown in table (A) or histogram (Figure 3.7B). As a loading control, total rLSD1 was quantified from western blots and the raw data is shown in table (B) and histogram (C). ns - not significant.

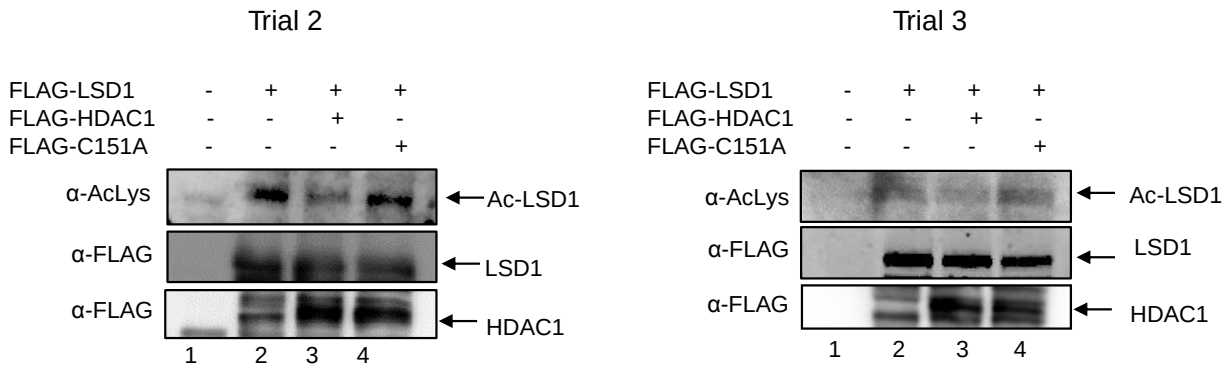


**Figure 3.13 – Repetitive trials for *in cellulo* deacetylation using overexpressed wild type or inactive C151A HDAC1 mutant.** FLAG-tagged wild type (WT) or C151A mutant HDAC1 were cotransfected with FLAG-tagged wild type LSD1 into HEK293 cells. FLAG tagged proteins were immunoprecipitated using anti-FLAG agarose beads, separated by SDS-PAGE, and immunoblotted with acetyl lysine (AcLys) or FLAG antibodies. Two trials are shown here, with the third shown in Figure 3.7C.

A

| | Trial 1 | Trial 2 | Trial 3 | Mean | Standard Error |
|---|---|---|---|---|---|
| LSD1 Ac-Lys | 100 | 100 | 100 | 100 | 0.0 |
| LSD1 Ac-Lys + WT HDAC1 | 31 | 43 | 34 | 36 | 4 |
| LSD1 Ac-Lys + C151A HDAC1 | 86 | 88 | 96 | 90 | 3 |

B

| | Trial 1 | Trial 2 | Trial 3 | Mean | Standard Error |
|---|---|---|---|---|---|
| LSD1 | 100 | 100 | 100 | 100 | 0.0 |
| LSD1 + WT HDAC1 | 100 | 104 | 91 | 98 | 4 |
| LSD1 + C151A HDAC1 | 93 | 101 | 92 | 95 | 3 |

C

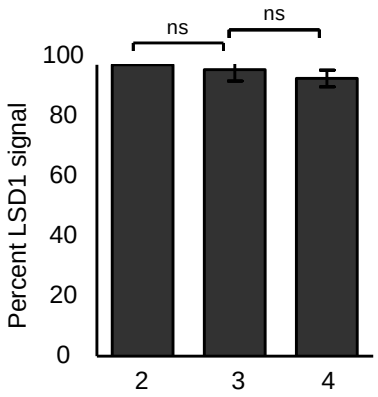


**Figure A.3.14- Quantification of *in cellulo* deacetylation assay.** The percent AcLys signal of FLAG-LSD1 was quantified from western blots using three independent trials and raw data is shown in table (A) or histogram (Figure 3.7D). C) As a loading control, total FLAG-LSD1 was quantified from Western blots and raw data is shown in table (B) and histogram (C). ns - not significant.

**Table A.3.1- *In vitro* demethylation assay of LSD1***

| | Trial 1 | Trial 2 | Trial 3 | Mean | Standard Error |
|---|---|---|---|---|---|
| LSD1+DMSO | 100 | 100 | 100 | 100 | 0.0 |
| LSD1+SHI-1:2 | 104 | 138 | 125 | 122 | 10 |
| LSD1+SAHA | 104 | 117 | 123 | 115 | 6 |

*HEK293 cells were transfected with FLAG-LSD1 and grown for 48 h. Then 10 μM SHI-1:2 or 10 μM SAHA was added for another 24 h, cells were harvested, and proteins were immunoprecipitated with anti-FLAG agarose beads. Half of the immunoprecipitate was subjected to LSD1 activity assay (Enzo Life Sciences) and the other half was analyzed by Western blotting with FLAG antibody. The fluorescence signal was background corrected using a reaction with all the components except the LSD1 enzyme. Then the signal of each sample was normalized to DMSO-treated LSD1 enzyme (set to 1). The

mean and the standard error from at least three independent trials are shown in Figure 3.8. Data is depicted in Figure 3.8.

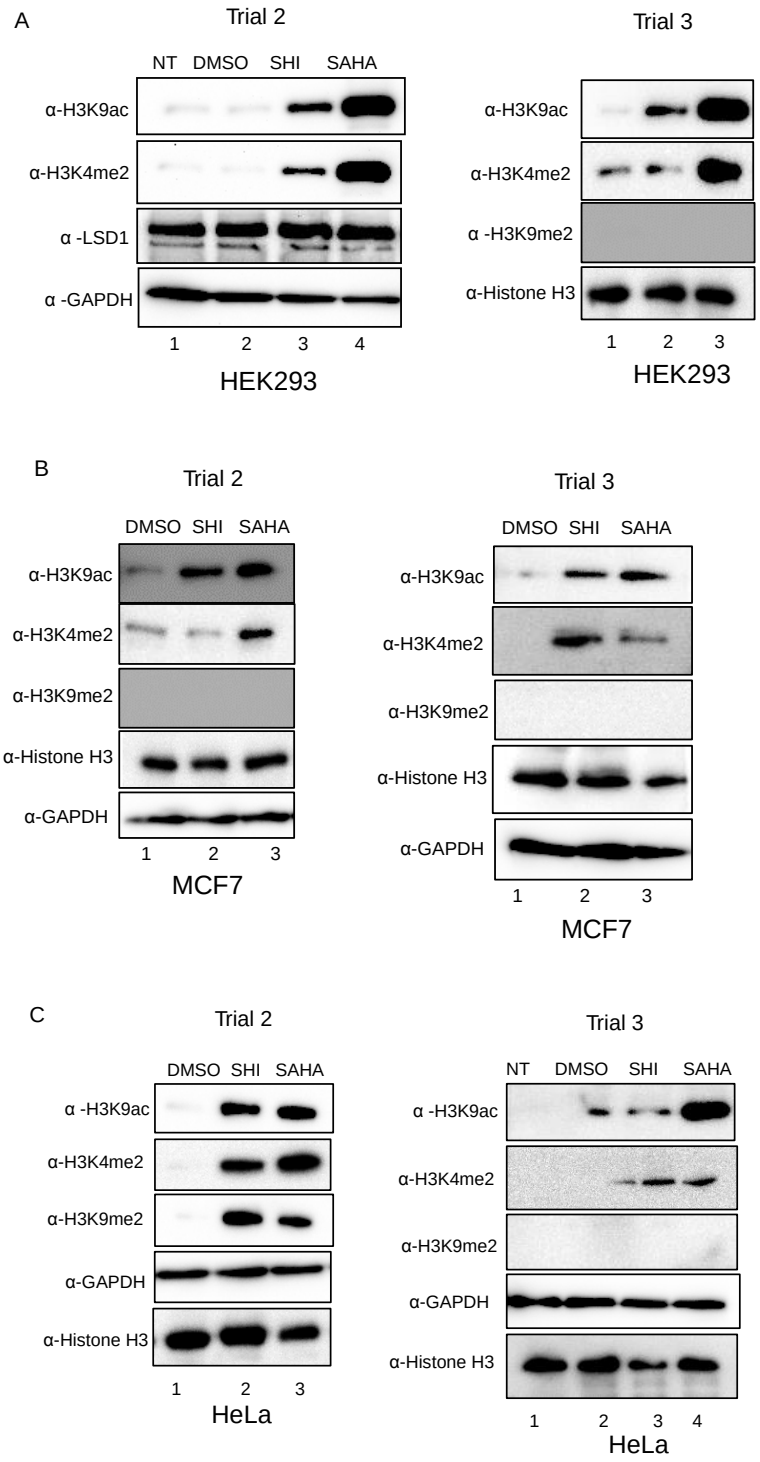

**Figure A.3.15 – Repetitive trials for *in cellulo* demethylation assays**. A) HEK293, B) MCF7, or C) HeLa cells were untreated (NT) or treated with DMSO, 10 µM SHI-1:2 or 10 µM SAHA for 24 h, harvested, lysed and proteins were separated by SDS-PAGE, followed by immunoblotting with LSD1, histone H3, histone H3K4me2, histone H3K9ac, and GAPDH antibodies. Two trials are shown here, with an additional trial shown in Figure 3.9.

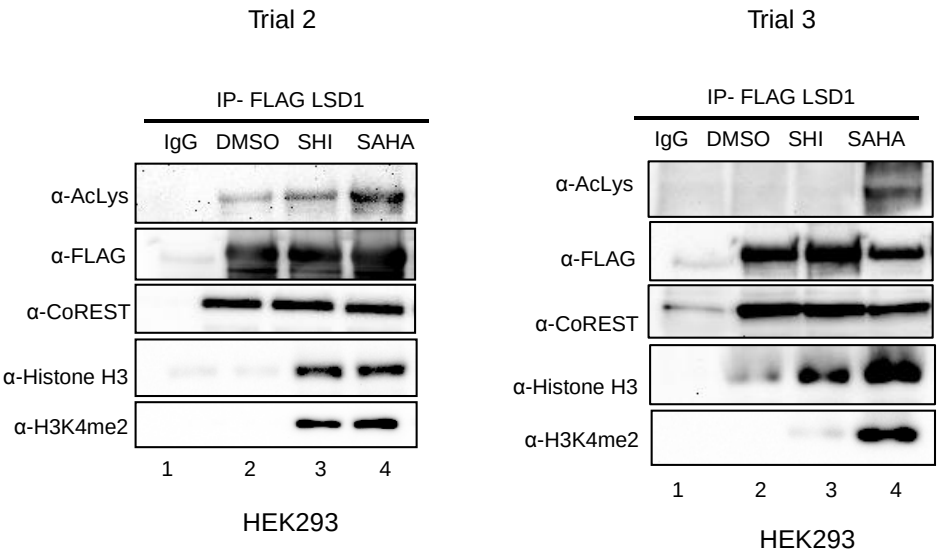


**Figure A.3.16 – Repetitive trials for overexpressed LSD1-H3 coimmunoprecipitation (Co-IP)**. FLAG-LSD1 was overexpressed in HEK293 and cells were untreated (IgG) or treated with DMSO or HDAC inhibitors to induce acetylation. Cells were harvested and proteins were immunoprecipitated with anti-FLAG agarose beads. Immunoprecipitates were analyzed by Western blotting with FLAG, acetyl lysine, histone H3, histone H3K4me2, histone H3K9me2, and CoREST antibodies. Two trials are shown here, with the third trial shown in Figure 3.10A.

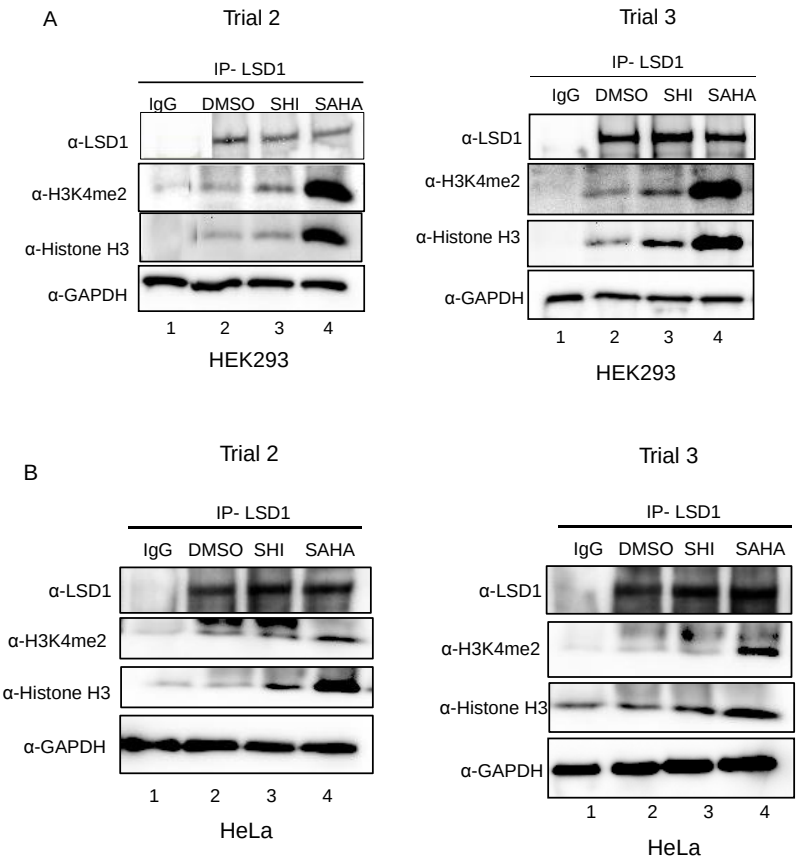


**Figure A.3.17 – Repetitive trials for endogenous LSD1-H3 Co-IP**. A) HEK293 cells or B) HeLa cells were untreated (IgG) or treated with DMSO or HDAC inhibitors, harvested, and endogenous LSD1 was immunoprecipitated. Western blotting was performed with LSD1, histone H3, and histone H3K4me2 antibodies. GAPDH was used as a loading control. Two trials are shown here, with the third trial shown in Figure 3.10B and C.

## A. Trial 1

### LSD1+DMSO

Peptide sequence- (K)EKDEmVEQEFNR(L)

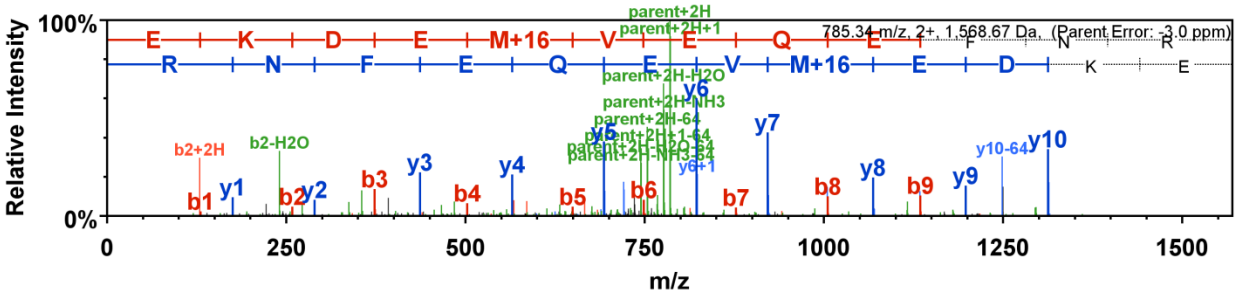


### LSD1+SHI1:2

Peptide sequence- (K)EKacDEMVEQEFNR(L)

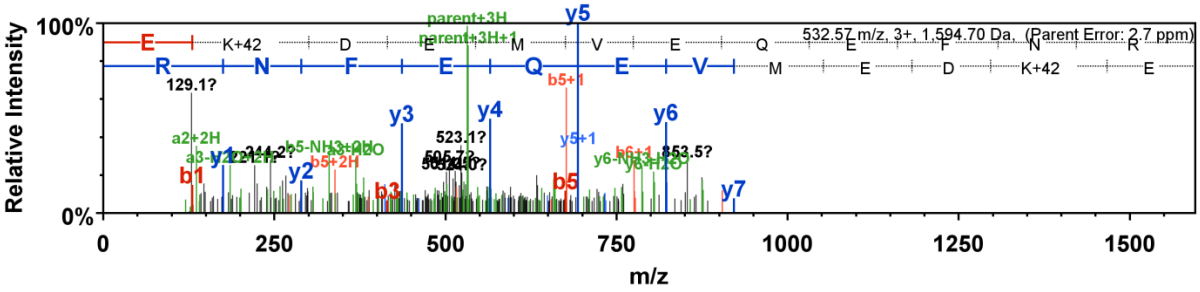

**B .Trial 2**

**LSD1+DMSO**

Peptide sequence- (K)EKDEMVEQEFNR(L)

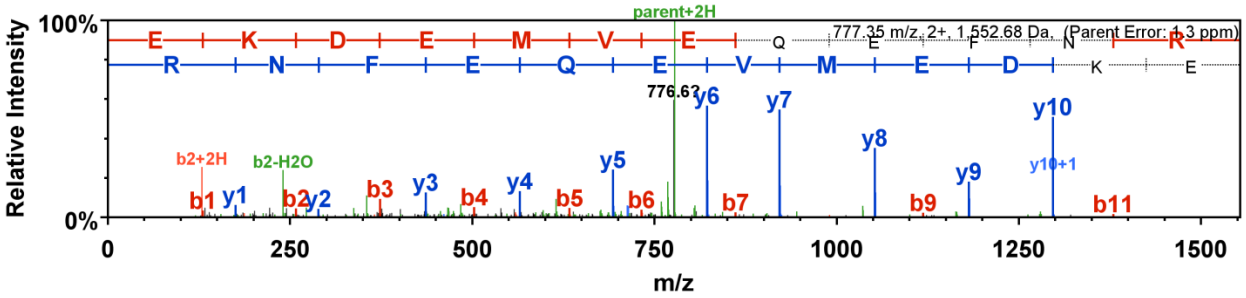


**LSD1+SHI-1:2**

Peptide sequence- (K)EKacDEmVEQEFNR(L)

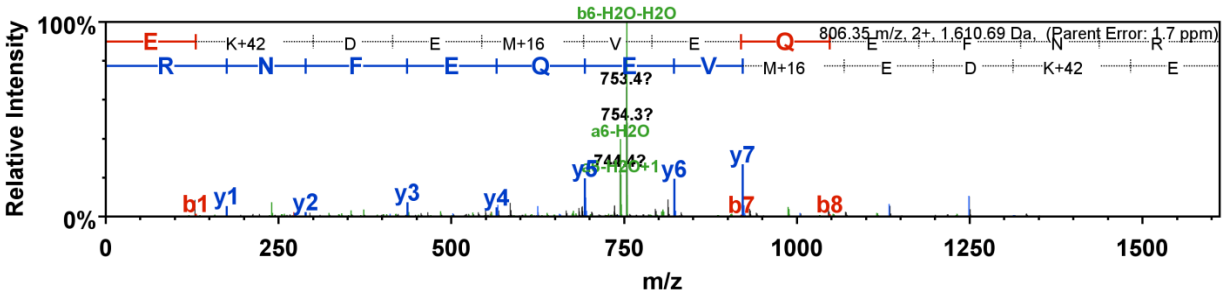

**LSD1+SAHA**

Peptide sequence- (K)EKDEmVEQEFNR(L)

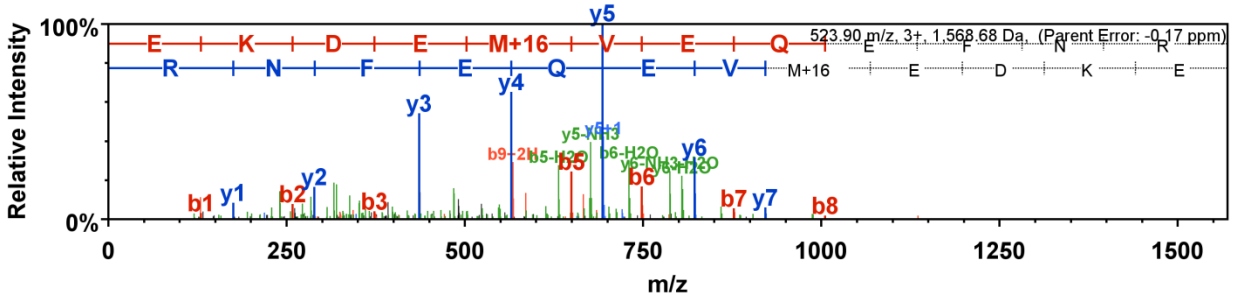


**C. Trial 3**

**LSD1+DMSO**

Peptide sequence- (K)EKDEmVEQEFNR(L)

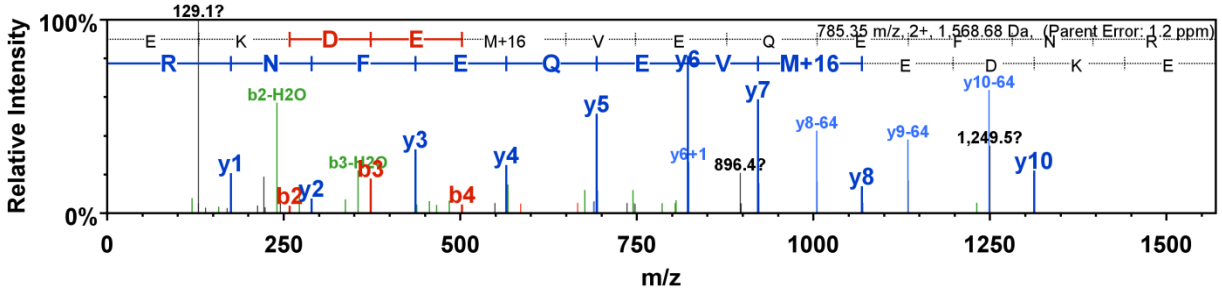

**LSD1+SAHA**

Peptide sequence- (K)EKacDEmVEQEFNR(L)

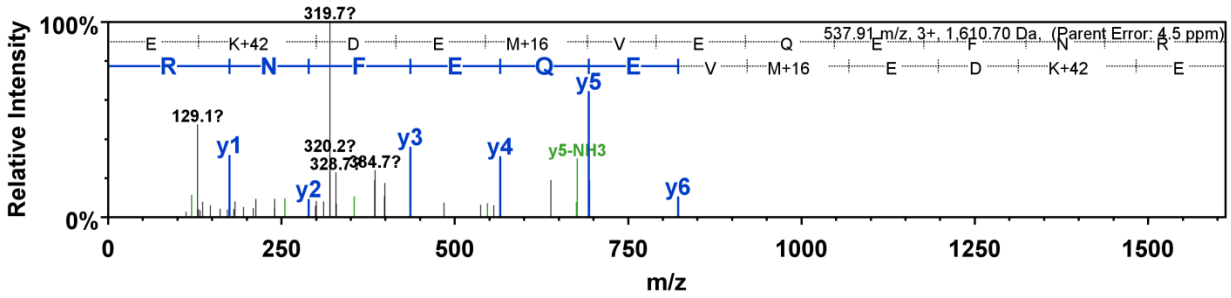


**Figure A.3.18 – Repetitive trials for MS analysis of K374 acetylation in LSD1.** Representative spectra for acetylated and unacetylated peptides of LSD1 identified from three independent trials. Data are represented in Table 3.2.

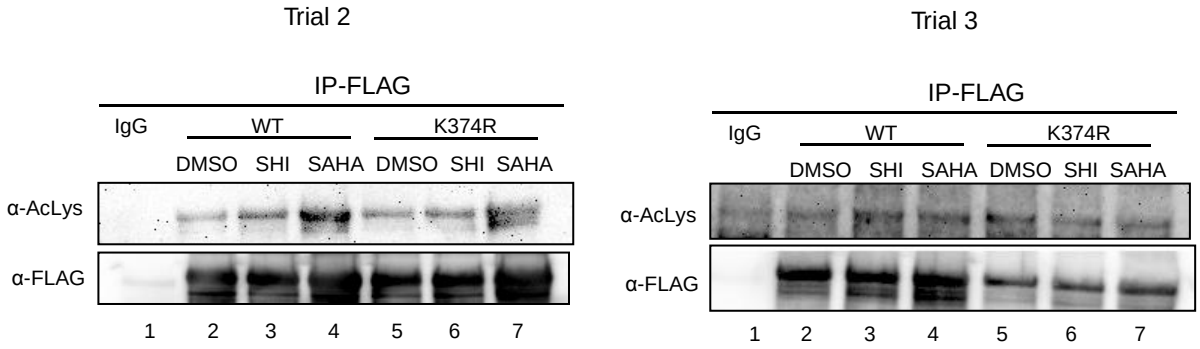


**Figure A.3.19- Repetitive trials for LSD1 acetylation at K374.** FLAG-tagged wild type or K374R mutant LSD1 were transfected into HEK293 cells, and cells were treated with HDAC1/2 selective inhibitor (SHI-1:2) or SAHA. FLAG-LSD1 was immunoprecipitated with FLAG antibody, subjected to SDS-PAGE separation, and immunoblotted with the FLAG and acetyl lysine antibodies. Two trials are shown here, with the third shown in Figure 3.11B.

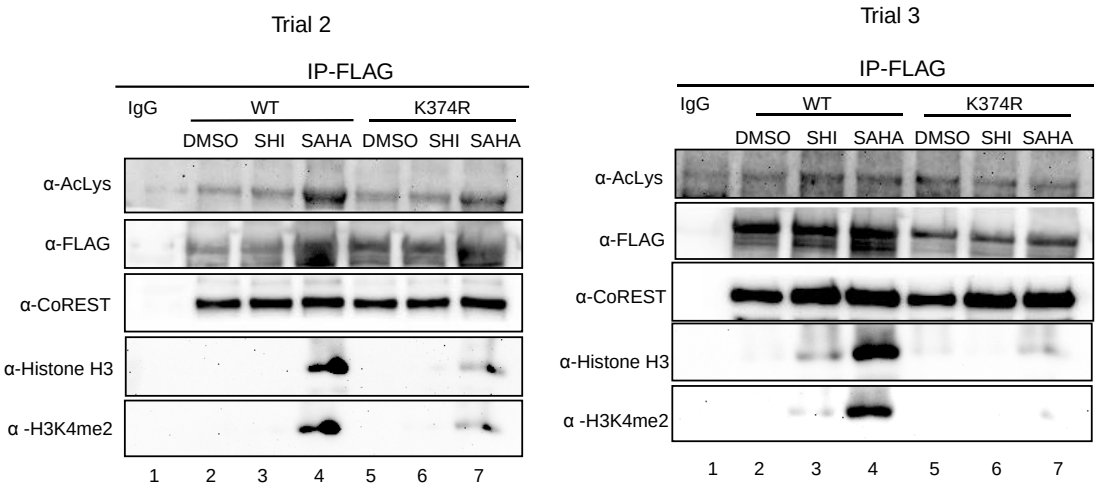


**Figure A.3.20- Repetitive trials for altered LSD1-H3 binding due to acetylation at K374.** FLAG-tagged wild type or K374R mutant LSD1 were transfected into HEK293 cells, and cells were treated with HDAC1/2 selective inhibitor (SHI-1:2) or SAHA. FLAG-LSD1 was immunoprecipitated with FLAG antibody, subjected to SDS-PAGE separation, and immunoblotted with indicated antibodies. Two trials are shown here, with the third shown in Figure 3.11C.

**Table A.3.2 – Real time PCR analysis of the SCN2A gene***

| SCN2A | Trial 1 | Trial 2 | Trial 3 | Trial 4 | Mean | Standard Error |
|---|---|---|---|---|---|---|
| NT | 1.4 | 3.9 | 1.7 | 2.6 | 2.4 | 0.6 |
| WT LSD1+DMSO | 1.0 | 1.0 | 1.0 | 1.0 | 1.0 | 0.0 |
| WT LSD1+SHI-1:2 | 7.8 | 5.9 | 2.7 | 5.0 | 5.4 | 1.0 |
| K374R LSD1+SHI-1:2 | 2.7 | 1.7 | 1.0 | 0.70 | 1.5 | 0.4 |

*Fold change calculated from four independent trials, mean and standard error are shown for SCN2A. Data depicted in Figure 3.12A.

**Table A.3.3 – Real time PCR analysis of the SCN3A gene***

| SCN3A | Trial 1 | Trial 2 | Trial 3 | Trial 4 | Mean | Standard Error |
|---|---|---|---|---|---|---|
| NT | 1.4 | 1.2 | 1.7 | - | 1.4 | 0.1 |
| WT LSD1+DMSO | 1.0 | 1.0 | 1.0 | 1.0 | 1.0 | 0.0 |
| WT LSD1+SHI-1:2 | 2.3 | 2.3 | 2.6 | 2.5 | 2.4 | 0.1 |
| K374R LSD1+SHI-1:2 | 0.40 | 0.80 | 1.2 | 1.2 | 0.90 | 0.2 |

*Fold change calculated from four independent trials, mean and standard error are shown for SCN3A. Data depicted in Figure 3.12B.

## APPENDIX C – CHAPTER 4 REPRODUCIBLE TRIALS

**Table A. 4.1- Percent deacetylase activities of HDAC1 F437 substitution mutants***

| Sample | Trial 1 | Trial 2 | Trial 3 | Trial 4 | Mean | Standard error (SE) |
|---|---|---|---|---|---|---|
| No protein | 4 | 10 | 1 | 11 | 7 | 2 |
| Wild type HDAC1 | 100 | 100 | 100 | 100 | 100 | 0 |
| H141A | 23 | 14 | 12 | 18 | 17 | 2 |
| F437C | 66 | 82 | 72 | 70 | 73 | 3 |
| F437L | 77 | 63 | 89 | ND | 76 | 8 |
| F437A | 75 | 68 | 93 | ND | 79 | 7 |
| F437S | 96 | 97 | 87 | ND | 93 | 3 |
| F437Y | 84 | 89 | 70 | ND | 84 | 5 |

*Wild type or mutant HDAC1 proteins were expressed as FLAG-tagged proteins in T-Ag Jurkat cells, and immunoprecipitated with anti-FLAG agarose beads. Catalytic activity was measured using an *in vitro* fluorescence assay (section 4.4.18). The table summarizes the mean percent activity of at least three independent trials (wild type is set to 100%) with standard error (data was depicted in Figure 4.1). The protein quantities used in the trials were confirmed by gel analysis, which is shown in Figure 4.1 and Figure A.4.1.

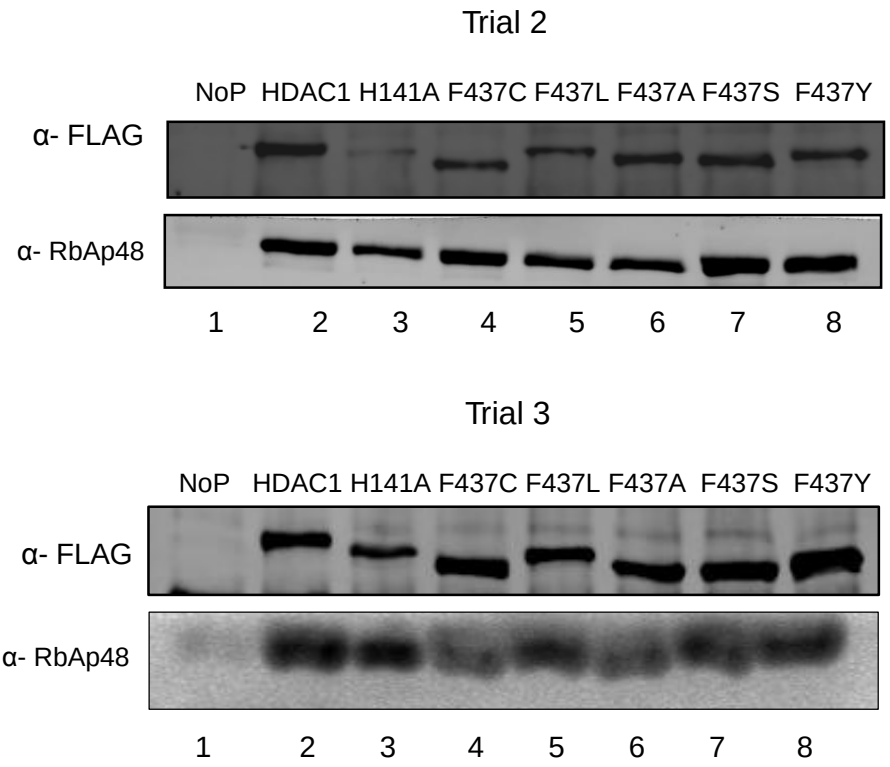


**Figure A.4.1 – Repetitive trials for the expression and coimmunoprecipitation of HDAC1 F437 mutants.** Wild type or mutant HDAC1 proteins were expressed as FLAG-tagged proteins in T-Ag Jurkat cells and immunoprecipitated with anti-FLAG agarose beads. Proteins were separated by SDS-PAGE, and immunoblotted with FLAG antibody (gel image) to assess protein levels or RbAp48 antibody. These gel images represent two independent trials, with the third shown in Figure 4.1.

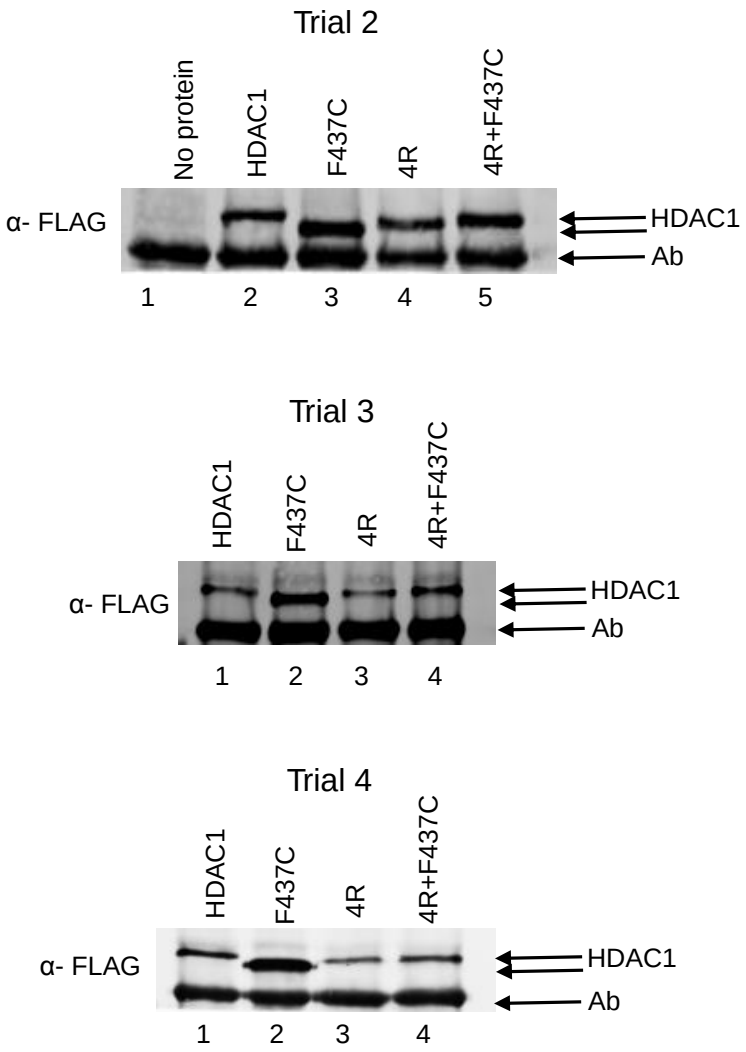


**Figure A.4.2 – Repetitive trials for the migration of deacetylation mimic mutants.** Wild type or mutant HDAC1 proteins were expressed as FLAG-tagged proteins in T-Ag Jurkat cells, immunoprecipitated with anti-FLAG agarose beads, separated by SDS-PAGE and immunoblotted with FLAG antibody. Three trials are shown here with the fourth shown in Figure 4.3A.

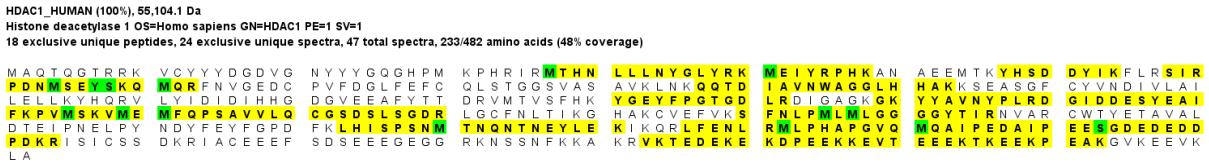


**Figure A.4.3 – Peptide sequences identified from the wild type HDAC1 immunoprecipitate (Trial 1).** Peptide sequences observed in the MS/MS analysis are highlighted in yellow, while modified amino acids are in green. The parameters were set to protein threshold 99%, peptide threshold 99% with minimum number of peptides set to 1. A spectrum for select peptides are shown in Figure A.4.4.

Peptide sequence - (R)mLPHAPGVQmQAIPEDAIPEEsGDEDEDDPDKR(I)

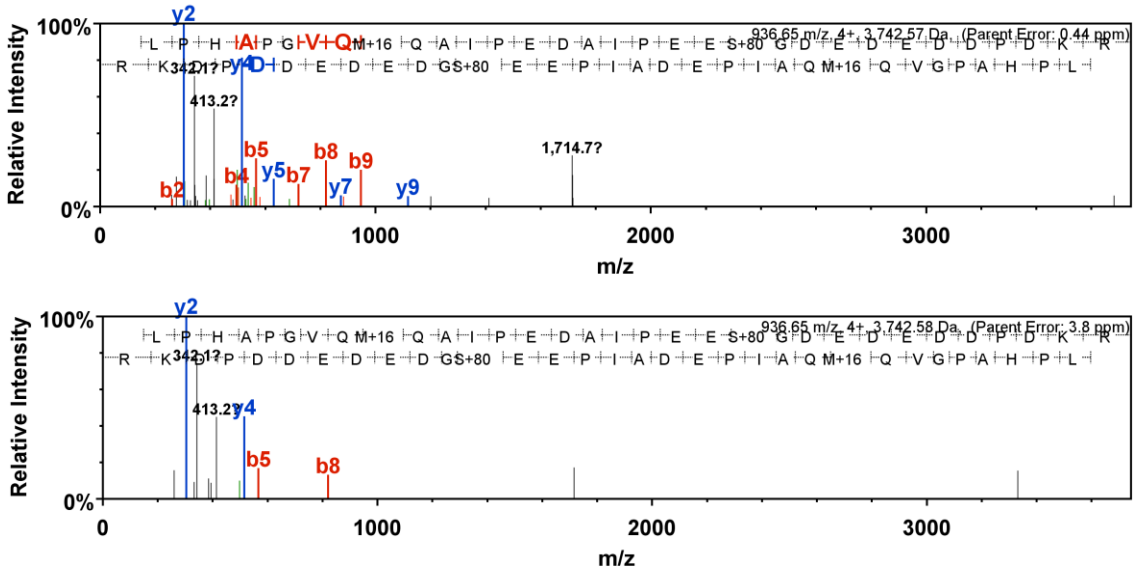


**Figure A.4.4 – Spectra of the phosphopeptide containing phosphorylated S393 (S+80) in wild type HDAC1 (Trial 1).**

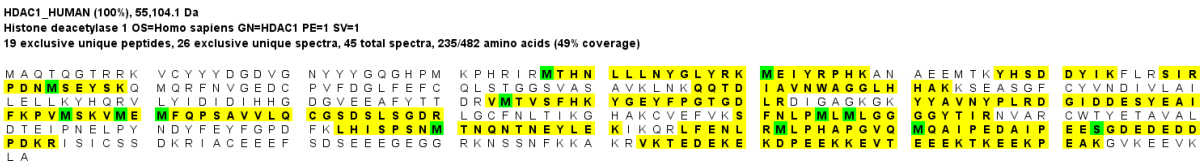


**Figure A.4.5 – Peptide sequences identified from the wild type HDAC1 immunoprecipitate (Trial 2).** Peptide sequences observed in the MS/MS analysis are highlighted in yellow, while modified amino acids are in green. The parameters were set to protein threshold 99%, peptide threshold 99% with minimum number of peptides set to 1. Spectra for select peptides are shown in Figure A.4.6.

Peptide sequence - (R)mLPHAPGVQmQAIPEDAIPEEsGDEDEDDPDKR(I)

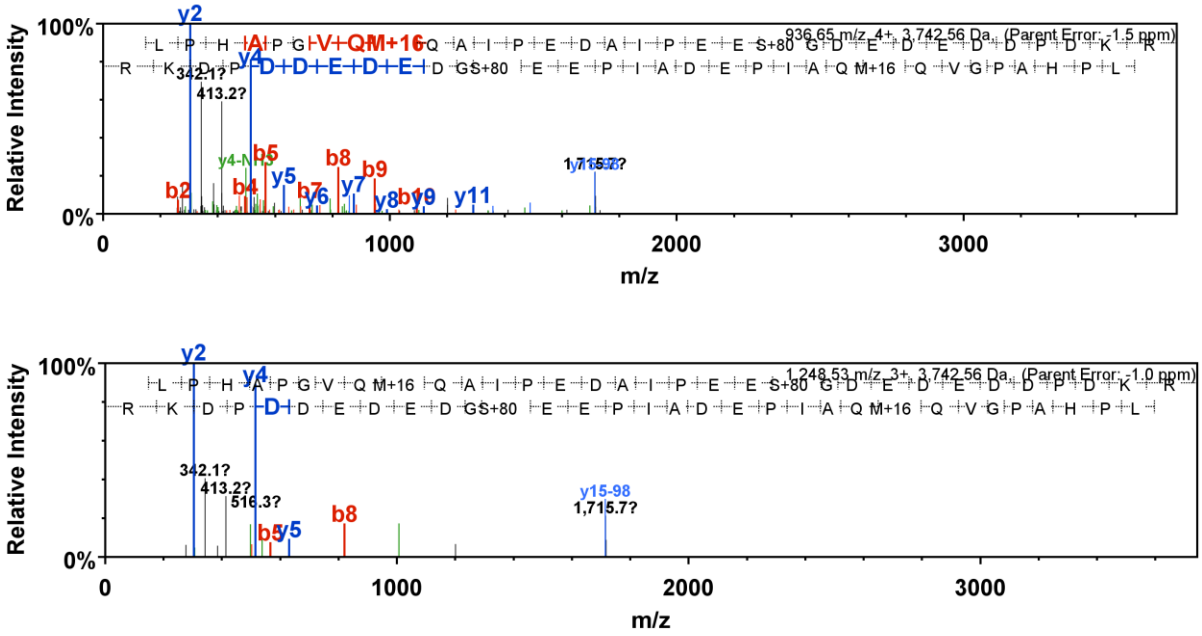


**Figure A.4.6 – Spectra of the phosphopeptide containing phosphorylated S393 (S+80) in wild type HDAC1 (Trial 2).**

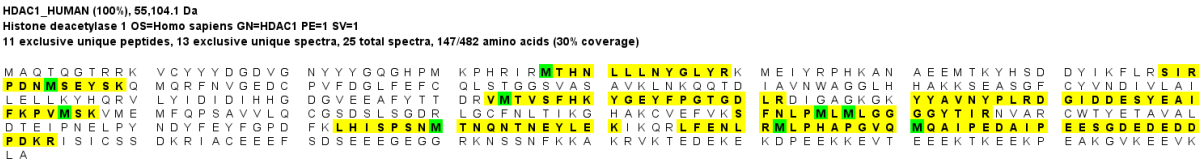


**Figure A.4.7 – Peptide sequences identified from the F437C HDAC1 immunoprecipitate (Trial 1).** Peptide sequences observed in the MS/MS analysis are highlighted in yellow, while modified amino acids are in green. The parameters were set to protein threshold 99%, peptide threshold 99% with minimum number of peptides set to 1. A spectrum for a select peptide is shown in Figure A.4.8.

Peptide sequence - (R)mLPHAPGVQmQAIPEDAIPEESGDEDEDDPDKR(I)

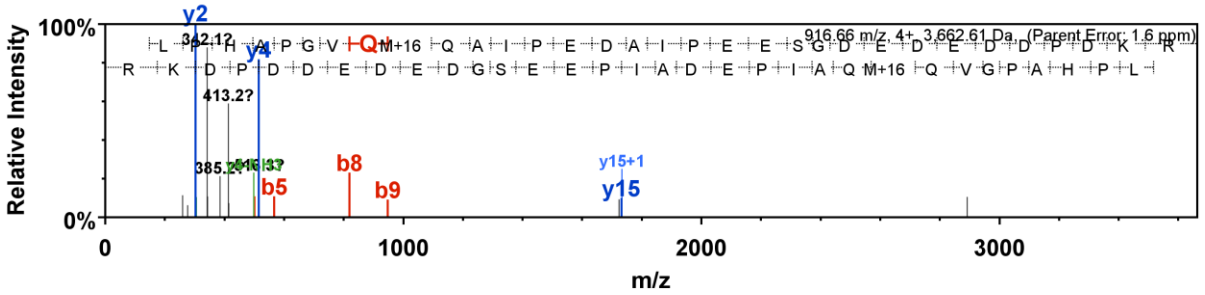


**Figure A.4.8 – Spectrum of the peptide containing S393 in F437C HDAC1 (Trial 1).**

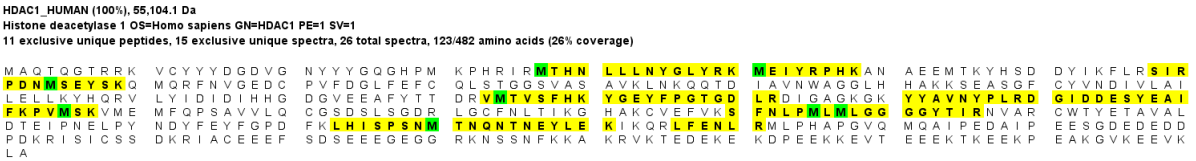


**Figure A.4.9 – Peptide sequences identified from the F437C HDAC1 immunoprecipitate (Trial 2).** Peptide sequences observed in the MS/MS analysis are highlighted in yellow, while modified amino acids are in green. The parameters were set to protein threshold 99%, peptide threshold 99% with minimum number of peptides set to 1. The peptide containing the S393 residue was not observed.

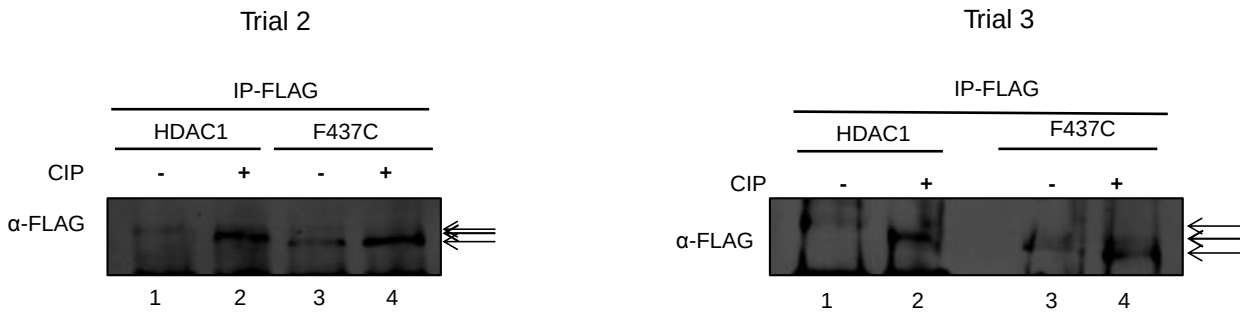


**Figure A.4.10 – Repetitive trials for the *in vitro* dephosphorylation assay.** Wild type or mutant HDAC1 proteins were expressed as FLAG-tagged proteins in T-Ag Jurkat cells, immunoprecipitated with anti-FLAG agarose beads and subjected to *in vitro* dephosphorylation with CIP (section 4.4.18). Then, proteins were separated by SDS-PAGE, and immunoblotted with FLAG antibody. Two trials are shown here with the third shown in the Figure 4.3B. Arrows indicate migration differences between wild type and F437C mutant.

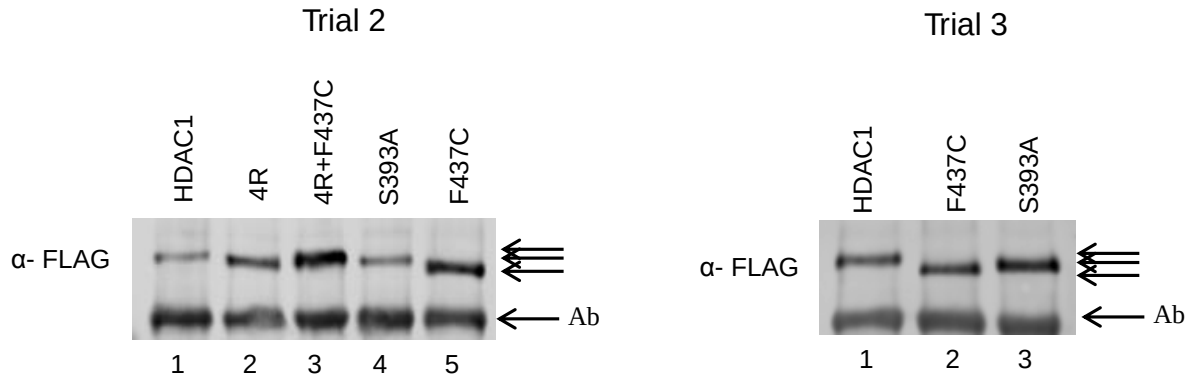


**Figure A.4.11 – Repetitive trials for the migration of the S393A mutant.** Wild type or mutant HDAC1 proteins were expressed as FLAG-tagged proteins in T-Ag Jurkat cells, immunoprecipitated with anti-FLAG agarose beads, separated by SDS-PAGE, and immunoblotted with FLAG antibody. Two trials are shown here with the third shown in the

Figure 4.3C. Arrows indicate migration difference between wild type and mutants and antibody (Ab).

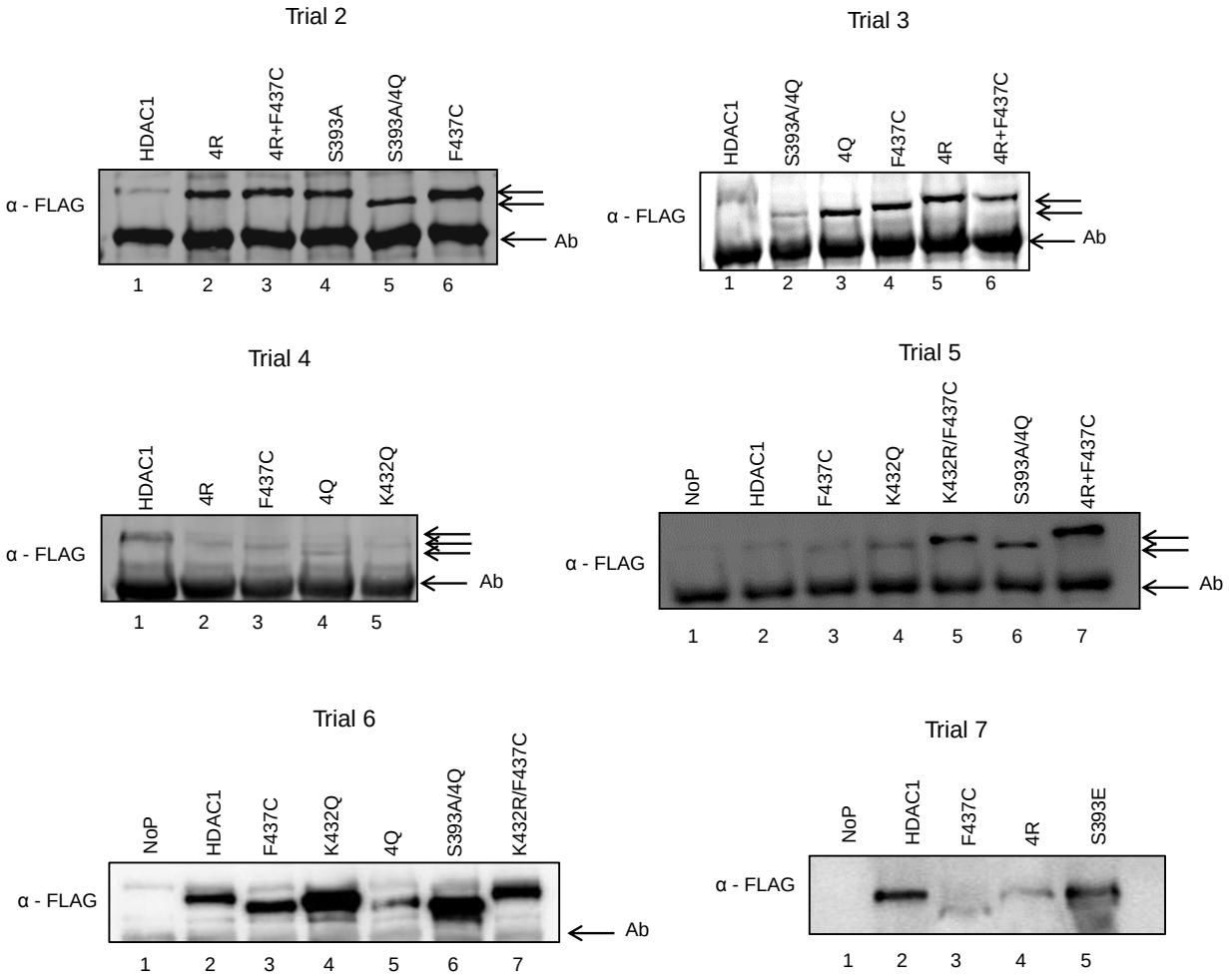


**Figure A.4.12 – Repetitive trials for the migration of acetylation mimic mutants.** Wild type or mutant HDAC1 proteins were expressed as FLAG-tagged proteins in T-Ag Jurkat cells, immunoprecipitated with anti-FLAG agarose beads, separated by SDS-PAGE, and immunoblotted with FLAG antibody. Five trials are shown here with the sixth shown in Figure 4.4. Arrows indicate the migration pattern of various acetylmimetic and acetylmutants compared to F437C and antibody (Ab).

# APPENDIX D – COPYRIGHT PERMISSIONS

Copyright Clearance Center RightsLink® Home Account Info Help Live Chat

nature publishing group

| | |
|---|---|
| **Title:** | Epigenetic protein families: a new frontier for drug discovery |
| **Author:** | Cheryl H. Arrowsmith, Chas Bountra, Paul V. Fish, Kevin Lee and Matthieu Schapira |
| **Publication:** | Nature Reviews Drug Discovery |
| **Publisher:** | Nature Publishing Group |
| **Date:** | May 1, 2012 |

Logged in as: Dhanusha Nalawansha LOGOUT



**Order Completed**

Thank you for your order.

This Agreement between Dhanusha A Nalawansha ("You") and Nature Publishing Group ("Nature Publishing Group") consists of your license details and the terms and conditions provided by Nature Publishing Group and Copyright Clearance Center.

Your confirmation email will contain your order number for future reference.

Get the printable license.

| | |
|---|---|
| License Number | 3926301042192 |
| License date | Aug 12, 2016 |
| Licensed Content Publisher | Nature Publishing Group |
| Licensed Content Publication | Nature Reviews Drug Discovery |
| Licensed Content Title | Epigenetic protein families: a new frontier for drug discovery |
| Licensed Content Author | Cheryl H. Arrowsmith, Chas Bountra, Paul V. Fish, Kevin Lee and Matthieu Schapira |
| Licensed Content Date | May 1, 2012 |
| Licensed Content Volume | 11 |
| Licensed Content Issue | 5 |
| Type of Use | reuse in a dissertation / thesis |
| Requestor type | academic/educational |
| Format | electronic |
| Portion | figures/tables/illustrations |
| Number of figures/tables/illustrations | 1 |
| High-res required | no |
| Figures | Figure 1 Covalent modification of histones and DNA |
| Author of this NPG article | no |
| Your reference number | |
| Title of your thesis / dissertation | Studies towards broadening the substrate profile and regulation of Histone deacetylase 1 |
| Expected completion date | Oct 2016 |
| Estimated size (number of pages) | 190 |
| Requestor Location | Dhanusha A Nalawansha<br>4757 Anthony Wayne Drive<br>Apt 12<br><br>DETROIT, MI 48201<br>United States<br>Attn: Dhanusha A Nalawansha |
| Billing Type | Invoice |
| Billing address | Dhanusha A Nalawansha |

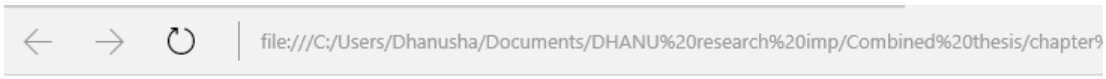


**NATURE PUBLISHING GROUP LICENSE TERMS AND CONDITIONS**

Aug 12, 2016

This Agreement between Dhanusha A Nalawansha ("You") and Nature Publishing Group ("Nature Publishing Group") consists of your license details and the terms and conditions provided by Nature Publishing Group and Copyright Clearance Center.

| | |
|---|---|
| License Number | 3926310472879 |
| License date | Aug 12, 2016 |
| Licensed Content Publisher | Nature Publishing Group |
| Licensed Content Publication | IBMS BonekEy |
| Licensed Content Title | Emergence of the osteo-epigenome in bone biology |
| Licensed Content Author | Shigeaki Kato, Kazuki Inoue, Min-Young Youn |
| Licensed Content Date | Jan 1, 2010 |
| Licensed Content Volume Number | 7 |
| Licensed Content Issue Number | 9 |
| Type of Use | reuse in a dissertation / thesis |
| Requestor type | academic/educational |
| Format | print and electronic |
| Portion | figures/tables/illustrations |
| Number of figures/tables/illustrations | 1 |
| High-res required | no |
| Figures | Figure 3 Histone modifications |
| Author of this NPG article | no |
| Your reference number | |
| Title of your thesis / dissertation | Studies towards broadening the substrate profile and regulation of Histone deacetylase 1 |
| Expected completion date | Oct 2016 |
| Estimated size (number of pages) | 190 |
| Requestor Location | Dhanusha A Nalawansha<br>4757 Anthony Wayne Drive<br>Apt 12<br><br>DETROIT, MI 48201<br>United States<br>Attn: Dhanusha A Nalawansha |
| Billing Type | Invoice |
| Billing Address | Dhanusha A Nalawansha<br>4757 Anthony Wayne Drive<br>Apt 12 |

Print This Page

Copyright Clearance Center

Note: Copyright.com supplies permissions but not the copyrighted content itself.

1 PAYMENT 2 REVIEW 3 CONFIRMATION

## Step 3: Order Confirmation

**Thank you for your order!** A confirmation for your order will be sent to your account email address. If you have questions about your order, you can call us at +1.855.239.3415 Toll Free, M-F between 3:00 AM and 6:00 PM (Eastern), or write to us at info@copyright.com. This is not an invoice.

**Confirmation Number: 11584169**
**Order Date: 08/14/2016**

If you paid by credit card, your order will be finalized and your card will be charged within 24 hours. If you choose to be invoiced, you can change or cancel your order until the invoice is generated.

**Payment Information**

Dhanusha Nalawansha
dhanusha@chem.wayne.edu
+1 (313)9093250
Payment Method: n/a

**Order Details**

### JOURNAL OF CLINICAL INVESTIGATION. ONLINE

| | |
|---|---|
| **Order detail ID:** | 70016876 |
| **Order License Id:** | 3927860945997 |
| **ISSN:** | 1558-8238 |
| **Publication Type:** | e-Journal |
| **Volume:** | |
| **Issue:** | |
| **Start page:** | |
| **Publisher:** | AMERICAN SOCIETY FOR CLINICAL INVESTIGATION |

| | |
|---|---|
| **Permission Status:** | Granted |
| **Permission type:** | Republish or display content |
| **Type of use:** | Republish in a thesis/dissertation |
| **Requestor type** | Academic institution |
| **Format** | Print, Electronic |
| **Portion** | chart/graph/table/figure |
| **Number of charts/graphs/tables/figures** | 1 |
| **Title or numeric reference of the portion(s)** | The Molecular targets of HDACs |
| **Title of the article or chapter the portion is from** | New and emerging HDAC inhibitors for cancer treatment |
| **Editor of portion(s)** | N/A |
| **Author of portion(s)** | Alison C. West1 and Ricky W. Johnstone1 |

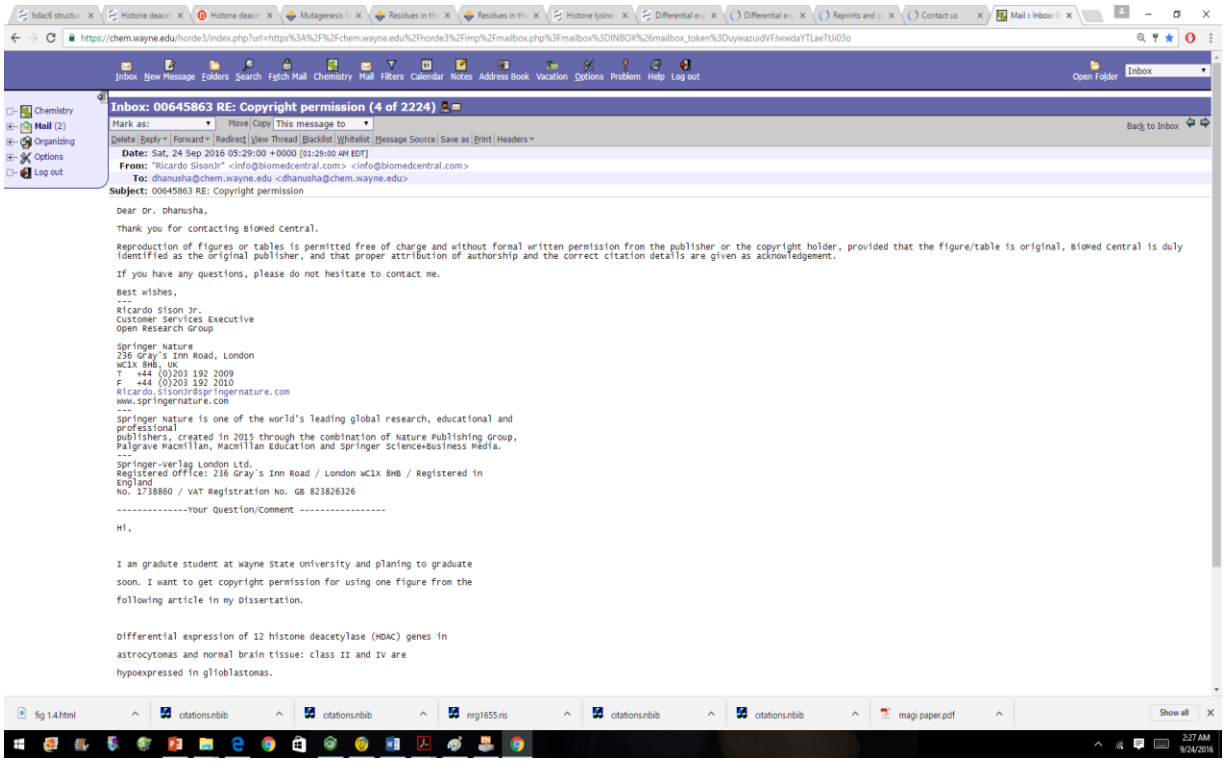

Inbox: 00645863 RE: Copyright permission (4 of 2224)

Date: Sat, 24 Sep 2016 05:29:00 +0000 [01:29:00 AM EDT]
From: "Ricardo SisonJr" <info@biomedcentral.com> <info@biomedcentral.com>
To: dhanusha@chem.wayne.edu <dhanusha@chem.wayne.edu>
Subject: 00645863 RE: Copyright permission

Dear Dr. Dhanusha,

Thank you for contacting BioMed Central.

Reproduction of figures or tables is permitted free of charge and without formal written permission from the publisher or the copyright holder, provided that the figure/table is original, BioMed Central is duly identified as the original publisher, and that proper attribution of authorship and the correct citation details are given as acknowledgement.

If you have any questions, please do not hesitate to contact me.

Best wishes,

Ricardo Sison Jr.
Customer Services Executive
Open Research Group

Springer Nature
236 Gray's Inn Road, London
WC1X 8HB, UK
T +44 (0)203 192 2009
F +44 (0)203 192 2010
Ricardo.SisonJr@springernature.com
www.springernature.com

Springer Nature is one of the world's leading global research, educational and professional
publishers, created in 2015 through the combination of Nature Publishing Group, Palgrave Macmillan, Macmillan Education and Springer Science+Business Media.

Springer-Verlag London Ltd.
Registered Office: 236 Gray's Inn Road / London WC1X 8HB / Registered in England
No. 1738860 / VAT Registration No. GB 823826326

----------Your Question/Comment ----------

Hi,

I am gradute student at Wayne State University and planing to graduate soon. I want to get copyright permission for using one figure from the following article in my Dissertation.

Differential expression of 12 histone deacetylase (HDAC) genes in astrocytomas and normal brain tissue: class II and IV are hypoexpressed in glioblastomas.

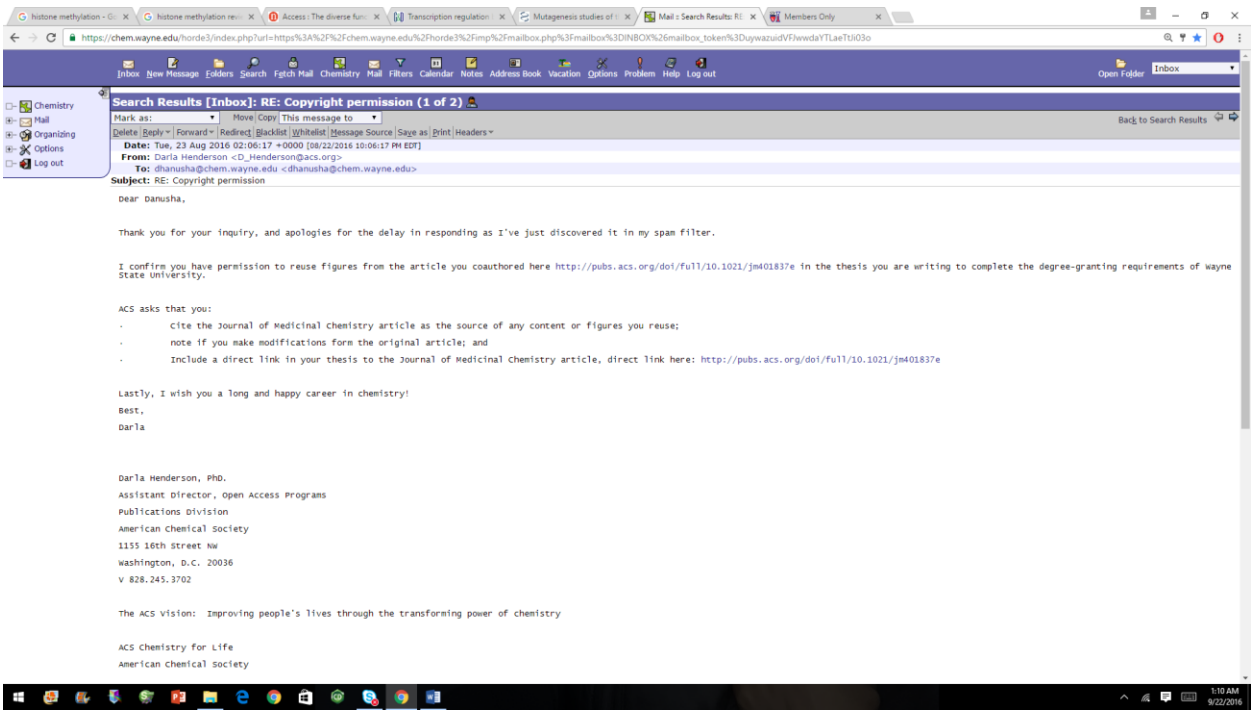

Search Results [Inbox]: RE: Copyright permission (1 of 2)

Date: Tue, 23 Aug 2016 02:06:17 +0000 [08/22/2016 10:06:17 PM EDT]
From: Darla Henderson <D_Henderson@acs.org>
To: dhanusha@chem.wayne.edu <dhanusha@chem.wayne.edu>
Subject: RE: Copyright permission

Dear Danusha,

Thank you for your inquiry, and apologies for the delay in responding as I've just discovered it in my spam filter.

I confirm you have permission to reuse figures from the article you coauthored here http://pubs.acs.org/doi/full/10.1021/jm401837e in the thesis you are writing to complete the degree-granting requirements of Wayne State University.

ACS asks that you:

- Cite the Journal of Medicinal Chemistry article as the source of any content or figures you reuse;
- note if you make modifications form the original article; and
- Include a direct link in your thesis to the Journal of Medicinal Chemistry article, direct link here: http://pubs.acs.org/doi/full/10.1021/jm401837e

Lastly, I wish you a long and happy career in chemistry!

Best,
Darla

Darla Henderson, PhD.
Assistant Director, Open Access Programs
Publications Division
American Chemical Society
1155 16th Street NW
Washington, D.C. 20036
V 828.245.3702

The ACS Vision: Improving people's lives through the transforming power of chemistry

ACS Chemistry for Life
American Chemical Society

Copyright Clearance Center RightsLink®

Home | Account Info | Help | Live Chat

Springer
the language of science

**Title:** Proteomic identification and functional characterization of MYH9, Hsc70, and DNAJA1 as novel substrates of HDAC6 deacetylase activity
**Author:** Linlin Zhang
**Publication:** Protein & Cell
**Publisher:** Springer
**Date:** Jan 1, 2014
Copyright © 2014, The Author(s)

Logged in as:
Dhanusha Nalawansha
Account #:
3001053831
LOGOUT

## Permissions Request

Copyright © 2016 Copyright Clearance Center, Inc. All Rights Reserved. Privacy statement. Terms and Conditions.
Comments? We would like to hear from you. E-mail us at customercare@copyright.com

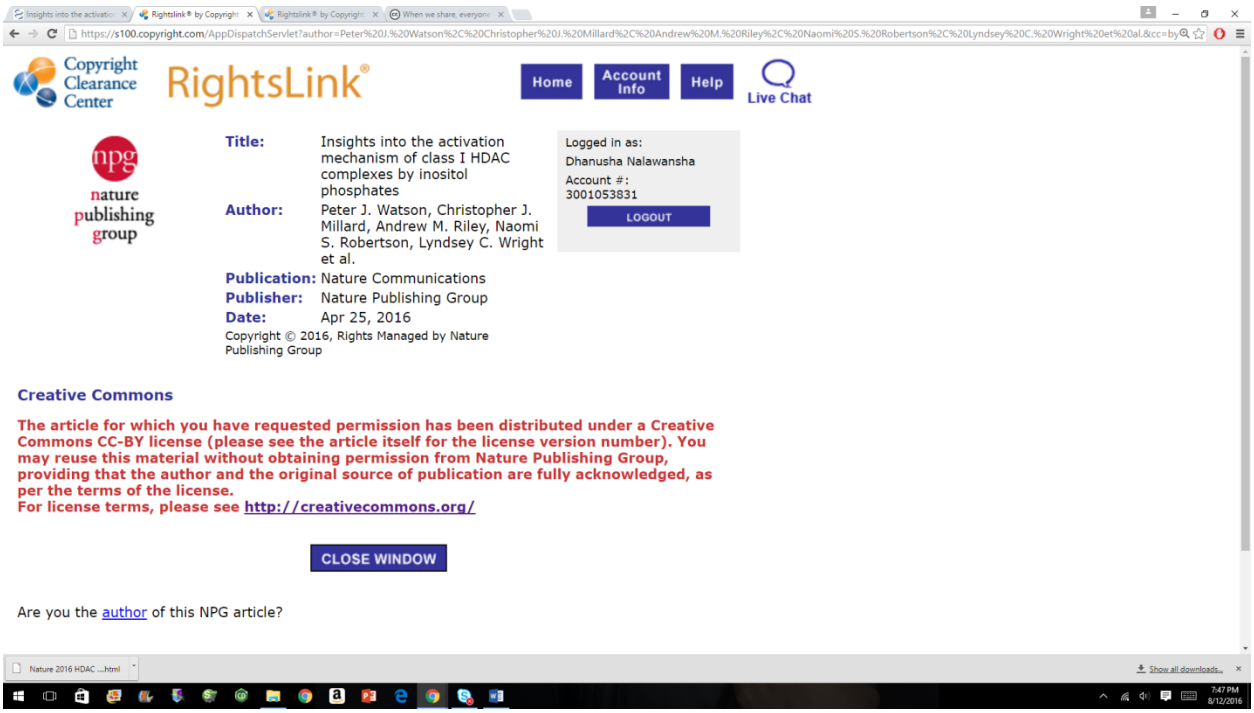

Copyright Clearance Center RightsLink®

Home | Account Info | Help | Live Chat

nature publishing group

**Title:** Insights into the activation mechanism of class I HDAC complexes by inositol phosphates
**Author:** Peter J. Watson, Christopher J. Millard, Andrew M. Riley, Naomi S. Robertson, Lyndsey C. Wright et al.
**Publication:** Nature Communications
**Publisher:** Nature Publishing Group
**Date:** Apr 25, 2016
Copyright © 2016, Rights Managed by Nature Publishing Group

Logged in as:
Dhanusha Nalawansha
Account #:
3001053831
LOGOUT

**Creative Commons**

**The article for which you have requested permission has been distributed under a Creative Commons CC-BY license (please see the article itself for the license version number). You may reuse this material without obtaining permission from Nature Publishing Group, providing that the author and the original source of publication are fully acknowledged, as per the terms of the license.**
**For license terms, please see http://creativecommons.org/**

CLOSE WINDOW

Are you the author of this NPG article?

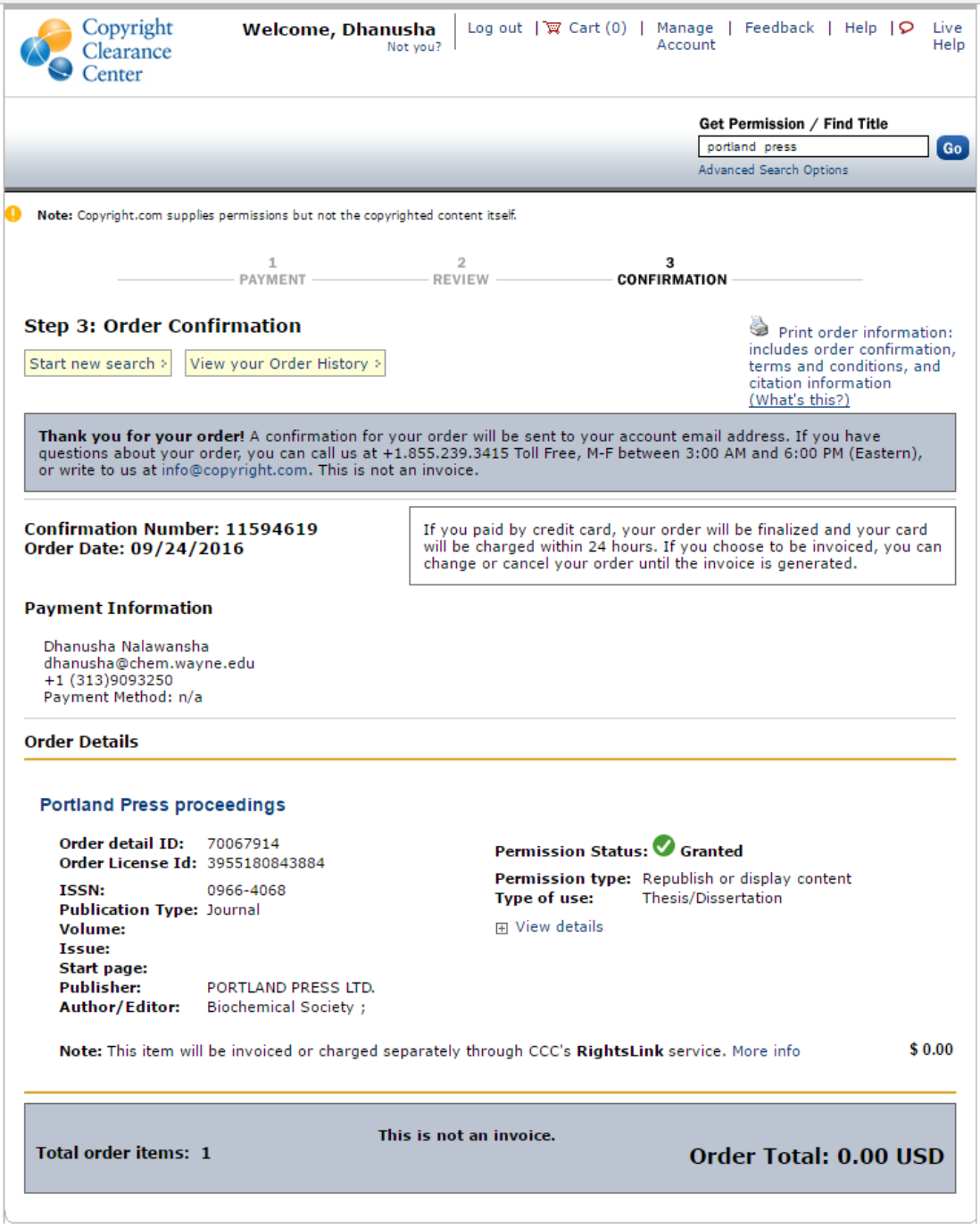

Copyright Clearance Center

Welcome, Dhanusha
Not you?

Log out | Cart (0) | Manage Account | Feedback | Help | Live Help

Get Permission / Find Title
portland press
Go
Advanced Search Options

**Note:** Copyright.com supplies permissions but not the copyrighted content itself.

1 PAYMENT — 2 REVIEW — 3 CONFIRMATION

## Step 3: Order Confirmation

Start new search | View your Order History

Print order information: includes order confirmation, terms and conditions, and citation information (What's this?)

**Thank you for your order!** A confirmation for your order will be sent to your account email address. If you have questions about your order, you can call us at +1.855.239.3415 Toll Free, M-F between 3:00 AM and 6:00 PM (Eastern), or write to us at info@copyright.com. This is not an invoice.

**Confirmation Number: 11594619**
**Order Date: 09/24/2016**

If you paid by credit card, your order will be finalized and your card will be charged within 24 hours. If you choose to be invoiced, you can change or cancel your order until the invoice is generated.

### Payment Information

Dhanusha Nalawansha
dhanusha@chem.wayne.edu
+1 (313)9093250
Payment Method: n/a

### Order Details

**Portland Press proceedings**

**Order detail ID:** 70067914
**Order License Id:** 3955180843884
**ISSN:** 0966-4068
**Publication Type:** Journal
**Volume:**
**Issue:**
**Start page:**
**Publisher:** PORTLAND PRESS LTD.
**Author/Editor:** Biochemical Society ;

**Permission Status:** Granted
**Permission type:** Republish or display content
**Type of use:** Thesis/Dissertation
View details

**Note:** This item will be invoiced or charged separately through CCC's **RightsLink** service. More info $ 0.00

**Total order items: 1**

**This is not an invoice.**

**Order Total: 0.00 USD**

nature publishing group

**Title:** Regulation of histone methylation by demethylimination and demethylation
**Author:** Robert J. Klose and Yi Zhang
**Publication:** Nature Reviews Molecular Cell Biology
**Publisher:** Nature Publishing Group
**Date:** Mar 7, 2007





## Review Order

Please review the order details and the associated terms and conditions.

No royalties will be charged for this reuse request although you are required to obtain a license and comply with the license terms and conditions. To obtain the license, click the Accept button below.

| | |
|---|---|
| Licensed Content Publisher | Nature Publishing Group |
| Licensed Content Publication | Nature Reviews Molecular Cell Biology |
| Licensed Content Title | Regulation of histone methylation by demethylimination and demethylation |
| Licensed Content Author | Robert J. Klose and Yi Zhang |
| Licensed Content Date | Mar 7, 2007 |
| Licensed Content Volume | 8 |
| Licensed Content Issue | 4 |
| Type of Use | reuse in a dissertation / thesis |
| Requestor type | academic/educational |
| Format | print and electronic |
| Portion | figures/tables/illustrations |
| Number of figures/tables/illustrations | 1 |
| High-res required | no |
| Figures | figure 3.4 |
| Author of this NPG article | no |
| Your reference number | |
| Title of your thesis / dissertation | Studies towards broadening the substrate profile and regulation of Histone deacetylase 1 |
| Expected completion date | Oct 2016 |
| Estimated size (number of pages) | 190 |
| Requestor Location | Dhanusha A Nalawansha<br>4757 Anthony Wayne Drive<br>Apt 12<br><br>DETROIT, MI 48201<br>United States<br>Attn: Dhanusha A Nalawansha |
| Total | 0.00 USD |

Edit Order Details

Edit Requestor Location This location may be used to determine your tax liability.

## REFERENCES


1. Khorasanizadeh, S. (2004) The nucleosome: from genomic organization to genomic regulation. *Cell* **116**, 259-272
2. Arrowsmith, C. H., Bountra, C., Fish, P. V., Lee, K., and Schapira, M. (2012) Epigenetic protein families: a new frontier for drug discovery. *Nature reviews. Drug discovery* **11**, 384-400
3. Lund, A. H., and van Lohuizen, M. (2004) Epigenetics and cancer. *Genes & development* **18**, 2315-2335
4. Vignali, M., Hassan, A. H., Neely, K. E., and Workman, J. L. (2000) ATP-dependent chromatin-remodeling complexes. *Molecular and cellular biology* **20**, 1899-1910
5. Jin, B., and Robertson, K. D. (2013) DNA methyltransferases, DNA damage repair, and cancer. *Advances in experimental medicine and biology* **754**, 3-29
6. Robertson, K. D. (2005) DNA methylation and human disease. *Nat Rev Genet* **6**, 597-610
7. Bannister, A. J., and Kouzarides, T. (2011) Regulation of chromatin by histone modifications. *Cell Research* **21**, 381-395
8. Kato, S., Inoue, K., and Youn, M.-Y. (2010) Emergence of the osteo-epigenome in bone biology. *IBMS BoneKEy* **7**, 314-324
9. Zhang, Y., and Reinberg, D. (2001) Transcription regulation by histone methylation: interplay between different covalent modifications of the core histone tails. *Genes & development* **15**, 2343-2360

10. Park, J. A., Kim, A. J., Kang, Y., Jung, Y. J., Kim, H. K., and Kim, K. C. (2011) Deacetylation and methylation at histone H3 lysine 9 (H3K9) coordinate chromosome condensation during cell cycle progression. *Molecules and cells* **31**, 343-349

11. Varier, R. A., and Timmers, H. T. (2011) Histone lysine methylation and demethylation pathways in cancer. *Biochimica et biophysica acta* **1815**, 75-89

12. Crunkhorn, S. (2015) Cancer: Targeting LSD1 in small cell lung cancer. *Nature reviews. Drug discovery* **14**, 602-602

13. Hayami, S., Kelly, J. D., Cho, H. S., Yoshimatsu, M., Unoki, M., Tsunoda, T., Field, H. I., Neal, D. E., Yamaue, H., Ponder, B. A., Nakamura, Y., and Hamamoto, R. (2011) Overexpression of LSD1 contributes to human carcinogenesis through chromatin regulation in various cancers. *International journal of cancer* **128**, 574-586

14. Eberharter, A., and Becker, P. B. (2002) Histone acetylation: a switch between repressive and permissive chromatin: Second in review series on chromatin dynamics. *EMBO Reports* **3**, 224-229

15. Kramer, O. H., Gottlicher, M., and Heinzel, T. (2001) Histone deacetylase as a therapeutic target. *Trends in endocrinology and metabolism: TEM* **12**, 294-300

16. Gregoretti, I. V., Lee, Y. M., and Goodson, H. V. (2004) Molecular evolution of the histone deacetylase family: functional implications of phylogenetic analysis. *Journal of molecular biology* **338**, 17-31

17. Taunton, J., Hassig, C. A., and Schreiber, S. L. (1996) A mammalian histone deacetylase related to the yeast transcriptional regulator Rpd3p. *Science* **272**, 408-411

18. Yang, W. M., Inouye, C., Zeng, Y., Bearss, D., and Seto, E. (1996) Transcriptional repression by YY1 is mediated by interaction with a mammalian homolog of the yeast global regulator RPD3. *Proceedings of the National Academy of Sciences of the United States of America* **93**, 12845-12850

19. Yang, W. M., Yao, Y. L., Sun, J. M., Davie, J. R., and Seto, E. (1997) Isolation and characterization of cDNAs corresponding to an additional member of the human histone deacetylase gene family. *The Journal of biological chemistry* **272**, 28001-28007

20. Buist, A., Blanchetot, C., Tertoolen, L. G., and den Hertog, J. (2000) Identification of p130cas as an in vivo substrate of receptor protein-tyrosine phosphatase alpha. *The Journal of biological chemistry* **275**, 20754-20761

21. Van den Wyngaert, I., de Vries, W., Kremer, A., Neefs, J., Verhasselt, P., Luyten, W. H., and Kass, S. U. (2000) Cloning and characterization of human histone deacetylase 8. *FEBS letters* **478**, 77-83

22. Grozinger, C. M., Hassig, C. A., and Schreiber, S. L. (1999) Three proteins define a class of human histone deacetylases related to yeast Hda1p. *Proceedings of the National Academy of Sciences of the United States of America* **96**, 4868-4873

23. Zhou, X., Marks, P. A., Rifkind, R. A., and Richon, V. M. (2001) Cloning and characterization of a histone deacetylase, HDAC9. *Proceedings of the National Academy of Sciences of the United States of America* **98**, 10572-10577

24. Kao, H. Y., Downes, M., Ordentlich, P., and Evans, R. M. (2000) Isolation of a novel histone deacetylase reveals that class I and class II deacetylases promote SMRT-mediated repression. *Genes & development* **14**, 55-66

25. Villagra, A., Sotomayor, E. M., and Seto, E. (2010) Histone deacetylases and the immunological network: implications in cancer and inflammation. *Oncogene* **29**, 157-173

26. Gao, L., Cueto, M. A., Asselbergs, F., and Atadja, P. (2002) Cloning and functional characterization of HDAC11, a novel member of the human histone deacetylase family. *The Journal of biological chemistry* **277**, 25748-25755

27. Lucio-Eterovic, A. K., Cortez, M. A., Valera, E. T., Motta, F. J., Queiroz, R. G., Machado, H. R., Carlotti, C. G., Jr., Neder, L., Scrideli, C. A., and Tone, L. G. (2008) Differential expression of 12 histone deacetylase (HDAC) genes in astrocytomas and normal brain tissue: class II and IV are hypoexpressed in glioblastomas. *BMC cancer* **8**, 243

28. Bressi, J. C., Jennings, A. J., Skene, R., Wu, Y., Melkus, R., De Jong, R., O'Connell, S., Grimshaw, C. E., Navre, M., and Gangloff, A. R. (2010) Exploration of the HDAC2 foot pocket: Synthesis and SAR of substituted N-(2-aminophenyl)benzamides. *Bioorganic & medicinal chemistry letters* **20**, 3142-3145

29. Millard, C. J., Watson, P. J., Celardo, I., Gordiyenko, Y., Cowley, S. M., Robinson, C. V., Fairall, L., and Schwabe, J. W. (2013) Class I HDACs share a common mechanism of regulation by inositol phosphates. *Molecular cell* **51**, 57-67

30. Watson, P. J., Fairall, L., Santos, G. M., and Schwabe, J. W. (2012) Structure of HDAC3 bound to co-repressor and inositol tetraphosphate. *Nature* **481**, 335-340

31. Bottomley, M. J., Lo Surdo, P., Di Giovine, P., Cirillo, A., Scarpelli, R., Ferrigno, F., Jones, P., Neddermann, P., De Francesco, R., Steinkuhler, C., Gallinari, P., and Carfi, A. (2008) Structural and functional analysis of the human HDAC4 catalytic domain reveals a regulatory structural zinc-binding domain. *The Journal of biological chemistry* **283**, 26694-26704

32. Schuetz, A., Min, J., Allali-Hassani, A., Schapira, M., Shuen, M., Loppnau, P., Mazitschek, R., Kwiatkowski, N. P., Lewis, T. A., Maglathin, R. L., McLean, T. H., Bochkarev, A., Plotnikov, A. N., Vedadi, M., and Arrowsmith, C. H. (2008) Human HDAC7 harbors a class IIa histone deacetylase-specific zinc binding motif and cryptic deacetylase activity. *The Journal of biological chemistry* **283**, 11355-11363

33. Vannini, A., Volpari, C., Filocamo, G., Casavola, E. C., Brunetti, M., Renzoni, D., Chakravarty, P., Paolini, C., De Francesco, R., Gallinari, P., Steinkuhler, C., and Di Marco, S. (2004) Crystal structure of a eukaryotic zinc-dependent histone deacetylase, human HDAC8, complexed with a hydroxamic acid inhibitor. *Proceedings of the National Academy of Sciences of the United States of America* **101**, 15064-15069

34. Somoza, J. R., Skene, R. J., Katz, B. A., Mol, C., Ho, J. D., Jennings, A. J., Luong, C., Arvai, A., Buggy, J. J., Chi, E., Tang, J., Sang, B. C., Verner, E., Wynands, R., Leahy, E. M., Dougan, D. R., Snell, G., Navre, M., Knuth, M. W., Swanson, R. V., McRee, D. E., and Tari, L. W. (2004) Structural snapshots of human HDAC8 provide insights into the class I histone deacetylases. *Structure (London, England : 1993)* **12**, 1325-1334

35. Watson, P. J., Millard, C. J., Riley, A. M., Robertson, N. S., Wright, L. C., Godage, H. Y., Cowley, S. M., Jamieson, A. G., Potter, B. V., and Schwabe, J. W. (2016) Insights into the activation mechanism of class I HDAC complexes by inositol phosphates. *Nature communications* **7**, 11262

36. Hai, Y., and Christianson, D. W. (2016) Histone deacetylase 6 structure and molecular basis of catalysis and inhibition. *Nature chemical biology* **12**, 741-747

37. Wambua, M. K., Nalawansha, D. A., Negmeldin, A. T., and Pflum, M. K. (2014) Mutagenesis Studies of the 14 Å Internal Cavity of Histone Deacetylase 1: Insights towards the Acetate Escape Hypothesis and Selective Inhibitor Design. *Journal of medicinal chemistry* **57**, 642-650

38. Weerasinghe, S. V., Estiu, G., Wiest, O., and Pflum, M. K. (2008) Residues in the 11 A channel of histone deacetylase 1 promote catalytic activity: implications for designing isoform-selective histone deacetylase inhibitors. *Journal of medicinal chemistry* **51**, 5542-5551

39. Chen, K., Zhang, X., Wu, Y. D., and Wiest, O. (2014) Inhibition and mechanism of HDAC8 revisited. *Journal of the American Chemical Society* **136**, 11636-11643

40. Gantt, S. M., Decroos, C., Lee, M. S., Gullett, L. E., Bowman, C. M., Christianson, D. W., and Fierke, C. A. (2016) General Base-General Acid Catalysis in Human Histone Deacetylase 8. *Biochemistry* **55**, 820-832

41. Zhang, Y., Ng, H. H., Erdjument-Bromage, H., Tempst, P., Bird, A., and Reinberg, D. (1999) Analysis of the NuRD subunits reveals a histone deacetylase core complex and a connection with DNA methylation. *Genes & development* **13**, 1924-1935

42. Hayakawa, T., and Nakayama, J. (2011) Physiological roles of class I HDAC complex and histone demethylase. *Journal of biomedicine & biotechnology* **2011**, 129383

43. Kelly, R. D., and Cowley, S. M. (2013) The physiological roles of histone deacetylase (HDAC) 1 and 2: complex co-stars with multiple leading parts. *Biochemical Society transactions* **41**, 741-749

44. Eom, G. H., Nam, Y. S., Oh, J. G., Choe, N., Min, H. K., Yoo, E. K., Kang, G., Nguyen, V. H., Min, J. J., Kim, J. K., Lee, I. K., Bassel-Duby, R., Olson, E. N., Park, W. J., and Kook, H. (2014) Regulation of acetylation of histone deacetylase 2 by p300/CBP-associated factor/histone deacetylase 5 in the development of cardiac hypertrophy. *Circulation research* **114**, 1133-1143

45. Lagger, G., Doetzlhofer, A., Schuettengruber, B., Haidweger, E., Simboeck, E., Tischler, J., Chiocca, S., Suske, G., Rotheneder, H., Wintersberger, E., and Seiser, C. (2003) The tumor suppressor p53 and histone deacetylase 1 are antagonistic regulators of the cyclin-dependent kinase inhibitor p21/WAF1/CIP1 gene. *Molecular and cellular biology* **23**, 2669-2679

46. Lagger, G., O'Carroll, D., Rembold, M., Khier, H., Tischler, J., Weitzer, G., Schuettengruber, B., Hauser, C., Brunmeir, R., Jenuwein, T., and Seiser, C. (2002) Essential function of histone deacetylase 1 in proliferation control and CDK inhibitor repression. *The EMBO journal* **21**, 2672-2681

47. Weichert, W. (2009) HDAC expression and clinical prognosis in human malignancies. *Cancer letters* **280**, 168-176

48. Zhang, Z., Yamashita, H., Toyama, T., Sugiura, H., Omoto, Y., Ando, Y., Mita, K., Hamaguchi, M., Hayashi, S., and Iwase, H. (2004) HDAC6 expression is correlated with better survival in breast cancer. *Clinical cancer research : an official journal of the American Association for Cancer Research* **10**, 6962-6968

49. Wilson, A. J., Byun, D. S., Popova, N., Murray, L. B., L'Italien, K., Sowa, Y., Arango, D., Velcich, A., Augenlicht, L. H., and Mariadason, J. M. (2006) Histone deacetylase 3 (HDAC3) and other class I HDACs regulate colon cell maturation and p21 expression and are deregulated in human colon cancer. *The Journal of biological chemistry* **281**, 13548-13558

50. Waltregny, D., North, B., Van Mellaert, F., de Leval, J., Verdin, E., and Castronovo, V. (2004) Screening of histone deacetylases (HDAC) expression in human prostate cancer reveals distinct class I HDAC profiles between epithelial and stromal cells. *European journal of histochemistry : EJH* **48**, 273-290

51. Oehme, I., Deubzer, H. E., Wegener, D., Pickert, D., Linke, J. P., Hero, B., Kopp-Schneider, A., Westermann, F., Ulrich, S. M., von Deimling, A., Fischer, M., and Witt, O. (2009) Histone deacetylase 8 in neuroblastoma tumorigenesis. *Clinical cancer research : an official journal of the American Association for Cancer Research* **15**, 91-99

52. Ropero, S., Fraga, M. F., Ballestar, E., Hamelin, R., Yamamoto, H., Boix-Chornet, M., Caballero, R., Alaminos, M., Setien, F., Paz, M. F., Herranz, M., Palacios, J., Arango, D., Orntoft, T. F., Aaltonen, L. A., Schwartz, S., Jr., and Esteller, M. (2006) A truncating mutation of HDAC2 in human cancers confers resistance to histone deacetylase inhibition. *Nature genetics* **38**, 566-569

53. Pacheco, M., and Nielsen, T. O. (2012) Histone deacetylase 1 and 2 in mesenchymal tumors. *Mod Pathol* **25**, 222-230

54. Glaser, K. B., Li, J., Staver, M. J., Wei, R. Q., Albert, D. H., and Davidsen, S. K. (2003) Role of class I and class II histone deacetylases in carcinoma cells using siRNA. *Biochemical and biophysical research communications* **310**, 529-536

55. Xie, H. J., Noh, J. H., Kim, J. K., Jung, K. H., Eun, J. W., Bae, H. J., Kim, M. G., Chang, Y. G., Lee, J. Y., Park, H., and Nam, S. W. (2012) HDAC1 inactivation induces mitotic defect and caspase-independent autophagic cell death in liver cancer. *PloS one* **7**, e34265

56. Barneda-Zahonero, B., and Parra, M. (2012) Histone deacetylases and cancer. *Molecular oncology* **6**, 579-589

57. Ishii, S., Kurasawa, Y., Wong, J., and Yu-Lee, L. Y. (2008) Histone deacetylase 3 localizes to the mitotic spindle and is required for kinetochore-microtubule attachment. *Proceedings of the National Academy of Sciences of the United States of America* **105**, 4179-4184

58. Grant, S., Easley, C., and Kirkpatrick, P. (2007) Vorinostat. *Nature reviews. Drug discovery* **6**, 21-22

59. Laubach, J. P., Moreau, P., San-Miguel, J. F., and Richardson, P. G. (2015) Panobinostat for the Treatment of Multiple Myeloma. *Clinical cancer research : an official journal of the American Association for Cancer Research* **21**, 4767-4773

60. Lee, H. Z., Kwitkowski, V. E., Del Valle, P. L., Ricci, M. S., Saber, H., Habtemariam, B. A., Bullock, J., Bloomquist, E., Li Shen, Y., Chen, X. H., Brown, J., Mehrotra, N., Dorff, S., Charlab, R., Kane, R. C., Kaminskas, E., Justice, R., Farrell, A. T.,

and Pazdur, R. (2015) FDA Approval: Belinostat for the Treatment of Patients with Relapsed or Refractory Peripheral T-cell Lymphoma. *Clinical cancer research : an official journal of the American Association for Cancer Research* **21**, 2666-2670

61. Prince, H. M., and Dickinson, M. (2012) Romidepsin for cutaneous T-cell lymphoma. *Clinical cancer research : an official journal of the American Association for Cancer Research* **18**, 3509-3515

62. Peart, M. J., Tainton, K. M., Ruefli, A. A., Dear, A. E., Sedelies, K. A., O'Reilly, L. A., Waterhouse, N. J., Trapani, J. A., and Johnstone, R. W. (2003) Novel mechanisms of apoptosis induced by histone deacetylase inhibitors. *Cancer research* **63**, 4460-4471

63. Mottamal, M., Zheng, S., Huang, T. L., and Wang, G. (2015) Histone deacetylase inhibitors in clinical studies as templates for new anticancer agents. *Molecules (Basel, Switzerland)* **20**, 3898-3941

64. Malvaez, M., McQuown, S. C., Rogge, G. A., Astarabadi, M., Jacques, V., Carreiro, S., Rusche, J. R., and Wood, M. A. (2013) HDAC3-selective inhibitor enhances extinction of cocaine-seeking behavior in a persistent manner. *Proceedings of the National Academy of Sciences of the United States of America* **110**, 2647-2652

65. Butler, K. V., Kalin, J., Brochier, C., Vistoli, G., Langley, B., and Kozikowski, A. P. (2010) Rational design and simple chemistry yield a superior, neuroprotective HDAC6 inhibitor, tubastatin A. *Journal of the American Chemical Society* **132**, 10842-10846

66. Balasubramanian, S., Ramos, J., Luo, W., Sirisawad, M., Verner, E., and Buggy, J. J. (2008) A novel histone deacetylase 8 (HDAC8)-specific inhibitor PCI-34051 induces apoptosis in T-cell lymphomas. *Leukemia* **22**, 1026-1034

67. Hassig, C. A., Tong, J. K., Fleischer, T. C., Owa, T., Grable, P. G., Ayer, D. E., and Schreiber, S. L. (1998) A role for histone deacetylase activity in HDAC1-mediated transcriptional repression. *Proceedings of the National Academy of Sciences of the United States of America* **95**, 3519-3524

68. Warrener, R., Chia, K., Warren, W. D., Brooks, K., and Gabrielli, B. (2010) Inhibition of histone deacetylase 3 produces mitotic defects independent of alterations in histone H3 lysine 9 acetylation and methylation. *Molecular pharmacology* **78**, 384-393

69. Zhao, S., Xu, W., Jiang, W., Yu, W., Lin, Y., Zhang, T., Yao, J., Zhou, L., Zeng, Y., Li, H., Li, Y., Shi, J., An, W., Hancock, S. M., He, F., Qin, L., Chin, J., Yang, P., Chen, X., Lei, Q., Xiong, Y., and Guan, K. L. (2010) Regulation of cellular metabolism by protein lysine acetylation. *Science* **327**, 1000-1004

70. Singh, B. N., Zhang, G., Hwa, Y. L., Li, J., Dowdy, S. C., and Jiang, S. W. (2010) Nonhistone protein acetylation as cancer therapy targets. *Expert review of anticancer therapy* **10**, 935-954

71. Scholz, C., Weinert, B. T., Wagner, S. A., Beli, P., Miyake, Y., Qi, J., Jensen, L. J., Streicher, W., McCarthy, A. R., Westwood, N. J., Lain, S., Cox, J., Matthias, P., Mann, M., Bradner, J. E., and Choudhary, C. (2015) Acetylation site specificities of lysine deacetylase inhibitors in human cells. *Nature biotechnology* **33**, 415-423

72. Zhang, L., Liu, S., Liu, N., Zhang, Y., Liu, M., Li, D., Seto, E., Yao, T. P., Shui, W., and Zhou, J. (2015) Proteomic identification and functional characterization of MYH9, Hsc70, and DNAJA1 as novel substrates of HDAC6 deacetylase activity. *Protein & cell* **6**, 42-54

73. Alam, N., Zimmerman, L., Wolfson, N. A., Joseph, C. G., Fierke, C. A., and Schueler-Furman, O. (2016) Structure-Based Identification of HDAC8 Non-histone Substrates. *Structure (London, England : 1993)* **24**, 458-468

74. Hubbert, C., Guardiola, A., Shao, R., Kawaguchi, Y., Ito, A., Nixon, A., Yoshida, M., Wang, X. F., and Yao, T. P. (2002) HDAC6 is a microtubule-associated deacetylase. *Nature* **417**, 455-458

75. Bali, P., Pranpat, M., Bradner, J., Balasis, M., Fiskus, W., Guo, F., Rocha, K., Kumaraswamy, S., Boyapalle, S., Atadja, P., Seto, E., and Bhalla, K. (2005) Inhibition of histone deacetylase 6 acetylates and disrupts the chaperone function of heat shock protein 90: a novel basis for antileukemia activity of histone deacetylase inhibitors. *The Journal of biological chemistry* **280**, 26729-26734

76. Kovacs, J. J., Murphy, P. J., Gaillard, S., Zhao, X., Wu, J. T., Nicchitta, C. V., Yoshida, M., Toft, D. O., Pratt, W. B., and Yao, T. P. (2005) HDAC6 regulates Hsp90 acetylation and chaperone-dependent activation of glucocorticoid receptor. *Molecular cell* **18**, 601-607

77. Luo, J., Su, F., Chen, D., Shiloh, A., and Gu, W. (2000) Deacetylation of p53 modulates its effect on cell growth and apoptosis. *Nature* **408**, 377-381

78. Martínez-Balbás, M. A., Bauer, U.-M., Nielsen, S. J., Brehm, A., and Kouzarides, T. (2000) Regulation of E2F1 activity by acetylation. *The EMBO journal* **19**, 662-671

79. Martinez-Balbas, M. A., Bauer, U. M., Nielsen, S. J., Brehm, A., and Kouzarides, T. (2000) Regulation of E2F1 activity by acetylation. *The EMBO journal* **19**, 662-671

80. Choudhary, C., Kumar, C., Gnad, F., Nielsen, M. L., Rehman, M., Walther, T. C., Olsen, J. V., and Mann, M. (2009) Lysine acetylation targets protein complexes and co-regulates major cellular functions. *Science* **325**, 834-840

81. Flint, A. J., Tiganis, T., Barford, D., and Tonks, N. K. (1997) Development of "substrate-trapping" mutants to identify physiological substrates of protein tyrosine phosphatases. *Proceedings of the National Academy of Sciences of the United States of America* **94**, 1680-1685

82. Wu, J., Katrekar, A., Honigberg, L. A., Smith, A. M., Conn, M. T., Tang, J., Jeffery, D., Mortara, K., Sampang, J., Williams, S. R., Buggy, J., and Clark, J. M. (2006) Identification of substrates of human protein-tyrosine phosphatase PTPN22. *The Journal of biological chemistry* **281**, 11002-11010

83. Motiwala, T., Datta, J., Kutay, H., Roy, S., and Jacob, S. T. (2010) Lyn kinase and ZAP70 are substrates of PTPROt in B-cells: Lyn inactivation by PTPROt sensitizes leukemia cells to VEGF-R inhibitor pazopanib. *Journal of cellular biochemistry* **110**, 846-856

84. Merritt, R., Hayman, M. J., and Agazie, Y. M. (2006) Mutation of Thr466 in SHP2 abolishes its phosphatase activity, but provides a new substrate-trapping mutant. *Biochimica et biophysica acta* **1763**, 45-56

85. Agazie, Y. M., and Hayman, M. J. (2003) Development of an efficient "substrate-trapping" mutant of Src homology phosphotyrosine phosphatase 2 and identification of the epidermal growth factor receptor, Gab1, and three other proteins as target substrates. *The Journal of biological chemistry* **278**, 13952-13958

86. Wang, D. F., Helquist, P., Wiech, N. L., and Wiest, O. (2005) Toward selective histone deacetylase inhibitor design: homology modeling, docking studies, and molecular dynamics simulations of human class I histone deacetylases. *Journal of medicinal chemistry* **48**, 6936-6947

87. Estiu, G., Greenberg, E., Harrison, C. B., Kwiatkowski, N. P., Mazitschek, R., Bradner, J. E., and Wiest, O. (2008) Structural origin of selectivity in class II-selective histone deacetylase inhibitors. *Journal of medicinal chemistry* **51**, 2898-2906

88. Cartron, P. F., Blanquart, C., Hervouet, E., Gregoire, M., and Vallette, F. M. (2013) HDAC1-mSin3a-NCOR1, Dnmt3b-HDAC1-Egr1 and Dnmt1-PCNA-UHRF1-G9a regulate the NY-ESO1 gene expression. *Molecular oncology* **7**, 452-463

89. Blangy, A., Lane, H. A., d'Herin, P., Harper, M., Kress, M., and Nigg, E. A. (1995) Phosphorylation by p34cdc2 regulates spindle association of human Eg5, a kinesin-related motor essential for bipolar spindle formation in vivo. *Cell* **83**, 1159-1169

90. Robbins, A. R., Jablonski, S. A., Yen, T. J., Yoda, K., Robey, R., Bates, S. E., and Sackett, D. L. (2005) Inhibitors of histone deacetylases alter kinetochore assembly by disrupting pericentromeric heterochromatin. *Cell cycle* **4**, 717-726

91. Taddei, A., Maison, C., Roche, D., and Almouzni, G. (2001) Reversible disruption of pericentric heterochromatin and centromere function by inhibiting deacetylases. *Nature cell biology* **3**, 114-120

92. Stevens, F. E., Beamish, H., Warrener, R., and Gabrielli, B. (2008) Histone deacetylase inhibitors induce mitotic slippage. *Oncogene* **27**, 1345-1354

93. Suzuki, J., Chen, Y. Y., Scott, G. K., Devries, S., Chin, K., Benz, C. C., Waldman, F. M., and Hwang, E. S. (2009) Protein acetylation and histone deacetylase expression associated with malignant breast cancer progression. *Clinical cancer research : an official journal of the American Association for Cancer Research* **15**, 3163-3171

94. Sawin, K. E., and Mitchison, T. J. (1995) Mutations in the kinesin-like protein Eg5 disrupting localization to the mitotic spindle. *Proceedings of the National Academy of Sciences of the United States of America* **92**, 4289-4293

95. Baradari, V., Huether, A., Hopfner, M., Schuppan, D., and Scherubl, H. (2006) Antiproliferative and proapoptotic effects of histone deacetylase inhibitors on gastrointestinal neuroendocrine tumor cells. *Endocrine-related cancer* **13**, 1237-1250

96. Ryu, J. K., Lee, W. J., Lee, K. H., Hwang, J. H., Kim, Y. T., Yoon, Y. B., and Kim, C. Y. (2006) SK-7041, a new histone deacetylase inhibitor, induces G2-M cell cycle arrest and apoptosis in pancreatic cancer cell lines. *Cancer letters* **237**, 143-154

97. Skoufias, D. A., DeBonis, S., Saoudi, Y., Lebeau, L., Crevel, I., Cross, R., Wade, R. H., Hackney, D., and Kozielski, F. (2006) S-trityl-L-cysteine is a reversible, tight binding inhibitor of the human kinesin Eg5 that specifically blocks mitotic progression. *The Journal of biological chemistry* **281**, 17559-17569

98. Jamaladdin, S., Kelly, R. D., O'Regan, L., Dovey, O. M., Hodson, G. E., Millard, C. J., Portolano, N., Fry, A. M., Schwabe, J. W., and Cowley, S. M. (2014) Histone deacetylase (HDAC) 1 and 2 are essential for accurate cell division and the pluripotency of embryonic stem cells. *Proceedings of the National Academy of Sciences of the United States of America* **111**, 9840-9845

99. Woolner, S., O'Brien, L. L., Wiese, C., and Bement, W. M. (2008) Myosin-10 and actin filaments are essential for mitotic spindle function. *The Journal of cell biology* **182**, 77-88

100. Yoon, H. G., Chan, D. W., Reynolds, A. B., Qin, J., and Wong, J. (2003) N-CoR mediates DNA methylation-dependent repression through a methyl CpG binding protein Kaiso. *Molecular cell* **12**, 723-734

101. Newbold, A., Salmon, J. M., Martin, B. P., Stanley, K., and Johnstone, R. W. (2014) The role of p21(waf1/cip1) and p27(Kip1) in HDACi-mediated tumor cell death and cell cycle arrest in the Emu-myc model of B-cell lymphoma. *Oncogene* **33**, 5415-5423

102. Blagosklonny, M. V., Robey, R., Sackett, D. L., Du, L., Traganos, F., Darzynkiewicz, Z., Fojo, T., and Bates, S. E. (2002) Histone deacetylase inhibitors all induce p21 but differentially cause tubulin acetylation, mitotic arrest, and cytotoxicity. *Molecular cancer therapeutics* **1**, 937-941

103. Chuang, C., Pan, J., Hawke, D. H., Lin, S. H., and Yu-Lee, L. Y. (2013) NudC deacetylation regulates mitotic progression. *PloS one* **8**, e73841

104. Krzysiak, T. C., Wendt, T., Sproul, L. R., Tittmann, P., Gross, H., Gilbert, S. P., and Hoenger, A. (2006) A structural model for monastrol inhibition of dimeric kinesin Eg5. *The EMBO journal* **25**, 2263-2273

105. Nalawansha, D. A., Gomes, I. D., Wambua, M. K., and Pflum, M. K. H (2016) Identification of Eg5 as an HDAC1 substrate using trapping mutants. *Cell chemical biology* **Submitted**

106. Lin, J., Lai, S., Jia, R., Xu, A., Zhang, L., Lu, J., and Ye, K. (2011) Structural basis for site-specific ribose methylation by box C/D RNA protein complexes. *Nature* **469**, 559-563

107. Tessarz, P., Santos-Rosa, H., Robson, S. C., Sylvestersen, K. B., Nelson, C. J., Nielsen, M. L., and Kouzarides, T. (2014) Glutamine methylation in histone H2A is an RNA-polymerase-I-dedicated modification. *Nature* **505**, 564-568

108. Jha, S., Shibata, E., and Dutta, A. (2008) Human Rvb1/Tip49 is required for the histone acetyltransferase activity of Tip60/NuA4 and for the downregulation of phosphorylation on H2AX after DNA damage. *Molecular and cellular biology* **28**, 2690-2700

109. Gorynia, S., Bandeiras, T. M., Pinho, F. G., McVey, C. E., Vonrhein, C., Round, A., Svergun, D. I., Donner, P., Matias, P. M., and Carrondo, M. A. (2011) Structural and functional insights into a dodecameric molecular machine - the RuvBL1/RuvBL2 complex. *Journal of structural biology* **176**, 279-291

110. Shen, X., Mizuguchi, G., Hamiche, A., and Wu, C. (2000) A chromatin remodelling complex involved in transcription and DNA processing. *Nature* **406**, 541-544

111. Shi, Y. J., Matson, C., Lan, F., Iwase, S., Baba, T., and Shi, Y. (2005) Regulation of LSD1 histone demethylase activity by its associated factors. *Molecular cell* **19**, 857-864

112. Shi, Y., Lan, F., Matson, C., Mulligan, P., Whetstine, J. R., Cole, P. A., Casero, R. A., and Shi, Y. (2004) Histone demethylation mediated by the nuclear amine oxidase homolog LSD1. *Cell* **119**, 941-953

113. Klose, R. J., and Zhang, Y. (2007) Regulation of histone methylation by demethylimination and demethylation. *Nat Rev Mol Cell Biol* **8**, 307-318

114. Singh, M. M., Manton, C. A., Bhat, K. P., Tsai, W. W., Aldape, K., Barton, M. C., and Chandra, J. (2011) Inhibition of LSD1 sensitizes glioblastoma cells to histone deacetylase inhibitors. *Neuro-oncology* **13**, 894-903

115. Forneris, F., Binda, C., Adamo, A., Battaglioli, E., and Mattevi, A. (2007) Structural basis of LSD1-CoREST selectivity in histone H3 recognition. *The Journal of biological chemistry* **282**, 20070-20074

116. Vellore, N. A., and Baron, R. (2013) Molecular dynamics simulations indicate an induced-fit mechanism for LSD1/CoREST-H3-histone molecular recognition. *BMC biophysics* **6**, 15

117. Baron, R., and Vellore, N. A. (2012) LSD1/CoREST is an allosteric nanoscale clamp regulated by H3-histone-tail molecular recognition. *Proceedings of the National Academy of Sciences of the United States of America* **109**, 12509-12514

118. Chen, Y., Yang, Y., Wang, F., Wan, K., Yamane, K., Zhang, Y., and Lei, M. (2006) Crystal structure of human histone lysine-specific demethylase 1 (LSD1). *Proceedings of the National Academy of Sciences of the United States of America* **103**, 13956-13961

119. Ropero, S., and Esteller, M. (2007) The role of histone deacetylases (HDACs) in human cancer. *Molecular oncology* **1**, 19-25

120. Jie, D., Zhongmin, Z., Guoqing, L., Sheng, L., Yi, Z., Jing, W., and Liang, Z. (2013) Positive expression of LSD1 and negative expression of E-cadherin correlate with metastasis and poor prognosis of colon cancer. *Digestive diseases and sciences* **58**, 1581-1589

121. Lim, S., Janzer, A., Becker, A., Zimmer, A., Schule, R., Buettner, R., and Kirfel, J. (2010) Lysine-specific demethylase 1 (LSD1) is highly expressed in ER-negative breast cancers and a biomarker predicting aggressive biology. *Carcinogenesis* **31**, 512-520

122. Lv, T., Yuan, D., Miao, X., Lv, Y., Zhan, P., Shen, X., and Song, Y. (2012) Over-expression of LSD1 promotes proliferation, migration and invasion in non-small cell lung cancer. *PloS one* **7**, e35065

123. Metzger, E., Wissmann, M., Yin, N., Muller, J. M., Schneider, R., Peters, A. H., Gunther, T., Buettner, R., and Schule, R. (2005) LSD1 demethylates repressive histone marks to promote androgen-receptor-dependent transcription. *Nature* **437**, 436-439

124. Lee, M. G., Wynder, C., Cooch, N., and Shiekhattar, R. (2005) An essential role for CoREST in nucleosomal histone 3 lysine 4 demethylation. *Nature* **437**, 432-435

125. Cao, C., Vasilatos, S. N., Bhargava, R., Fine, J. L., Oesterreich, S., Davidson, N. E., and Huang, Y. (2016) Functional interaction of histone deacetylase 5 (HDAC5) and lysine-specific demethylase 1 (LSD1) promotes breast cancer progression. *Oncogene*

126. Lee, M. G., Wynder, C., Bochar, D. A., Hakimi, M. A., Cooch, N., and Shiekhattar, R. (2006) Functional Interplay between Histone Demethylase and Deacetylase Enzymes. *Molecular and cellular biology* **26**, 6395-6402

127. Forneris, F., Battaglioli, E., Mattevi, A., and Binda, C. (2009) New roles of flavoproteins in molecular cell biology: histone demethylase LSD1 and chromatin. *The FEBS journal* **276**, 4304-4312

128. Pilotto, S., Speranzini, V., Marabelli, C., Rusconi, F., Toffolo, E., Grillo, B., Battaglioli, E., and Mattevi, A. (2016) LSD1/KDM1A mutations associated to a newly described form of intellectual disability impair demethylase activity and binding to transcription factors. *Human molecular genetics*

129. Luo, H., Shenoy, A. K., Li, X., Jin, Y., Jin, L., Cai, Q., Tang, M., Liu, Y., Chen, H., Reisman, D., Wu, L., Seto, E., Qiu, Y., Dou, Y., Casero, R. A., Jr., and Lu, J. (2016) MOF Acetylates the Histone Demethylase LSD1 to Suppress Epithelial-to-Mesenchymal Transition. *Cell reports*

130. Piao, L., Suzuki, T., Dohmae, N., Nakamura, Y., and Hamamoto, R. (2015) SUV39H2 methylates and stabilizes LSD1 by inhibiting polyubiquitination in human cancer cells. *Oncotarget* **6**, 16939-16950

131. Gamazon, E. R., Huang, R. S., Cox, N. J., and Dolan, M. E. (2010) Chemotherapeutic drug susceptibility associated SNPs are enriched in expression quantitative trait loci. *Proceedings of the National Academy of Sciences* **107**, 9287-9292

132. Sripichai, O., and Fucharoen, S. (2007) Genetic polymorphisms and implications for human diseases. *Journal of the Medical Association of Thailand = Chotmaihet thangphaet* **90**, 394-398

133. Kebir, O., Chaumette, B., Fatjo-Vilas, M., Ambalavanan, A., Ramoz, N., Xiong, L., Mouaffak, F., Millet, B., Jaafari, N., DeLisi, L. E., Levinson, D., Joober, R., Fananas, L., Rouleau, G., Dubertret, C., and Krebs, M. O. (2014) Family-based association study of common variants, rare mutation study and epistatic interaction detection in HDAC genes in schizophrenia. *Schizophrenia research* **160**, 97-103

134. Kim, T., Park, J. K., Kim, H. J., Chung, J. H., and Kim, J. W. (2010) Association of histone deacetylase genes with schizophrenia in Korean population. *Psychiatry research* **178**, 266-269

135. Zeng, Z., Liao, R., Yao, Z., Zhou, W., Ye, P., Zheng, X., Li, X., Huang, Y., Chen, S., and Chen, Q. (2014) Three single nucleotide variants of the HDAC gene are associated with type 2 diabetes mellitus in a Chinese population: a community-based case-control study. *Gene* **533**, 427-433

136. Park, B. L., Kim, Y. J., Cheong, H. S., Lee, S. O., Han, C. S., Yoon, J. H., Park, J. H., Chang, H. S., Park, C. S., Lee, H. S., and Shin, H. D. (2007) HDAC10 promoter polymorphism associated with development of HCC among chronic HBV patients. *Biochemical and biophysical research communications* **363**, 776-781

137. Pflum, M. K., Tong, J. K., Lane, W. S., and Schreiber, S. L. (2001) Histone deacetylase 1 phosphorylation promotes enzymatic activity and complex formation. *The Journal of biological chemistry* **276**, 47733-47741

138. Kim, M. H., Kim, S. H., Kim, Y. K., Hong, S. J., Min, K. U., Cho, S. H., and Park, H. W. (2013) A polymorphism in the histone deacetylase 1 gene is associated with the response to corticosteroids in asthmatics. *The Korean journal of internal medicine* **28**, 708-714

139. Swett, R. J., Elias, A., Miller, J. A., Dyson, G. E., and Andres Cisneros, G. (2013) Hypothesis driven single nucleotide polymorphism search (HyDn-SNP-S). *DNA repair* **12**, 733-740

140. Ryslava, H., Doubnerova, V., Kavan, D., and Vanek, O. (2013) Effect of posttranslational modifications on enzyme function and assembly. *Journal of proteomics* **92**, 80-109

141. Brandl, A., Heinzel, T., and Kramer, O. H. (2009) Histone deacetylases: salesmen and customers in the post-translational modification market. *Biology of the cell / under the auspices of the European Cell Biology Organization* **101**, 193-205

142. Qiu, Y., Zhao, Y., Becker, M., John, S., Parekh, B. S., Huang, S., Hendarwanto, A., Martinez, E. D., Chen, Y., Lu, H., Adkins, N. L., Stavreva, D. A., Wiench, M., Georgel, P. T., Schiltz, R. L., and Hager, G. L. (2006) HDAC1 acetylation is linked

to progressive modulation of steroid receptor-induced gene transcription. *Molecular cell* **22**, 669-679

143. Segre, C. V., and Chiocca, S. (2011) Regulating the regulators: the post-translational code of class I HDAC1 and HDAC2. *Journal of biomedicine & biotechnology* **2011**, 690848

144. Karwowska-Desaulniers, P., Ketko, A., Kamath, N., and Pflum, M. K. (2007) Histone deacetylase 1 phosphorylation at S421 and S423 is constitutive in vivo, but dispensable in vitro. *Biochemical and biophysical research communications* **361**, 349-355

145. Weichert, W., Roske, A., Gekeler, V., Beckers, T., Ebert, M. P., Pross, M., Dietel, M., Denkert, C., and Rocken, C. (2008) Association of patterns of class I histone deacetylase expression with patient prognosis in gastric cancer: a retrospective analysis. *The Lancet. Oncology* **9**, 139-148

146. Yang, H., Yan, B., Liao, D., Huang, S., and Qiu, Y. (2015) Acetylation of HDAC1 and degradation of SIRT1 form a positive feedback loop to regulate p53 acetylation during heat-shock stress. *Cell death & disease* **6**, e1747

147. Shahar, O. D., Gabizon, R., Feine, O., Alhadeff, R., Ganoth, A., Argaman, L., Shimshoni, E., Friedler, A., and Goldberg, M. (2013) Acetylation of lysine 382 and phosphorylation of serine 392 in p53 modulate the interaction between p53 and MDC1 in vitro. *PloS one* **8**, e78472

148. Wu, S. Y., and Chiang, C. M. (2009) Crosstalk between sumoylation and acetylation regulates p53-dependent chromatin transcription and DNA binding. *The EMBO journal* **28**, 1246-1259

149. Lai, L.-C., Tsai, M.-H., Chen, P.-C., Chen, L. H., Hsiao, J.-H., Chen, S.-K., Lu, T.-P., Lee, J.-M., Hsu, C.-P., Hsiao, C. K., and Chuang, E. Y. (2014) SNP rs10248565 in HDAC9 as a novel genomic aberration biomarker of lung adenocarcinoma in non-smoking women. *Journal of Biomedical Science* **21**, 1-9

150. Glozak, M. A., and Seto, E. (0000) Histone deacetylases and cancer. *Oncogene* **26**, 5420-5432

151. Müller, B. M., Jana, L., Kasajima, A., Lehmann, A., Prinzler, J., Budczies, J., Winzer, K.-J., Dietel, M., Weichert, W., and Denkert, C. (2013) Differential expression of histone deacetylases HDAC1, 2 and 3 in human breast cancer - overexpression of HDAC2 and HDAC3 is associated with clinicopathological indicators of disease progression. *BMC cancer* **13**, 1-8

152. Osada, H., Tatematsu, Y., Saito, H., Yatabe, Y., Mitsudomi, T., and Takahashi, T. (2004) Reduced expression of class II histone deacetylase genes is associated with poor prognosis in lung cancer patients. *International journal of cancer* **112**, 26-32

## ABSTRACT

**STUDIES TOWARDS BROADENING THE SUBSTRATE PROFILE AND REGULATION OF HISTONE DEACETYLASE 1**

by

**DHANUSHA ASHANTHI NALAWANSHA**

**December 2016**

**Advisor:** Dr. Mary Kay H. Pflum

**Major:** Chemistry (Biochemistry)

**Degree:** Doctor of Philosophy

Aberrant expression of histone deacetylase 1 (HDAC1) is implicated in multiple diseases, including cancer. As a consequence, HDAC1 has emerged as an important therapeutic target for drug development. HDAC1 regulates key cellular processes, such as cell proliferation, apoptosis, and cell survival, by deacetylating both histone and non-histone substrates. Due to the lack of simple tools to identify physiological substrates of HDAC1, the full spectrum of HDAC1 activities in the cell remains unclear. Here, we employed a substrate trapping strategy to discover cellular substrates of HDAC1. Using this approach, we identified mitosis-related protein Eg5 as a substrate. HDAC1 colocalizes with Eg5 during mitosis, suggesting a role for HDAC1 in the mitotic defects observed with HDAC inhibitor drugs.

By extending our substrate trapping strategy to HEK293 cells, we identified lysine specific demethylase 1 (LSD1) as an HDAC1 substrate. Significantly, LSD1 is overexpressed in multiple cancers and has emerged as a potential anti-cancer drug target. LSD1 is typically found in association with another epigenetic enzyme, histone deacetylase1 (HDAC1). HDAC and LSD1 inhibitor compounds have been tested as

combination anti-cancer agents. However, the functional link between LSD1 and HDAC has yet to be understood in detail. Here we uncovered that HDAC1 mediated deacetylation of LSD1 at K374 in the substrate binding lobe, which affected the histone 3 binding and gene expression activity of LSD1. The mechanistic link between HDAC1 and LSD1 established here suggests that HDAC inhibitors influence LSD1 activity, which will ultimately guide drug design targeting epigenetic enzymes. Discovery of novel substrates using trapping mutants will reveal the full activities of HDAC1 in both physiological and pathological conditions, which will lead to a better understanding of HDAC inhibitor mechanism of action.

My second project focused on studying the effect of Single nucleotide polymorphisms (SNPs) of HDAC1. HDAC1 is upregulated in multiple diseases, and has emerged as an important therapeutic target for drug development. SNPs in multiple genes are often linked to the diseases, such as cancer. Here, we used the Hypothesis driven SNP search (HyDn-SNP-S) program to identify a HDAC1 SNP-F437C. The presence of SNP-F437C on HDAC1 affected acetylation at K432 and phosphorylation at S393, which ultimately altered enzymatic activity. These studies shed insights into the altered posttranslational modifications caused by HDAC1 exonic SNP. The study also revealed the significance of studying SNPs of HDAC in understanding the mechanisms leading to HDAC deregulation in cancer.

# AUTOBIOGRAPHICAL STATEMENT

DHANUSHA ASHANTHI NALAWANSHA

## EDUCATIONAL BACKGROUND

**Ph.D.,** Biological Chemistry (September 2011- October 2016)
Department of Chemistry, Wayne State University, Detroit MI
Dissertation title: Studies towards broadening the substrate profile and regulation of Histone Deacetylase1.
Advisor: Prof. Mary Kay H. Pflum

**BS.**, Molecular biology and Biochemistry (July 2006- August 2010)
Department of Chemistry, University of Colombo, Sri Lanka,
Thesis title: Cloning and characterization of *E. coli* leader peptidase
Advisors: Prof. N. V Chandrasekharan and Prof. U. Ratnayake

## AWARDS AND HONORS

- Thomas C. Rumble fellowship: Awarded by Graduate school, for superior academic achievement, Wayne State University, September 2014 - May 2015
- Graduate professional student travel award: From Wayne State University, January 2015
- Second place for the best research poster at the Graduate and Postdoctoral Symposium, Wayne State University, March 2016

## PUBLICATIONS

- Magdalene K. Wambua, **Dhanusha A. Nalawansha**, Ahmed T. Negmeldin, and Mary Kay H. Pflum, Mutagenesis Studies of the 14 Å Internal Cavity of Histone Deacetylase 1: Insights toward the Acetate - Escape Hypothesis and Selective Inhibitor Design, *J. Med. Chem.*, **2014**, *57* (3), 642–650
- **Dhanusha A. Nalawansha**, Inosha D. Gomes, Magdalene K. Wambua and Mary Kay H. Pflum, Identification of Eg5 as a HDAC1 substrate using trapping mutants, *Cell Chem. Biol., 2016, in revision.*
- **Dhanusha A. Nalawansha** and Mary Kay H. Pflum, LSD1 substrate binding and gene expression are affected by HDAC1-mediated deacetylation *ACS Chem. Bio., 2016, in revision.*
- **Dhanusha A. Nalawansha**, Rebecca J. Swett, Andres G. Cisneros and Mary Kay H. Pflum, HDAC1 SNP reveals a crosstalk between acetylation and phosphorylation, *Manuscript in preparation.*